



**DTIC FILE COPY**

2

**Naval Ocean Research and  
Development Activity**  
Stennis Space Center, Mississippi 39529-5004

**NORDA Technical Note 414**  
December 1988

**AD-A205 148**

**Proceedings of the Very Low Frequency (VLF)  
Ambient Noise Workshop:  
20-21 September 1988**

*(This document contains the unclassified presentations only.)*

**DTIC**  
**SELECTED**  
**S** **D**  
MAR 10 1989

Compiled by:  
**Ronald A. Wagstaff**  
Ocean Acoustics Division  
Ocean Acoustics and Technology Directorate

**Marshall R. Bradley**  
**Laurie A. Jugan**  
Planning Systems, Incorporated  
Slidell, Louisiana

89 3 08 207

Approved for public release; distribution is unlimited.



## Table of Contents

	<u>Page</u>
Abstract .....	i
Table of Contents .....	ii
I. Introduction .....	1
II. Participants .....	3
III. Agenda .....	7
IV. Summary .....	11
V. Presentations .....	37
"Opening Remarks," R. Wagstaff .....	39
"Influence of Noise Source Distributions and Propagation Mechanisms on Noise Field Directionality," M. Bradley/R. Wagstaff .....	51
"Distant Storm Noise," J. Wilson .....	121
"Shelf Shipping Noise," W. Hodgkiss .....	173
"Noise Floor Mechanisms," R.D. Gaul/ A. Wittenborn .....	193
"AEAS Noise Modeling Program - Directions/Needs," E. Chaika .....	227
"Noise Holes - Measured and Modeled," R. Heitmeyer .....	265
"System/Self/Flow Noise," J. Gottwald .....	279
"Ambient/Pseudo/Self Noise on VLA," P. Mikhalevsky/H. Freese .....	377
"SURTASS Noise Field Measurements," E. Holstrom/S. Kooney/M. Bradley .....	471
"VLA Measurements," W. Hodgkiss .....	513
"Noise Modal Filtering to Enhance Array Gain," T. Yang .....	567
"Opportunities for Analysis of Previously Recorded Data," J. Shooter/S. Mitchell .....	621

**Proceedings of the  
Very Low Frequency (VLF) Ambient Noise Workshop:  
20-21 September 1988**

**Naval Ocean Research and Development Activity  
Stennis Space Center, MS 39529-5004**

**I. INTRODUCTION**

A significant number of measurements of acoustic and ambient noise environmental data have been made over the past 15 years. Unfortunately, the processing, analysis, and reporting of these measurements have not been pursued at a commensurate level. It seems that there are always more funds available for measurement than for analysis. Hence, it is reasonable to assume that present data which have not received complete processing attention may contain some undiscovered gems that could be extremely valuable to a current program. Furthermore, these gems may be "mined" at relatively low cost compared to the cost of fielding an experiment to reacquire the data. The key, of course, is to scrutinize the data very closely to determine if the potential for gems existing in the data is high, the quality of the storage medium is adequate, and the necessary ancillary information is available. This includes deployment logs, environmental measurements, and descriptions of measurement conditions that include factors influencing the processing and analysis of the data. An additional consideration, some corporate knowledge must still exist concerning the data. These concerns were the motivating factors for conducting this VLF ambient noise workshop.

There was an additional motivating factor for conducting this workshop. Such a workshop presents an excellent opportunity to summarize the current state of knowledge of VLF ambient noise and any critical deficiencies, at least in so far as the HGI program is concerned. Hence, VLF ambient noise was reviewed in a focused way by inviting specific researchers to give presentations on particular topics and to tailor those presentations to the needs of the HGI program. The topics were not limited to data alone, but included presentations on factors that influence the quality of the data, such as system noise and flow noise, on acoustic propagation mechanisms that influence the noise, noise source characteristics and distributions, and the processing of noise data by the same algorithms that might be used to process signal data from a high gain array.

Due to the short time constraints for organizing and conducting this workshop, each speaker was asked to prepare a viewgraph presentation on a particular topic and to provide the organizers with an annotated hard copy of their viewgraphs. These viewgraphs are included in these Proceedings. Two volumes, one unclassified and one classified, were compiled to facilitate ease of distribution and handling.

Following this Introduction, a list of workshop participants can be found (Section II). Section III gives the agenda of the two day workshop, and Section IV contains viewgraphs which give a summary of the workshop and recommendations for future efforts. Section V contains the annotated hard copies of the viewgraphs from the presentations by the speakers. Unfortunately, not all of the presentations were annotated by the authors.



## II. PARTICIPANTS

The following is a list of those people who participated in the VLF Ambient Noise Workshop. Below each name, a full address is provided.

1. Marshall Bradley  
PSI  
115 Christian Lane  
Slidell, LA 70458
2. J. Ernest Breeding, Jr.  
NORDA  
Code 245  
Stennis Space Center, MS 39529
3. John Campbell  
NORDA  
Code 224  
Stennis Space Center, MS 39529
4. William Carey  
NUSC  
New London, CT 06320
5. Edward Chaika  
ONR Detachment  
Building 1100  
Stennis Space Center, MS 39529
6. Johanan L. Codona  
AT&T Bell Labs  
WH14B-419  
Whippany, NJ 07981
7. J.P. Feuillet  
SPAWAR  
Space & Naval Warfare Command  
Washington, DC 20375
8. Craig Fisher  
NORDA  
Code 245  
Stennis Space Center, MS 39529
9. Dr. Edward Franchi  
NORDA  
Code 200  
Stennis Space Center, MS 39529
10. Herb Freese  
SAIC  
1710 Goodridge Drive  
McLean, VA 22102
11. R.D. Gaul  
Blue Sea Corporation  
Suite 317  
14300 Cornerstone Village Dr.  
Houston, TX 77014
12. T.G. Goldsberry  
NORDA  
Code 240  
Stennis Space Center, MS 39529
13. J.T. Gottwald  
G/J Associates  
P.O. Box 3259  
968 Yachtsman Way  
Annapolis, MD 21403
14. Richard Heitmeyer  
NRL  
Code 512  
Washington, DC 20375
15. W.S. Hodgkiss  
Marine Physical Lab  
Scripps Institute of Oceanography  
San Diego, CA 92152
16. E.K. Holmstrom  
COMOCEANSYSPAC  
P.O. Box 1390  
Pearl Harbor, HI 96860-7550
17. Stephanie Kooney  
NORDA  
Code 245  
Stennis Space Center, MS 39529
18. K.W. Lackie  
ONR/AEAS  
Code 125  
800 North Quincy Street  
Arlington, VA 22217
19. Yung P. Lee  
SAIC  
1710 Goodridge Drive  
McLean, VA 22102
20. Joe Lombardo  
JHU/APL  
Laurel, MD 20707



21. Jack McDermid  
NORDA  
Code 211  
Stennis Space Center, MS 39529
22. S.W. Marshall  
BBN  
1300 North 17th Street  
Arlington, VA 22209
23. Peter Mikhalevsky  
SAIC  
1710 Goodridge Drive  
(MS T-3-5)  
McLean, VA 22102
24. S.K. Mitchell  
ARL:UT  
Applied Research Labs  
Box 8029  
Austin, TX 78713
25. Joal J. Newcomb  
NORDA  
Code 245  
Stennis Space Center, MS 39529
26. John Perkins  
NRL  
Code 5160  
Washington, DC 20375-5000
27. William Renner  
SAIC  
1710 Goodridge Drive  
McLean, VA 22102
28. J.W. Reese  
NOSC  
Code 715  
San Diego, CA 92152
29. Jack Shooter  
ARL:UT  
P.O. Box 8029  
Austin, TX 78713
30. R.A. Wagstaff  
NORDA  
Code 245  
Stennis Space Center, MS 39529
31. James H. Wilson  
WAR, Inc.  
PRL, Inc.  
6309 Carpinteria Avenue  
Carpinteria, CA 93013
32. A.F. Wittenborn  
Blue Sea Corporation  
3405 Southill  
Austin, TX 78703
33. T.C. Yang  
NRL  
4555 Overlook Avenue  
Washington, DC 20375



### III. AGENDA

The presentations for this workshop covered several broad topics: Noise Field Mechanisms, Modeling, System Noise, "Stationary" Horizontal Arrays, Towed Horizontal Arrays, Vertical Arrays, and Data Processing Proposals. Presentation summaries consisting of viewgraphs with annotations (when available) can be found in Section V of this report or in a companion classified report. The presentations were given in the following order:

#### HGI/AEAS VLF AMBIENT NOISE WORKSHOP AGENDA

**20 Sep 1988**

- 0900 Opening Remarks: R. Wagstaff (NORDA)
- 0910 Welcome Address: Dr. E.R. Franchi
- 0920 Workshop Sponsors' Comments: N. Booth (ONT)/AEAS Rep. (ONR)

#### **NOISE FIELD MECHANISMS (J. Reese/NOSC)**

- 0930 Influence of Noise Source Distributions and Propagation Mechanisms on Noise Field Directionality: M. Bradley (PSI)/R. Wagstaff (NORDA)
- 1000 Distant Storm Noise: J. Wilson (WAR, Inc.)
- 1030 BREAK
- 1045 Shelf Shipping Noise: W. Hodgkiss (MPL)
- 1115 Noise Floor Mechanisms: R.D. Gaul/A. Wittenborn (BSC)

#### **MODELING (J. Reese/NOSC)**

- 1330 AEAS Noise Modeling Program - Directions/Needs: E. Chaika
- 1400 Noise Holes-Measured and Modeled: R. Heitmeyer (NRL)

#### **SYSTEM NOISE (W. Hodgkiss/MPL)**

- 1430 System/Self/Flow Noise: J. Gottwald (J/G Assoc.)
- 1500 BREAK
- 1515 VLF Self Noise Observed in SURTASS\*: J. Reese (NOSC)
- 1545 Ambient/Pseudo/Self Noise on VLA: P. Mikhalevsky/H. Freese (SAIC)
- 1615 ADJOURN

---

\* Viewgraphs are contained in a companion classified report.



21 Sep 1988

**"STATIONARY" HORIZONTAL ARRAYS (S. Marshall/BBN)**

- 0830 OMAT Beam Noise Data/Down Slope Conversion\*: P. Herstein/P. Koenigs/W. Carey (NUSC)  
0900 LBA Data: J. Codona\* (BTL)

**TOWED HORIZONTAL ARRAYS (S. Marshall/BBN)**

- 0930 Towed Array Data Overview\*: M. Bradley (PSI)/B. Palmer (NRL)/R. Wagstaff (NORDA)  
1000 LAMBDA II and III Results\*: R. Wagstaff (NORDA)  
1030 BREAK  
1045 VLF-MF, MFA and QRSS Data\*: W. Carey (NUSC)  
1115 APL/JHU Measurements\*: J. Lombardo (APL/JHU)  
1145 SURTASS Noise Field Measurements: E. Holmstrom (COSP)/S. Kooney (NORDA)/ M. Bradley (PSI)  
1215 LUNCH

**VERTICAL ARRAYS (W. Carey/NUSC)**

- 1330 VLA Measurements: W. Hodgkiss (MPL)  
1400 Noise Model Filtering to Enhance Array Gain: T. Yang (NRL)  
1430 BREAK

**DATA PROCESSING PROPOSALS (R. Wagstaff/NORDA)**

- 1445 Opportunities for Analysis of Previously Recorded Data: J. Shooter/S. Mitchell (ARL/UT)  
1500 Other Proposals?  
1600 Adjourn Workshop

---

\* Viewgraphs are contained in a companion classified report.



#### IV. SUMMARY

As a result of this workshop, VLF ambient noise was reviewed in light of HGI Program objectives. It is evident that the general principles governing ambient noise between 10 and 100 Hz are well understood. This understanding was used to develop criteria for future program efforts. Toward this end, some existing data sets were determined as candidates for reprocessing tailored to HGI investigations. The following set of viewgraphs summarizes the findings of the workshop.





# PROCEEDINGS ACCOMPLISHMENTS

---

- A BALANCED REVIEW OF 10-100 Hz NOISE
  - MECHANISMS
  - PROPAGATION
  - DATA
- CONSENSUS AGREEMENT THAT GENERAL PROPERTIES OF 10-100 Hz NOISE FIELD ARE WELL UNDERSTOOD
- NUMEROUS EXAMPLES OF AG IN EXCESS OF DI FOR CONVENTIONALLY PROCESSED HORIZONTAL ARRAYS
- CANDIDATE DATA SETS FOR REPROCESSING IDENTIFIED





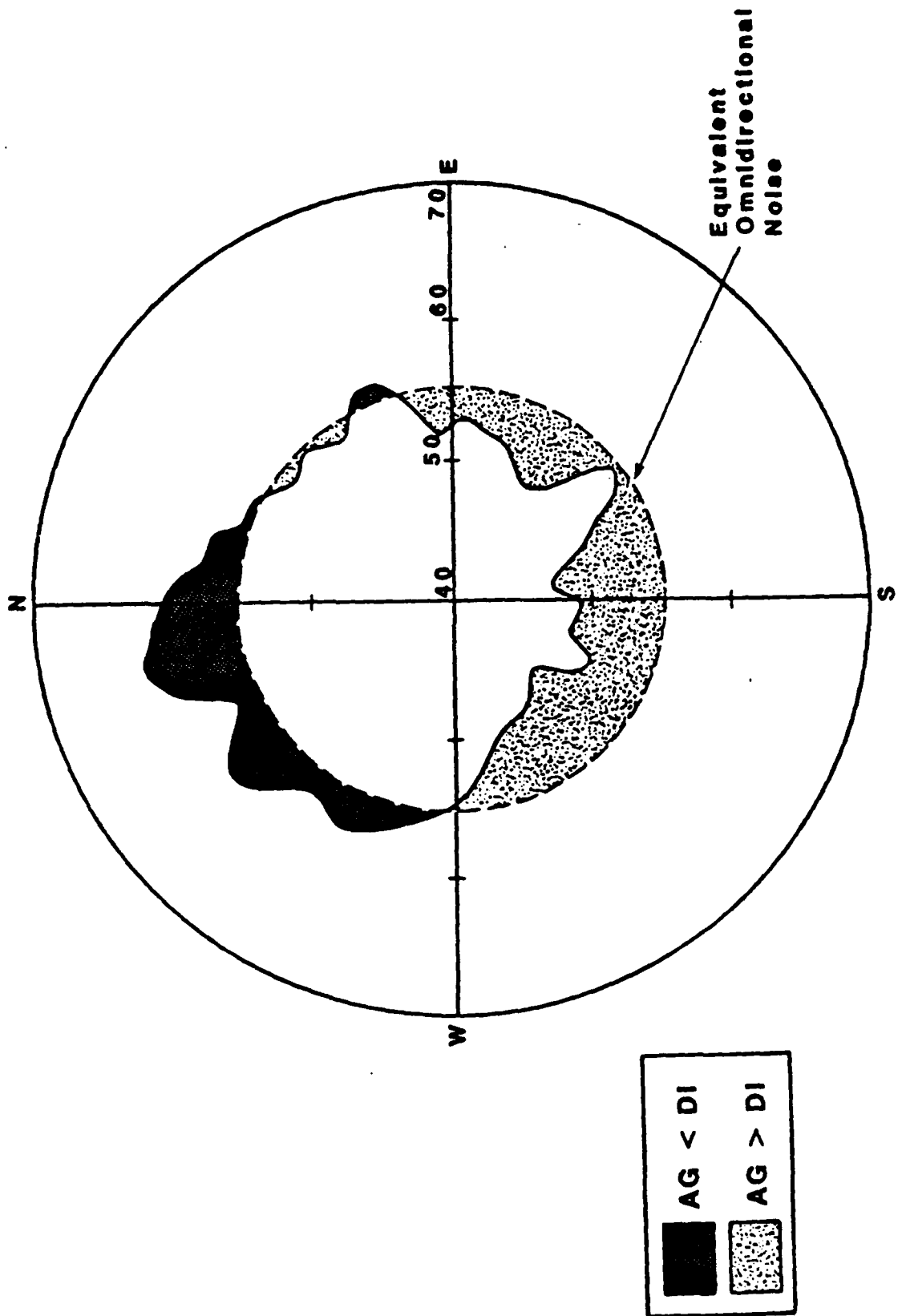
# EXAMPLES OF ARRAY GAIN GREATER THAN DIRECTIVITY INDEX

ARRAY GAIN EXCEEDS DIRECTIVITY INDEX WHEN  
ACTUAL BEAM NOISE IS LESS THAN THE  
EQUIVALENT OMNIDIRECTIONAL BEAM NOISE





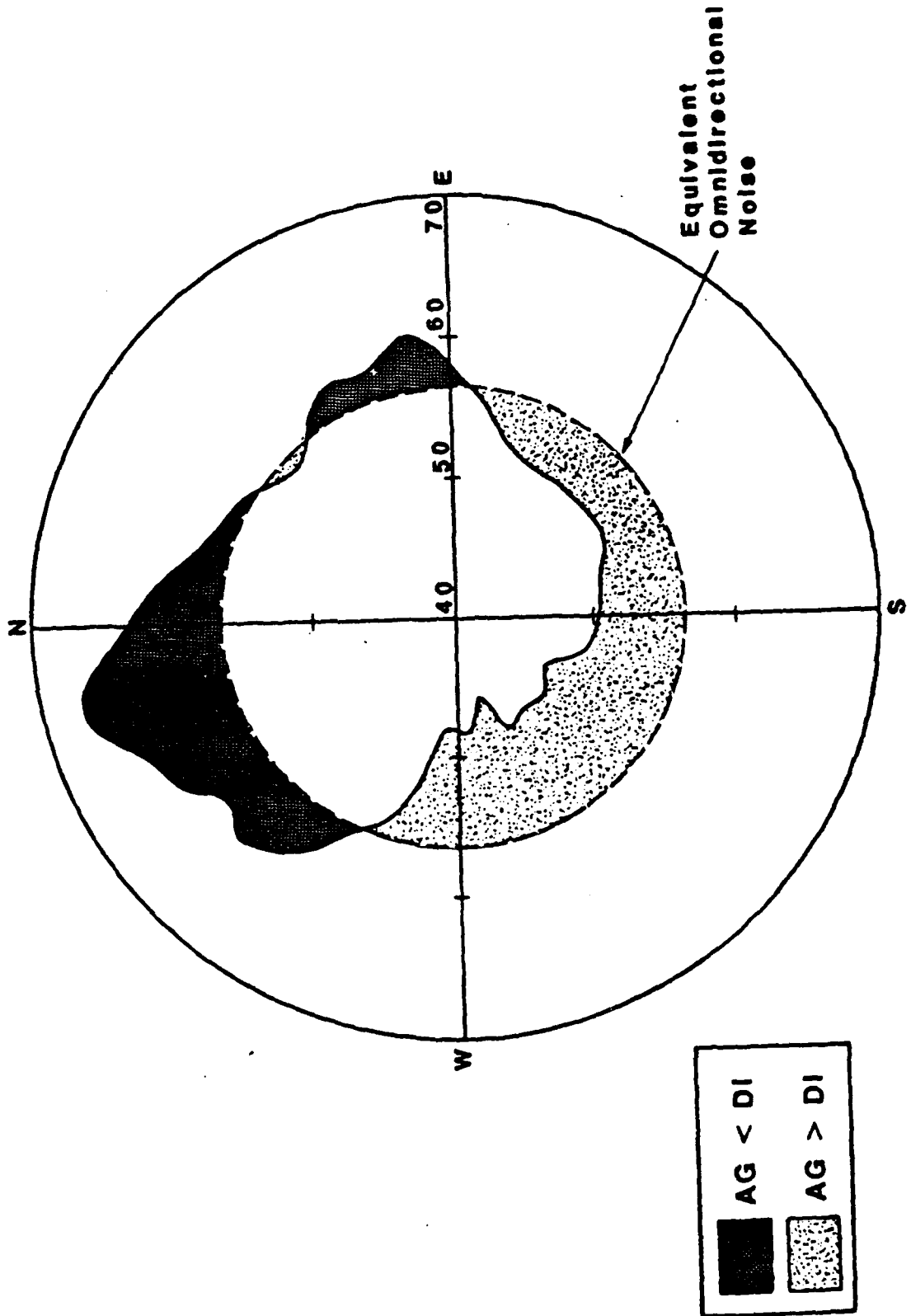
# SEARCHLIGHT BEAM NOISE LEVELS at 9 Hz







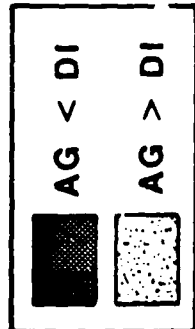
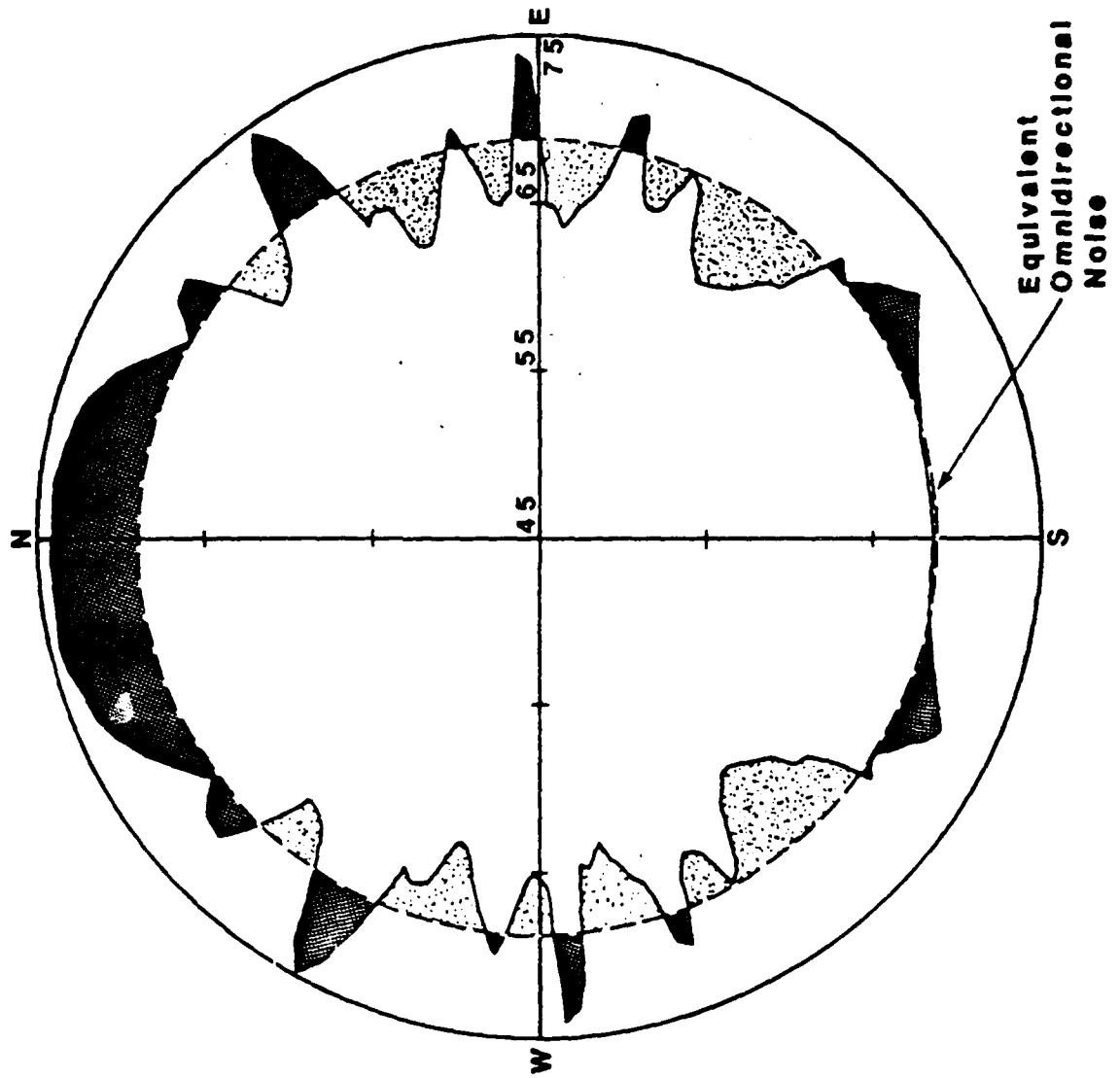
# SEARCHLIGHT BEAM NOISE LEVELS at 19 Hz





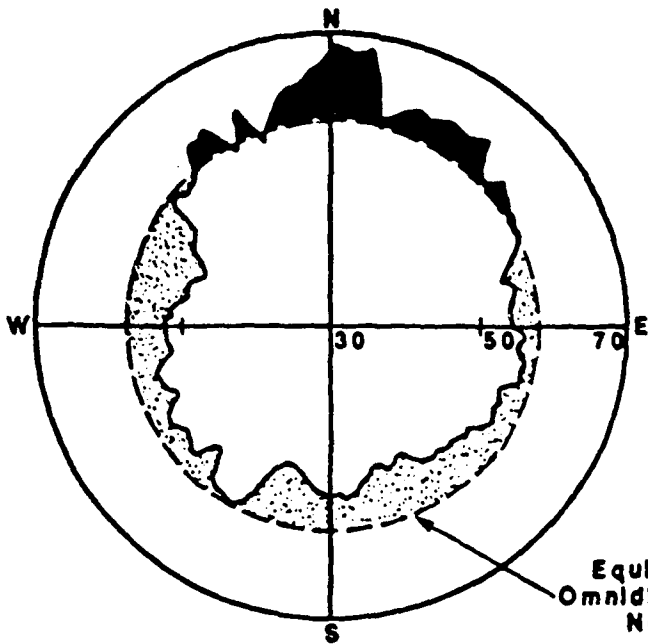


# TOWED ARRAY BEAM NOISE LEVELS at 25 Hz

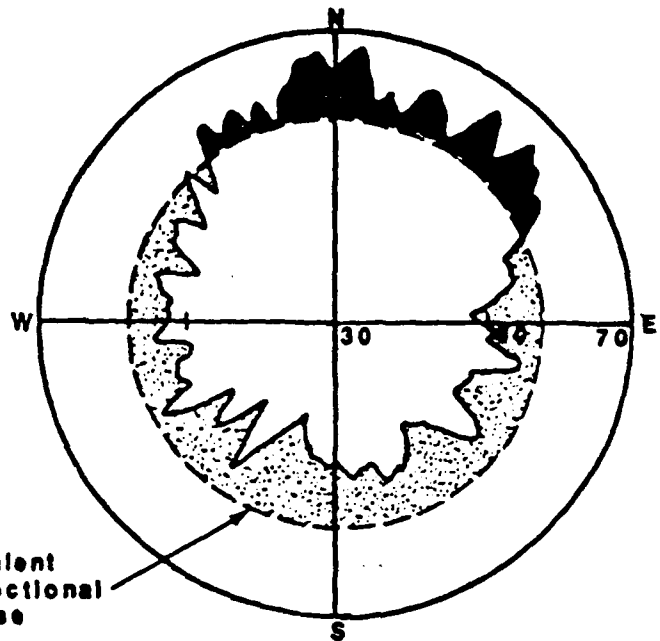




# SEARCHLIGHT BEAM NOISE LEVELS

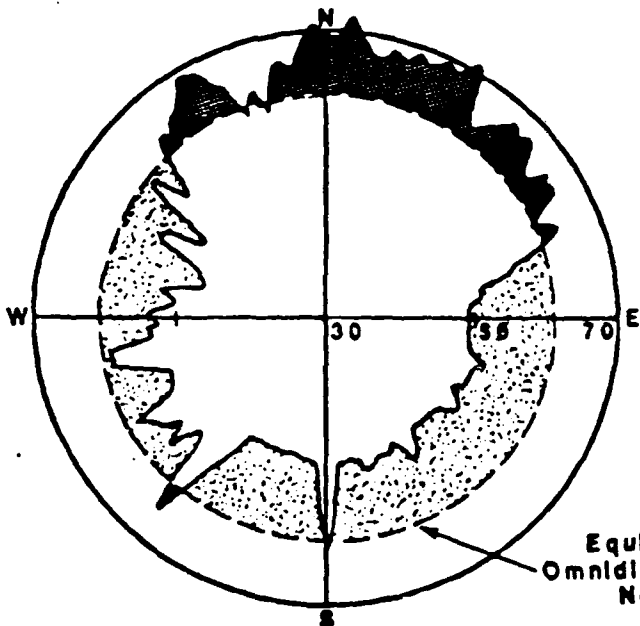


15 Hz

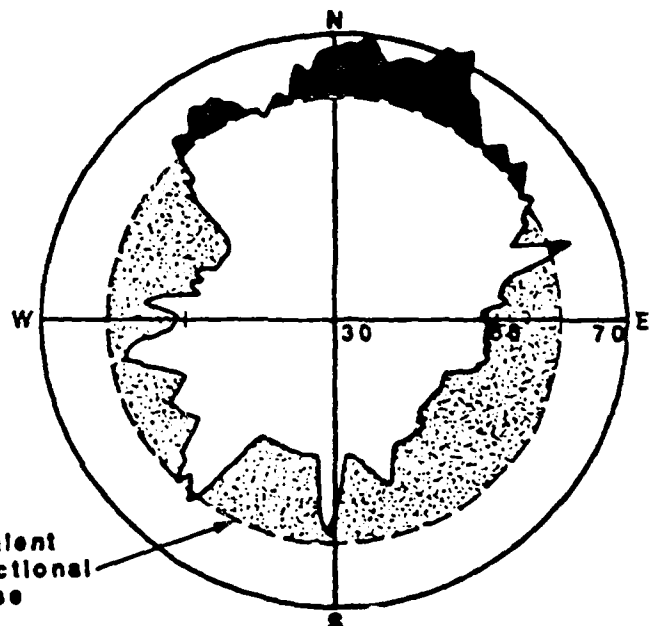


25 Hz

Equivalent  
Omnidirectional  
Noise

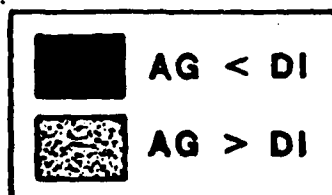


49 Hz



60 Hz

Equivalent  
Omnidirectional  
Noise

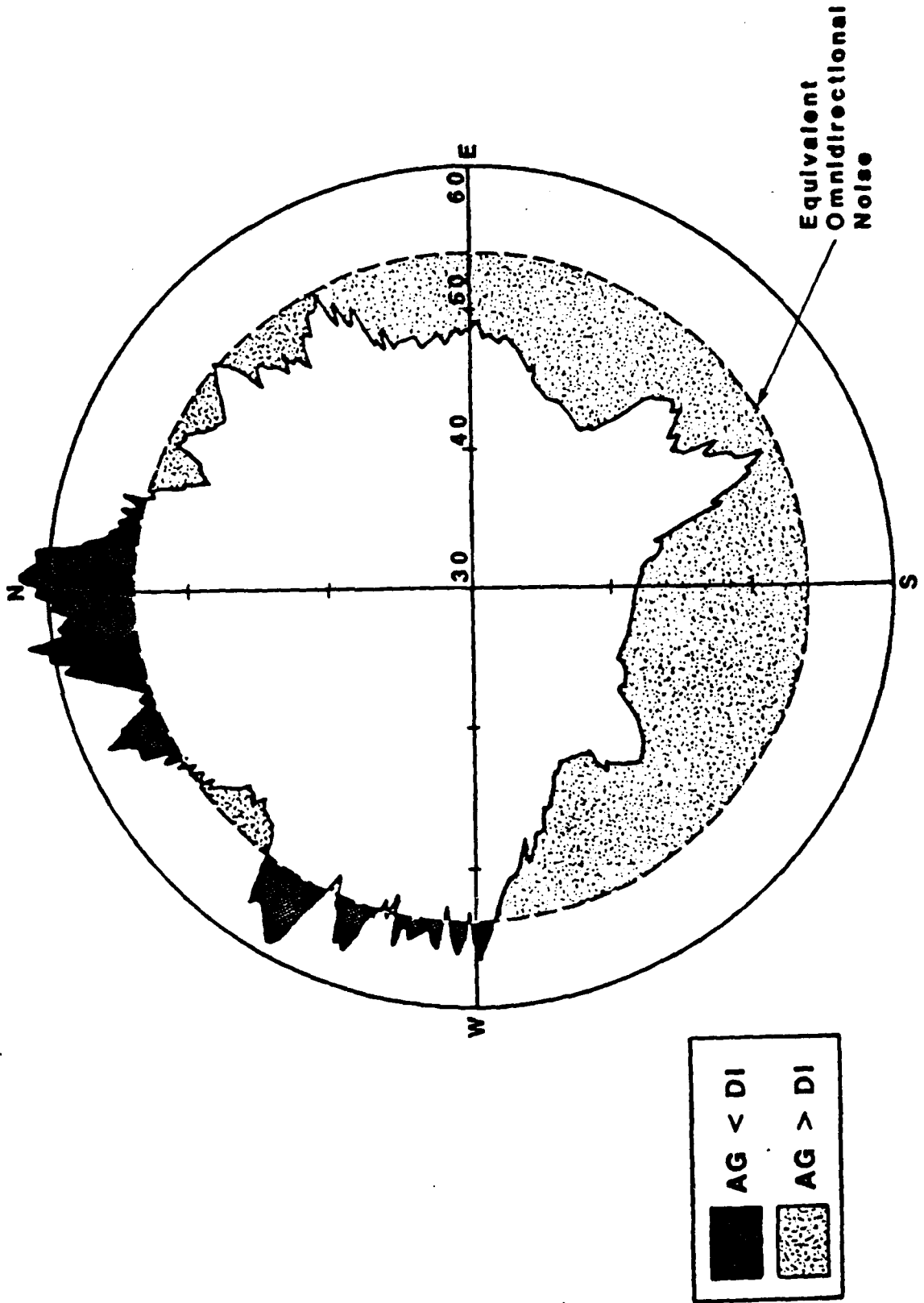






# SEARCHLIGHT BEAM NOISE LEVELS

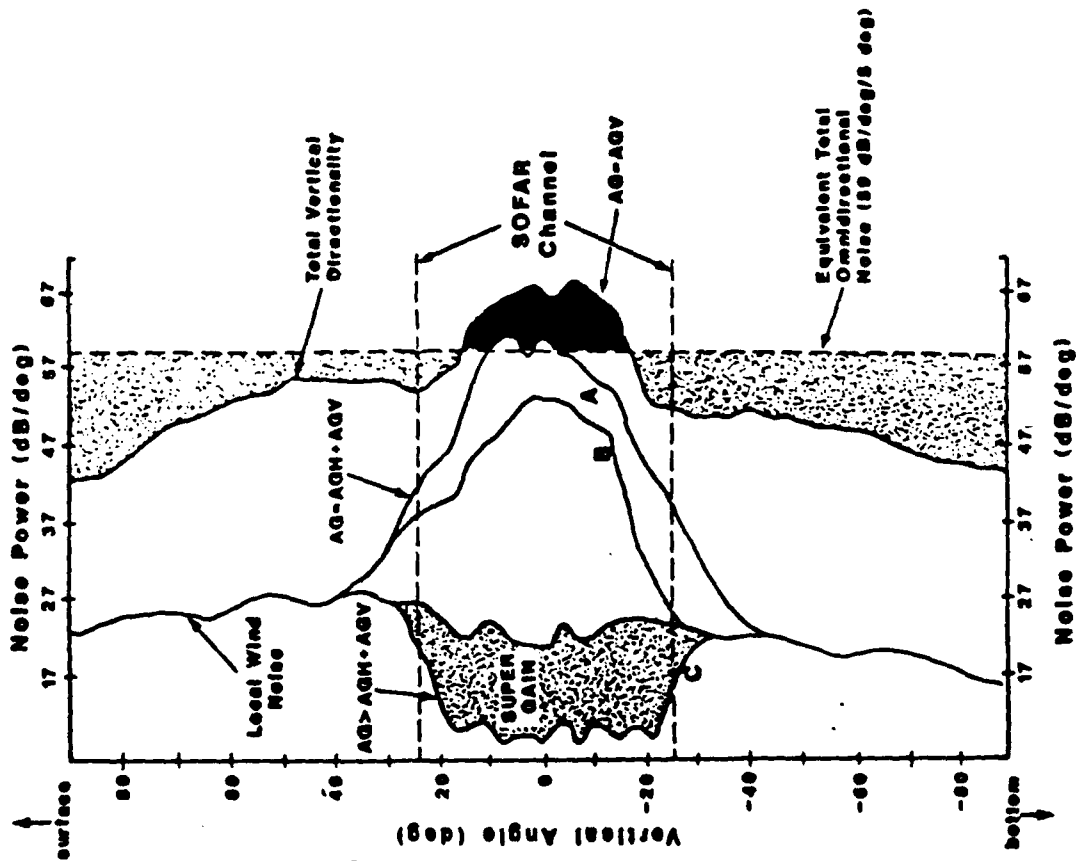
at 11 Hz



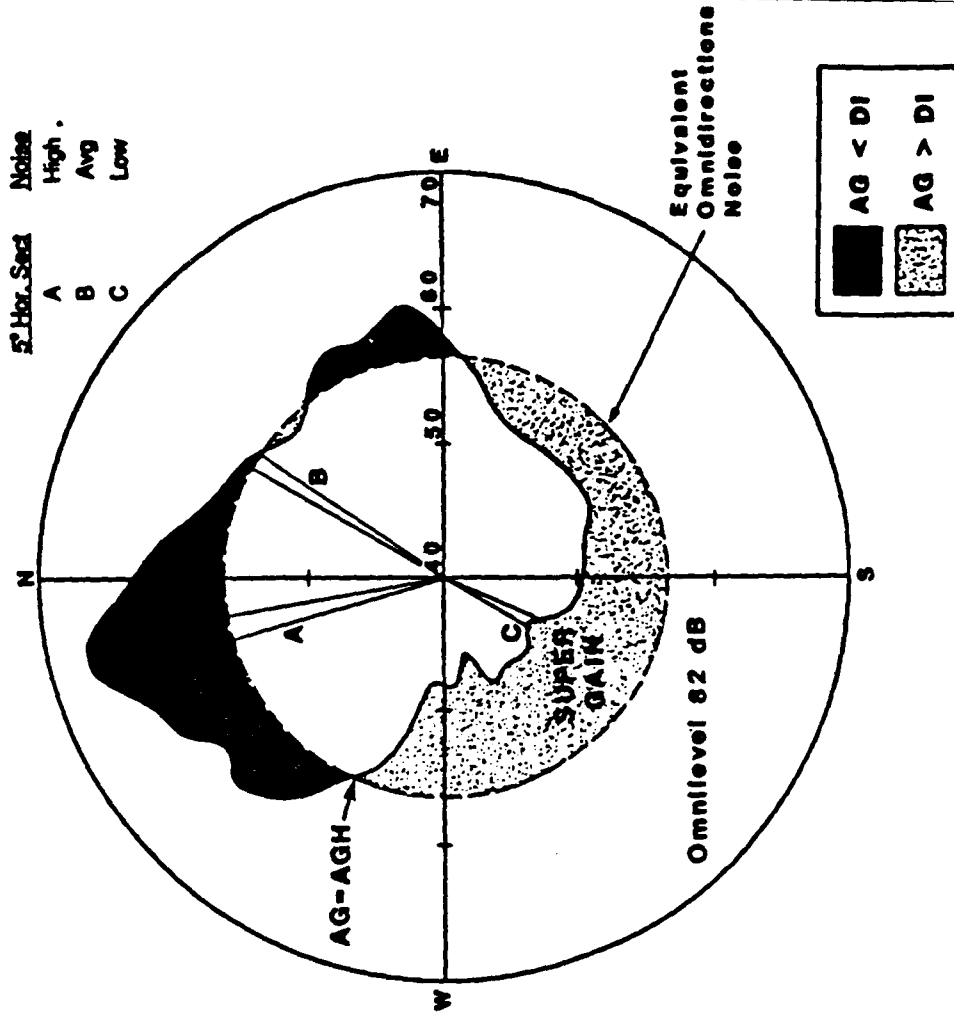




# MEASUREMENTS AND ESTIMATES OF THE POTENTIAL FOR SUPER GAIN IN THE HORIZONTAL AND VERTICAL



Time Averaged and Spatially Smoothed  
Horizontal Directionality at 19 Hz  
(dB/deg)







# CANDIDATE DATA SETS FOR ADDITIONAL PROCESSING

	Data	Pro	Con	Applicability to HGI Goals	AG > DI	Proposal
<b>SURTASS</b>	Beam Noise Stats, Horiz. Direct.	"High" Resolution, Large Quantity	Lack of Support EVA Data	Depth, Width & Occurrence of Noise Holes, Site Selection, Model Validation	Yes, > 10 dB	NORDA
<b>OMAT</b>	Beam Noise Stats	"Stationary" Array	Deformed Array, Side Lobe Control	Width & Occurrence of Noise Holes, Model Validation	Probably	NUSC, BBN
<b>VDABS</b>	Omni/Vert, T, Z Site Variability	Multiple Sites	Low Resolution	Model Validation	NA	ARL/UT
<b>CHURCH OPAL</b>	Omni Noise Floor Characterization	Noise Floor is Important Concept	Omni Only	Local Noise Generation, Noise Floor Upper Bound	NA	Blue Seas
<b>MPL VLA</b>	High Resolution Vert. Direct.	Long Aperture	Many Artifacts	Suitable for HGI System Processing, i.e., MFP	Yes	MPL





## PRESENT STATUS

- **LOW FREQUENCY AMBIENT NOISE FIELD GROSS STRUCTURE IS WELL UNDERSTOOD**
- **PERFORMANCE OF CONVENTIONAL SYSTEMS IS PREDICTABLE**
- **ADDITIONAL PROCESSING OF EXISTING DATA SETS APPROPRIATE FOR**
  - **INVESTIGATION OF SOME FUNDAMENTAL MECHANISMS OF SIGNIFICANCE TO HGI**
  - **PRESENT MODEL VALIDATION**
  - **DESIGN AND PERFORMANCE PREDICTION OF NEXT GENERATION HGI MEASUREMENT SYSTEM**
- **DATA WHICH DEFINE THE LIMITING NOISE FLOOR DO NOT EXIST BECAUSE THE NEED FOR ULTRA HIGH GAIN AGAINST THE NOISE WAS NOT PREVIOUSLY PERCEIVED**
- **CAPABILITY TO MAKE THESE MEASUREMENTS CURRENTLY EXISTS**
- **HGI SYSTEM PERFORMANCE NOT CURRENTLY PREDICTABLE**





## RECOMMENDATIONS

- EXAMINE MODEL DEFICIENCIES AND PROJECTED HGI MEASUREMENTS TO DEFINE THE REQUIREMENTS FOR ADDITIONAL DATA PROCESSING OF EXISTING DATA
  - VERTICALLY ORIENTED MEASUREMENT PROGRAM CAN BE SUPPLEMENTED WITH PREVIOUS HORIZONTAL ARRAY DATA
  - UPPER BOUNDS ON NOISE FLOOR CAN BE CHARACTERIZED BY PREVIOUS VERTICAL STRING HYDROPHONE MEASUREMENTS
- USE CURRENT CAPABILITIES TO MEASURE THE SPATIAL AND TEMPORAL CHARACTERISTICS OF THE BASAL NOISE DENSITY AND RELATE TO NOISE SOURCE DISTRIBUTION AND PROPAGATION MECHANISMS
- DEVELOP THE CAPABILITY TO PREDICT THE INFLUENCE OF THE BASAL NOISE DENSITY ON ADVANCED PROCESSORS





## SUMMARY

- NEED DATA TO QUANTIFY ANGULAR DISTRIBUTIONS OF LOW LEVEL NOISE IN DEEP SOUND CHANNEL
- NEED TO INCLUDE DISTANT STORMS TO AGREE WITH DATA
- CHURCH OPAL DATA ARE GOOD FOR INVESTIGATING BROADBAND SPECTRAL HOLES
- FLOW NOISE BELOW 10 Hz DROPPED 20 dB FOR SURTASS DIW
- VLA BEHAVED LIKE A STICK
- LONG ARRAY WAS OUT OF FOCUS FOR MOST RANGES DUE TO LONG APERTURE
- NEAR FIELD BOTTOM INTERACTION LIMITED COHERENCE
- MUCH OF DATA DISCUSSED COULD BE REPROCESSED TO ADDRESS ISSUES IMPORTANT TO HGI



## V. PRESENTATIONS

This section contains copies of the viewgraphs used for the presentations made at the VLF Ambient Noise Workshop. Annotations to the viewgraphs are also provided when available. As previously indicated, some viewgraphs are omitted from this report, and are contained in a companion classified report.



# OPENING REMARKS

R. WAGSTAFF (NORDA)





# VLF AMBIENT NOISE WORKSHOP

**ORGANIZERS:**

R. A. WAGSTAFF, NORDA  
M. BRADLEY, PSI

**HOST:**

NORDA/USM

**SPONSORS:**

ONT (HIGH GAIN INITIATIVE PROGRAM)  
AEAS PROGRAM





# ONT/AEAS VLF AMBIENT NOISE WORKSHOP

## PURPOSE:

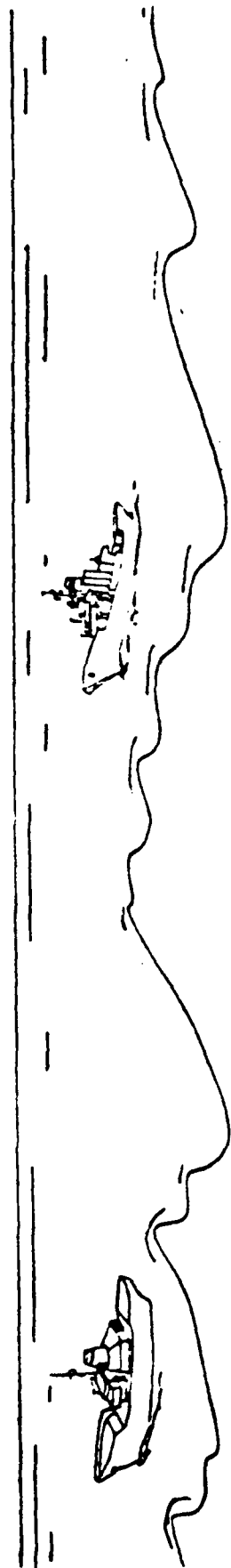
- SUMMARIZE VLF NOISE, PROPAGATION MECHANISMS
- EVIDENCE OF AG > DI
- ADDITIONAL DATA PROCESSING/ANALYSIS
- IDENTIFY DATA SETS
- GENERATE PROPOSALS

In the past the Navy ASW effort has focused on signal studies and ignored the ambient noise, where the most significant gains can be achieved.





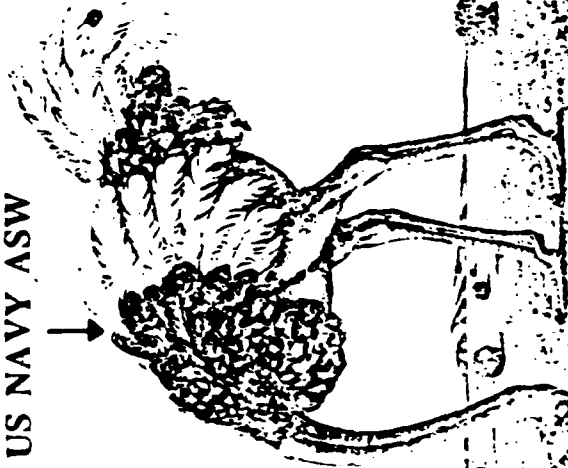
# PAST ASW POSTURE



**NOISE**



US NAVY ASW



**SIGNAL**

The objectives of the workshop as stated by the HGI program manager.



# AMBIENT NOISE WORKSHOP

## MAJOR HIGH GAIN QUESTION:

CAN WE ACHIEVE  
ARRAY GAIN > DIRECTIVITY  
INDEX  
BY AT LEAST 15 dB?

## FOCUS:

1. Determine if evidence exists that the Ambient Noise Field is such that Array Gain >> Directivity Index can be achieved with a High Gain Array.
  - Summarize the evidence.
    - VLF Frequency Range
    - Quantitative
    - Fully Annotated
    - Probability of Occurrence
2. Determine if further analysis of existing data will improve our ability to answer the question.
  - List the data sets.
  - Define the questions to be answered.
  - List the benefits and limitations of the analysis.





# AMBIENT NOISE WORKSHOP

## AS TIME ALLOWS:

3. Develop lists of phenomena that suggest
  - AG >> DI.
  - AG  $\approx$  DI.
4. Recommend experimental or analytical approaches for estimating the magnitude of the phenomena.

## EXPECTED PRODUCT:

- Summary Viewgraphs on each of the above items at conclusion of meeting.
- Outline of Report at conclusion of meeting.
- Report with selected viewgraphs and/or illustrative results.  
Mid October



**INFLUENCE OF NOISE SOURCE  
DISTRIBUTIONS AND  
PROPAGATION MECHANISMS ON  
NOISE FIELD DIRECTIONALITY**

**M. BRADLEY (PSI) / R. WAGSTAFF (NORDA)**





**INFLUENCE OF NOISE SOURCE  
DISTRIBUTIONS AND PROPAGATION  
MECHANISMS ON NOISE FIELD  
DIRECTIONALITY**

**Marshall Bradley  
Ron Wagstaff**



# LOW FREQUENCY

# NOISE SOURCES

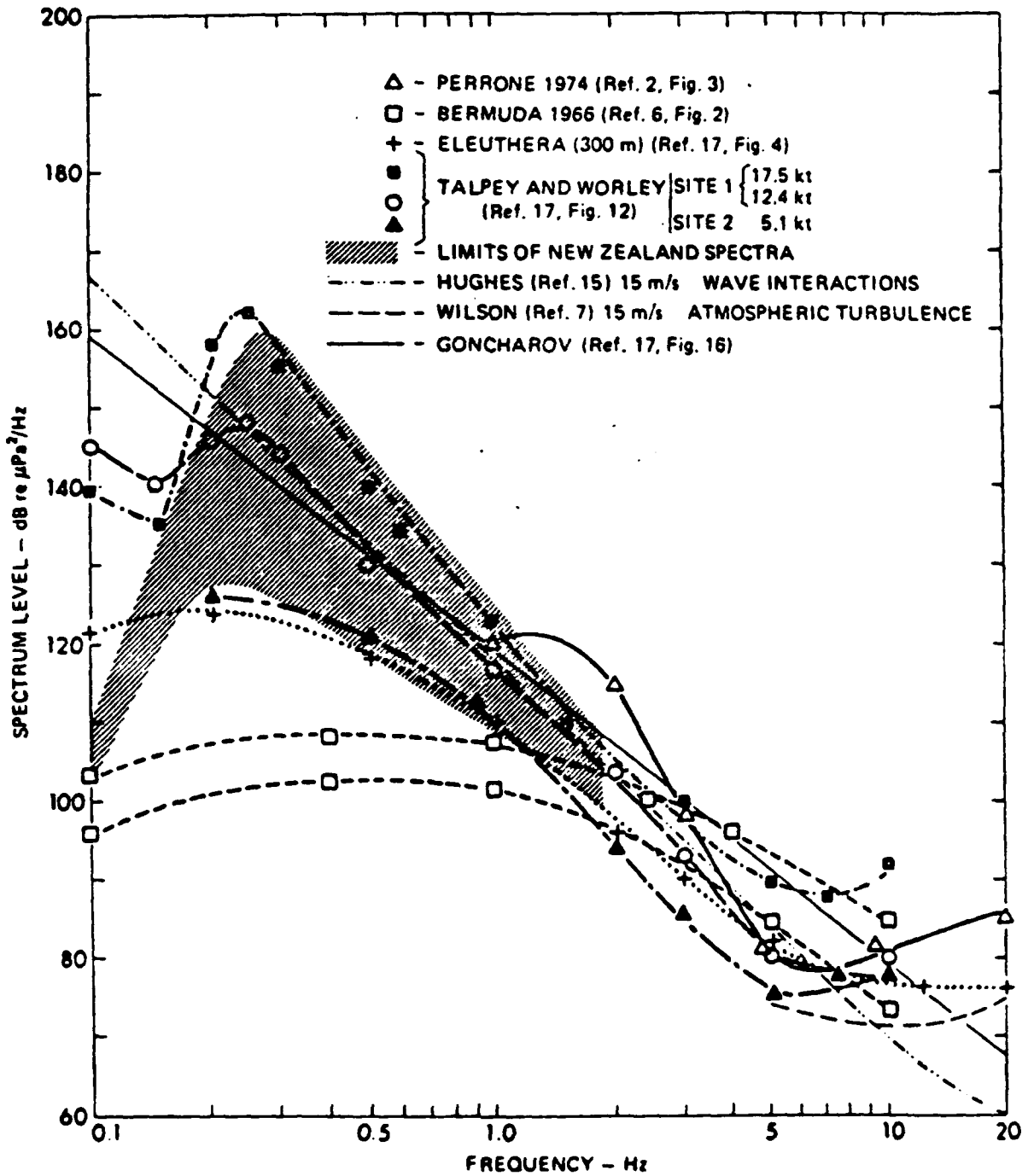






# VLF AMBIENT NOISE

## Kibblewhite (1985)



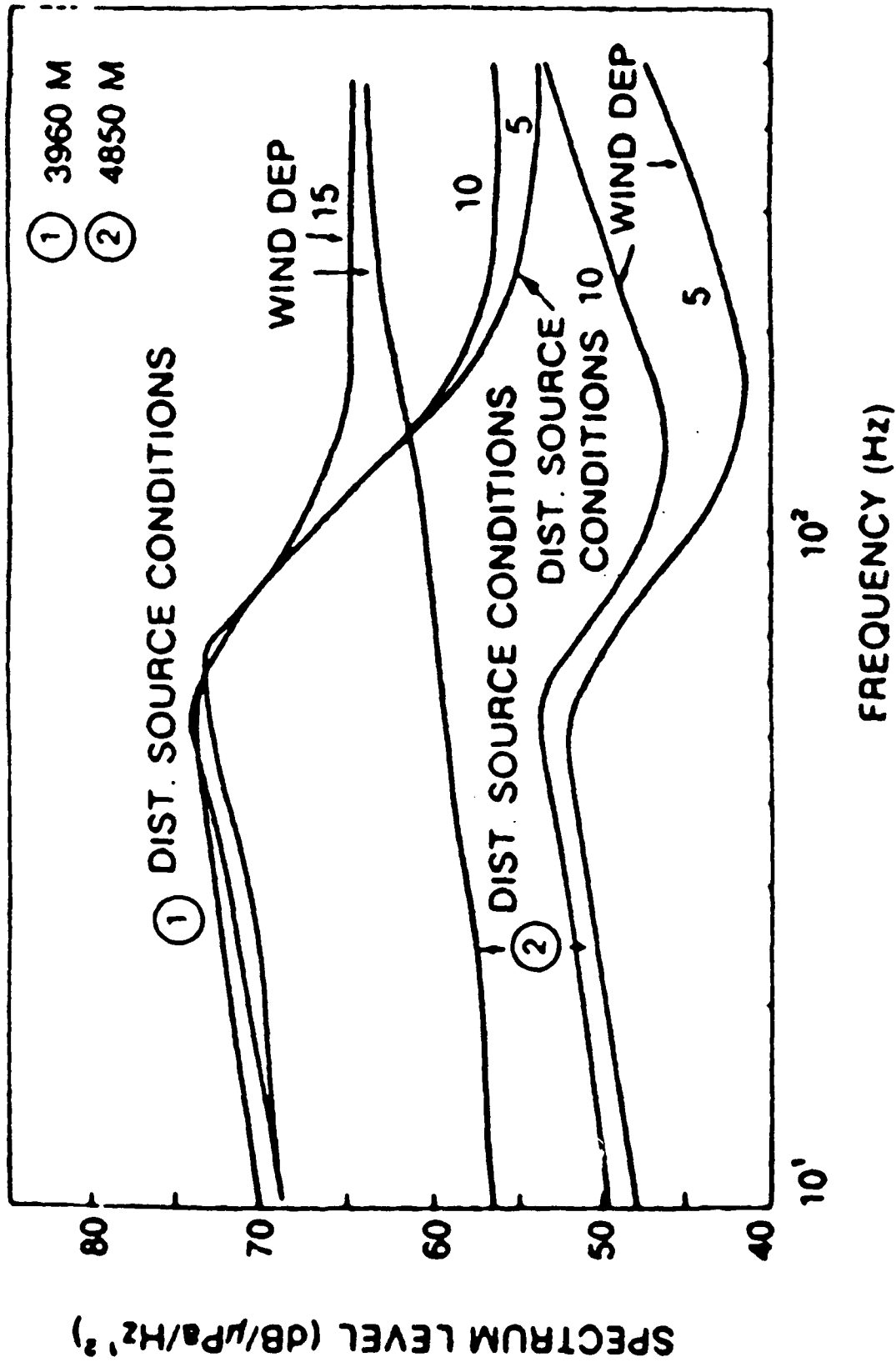
### Wind Component of VLF Noise

This slide shows measurements of omnidirectional ambient noise made during the CHURCH OPAL exercise by Wittenborn (1976). Data from two hydrophones are shown; one hydrophone is in the sound channel and the other is below critical depth. There is an indication that both curves are affected by noise from distant sources (note similarities in shape), however the sound channel hydrophone is dominated by distant source noise. The deeper hydrophone shows a pronounced wind dependence in the 10-100 Hz frequency region.



# WIND COMPONENT OF VLF NOISE

Wittenborn (1976)

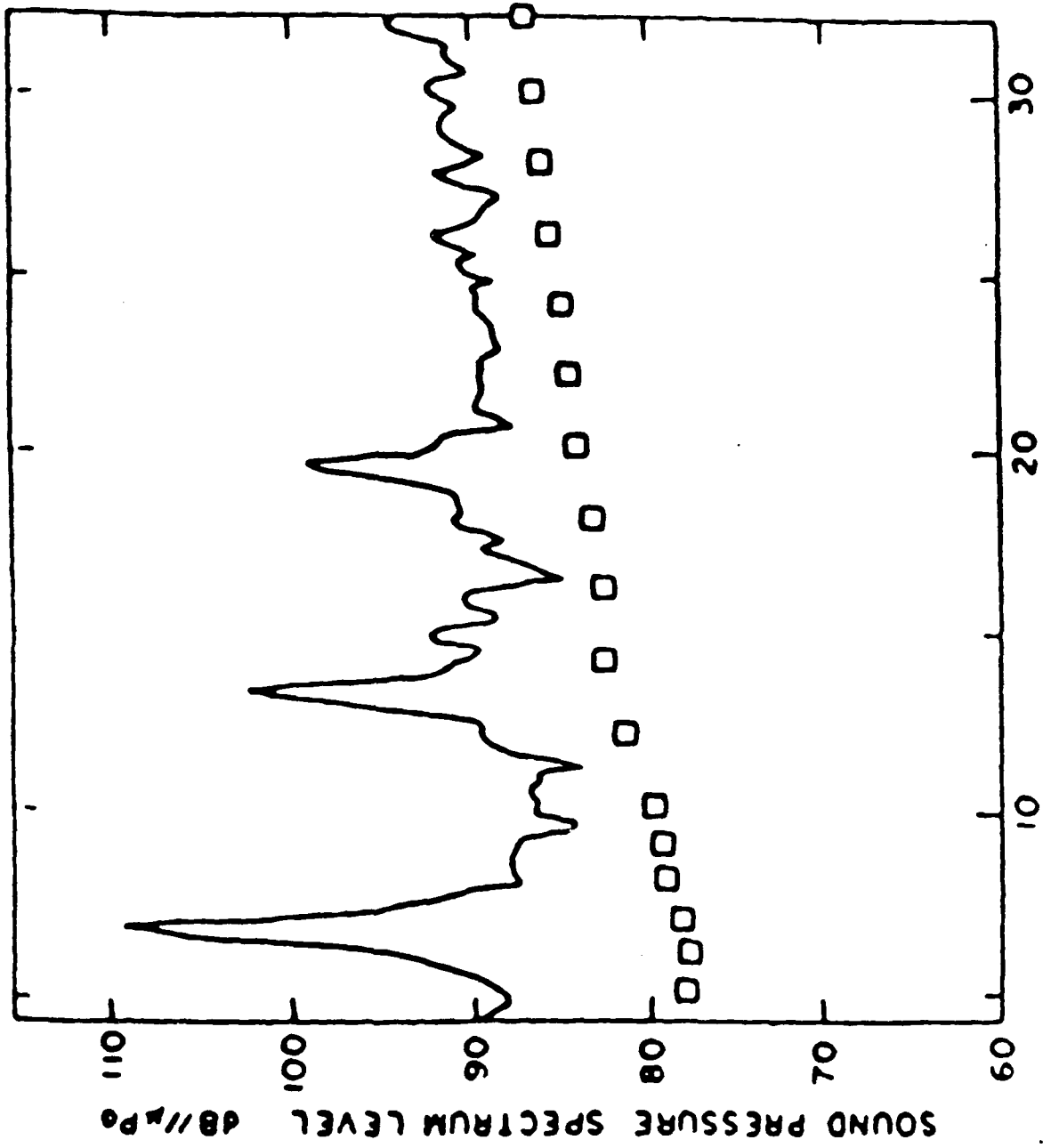


### VLF Shipping Noise

This slide shows noise measurements made by McGrath in 1976 at a near-bottom hydrophone at a location near the Mid Atlantic ridge off the Azores. The lower data are the background noise level. The upper curve is a measured ship noise spectrum. The ship has significant acoustic energy output down to at least 5 Hz. The tonal nature of the spectrum is clearly evident.

# VLF SHIPPING NOISE

McGrath (1976)







**AMBIENT**

**NOISE**

**PHYSICS**

### Vertical Structure for Noise due to Ships and Wind/Sea-State Disturbance, Nearby and Distant

In the frequency range 10-100 Hz, the primary sources of ambient noise in non-Arctic waters are ships and wind/sea-state disturbance. Shipping noise is dominant in most circumstances.

Shipping noise or wind noise arriving at a sensor can originate either nearby that sensor or at distances greatly removed from that sensor.

The noise generated by nearby surface wind/sea-state disturbance arrives at a sensor from paths with vertical arrival angles that are well off the horizontal, both vertically up and vertically down. This component of noise is approximately constant in azimuth and continuously distributed in the vertical dimension with the possible exception of a noise notch near horizontal.

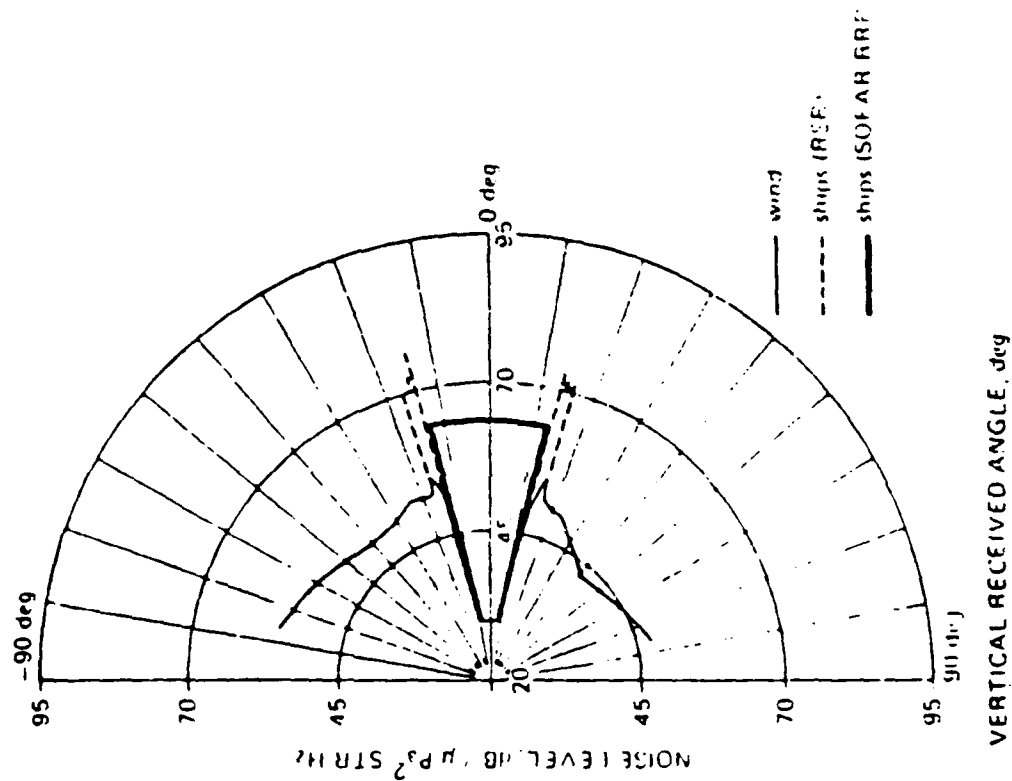
Locally generated surface ship noise will also arrive at angles well off the horizontal. Its azimuthal distribution depends upon ship locations.

Noise generated by distant ships and distant wind/sea-state disturbance travels from distant regions by way of different ray paths. This noise is responsible for filling the noise notch in a vertical directionality measurement at a depth near the sound channel axis.

This slide shows the vertical arrival structure for the various components of low frequency ambient noise. The narrow solid curve corresponds to the noise due to nearby wind/sea-state disturbance. The component below the horizontal is lower in level than the corresponding component above the horizontal because the upward travelling rays have larger path lengths from the nearby surface than the others and at the more vertical down angles the noise experiences bottom losses before arriving at the sensor location. The dashed curve corresponds to shipping noise that arrives via RSR ray paths. This noise is concentrated between the Sofar channel limiting ray angles and the angles for bottom interaction. The solid curve near the horizontal corresponds to distant shipping and distant wind/sea-state disturbance noise that travels via RR paths and experiences cylindrical spreading. It is quite likely that this component of noise will not be a constant level as a function of vertical angle as illustrated in this slide. In fact, measurements by Hodgkiss and Fisher indicate that there is evidence of arrival structure due to individual ships in this angular region.



# VERTICAL STRUCTURE FOR NOISE DUE TO SHIPS AND WIND/SEA-STATE DISTURBANCE, NEARBY AND DISTANT



Ambient Noise Vertical Directionality  
Axelrod et al (1965)

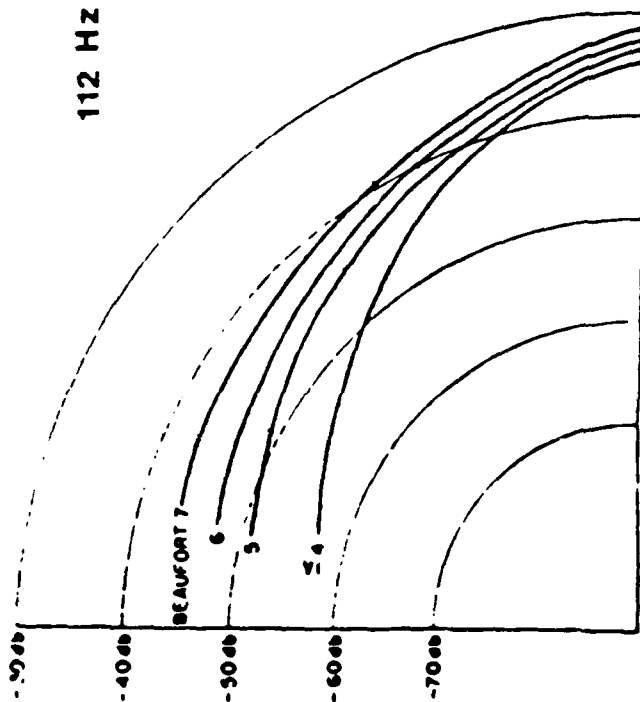
This slide shows measurements of ambient noise vertical directionality made in 2400 fathoms of water off Bermuda from a 300 foot array mounted 110 feet off the bottom. As sea state increases the intensity of noise arriving at high angles also increases. At 891 Hz much less noise arrives at angles near the horizontal than does at 112 Hz.



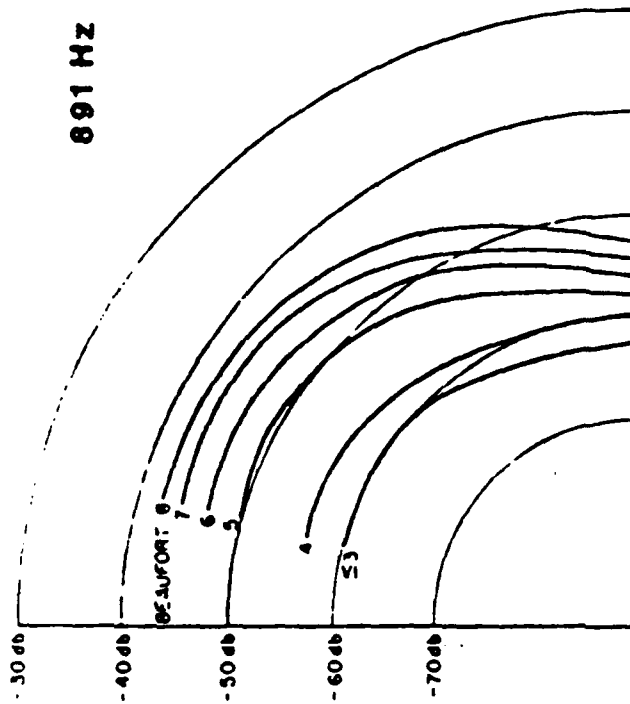
# AMBIENT NOISE VERTICAL DIRECTONALITY

(E.H. Axelrod, et al., JASA Vol. 37, 1965)

LOW FREQUENCY (<300 Hz)  
SHIPPING DOMINATED



HIGH FREQUENCY (>500 Hz)  
WIND DOMINATED



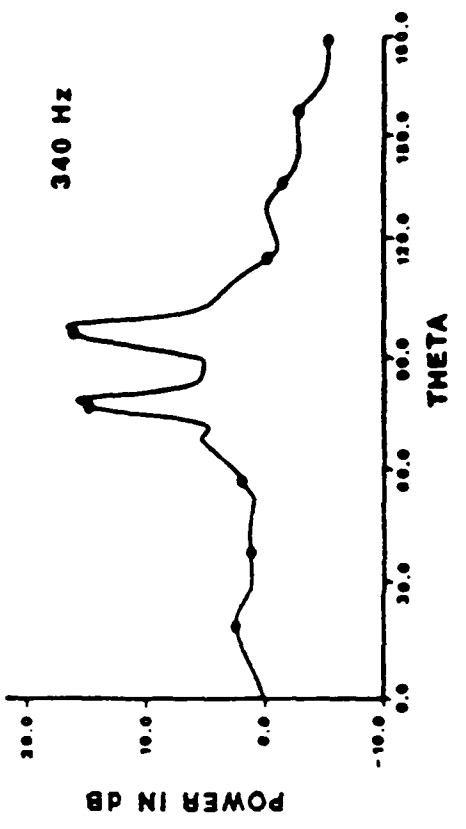
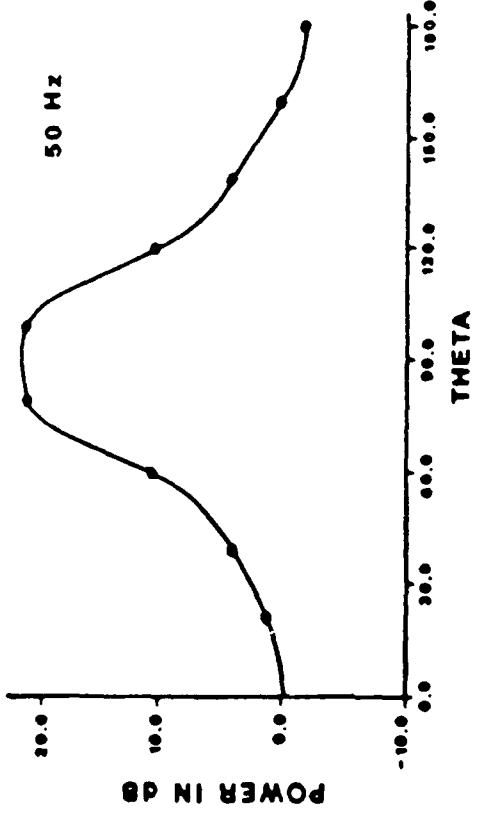
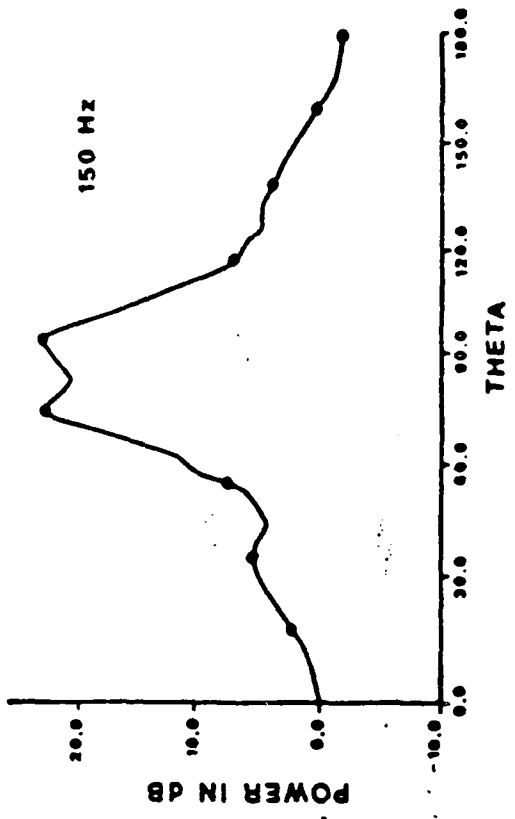
SPECTRUM LEVEL IN dB//  $\mu\text{Pa}^2$  / STERADIAN / CYCLE PER SECOND

### Variation of Ambient Noise Vertical Directionality with Frequency

This slide shows data collected by Anderson (1972). These data were measured south of Bermuda with a vertical array of 26 hydrophones spaced over 110 m. This corresponds to 1/2 wavelength spacing at 170 Hz. The array center was at a depth of 236 m in the deep sound channel. The deep sound channel axis was at a depth of 110 m.

The peaks at 340, 150, and 50 Hz at  $90^\circ \pm 9.5^\circ$  correspond to the limiting RSR arrival angle. There is pronounced filling of the vertical noise notch at 50 and 150 Hz. This is not the case at 340 Hz. The filling of the noise notch at lower frequencies indicates that significant portion of the received noise energy is not locally generated.

# VARIATION OF AMBIENT NOISE VERTICAL DIRECTIONALITY WITH FREQUENCY

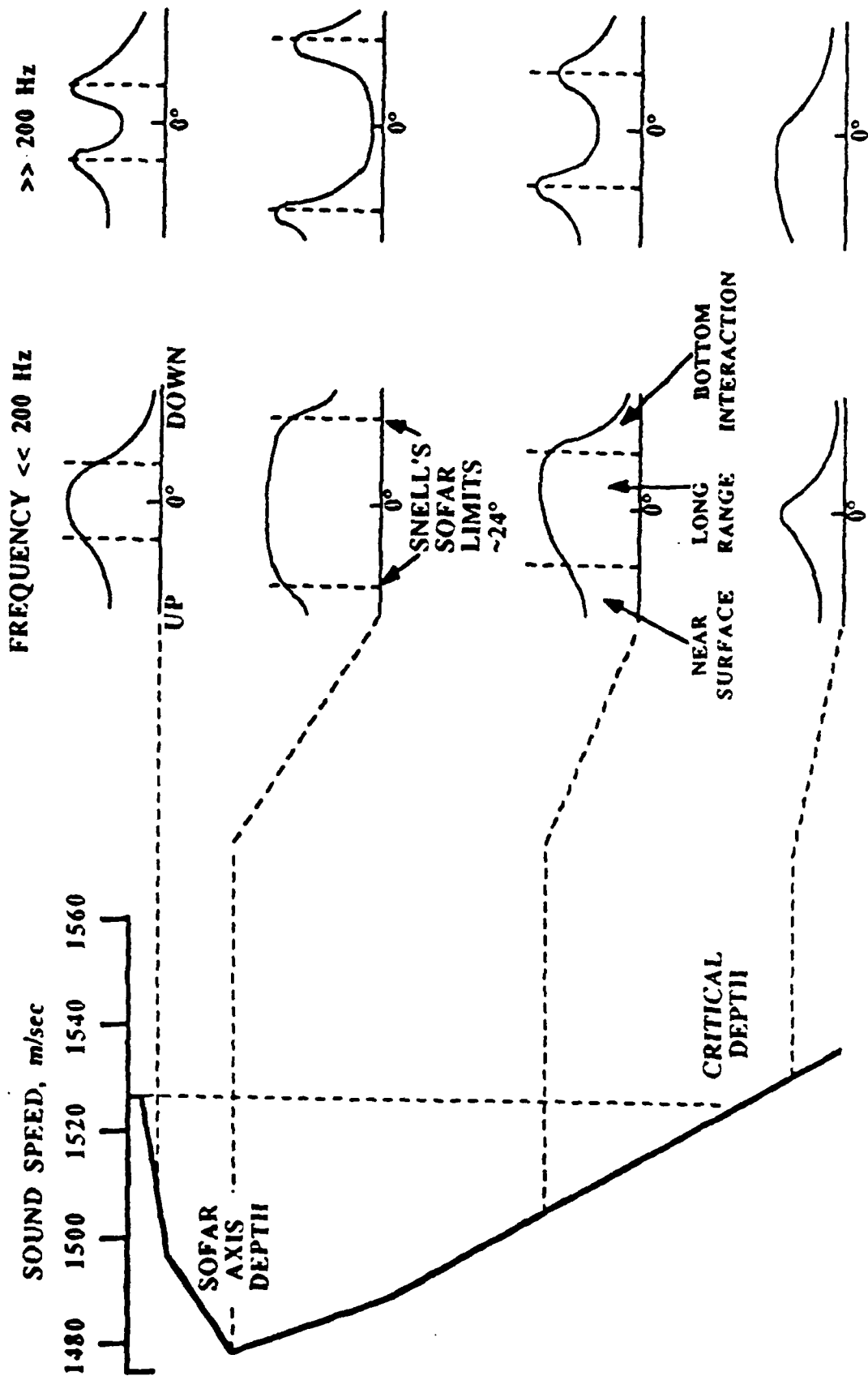


### Noise Vertical Structure vs Frequency/Depth

This slide shows how the vertical directionality of low frequency ambient noise might vary with depth and frequency at a typical deep water site. At frequencies above 200 Hz the Sofar channel component of noise is greatly reduced by attenuation. Snell's Law can be used to calculate the variation in vertical directionality with changes in receiver depth.



# NOISE VERTICAL STRUCTURE VS FREQ/DEPTH



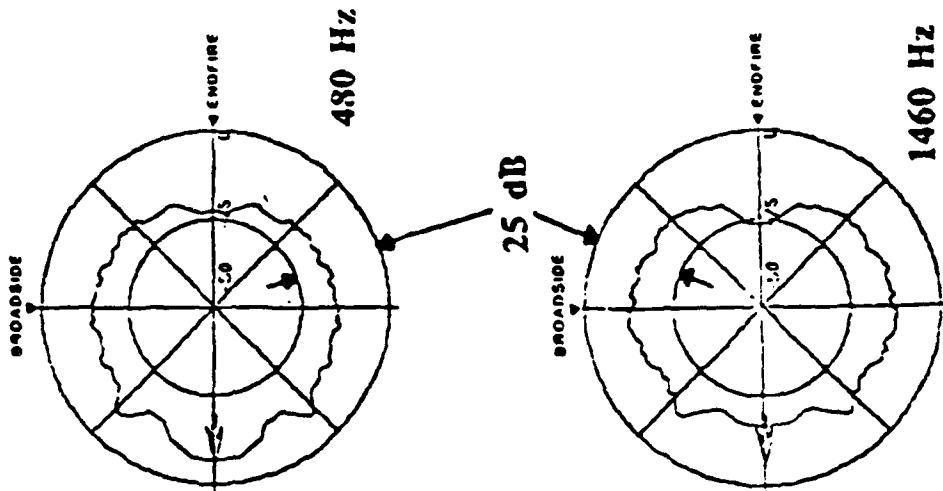
### Measurement of HF Sofar Noise Notch by a Towed Array

The HF Sofar noise notch can be measured with a horizontal towed array as well as a vertical array. The endfire beams of the horizontal array do not receive energy generated locally at the ocean surface. This slide shows the dramatic drop in aft endfire beam noise levels at 1460 Hz versus 480 Hz.

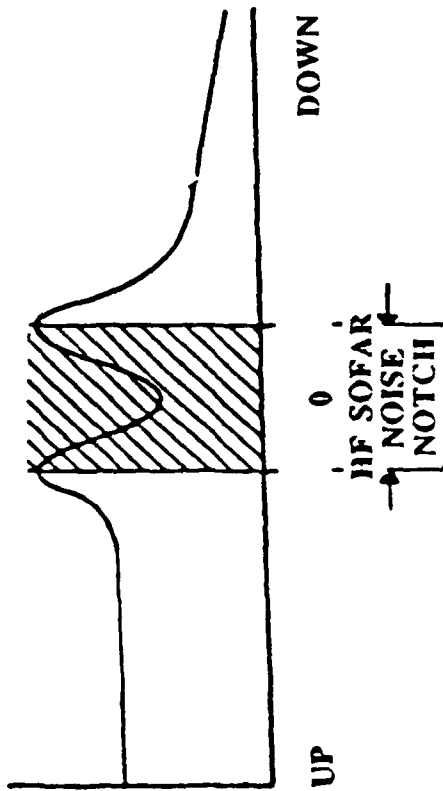


# MEASUREMENT OF HF SOFAR NOISE NOTCH BY A TOWED ARRAY

## HORIZONTAL LINE ARRAY



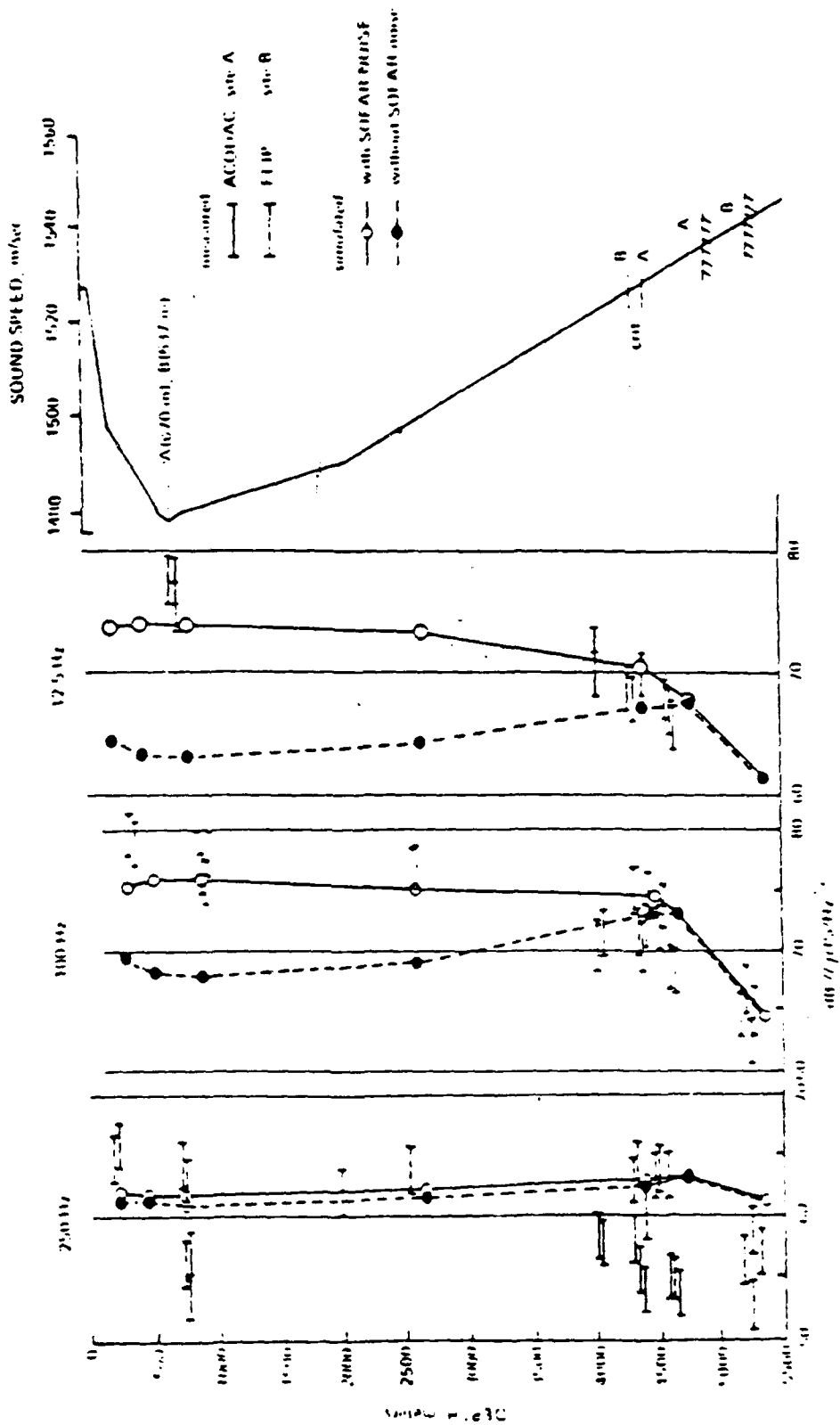
## NOISE VERTICAL STRUCTURE



### Noise Field Depth Dependence

In many locations, the Sofar channel component of noise is by far the dominant noise component. From the standpoint of modeling, if the Sofar noise component at these locations is not properly accounted for, then key features in the noise field, in particular depth dependence, will be incorrectly predicted. This slide shows calculations of the noise depth dependence at a Northeast Pacific Ocean site, both with and without the Sofar component. When the Sofar component is included, model predictions compare favorably with data.

# NOISE FIELD DEPTH DEPENDENCE

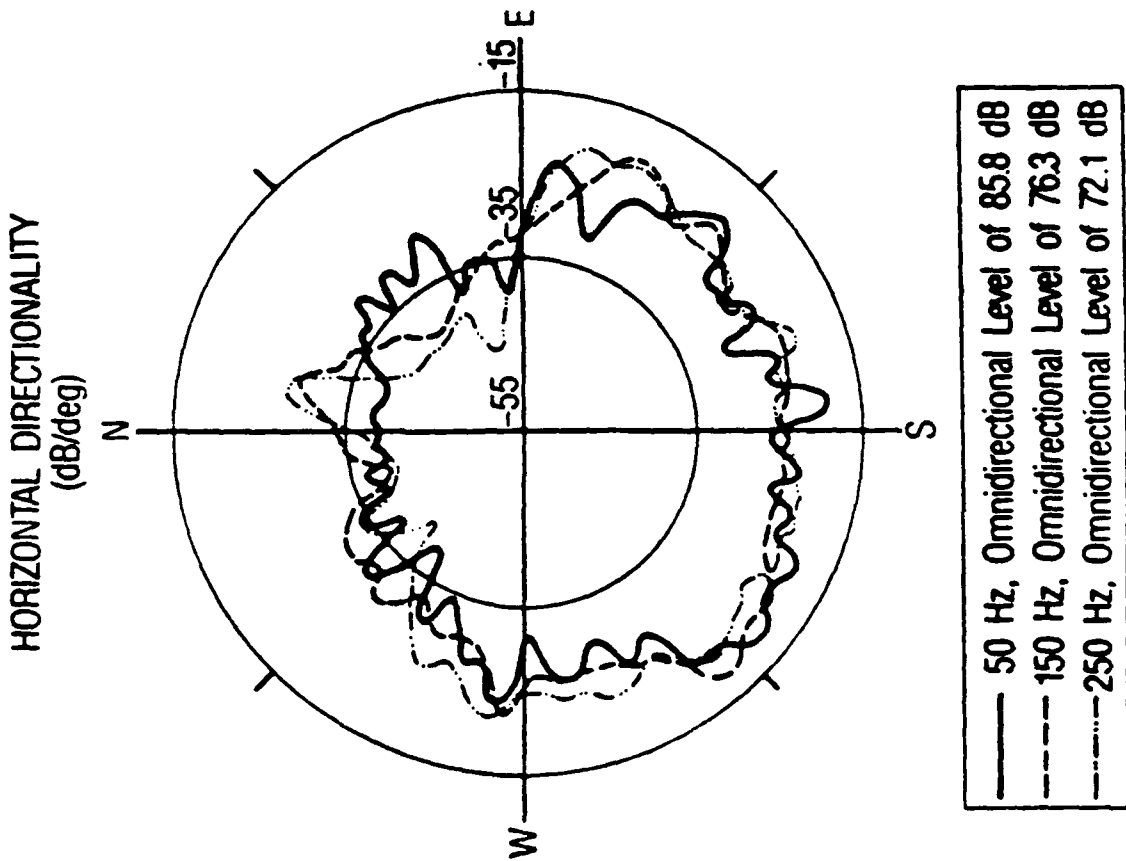


### Shipping Noise Horizontal Directionality Frequency Dependence

This slide shows horizontal directionality measurements at a Northwest Pacific Ocean site at 50, 150 and 250 Hz. At each frequency, the directionality is approximately the same - indicating that at this location shipping noise was dominant up to 250 Hz.



# SHIPPING NOISE HORIZONTAL DIRECTIONALITY FREQUENCY DEPENDENCE







# AMBIENT NOISE PROPAGATION MECHANISMS

### Sound Channel Noise Coupling Mechanisms

Distant noise generated by near surface sources can couple into the deep sound channel by at least two mechanisms:

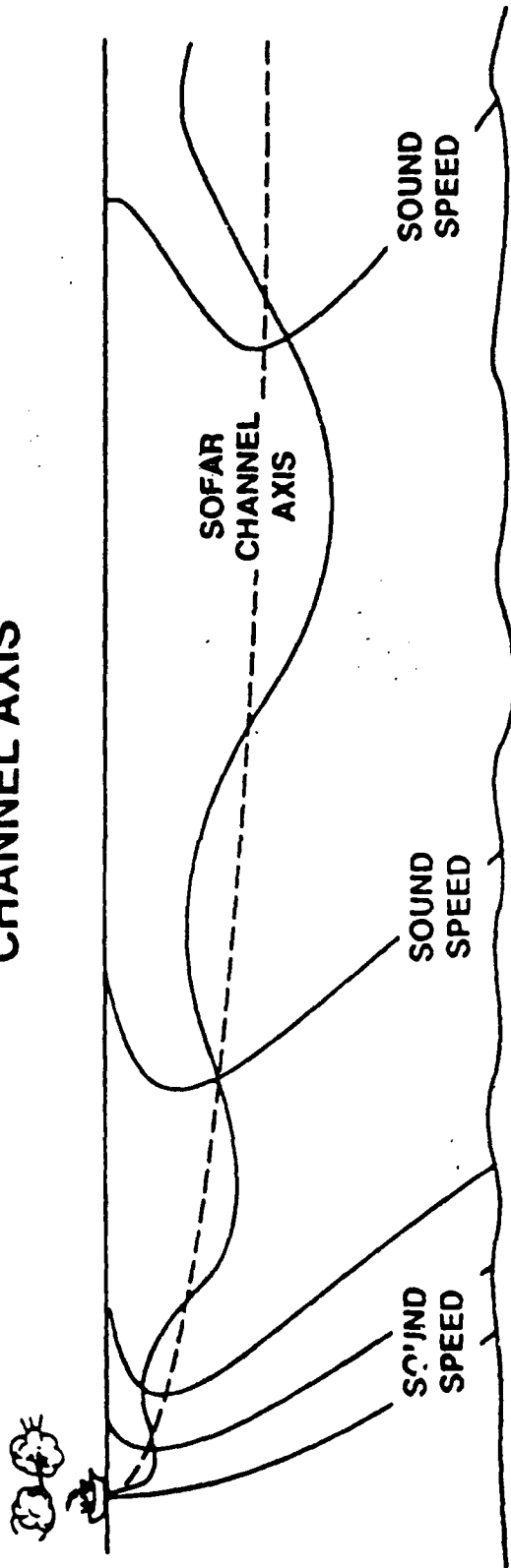
1. High latitude shoaling of the sound channel axis.
2. Down slope conversion.

This slide illustrates the first case. At high latitudes, ocean waters are colder and the deep sound channel axis is at shallower depths. Sound propagating to the south bends towards the minimum sound velocity and as a result of the keeping of the sound channel axis to the south, this sound is concentrated at deeper depths and shallower arrival angles than locally generated sound would be.



# SOUND CHANNEL NOISE COUPLING MECHANISMS

## HIGH LATITUDE SHOALING OF SOUND CHANNEL AXIS

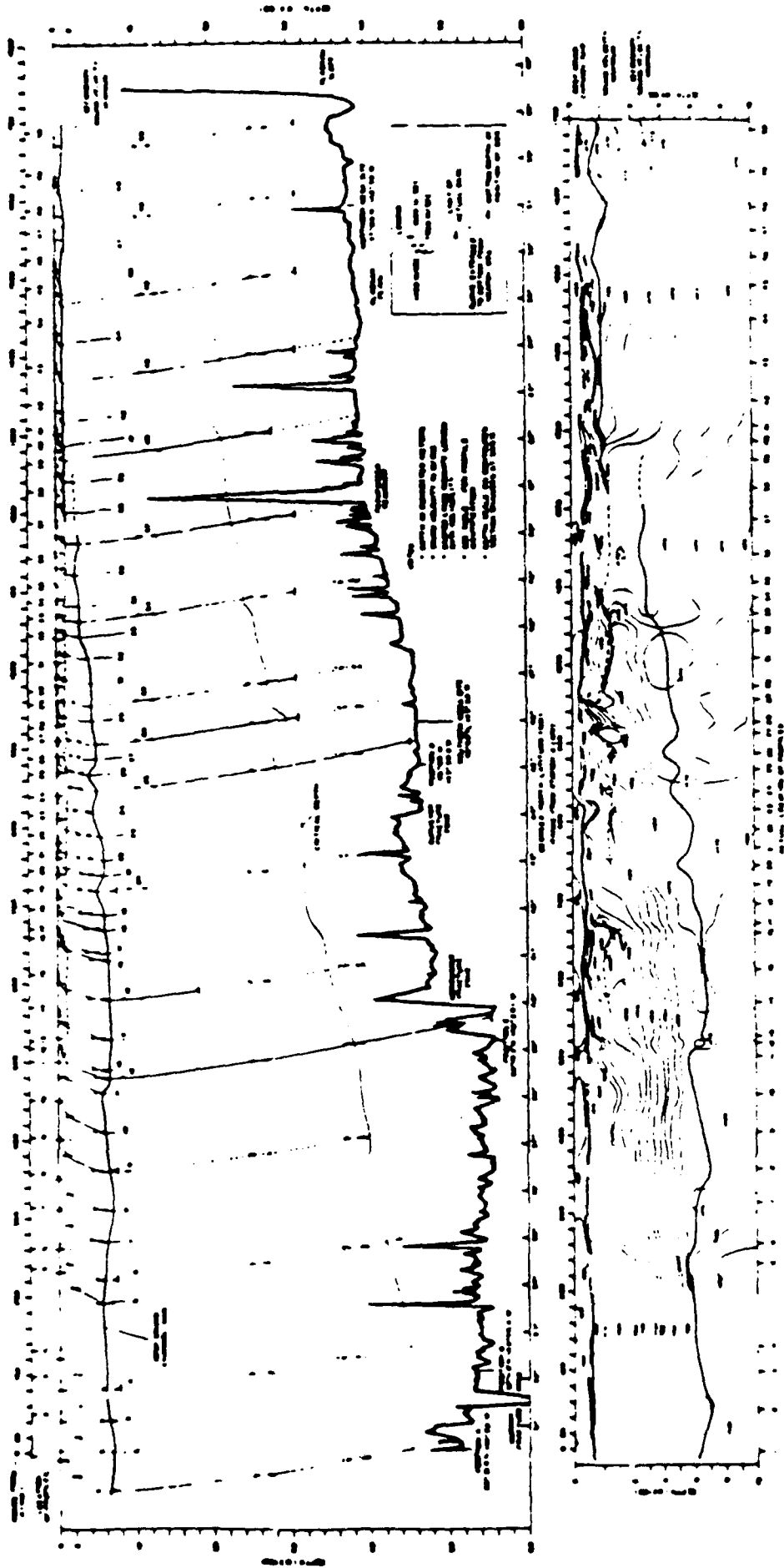


Sound Speed Structure in the CHURCH ANCHOR Exercise Area

This slide shows an environmental cross section based upon data taken during the CHURCH ANCHOR exercise. The shoaling of the deep sound channel axis is evident.



# SOUND-SPEED STRUCTURE IN THE CHURCH ANCHOR EXERCISE AREA



### Wind Noise Generation Areas

This slide displays a map of the world showing Bannister's high latitude noise lanes. The southern wind noise lanes show a seasonal dependence in geographic extent due to changes in pack ice location. The right hand side of the slide shows the variation of wind speed with latitude.

Bannister defined wind noise lanes at high latitudes within which the noise from sources at the surface could become coupled into the Sofar channel and travel throughout the oceans with relatively low loss. He hypothesized that because of the vast areas over which the coupling could take place and also because those were the areas of highest and longest duration of wind and sea states, the resulting component of noise could be equal to the low-frequency omnidirectional ambient noise levels that have been measured at various locations of wide geographic distribution. This component of noise is confined to the Sofar channel, arrives within the angular limits of the Sofar channel limiting ray angles, and can only be measured by sensors located in the Sofar channel.

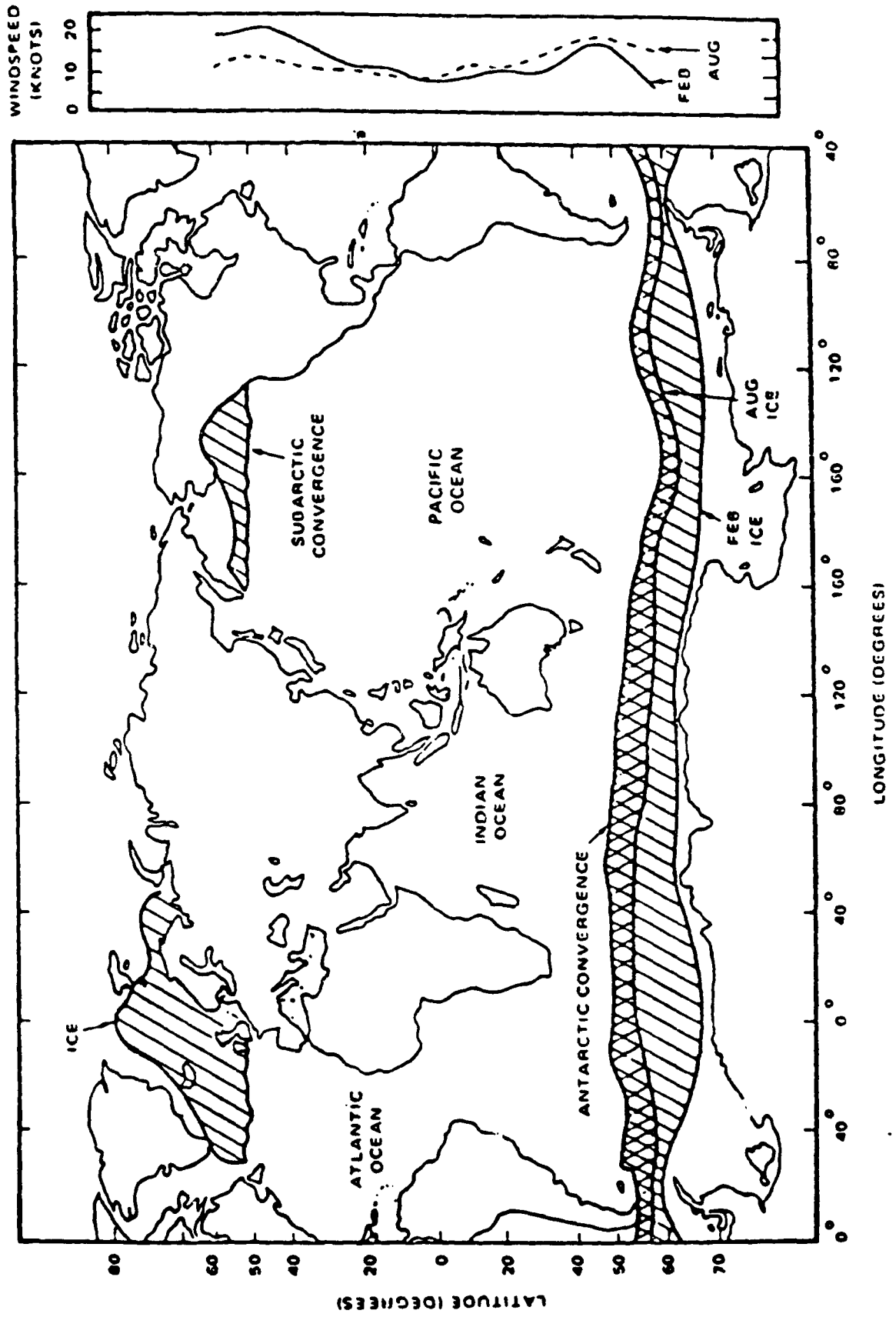
This noise is due to wind/sea-state disturbance and consequently does not possess discrete frequency lines similar to shipping noise.

It could well form the limiting background against which a high gain system would need to operate.



# WIND NOISE GENERATION AREAS

(R. W. Bannister, JASA Vol. 79, 1986)



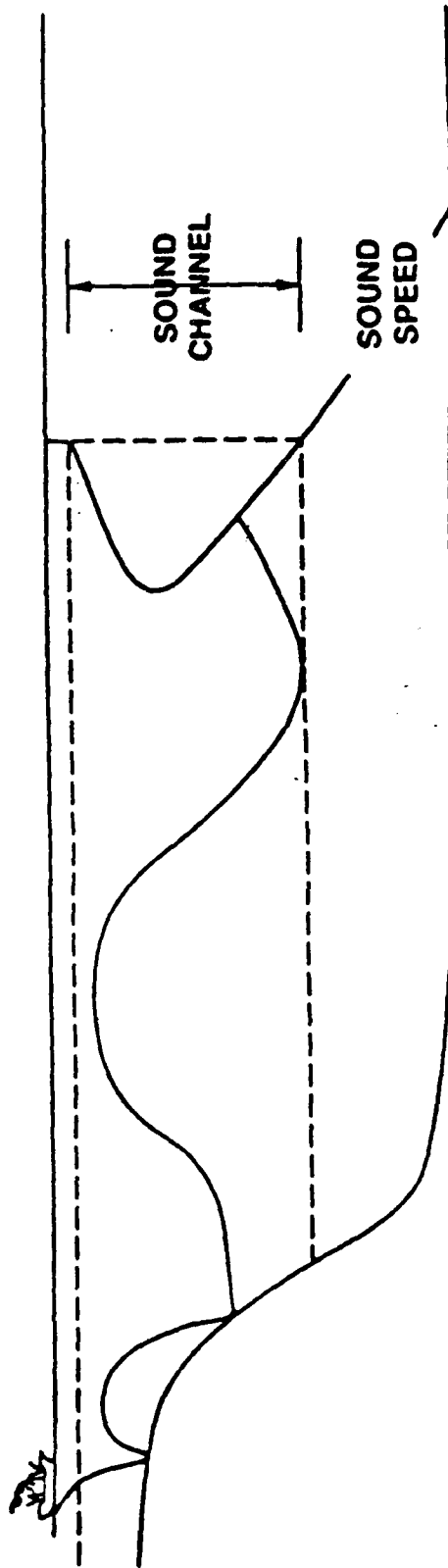
### Sound Channel Noise Coupling Mechanisms

The second mechanism is illustrated in this figure. Each reflection of sound bends the ray path towards the horizontal by twice the slope angle. Generally not many reflections are required to bend the ray path toward the horizontal sufficiently to avoid additional bottom interactions. Once the boundary losses are eliminated cylindrical spreading begins and the associated spreading losses are low. Noise generated along basin boundaries and seamounts can experience this favorable type of propagation.



# SOUND CHANNEL NOISE COUPLING MECHANISMS

## DOWN SLOPE CONVERSION

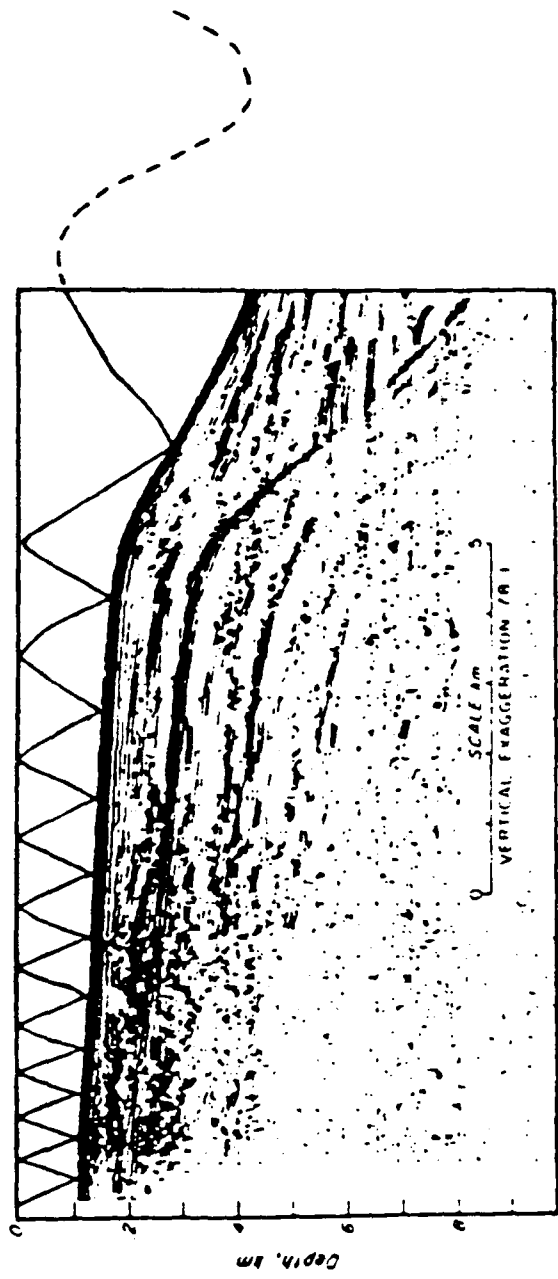


Downslope Enhancement, Northrop (1968)

This slide shows a ray trace taken from Northrop (1968) based upon bathymetry in the Point Arena area. Steep rays are converted into shallow rays. At each bottom bounce on a slope, the ray angle with respect to the horizontal is increased by twice the slope angle.

# DOWNSLOPE ENHANCEMENT

Northrop (1968)



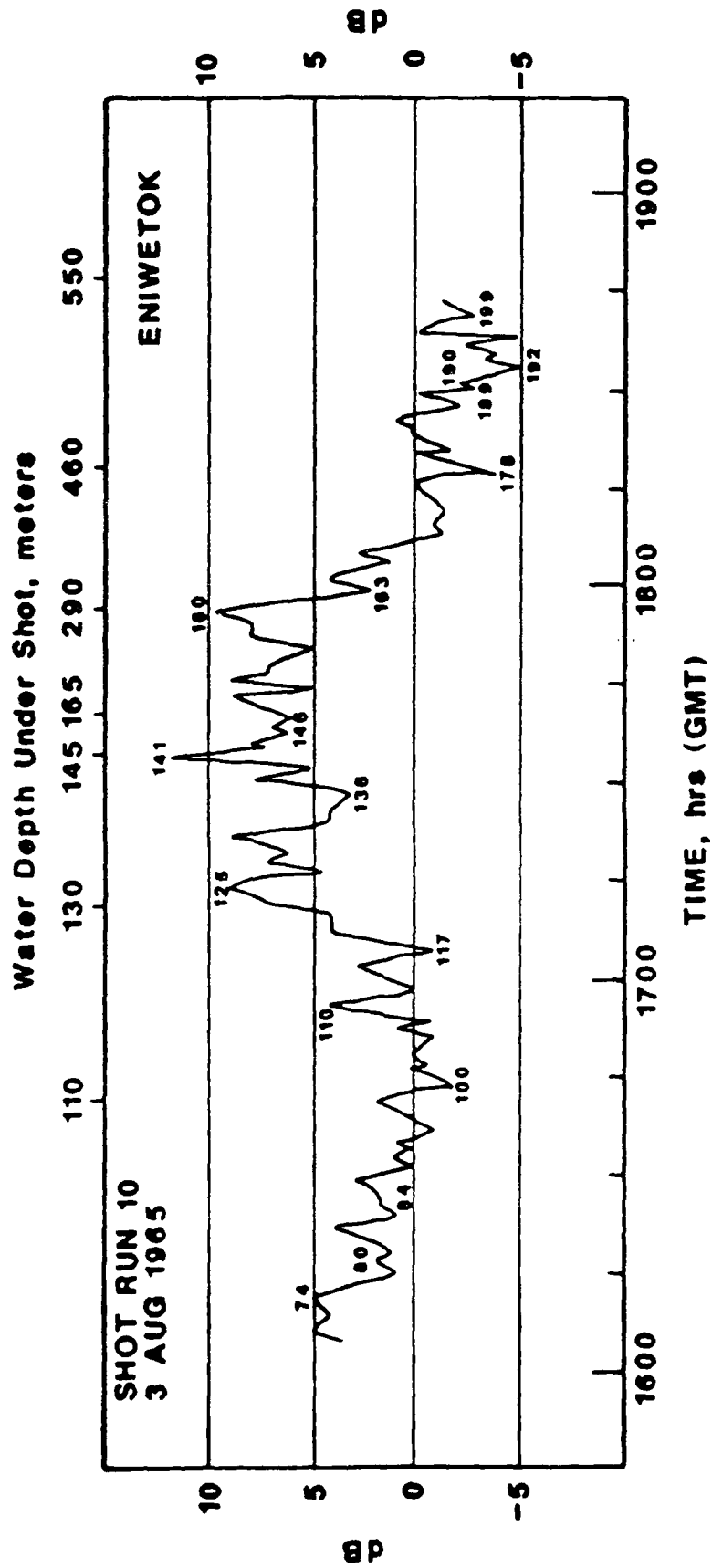
Downslope Enhancement, Northrop, et al (1968)

This slide shows transmission loss data from Northrop (1968). Shots were dropped off Point Arena, California over the continental shelf and slope. The hydrophone receiver was located at Eniwetok. The best transmission occurred for shots dropped in waters with depths in the 120-160 m range. These locations were just over the edge of the continental slope.



# DOWNSLOPE ENHANCEMENT

Northrop et al (1968)

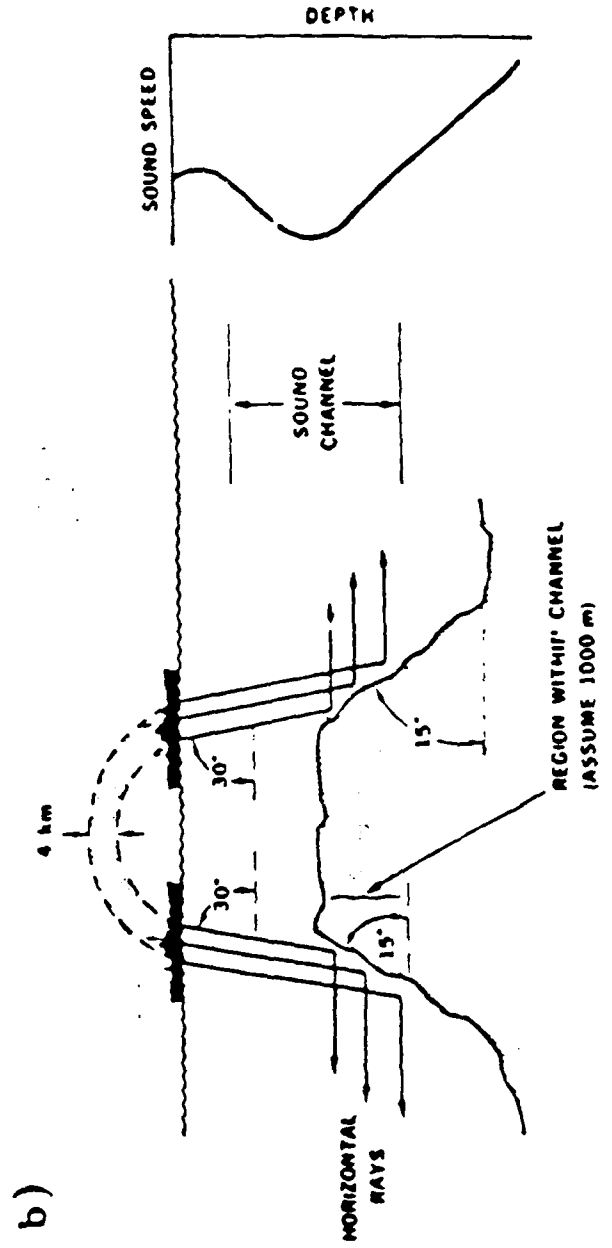
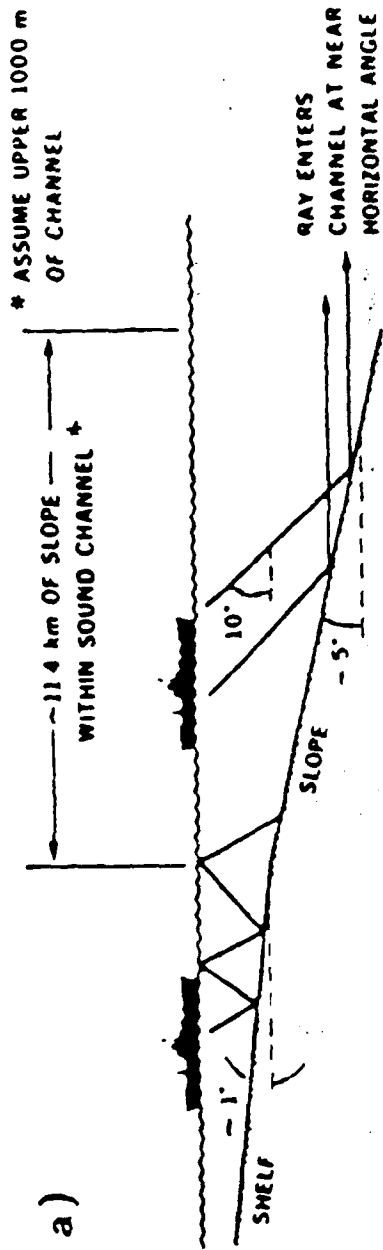


Conversion of High Angle Ray Paths to Near by Horizontal Ray Paths  
by Reflection off a Sloping Bottom

Coupling into the deep sound channel via downslope slope enhancement can also occur over  
seamounts.



# CONVERSION OF HIGH-ANGLE RAY PATHS TO NEARBY HORIZONTAL RAY PATHS BY REFLECTION OFF A SLOPING BOTTOM



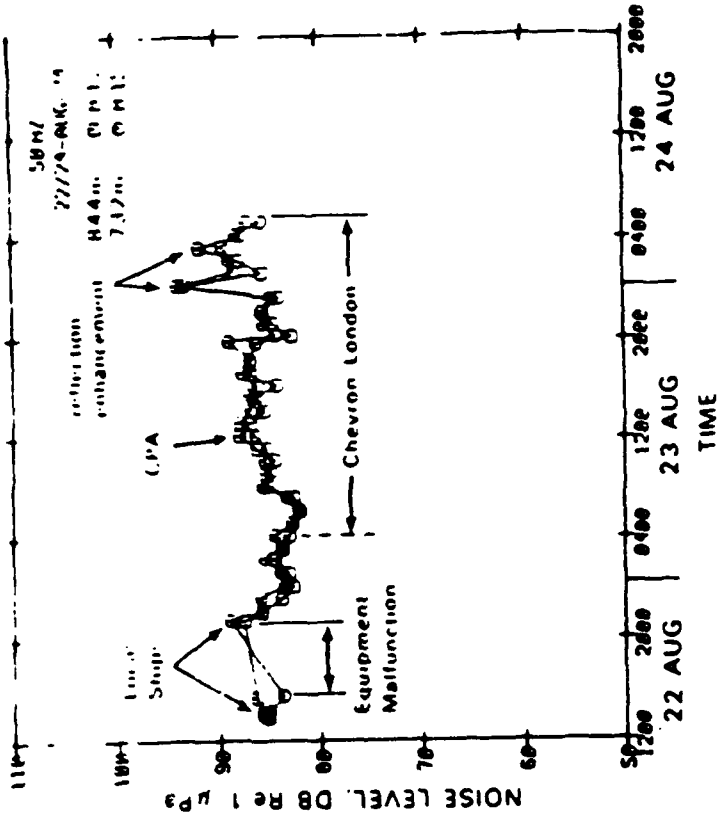
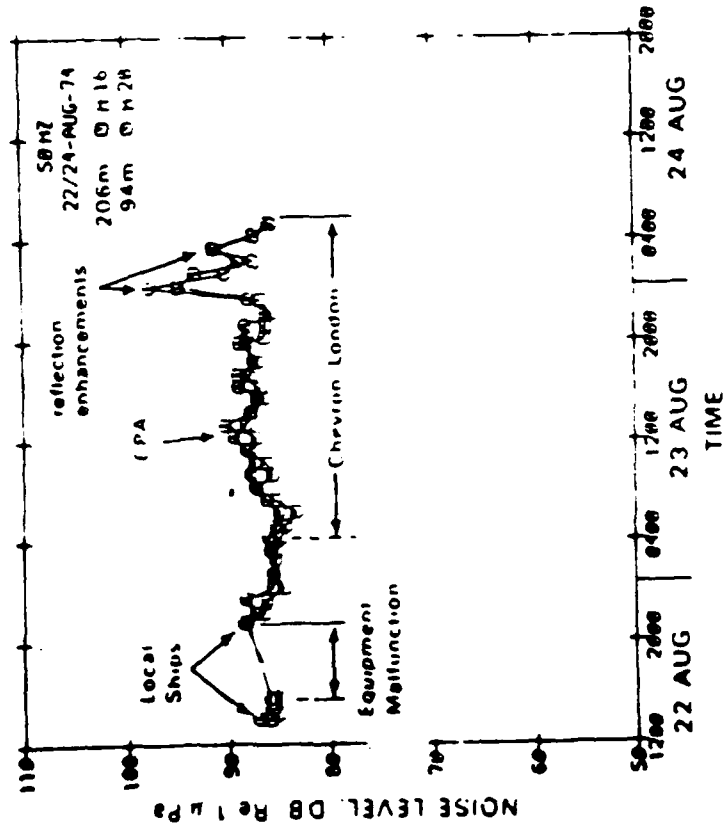
Downslope Enhancement, Morris (1978)

This slide shows transmission loss data from Morris (1978). The source was a ship of opportunity, the Chevron London. The receiver was flip. The best transmission occurred when the ship passed a seamount and later, when the ship approached the continental slope.



# DOWNSLOPE ENHANCEMENT

Morris (1978)

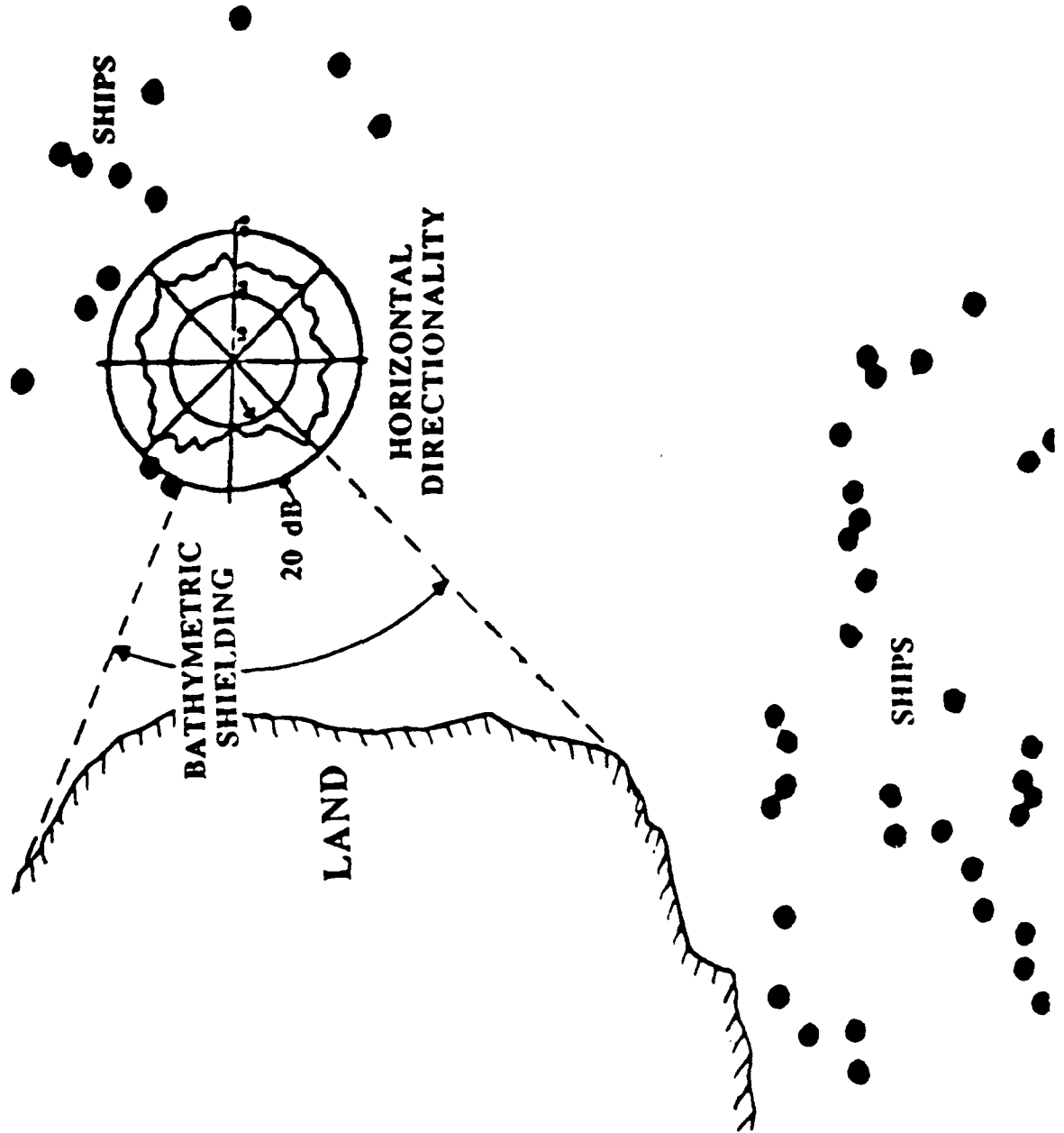


### Bathymetric Effects

Bathymetric effects can have a significant impact on noise horizontal directionality. This slide shows how bathymetric shielding can have a nearly 20 dB effect on noise horizontal directionality at a Mediterranean site.



# BATHYMETRIC EFFECTS



### Measured Ambient Noise System Dependence

The observed properties of the ambient noise field depend upon the system used to make the measurement. In order to make measurements of the fine structure of the noise field, high resolution systems with low side-lobe levels must be used. Bandwidths and averaging times must be carefully selected with regard to the application in mind.



# MEASURED AMBIENT NOISE SYSTEM DEPENDENCE

- OMNIDIRECTIONAL SYSTEM
- DIRECTIONAL SYSTEM
  - VERTICAL
  - HORIZONTAL
  - OTHER
- AVERAGING TIME/BANDWIDTH
  - NARROWBAND
  - BROADBAND

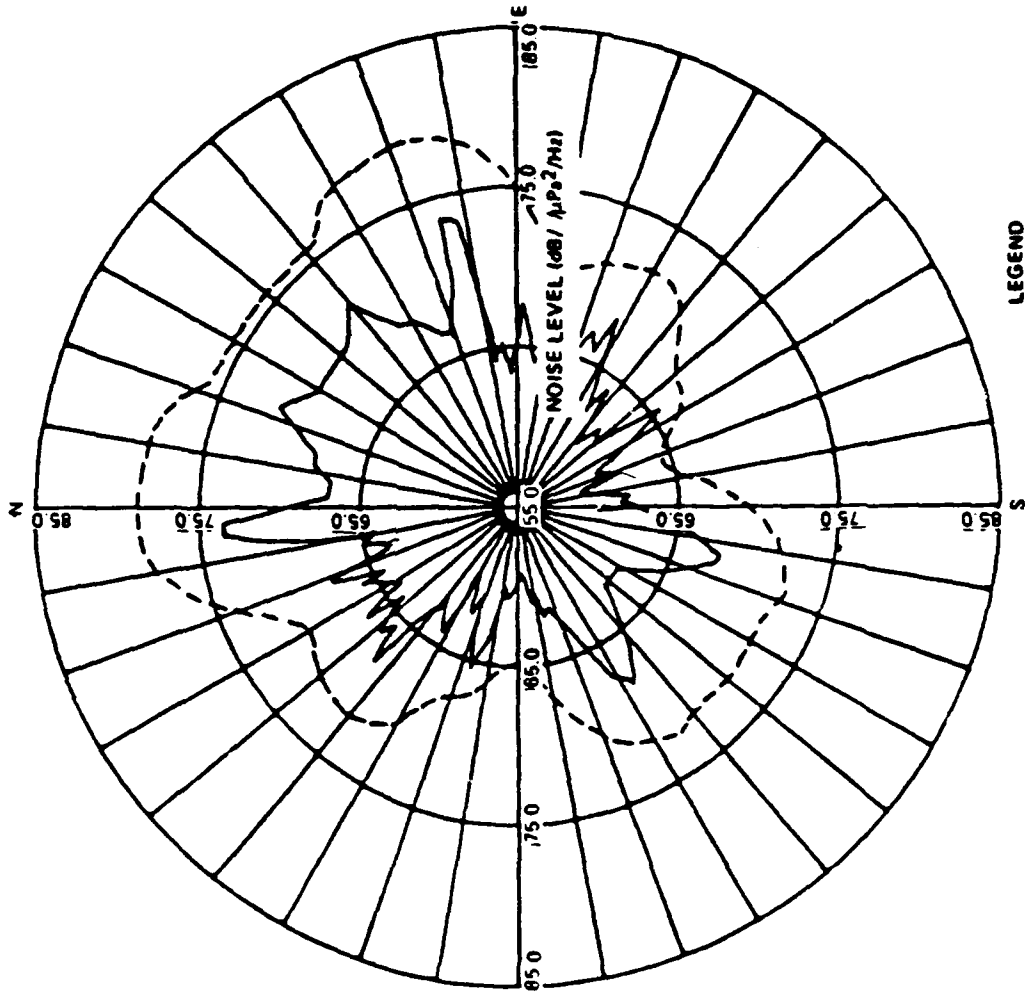
### Array Aperture Effects on Measurement of Noise Field Properties

This slide shows measured beam noise levels at 50 Hz with mid-frequency and high frequency sub-arrays of a towed array. The mid-frequency subarray has a length of about 800 m. The high-frequency subarray has a length of 300 m. As expected the wider beams of the high-frequency subarray produce higher beam noise levels. An additional feature of the data is that the fine scale noise directionality cannot be observed with the low resolution system.

# ARRAY APERTURE EFFECTS ON MEASUREMENT OF NOISE FIELD PROPERTIES



BEAM RESPONSE DATA



LEGEND

- MID-FREQUENCY SUB-ARRAY, 60 Hz
- - - HIGH-FREQUENCY SUB-ARRAY, 60 Hz

Pacific Ocean Shipping HITS Shipping Database, Fall Case

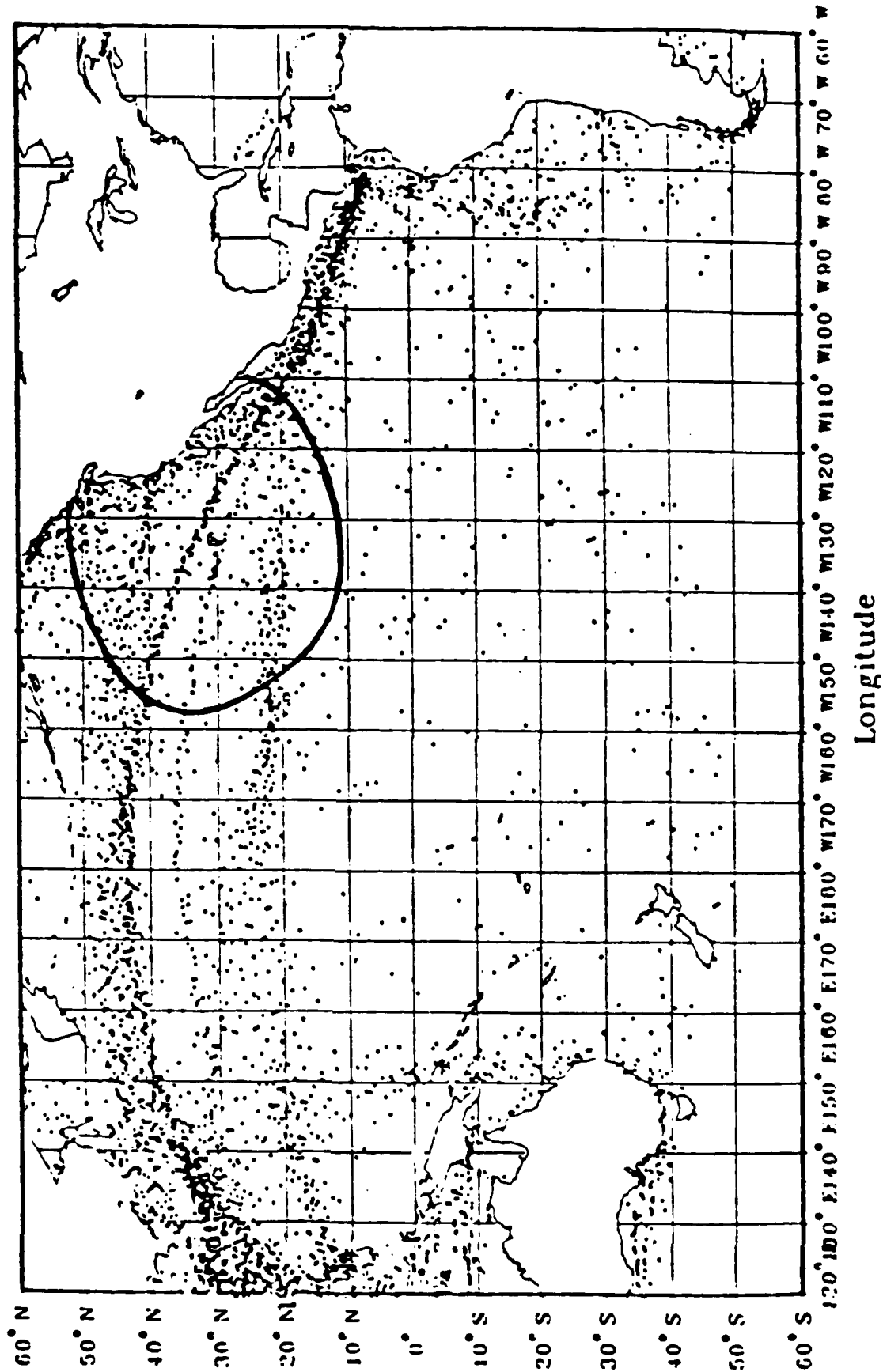
This slide shows a representative set of discrete shipping locations based upon the HITS shipping distribution. The circle encompasses the nearest 700 ships about the receiver location.



# PACIFIC OCEAN SHIPPING

## HITS SHIPPING DATABASE

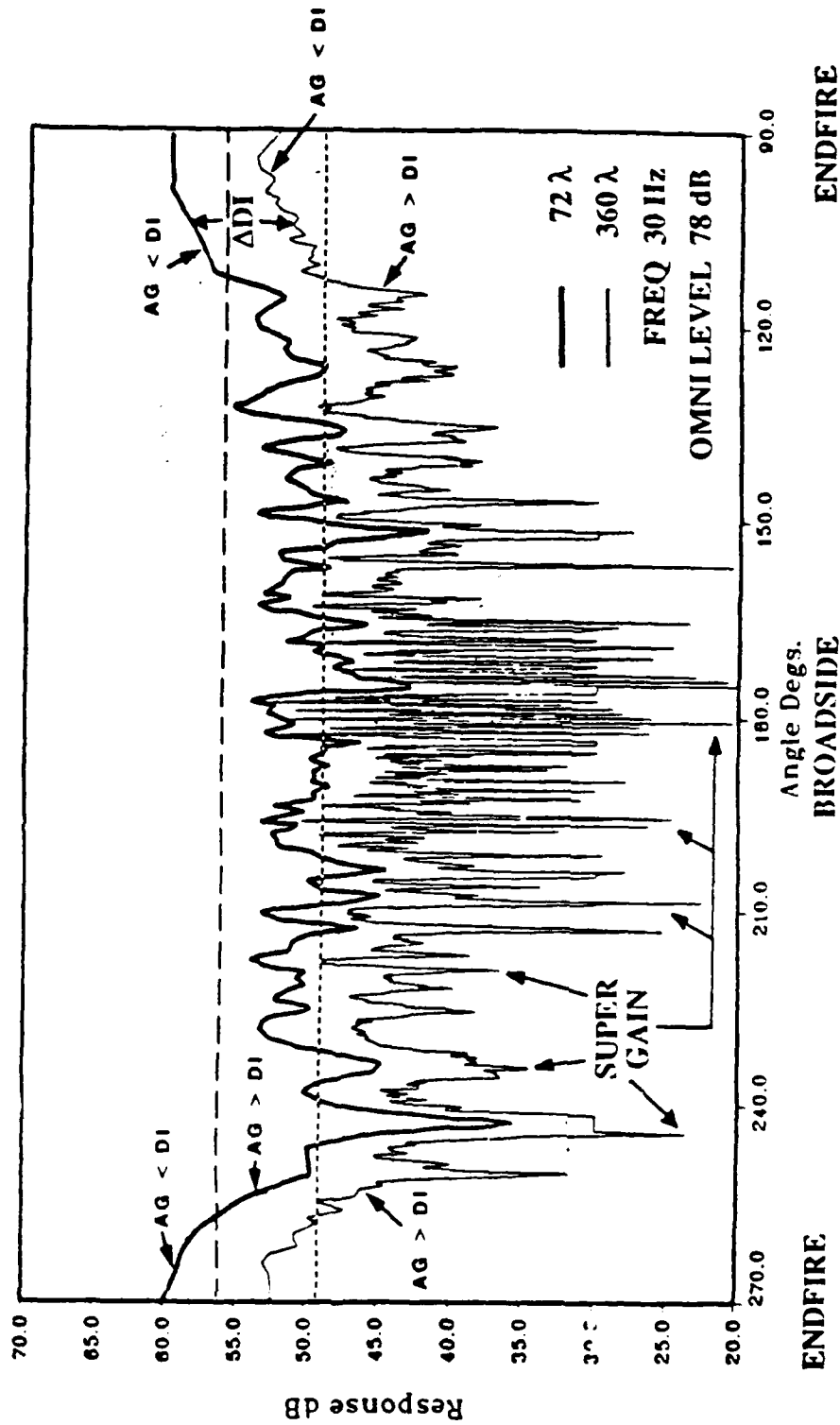
### FALL CASE



Line Array Beam Noise: Nearest 700 Ships

Using the ships locations shown in the previous slide, model predictions of beam noise were made for a  $72 \lambda$  array and a  $360 \lambda$  array. The frequency is 30 Hz. No wind noise is included. The  $360 \lambda$  array clearly has the capacity to see between ships, indicating the possibility of super gain. The degree of super gain possible will depend, from an environmental standpoint, on the underlying background level not attributable to discrete sources.

# LINE ARRAY BEAM NOISE: NEAREST 700 SHIPS



Equivalent Omni Beam Noise  
 - - - - - 72λ Array  
 ······· 360λ Array





# AMBIENT NOISE PERSISTENCE/ REPEATABILITY





**PERSISTENCE OF LOW  
FREQUENCY NOISE  
DIRECTIONALITY**

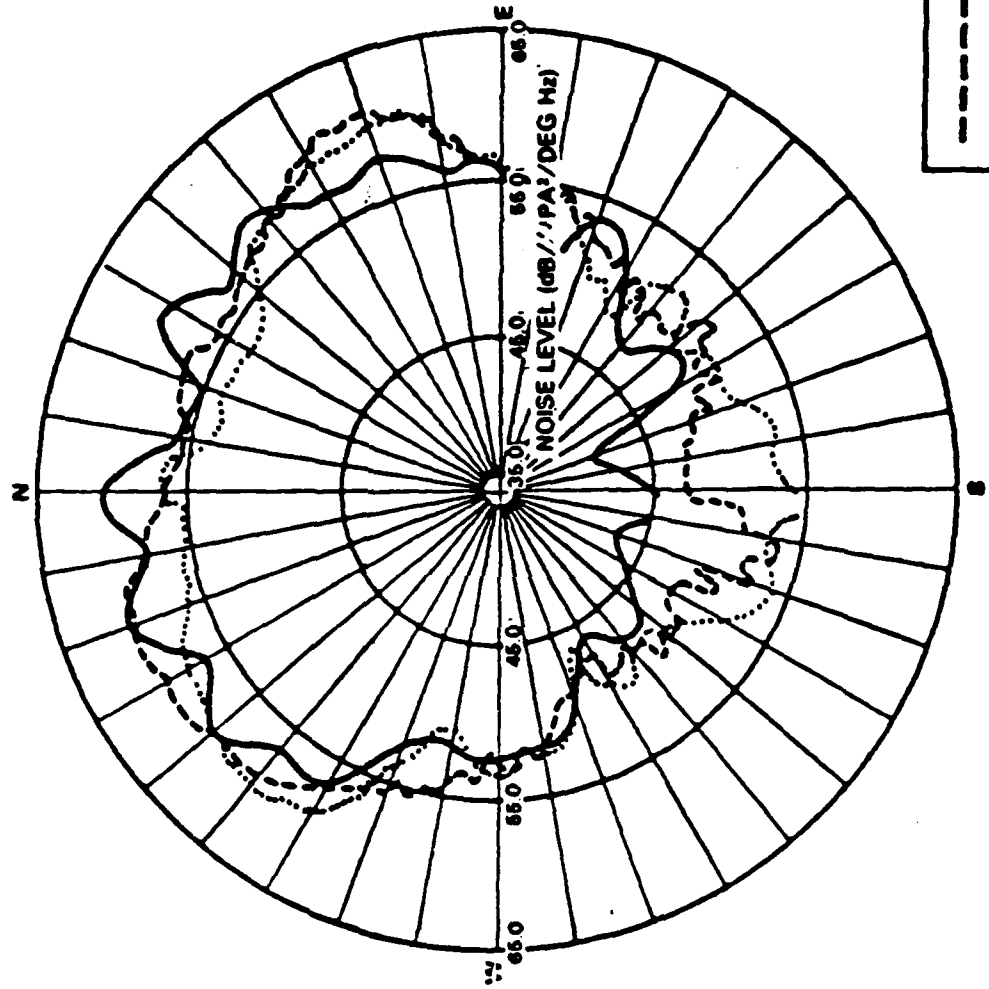
Long Term Persistence of Broadscale Horizontal Directionality at 50 Hz

This slide shows horizontal directionality data taken during exercises conducted in 1973, 1975, and 1979 at approximately the same location. The patterns are quite similar indicating that the low frequency noise directionality repeats over long time periods.



# LONG TERM PERSISTENCE OF BROADSCALE HORIZONTAL DIRECTIONALITY AT 50 HZ

HORIZONTAL DIRECTIONALITY:



- CHURCH ANCHOR
- CHURCH OPAL
- ..... CHURCH STROKE ONE

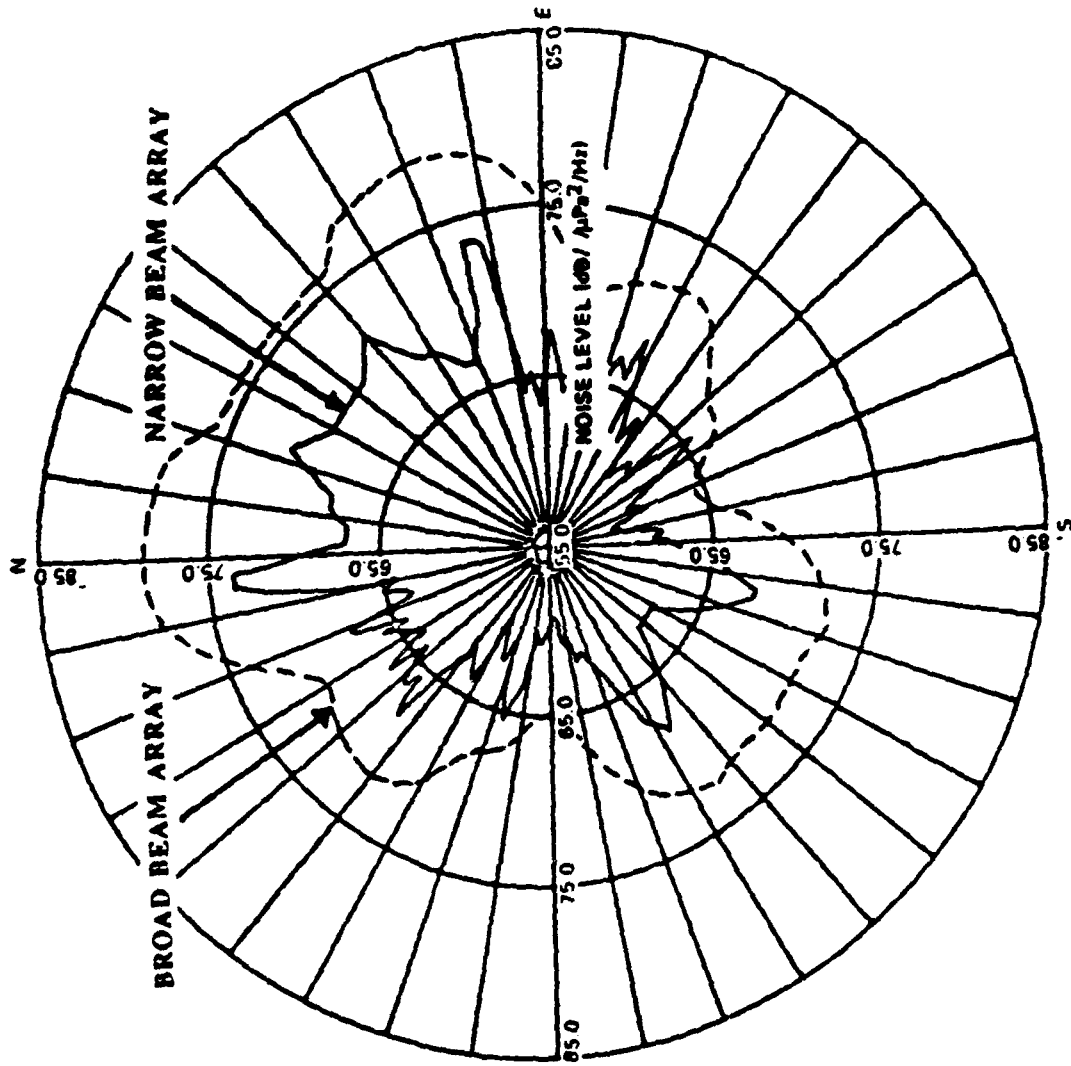
### Measured Broad Beam vs Narrow Beam Statistics

This slide shows the effect of array beamwidth on beam noise. The data were taken using a multiple aperture towed array. The narrow beam aperture begins to resolve some of the fine structure in the noise field. The broad beam array is not sensitive to this fine structure.



# MEASURED BROAD BEAM VS NARROW BEAM STATISTICS

50 Hz BEAM RESPONSE DATA



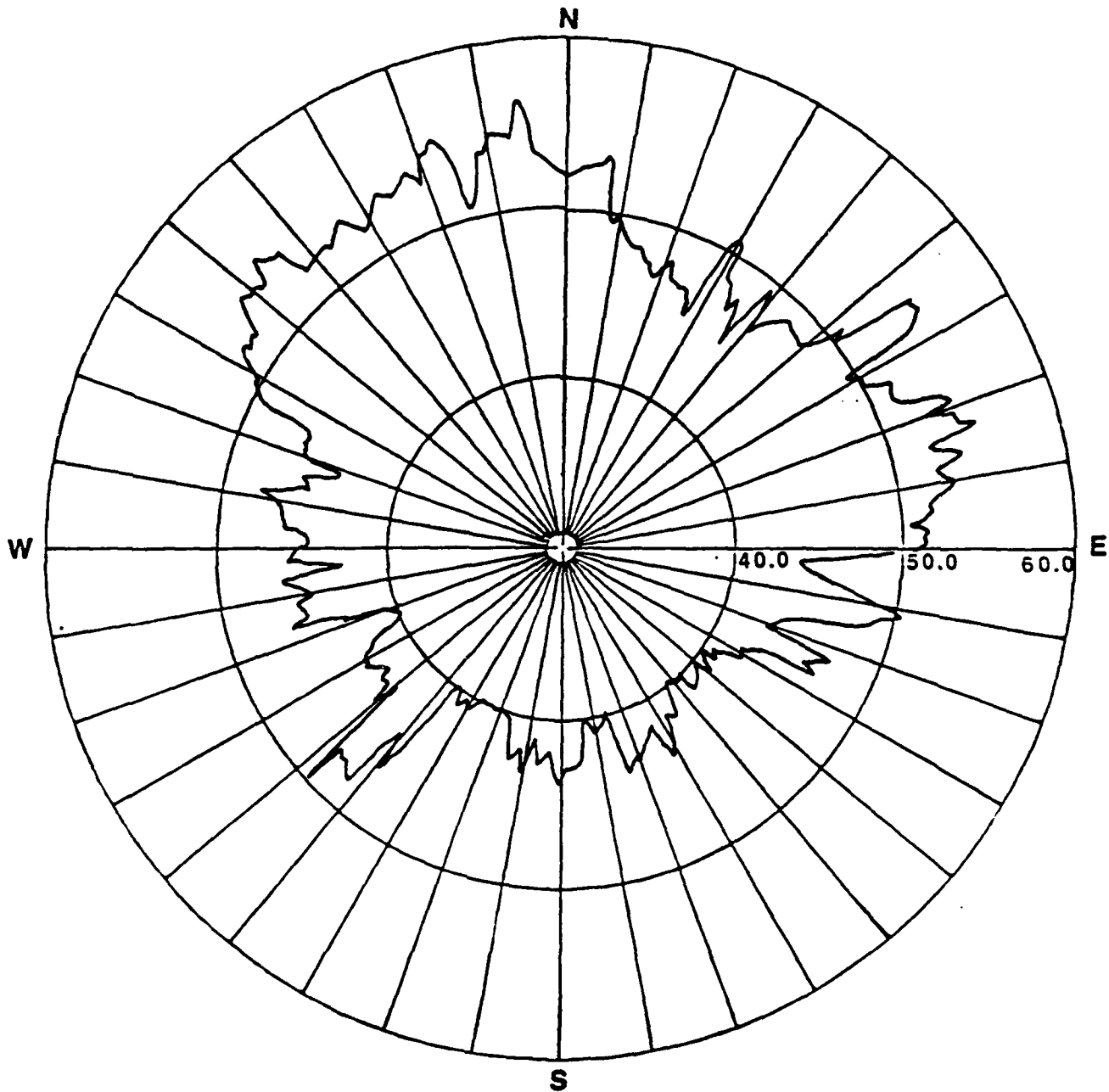
**Measured CHURCH ANCHOR Data**

**This slide and the next show how noise directionality persists on shorter time scales. These measurements differ by several hours but the patterns are much the same.**



# MEASURED CHURCH ANCHOR DATA

## HORIZONTAL DIRECTIONALITY



POLYGON NUMBER 5311, 5 SIDES, 100 Hz

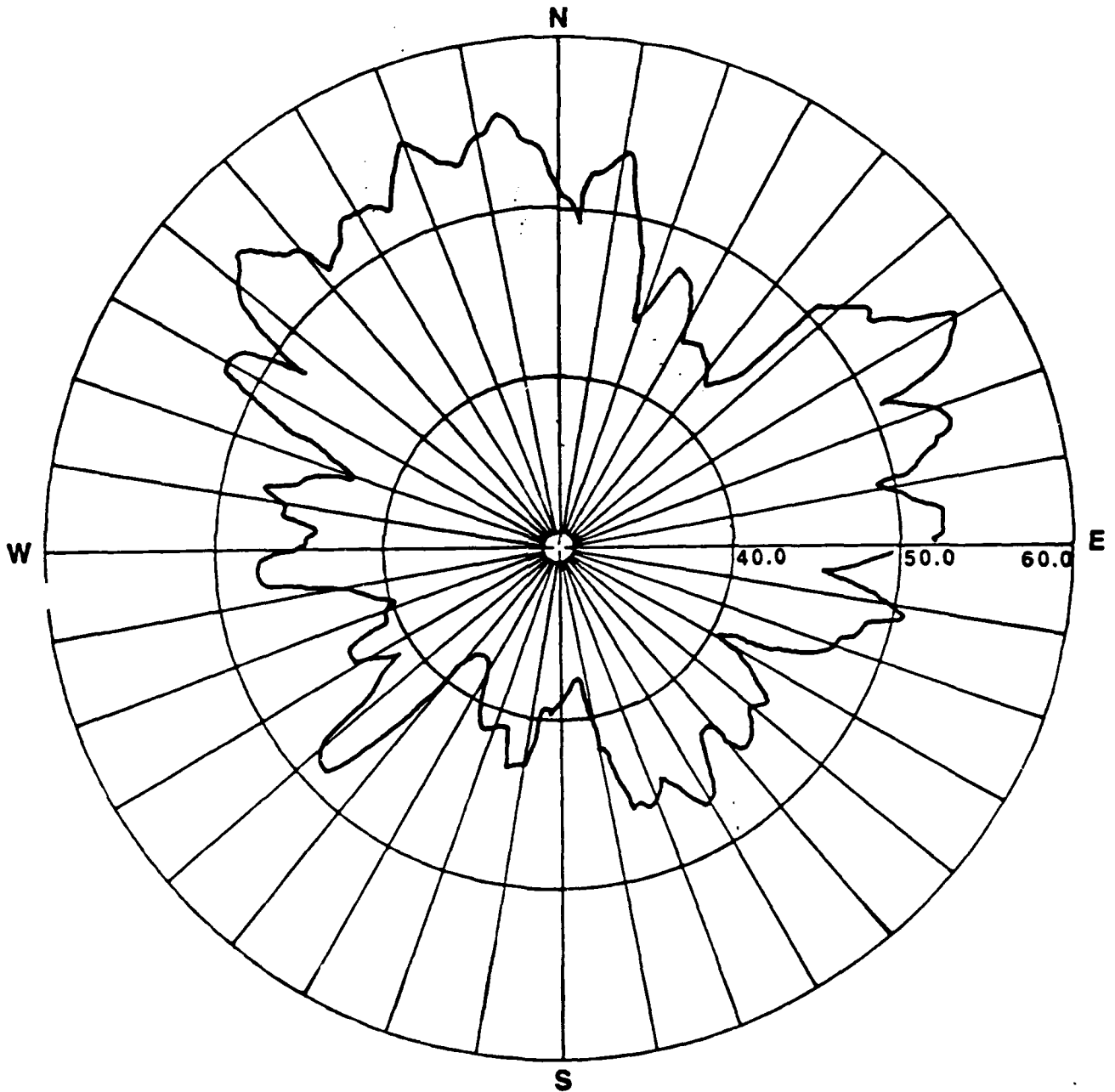
OMNI LEVEL - 74.9 dB





# MEASURED CHURCH ANCHOR DATA

## HORIZONTAL DIRECTIONALITY



POLYGON 5311, 2 SIDES, 100 Hz

OMNI LEVEL - 75.3 dB





## OBSERVATIONS

- **LOW FREQUENCY AMBIENT NOISE FIELD GROSS STRUCTURE IS WELL UNDERSTOOD**
  - VERTICAL AND HORIZONTAL DIRECTIONALITY
  - DEPTH DEPENDENCE
- **DOMINANT NOISE PROPAGATION MECHANISMS ARE UNDERSTOOD AND MODELABLE**
- **A VARIETY OF BOTTOM INTERACTION EFFECT HAVE BEEN OBSERVED BUT ARE NOT UNIVERSALLY QUANTIFIABLE**
- **THE ANGULAR DISTRIBUTION OF THE SOFAR CHANNEL LOWER LEVEL BACKGROUND NOISE IS NOT WELL UNDERSTOOD**
  - MEASUREMENTS TO SUPPORT MODELING DO NOT EXIST



**DISTANT STORM NOISE**

**J. WILSON (WAR, INC.)**



## **PRESENTATION OUTLINE**

Dr. James H. Wilson  
WAR, Inc.

### **EMPIRICAL SEA SURFACE AMBIENT NOISE MODEL RESULTS**

- Storm noise model shows that distant storm noise can provide "noise floor" for long horizontal arrays looking between ships

### **AT- SEA MEASUREMENT CONCEPT**

- Inexpensive, low risk method to collect long time series data
- Beam data to be transmitted via ARGOS

### **MEASUREMENT NEEDS FOR THEORIES**

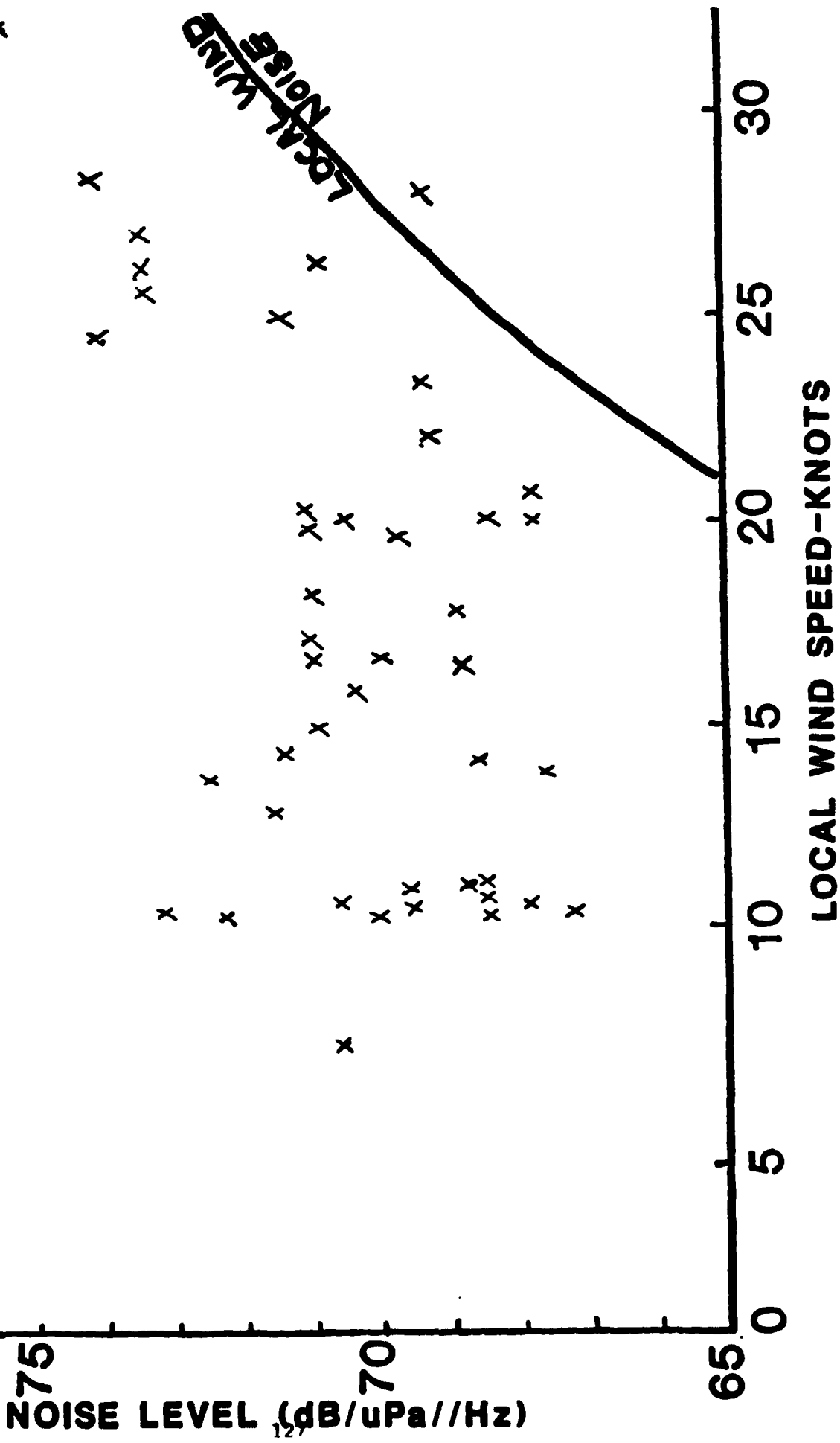
- Lack of supporting environmental data is a major problem in current data sets



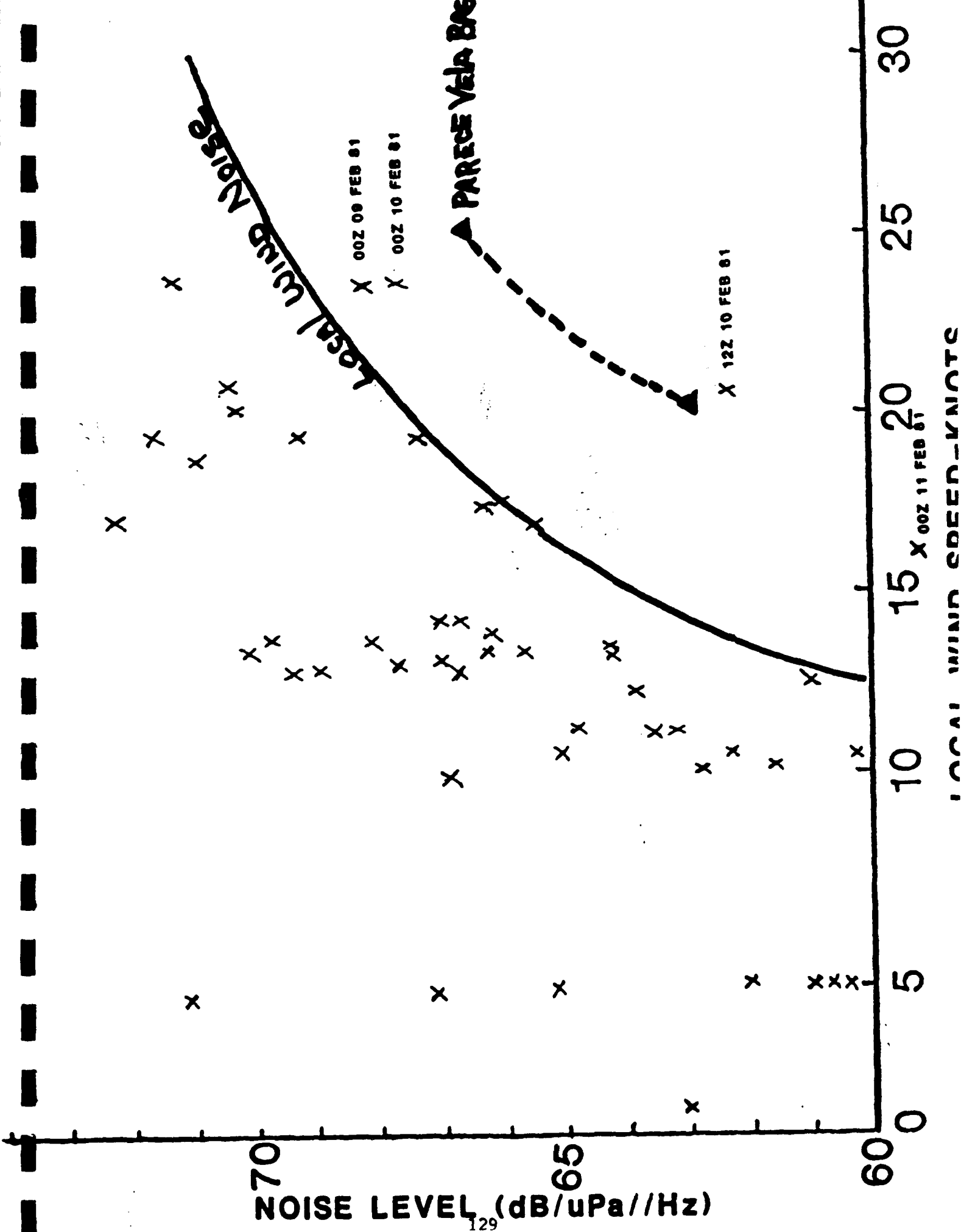
# STORM NOISE MODEL

- SOURCE LEVEL DENSITY
- SOURCE DIRECTIVITY PATTERN
- SOURCE SURFACE DISTRIBUTION
- TRANSMISSION LOSS MODEL

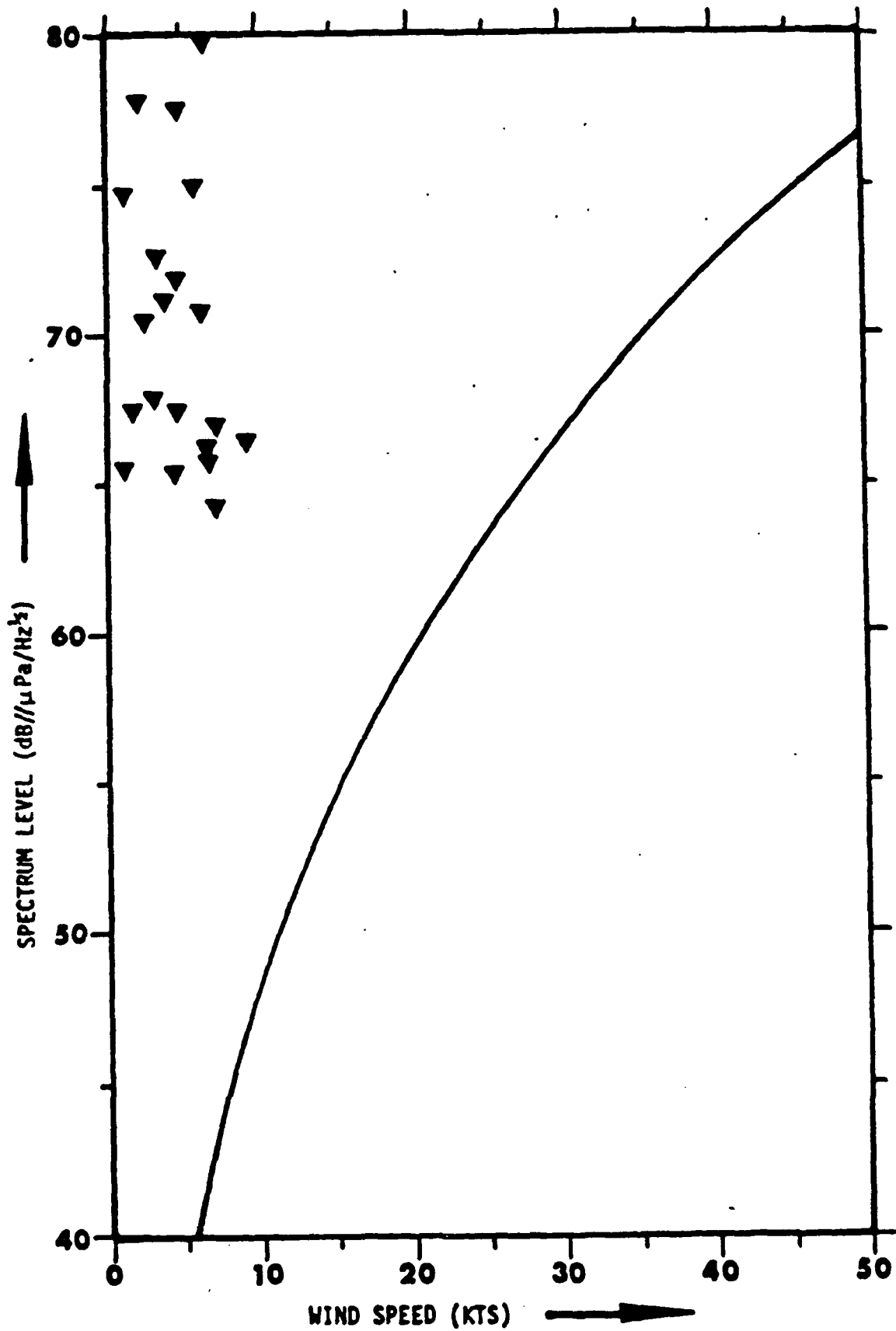






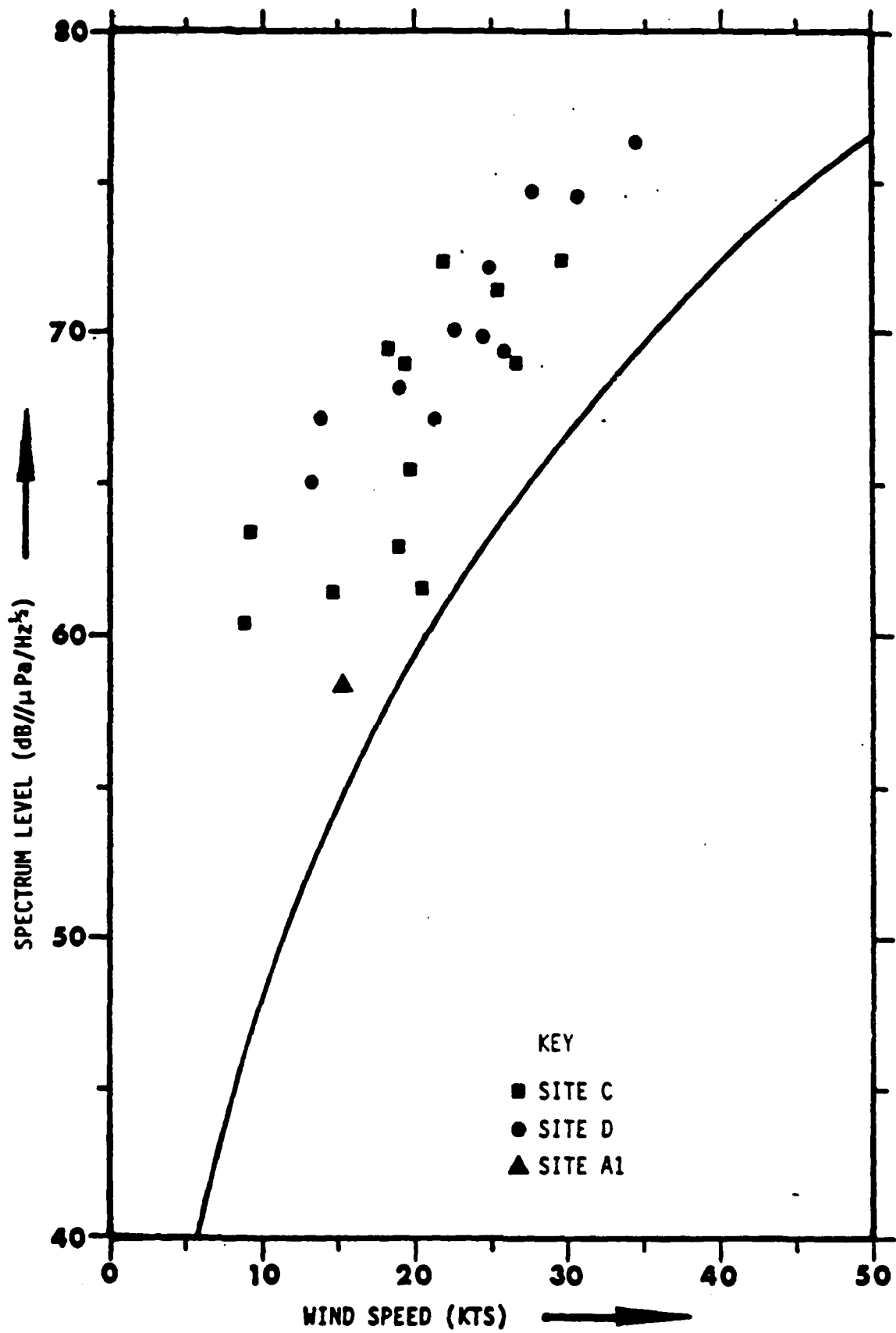






12.5 Hz NOISE DATA MEASURED AT A SITE NEAR A MAJOR SHIPPING LANE

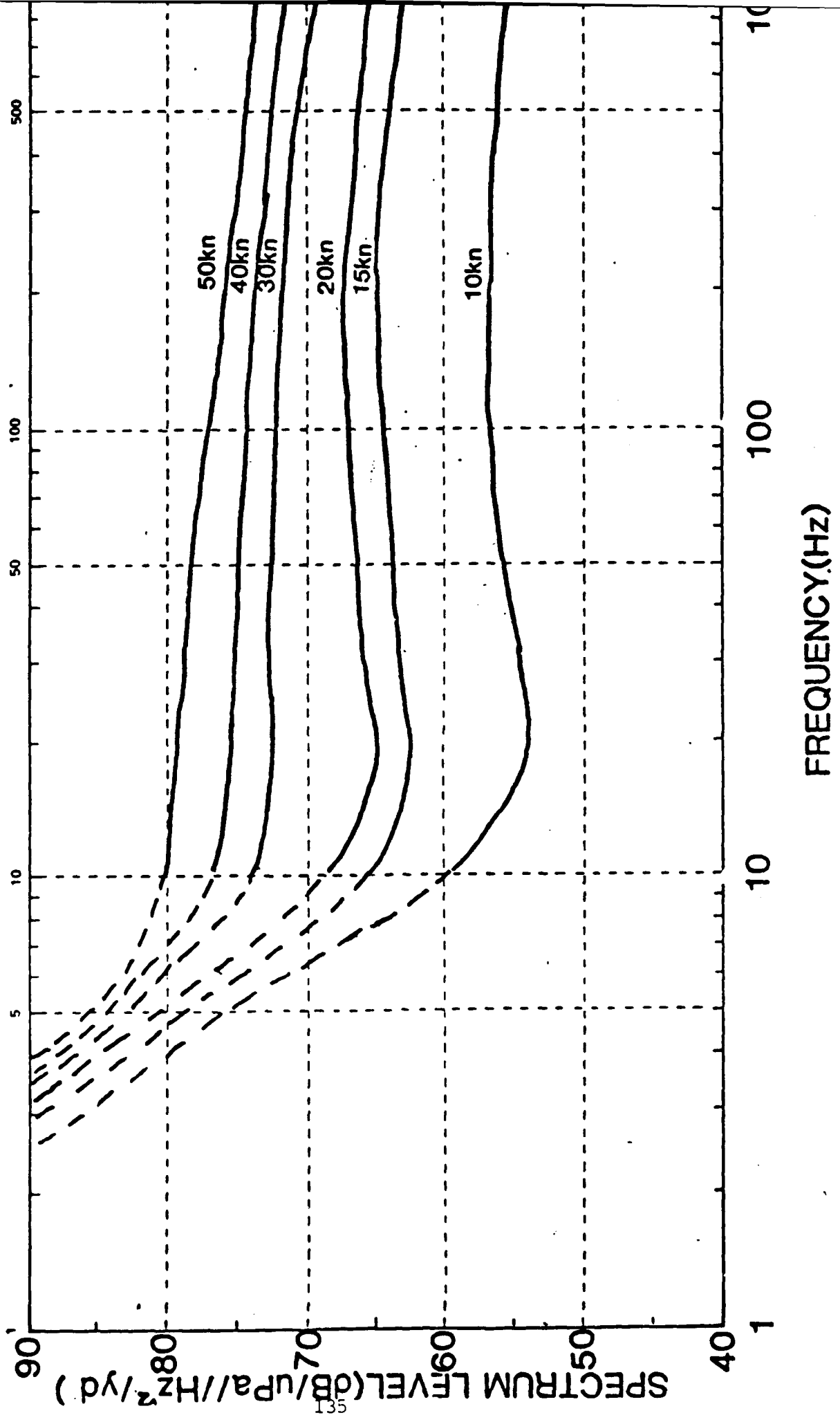




12.5 Hz NOISE DATA MEASURED AT THREE SITES DISTANT FROM MAJOR SHIPPING LANES

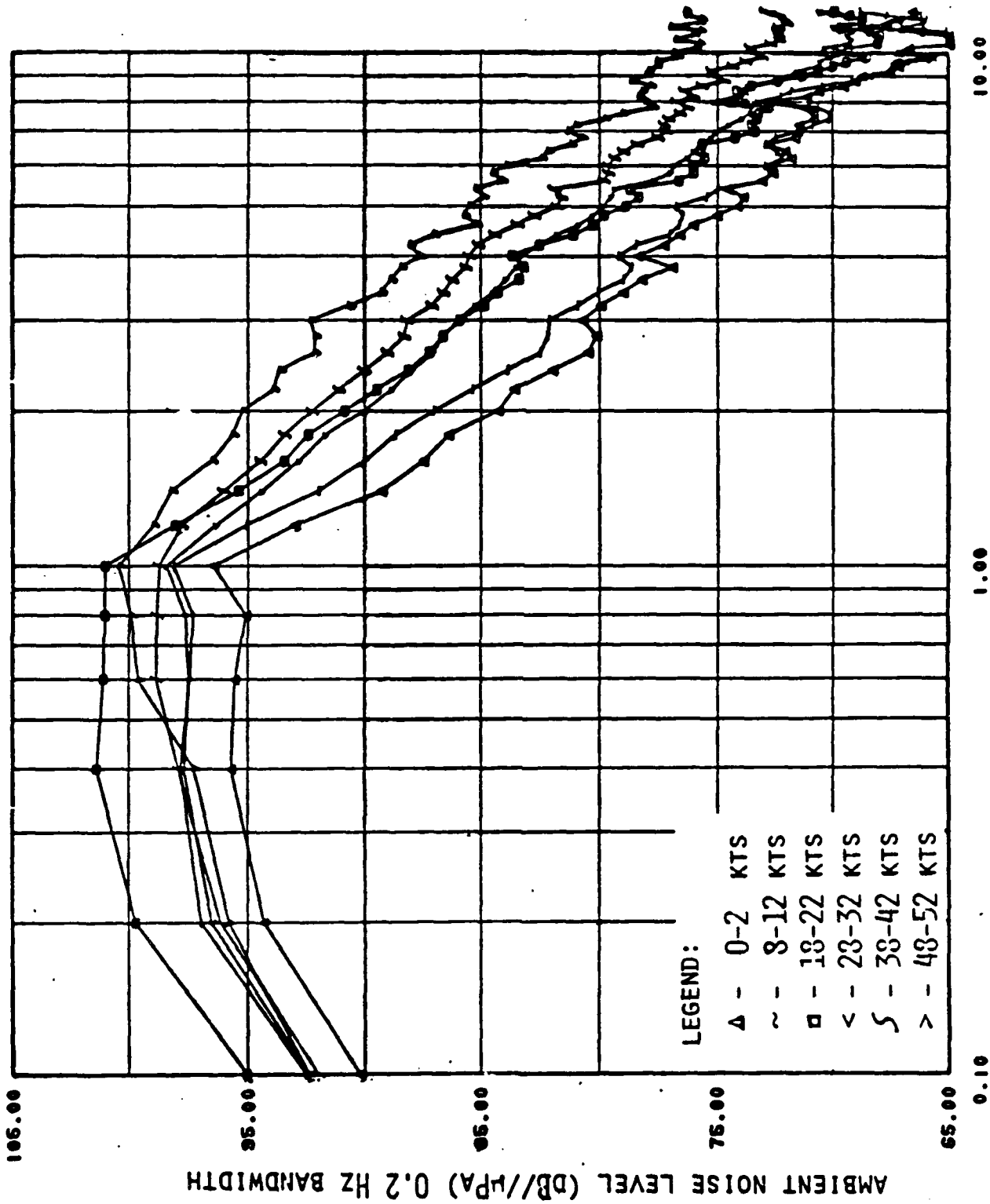


# SOURCE LEVEL DENSITY

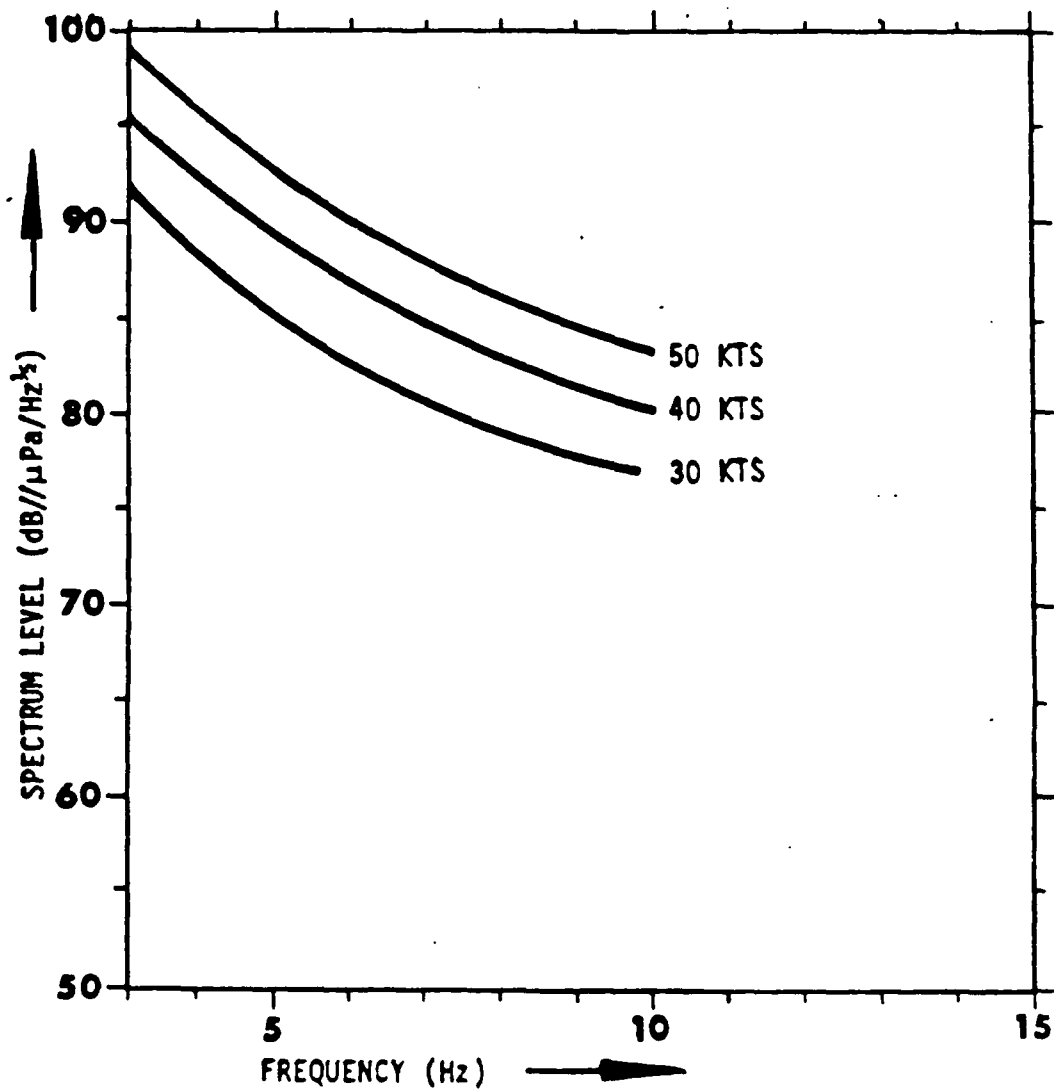




VLF AMBIENT NOISE LEVELS NEAR BERMUDA

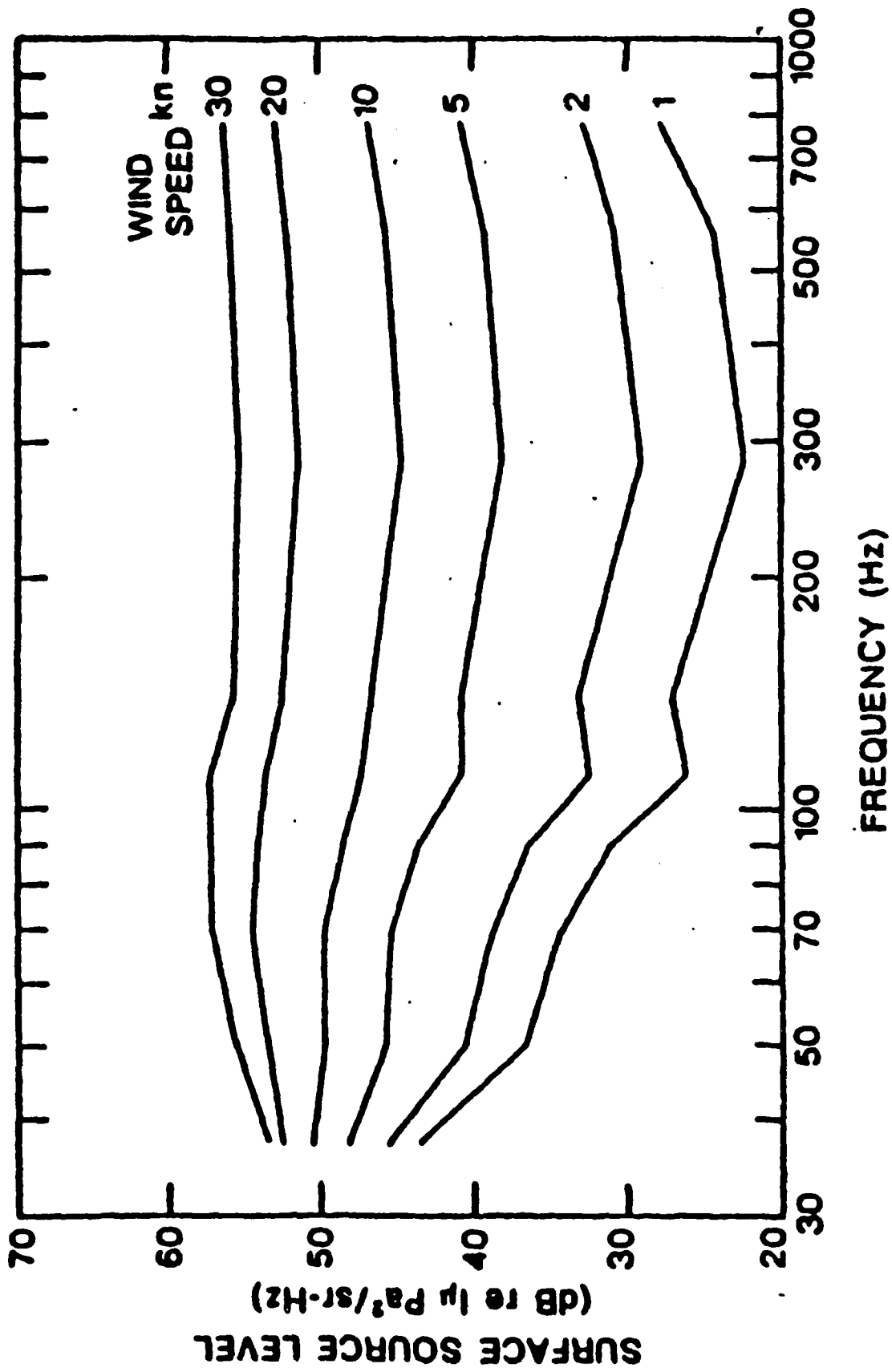






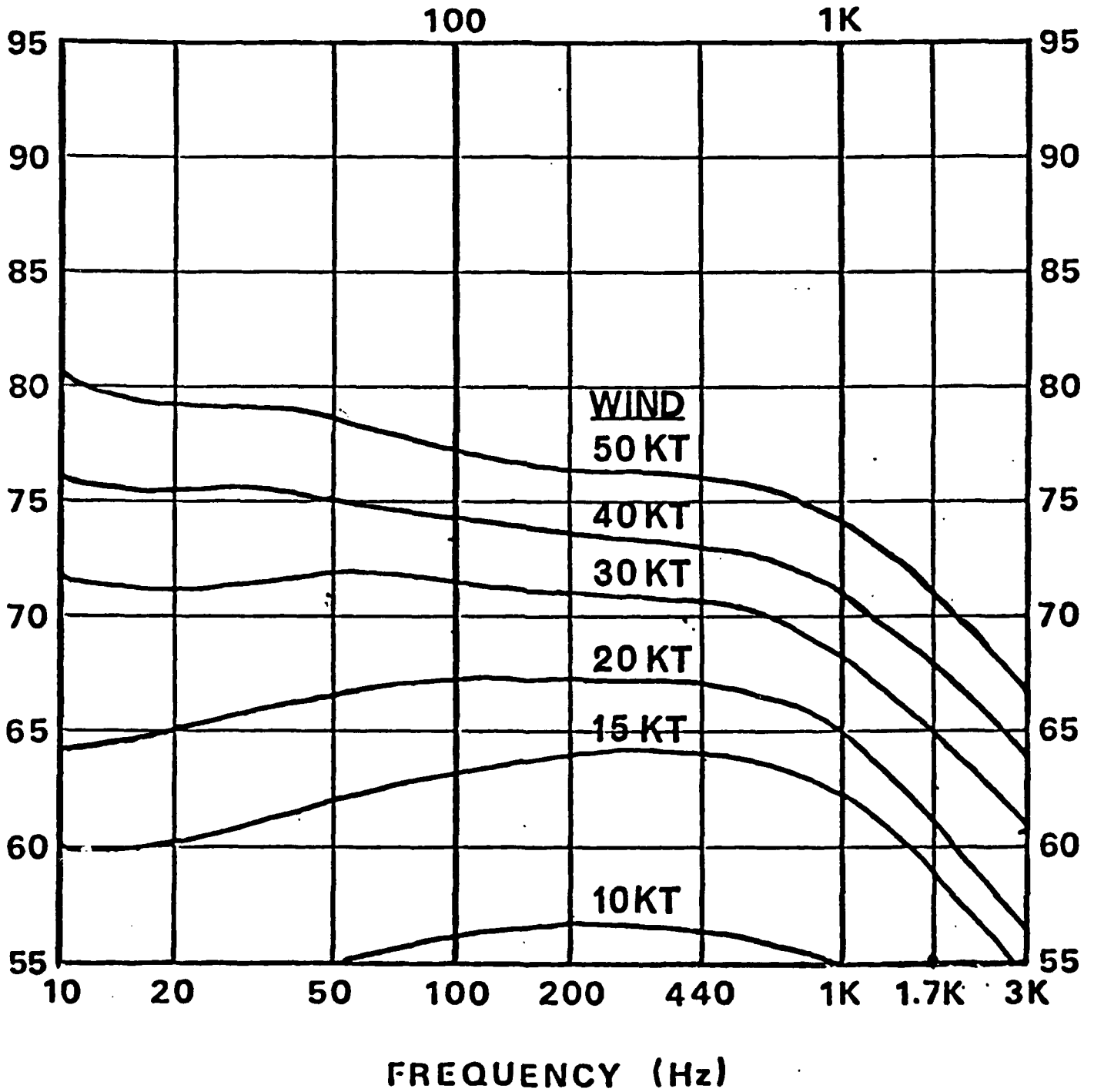
WIND SPEED DEPENDENCE OF PERRONE'S MEASURED NOISE DATA







MEAN AMBIENT NOISE  
DUE TO WIND AND WAVES

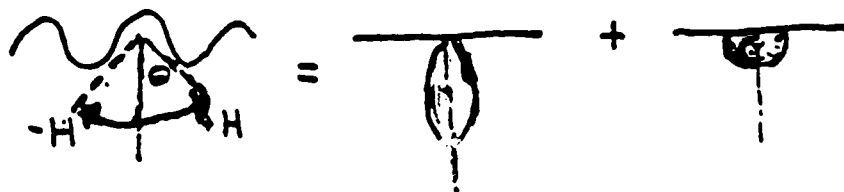




# ROCKING DIPOLE

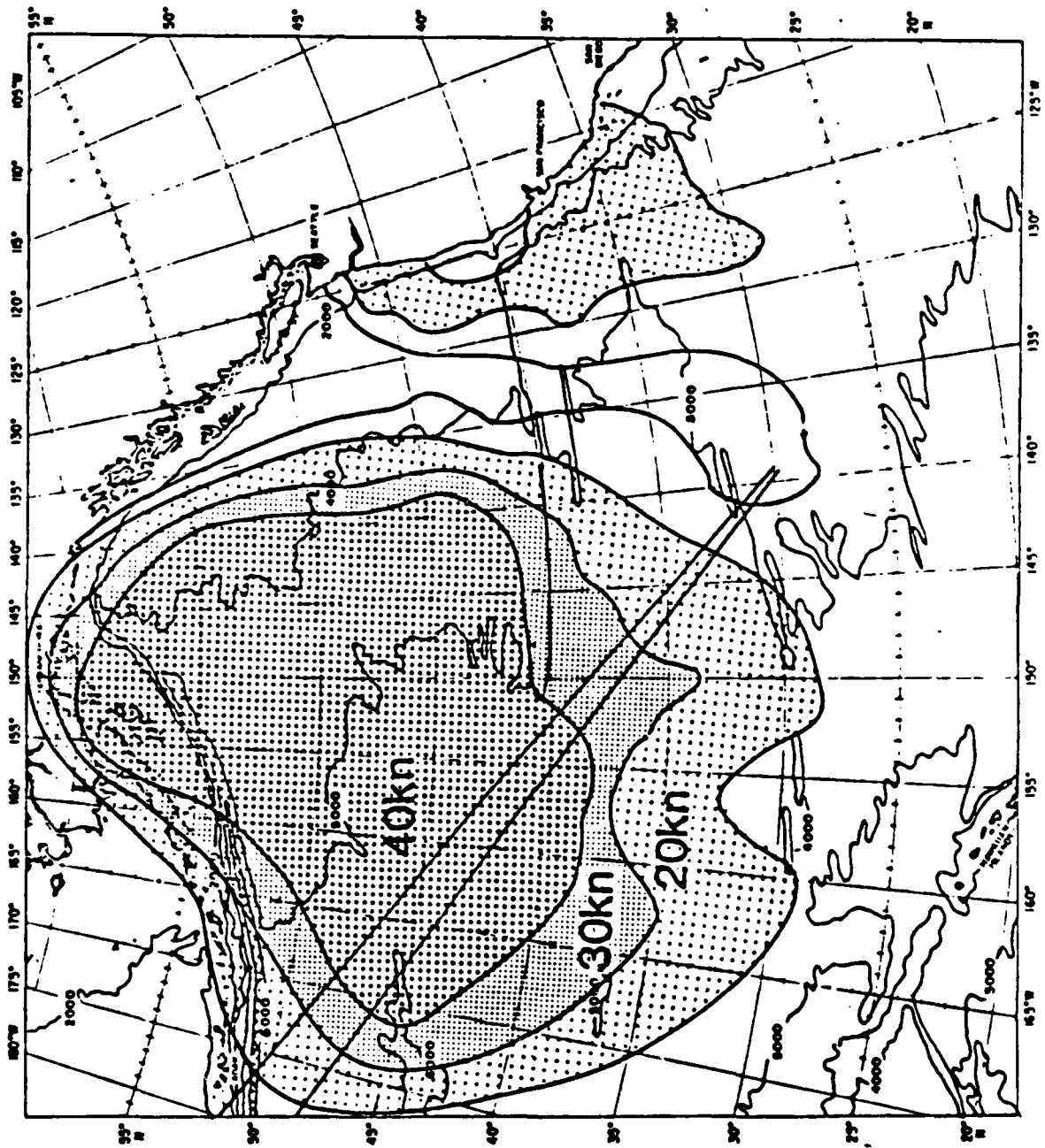
- SEPARATION INTO PURE DIPOLE & MONOPOLE TERMS

$$R(\theta) = J_0(2H)\cos^2(\theta) + (1 - J_0(2H))/2$$

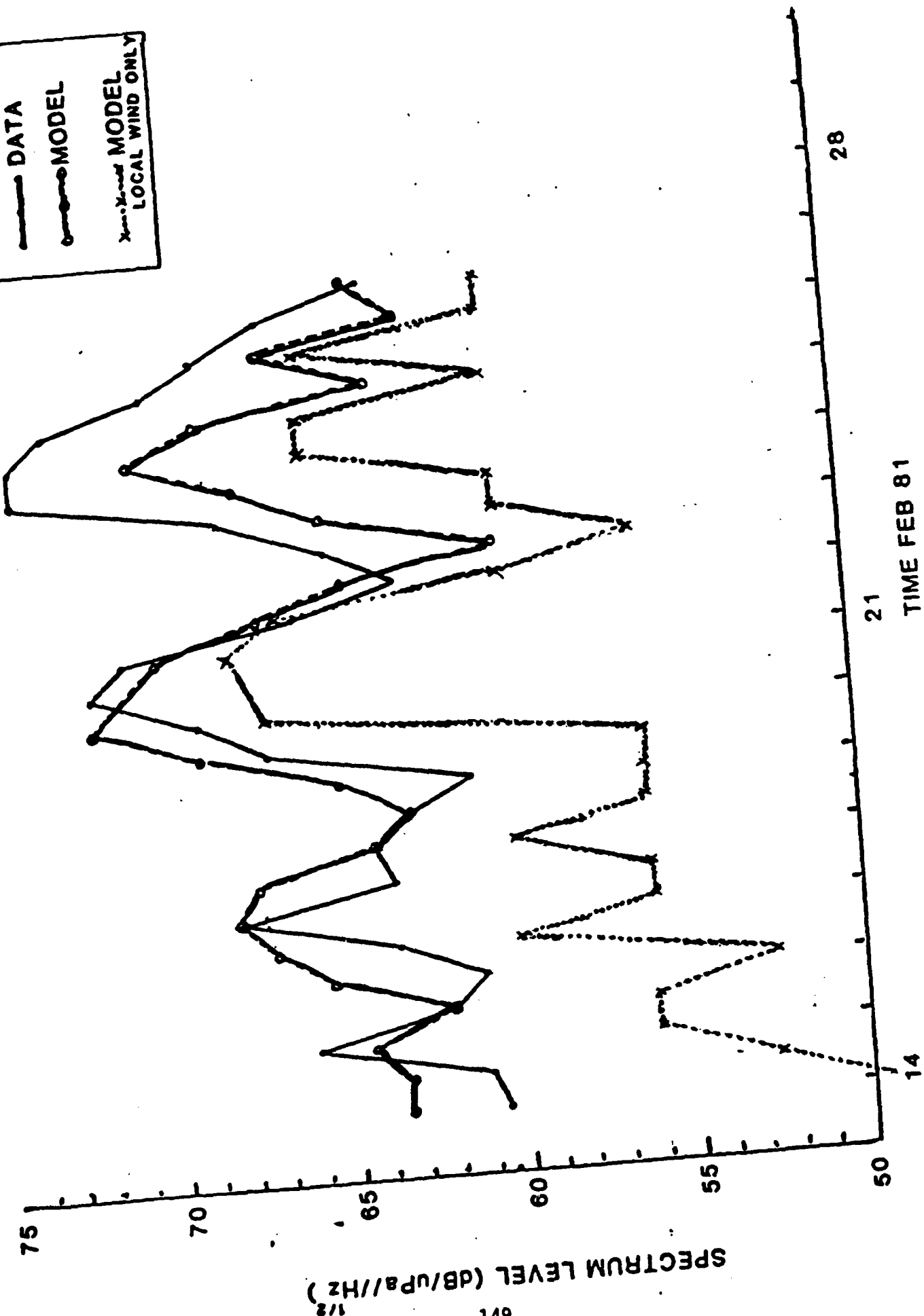
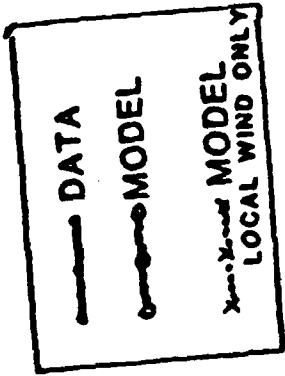


- DIPOLE ASSUMED TO ROCK BETWEEN  $\pm H^\circ$
- SURFACE MONOPOLE/DIPOLE TRANSMISSION LOSS





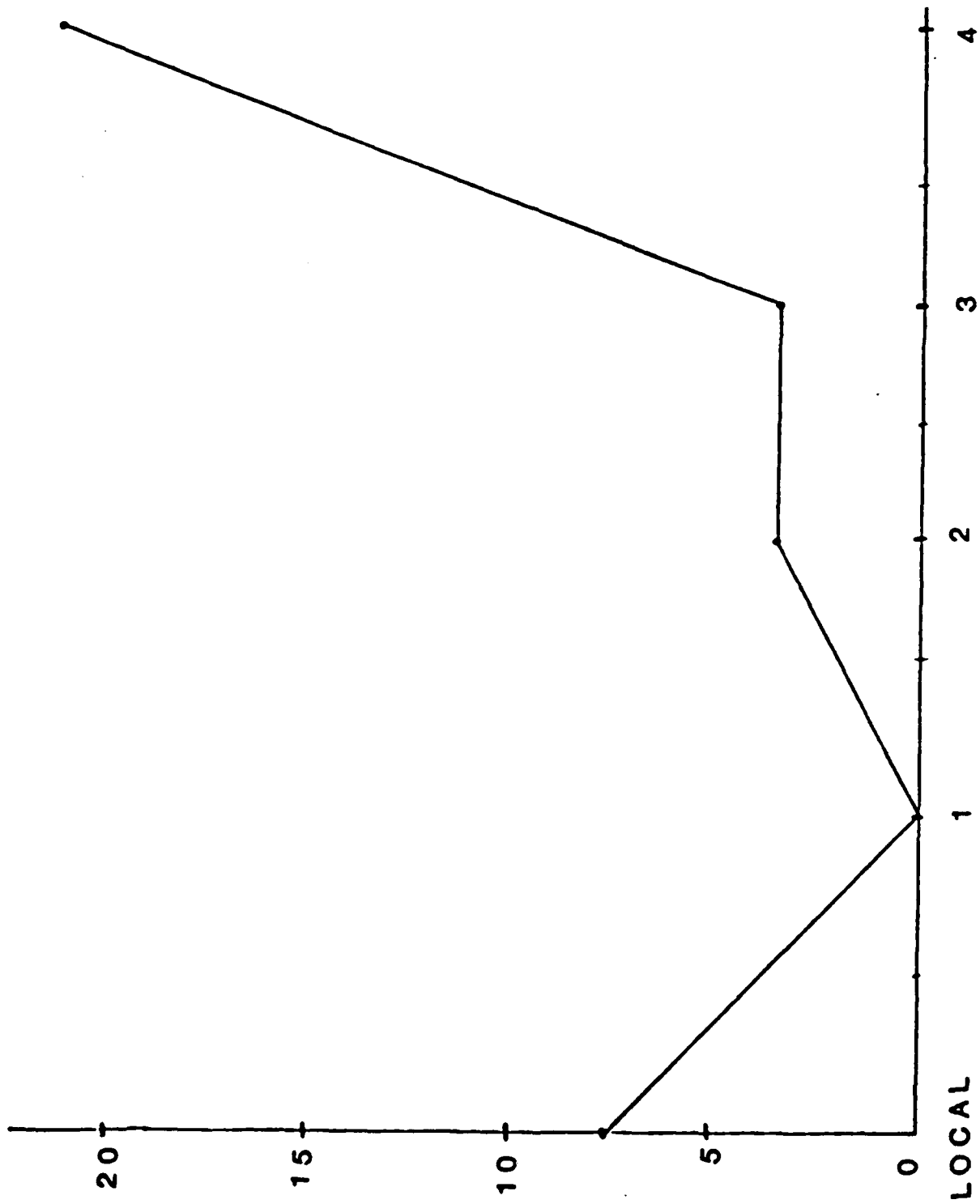




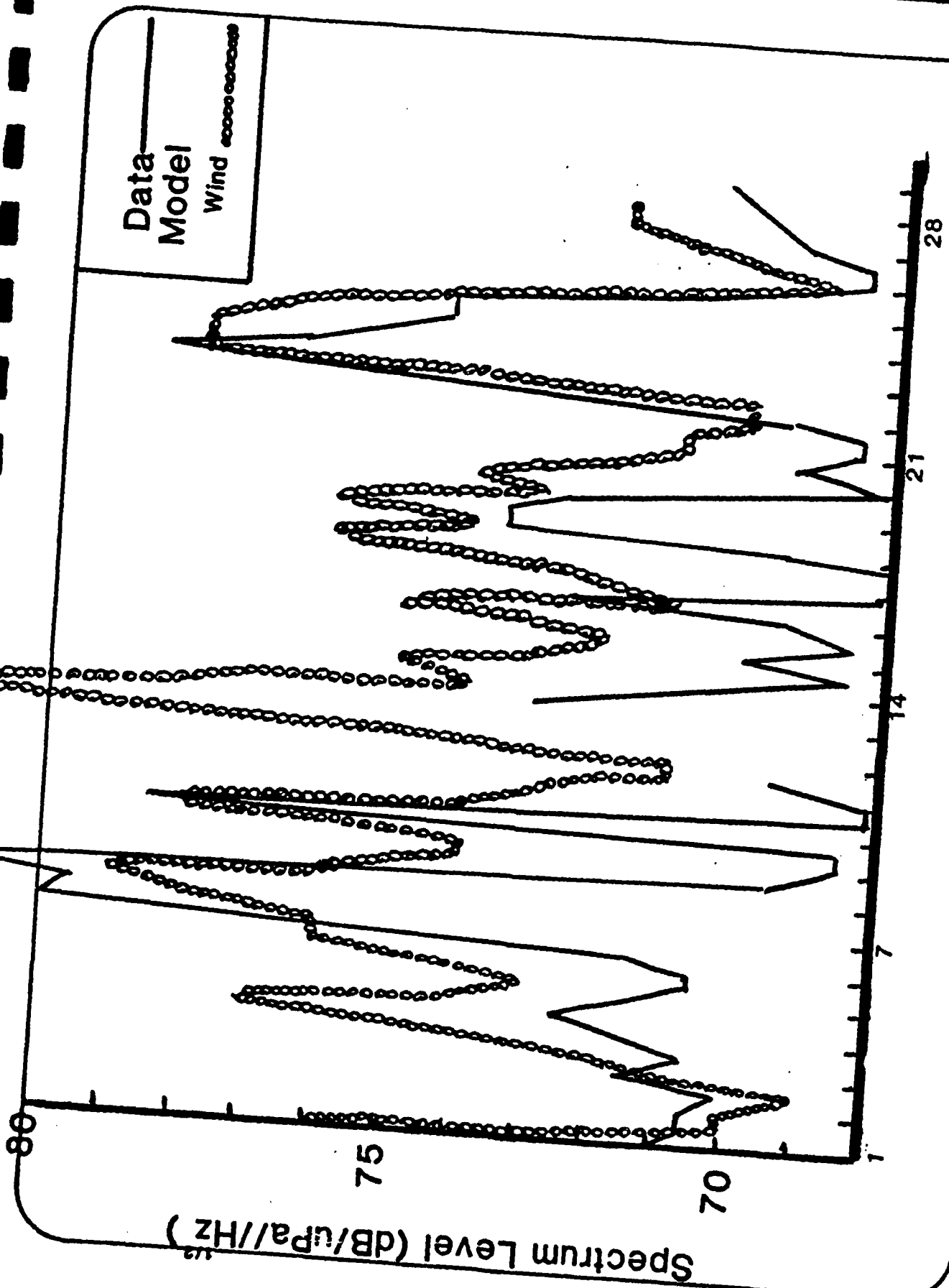
$\frac{1}{2}$   
 SPECTRUM LEVEL (dB/ $\mu$ Pa//Hz)



RELATIVE POWER IN EACH TL SECTOR(DB)







Time February 1981



(U) Figure B-1 Site A Model/Data Comparison-10 Hz (6)



**NOSCC**

**LOW-FREQUENCY STORM NOISE**

- REMOTE SENSING OF WIND FIELD
- PREDICTION OF NOISE SOURCE FIELD
- PROPAGATION OF NOISE TO ARRAY SITE
- ANALYSIS SYNOPSIS TO GLOBAL COVERAGE

COPIES AVAILABLE FROM OUR

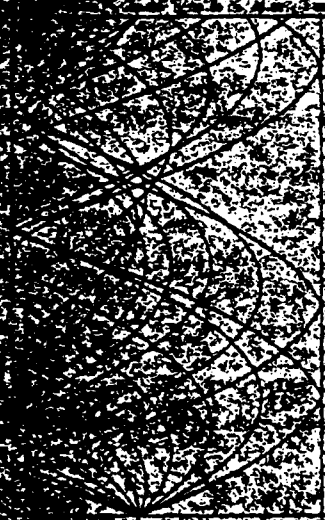


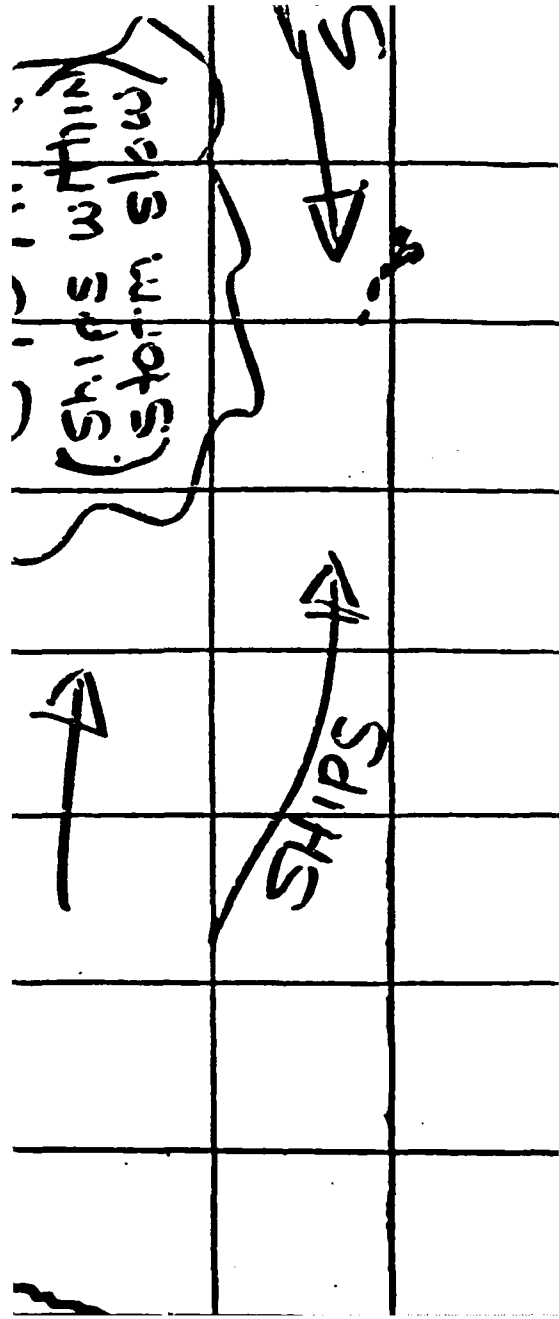
Figure 1 (10)

Aug 11 8 1076 - 6053 Wind Vectors  
 150 170 180 160 140 130 120 110  
 100 90 80 70 60 50 40 30 20 10 0



1B1834







## ***MEASUREMENT CONCEPT***

**COLLECT AND TRANSMIT DATA FOR LONG  
PERIODS OF TIME AT SEVERAL LOCATIONS**

**MINIMIZE EXPENSE**

**MINIMIZE RISK OF LOSING DATA DURING  
AT-SEA RECOVERY**



# ***MEASUREMENT ASSETS***

**WAVES AIR-SEA INTERACTION**

**DRIFTING(WASID) BUOY**

**DEEP MOORED BUOY (DMB)**

**ARGOS DATA TRANSMISSION SYSTEM**



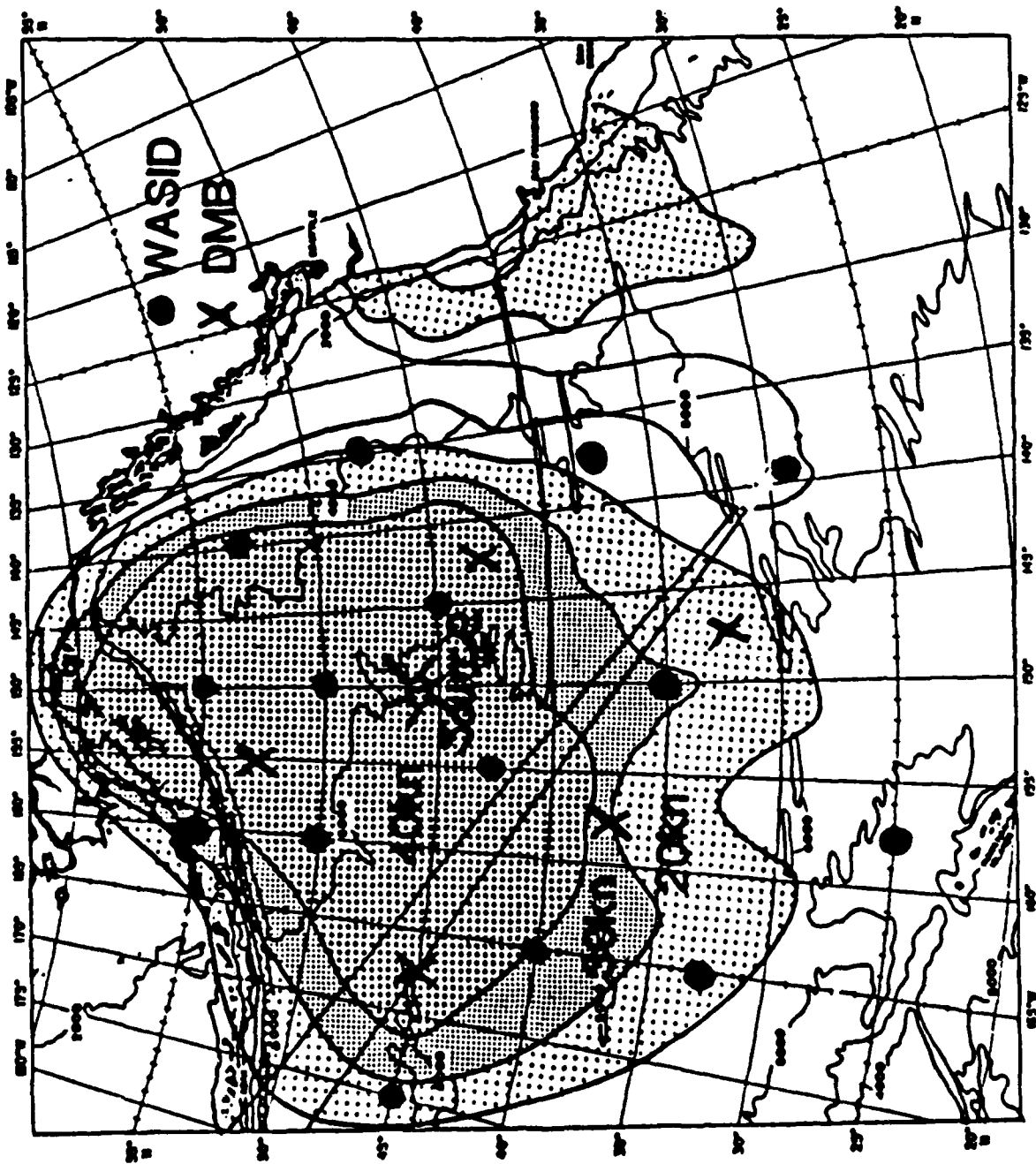


FIGURE 1. PROPOSED EXERCISE SCENARIO



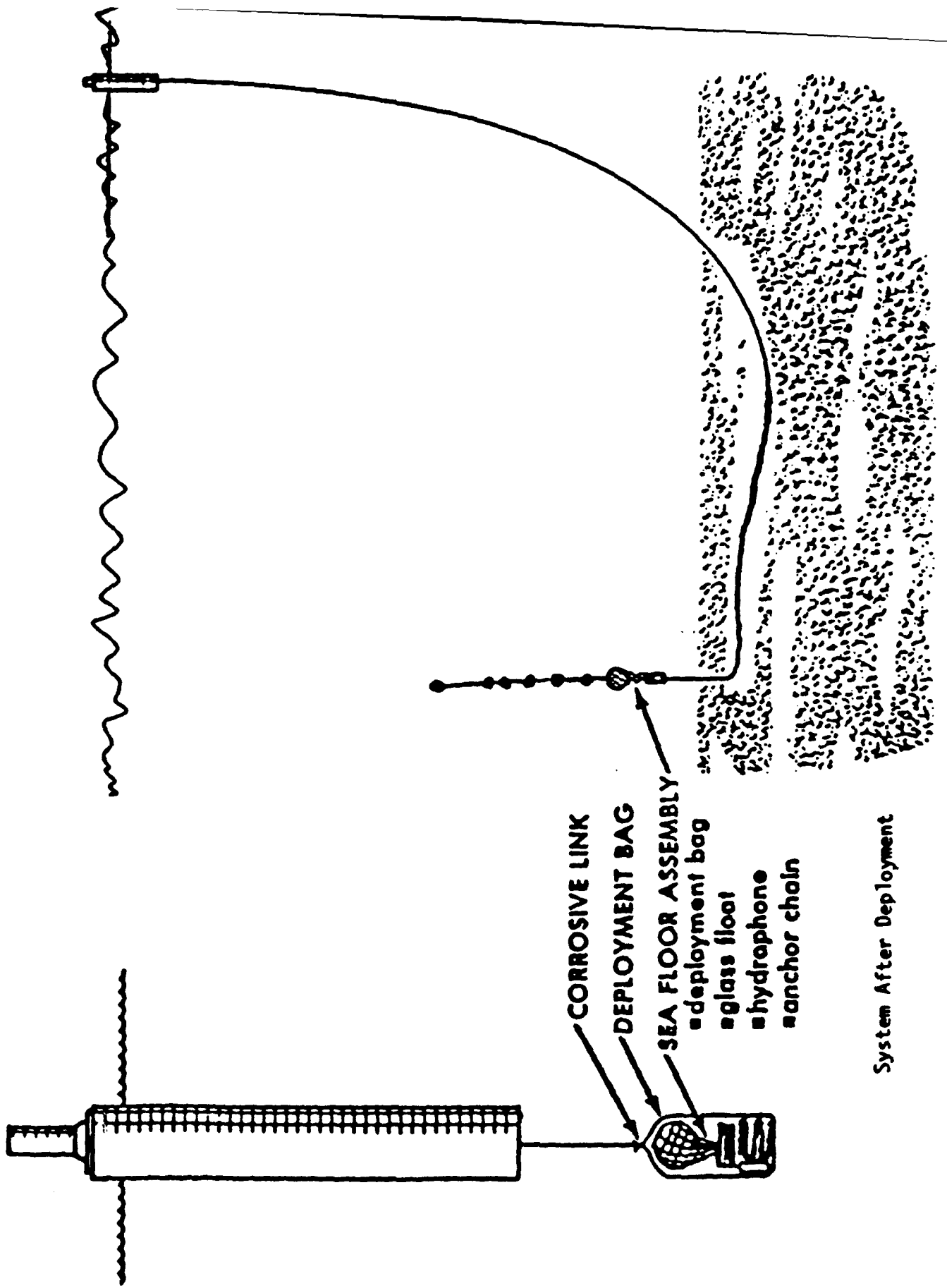
OCEAN SURFACE ENVIRONMENTAL PARAMETERS  
THAT ARE FEASIBLE TO MEASURE

- Wind speed vertical profile (3 different heights)
- Low frequency wave spectrum
- Barometric pressure
- Air and sea temperature
- Subsurface bubble density\*
- Ocean Turbulence\*
- High frequency wave spectra\*
- Microseismic activity\*

\* System currently not capable of measuring this parameter.



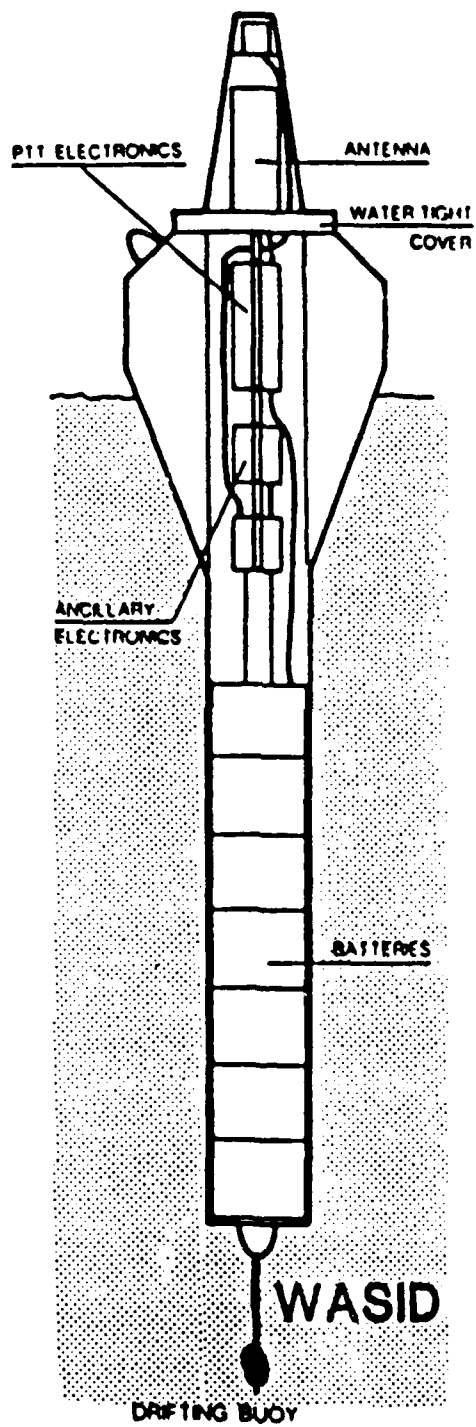
# DEEP MOORED BUOY



- CORROSIVE LINK
- DEPLOYMENT BAG
- SEA FLOOR ASSEMBLY
  - deployment bag
  - glass float
  - hydrophone
  - anchor chain

System After Deployment







## CONCLUSIONS

- Currently, open ocean ambient noise measurements are not adequate to determine source level density function to validate theories of ocean surface physical mechanisms.
- Ambient noise measurements can yield ocean surface sound levels only after propagation effects have been removed from the data.
- Some accepted (?) results from ambient noise analyses.
  - spectra have three regions with similar slopes within each region
  - wind speed dependence has at least two physical regions (divided by ~ 10 knots)



# **SHELF SHIPPING NOISE**

**W. HODGKISS (MPL)**



# Shelf Shipping Noise

W. S. Hodgkiss

Marine Physical Laboratory  
Scripps Institution of Oceanography  
San Diego, CA 92152

HGI/AEAS VLF Ambient Noise  
Workshop

September 20, 1988



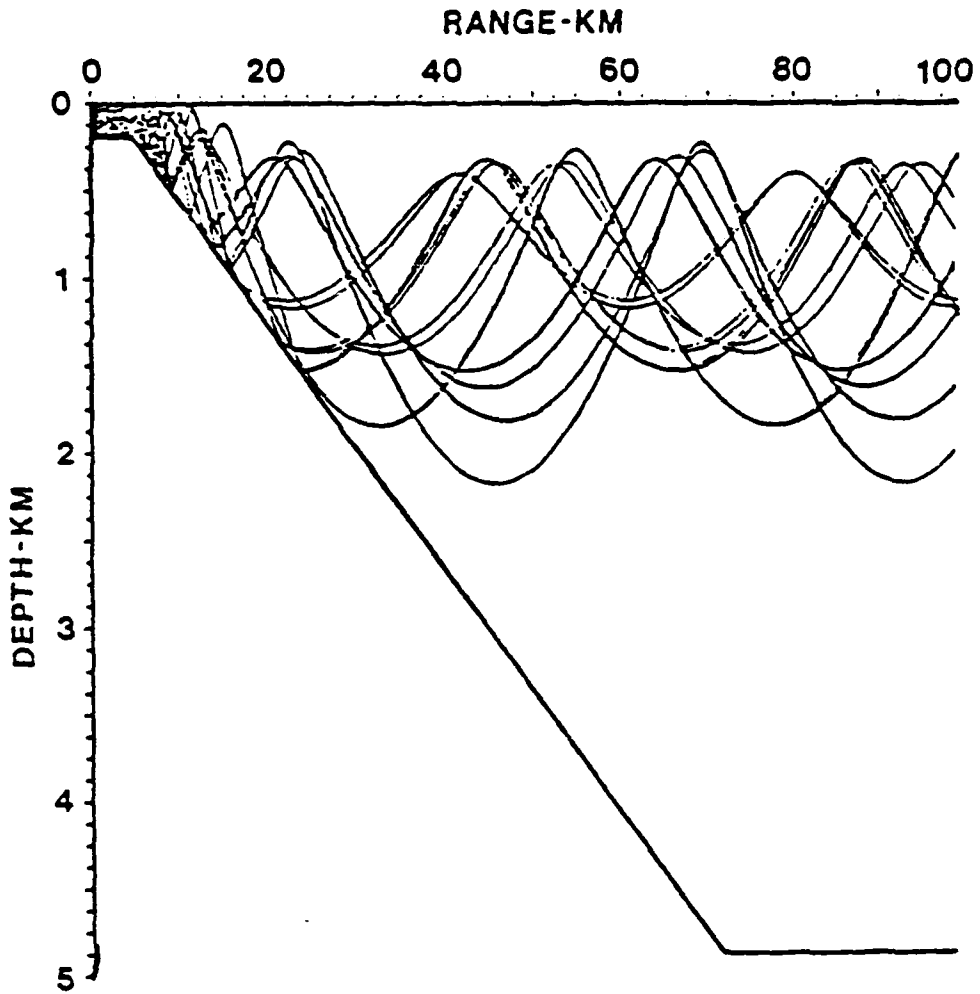


Figure 1. Ray trace for a 10 m source 5 km from the edge of a  $4^\circ$  slope [1].



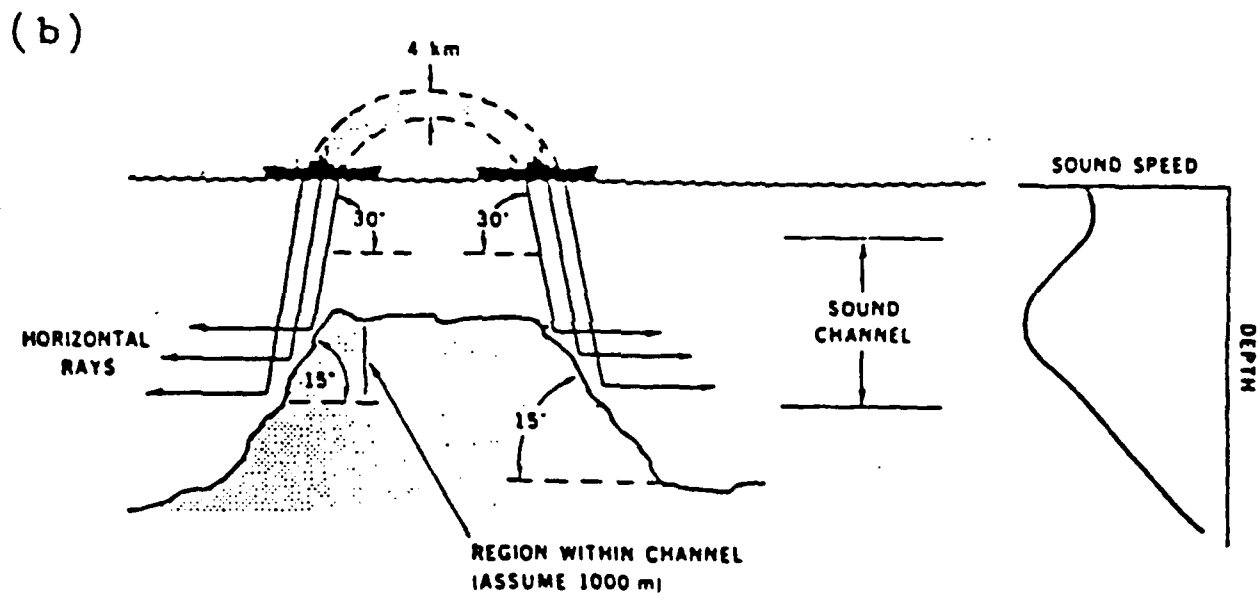
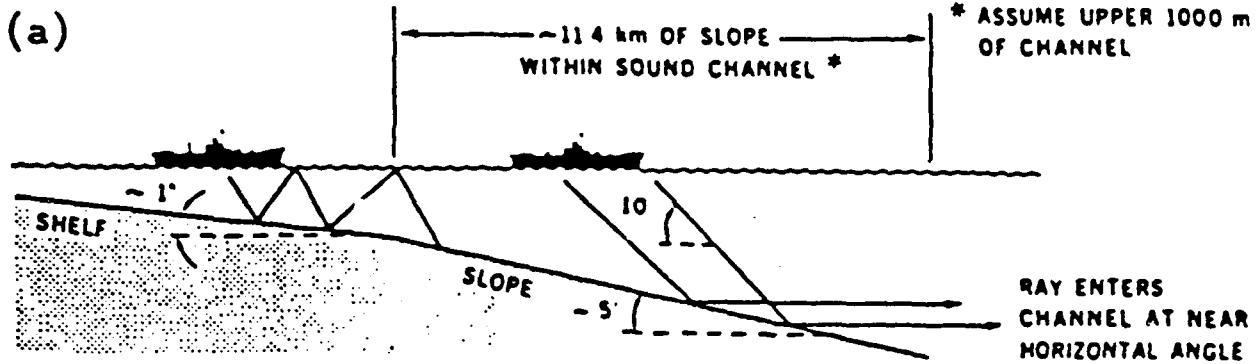
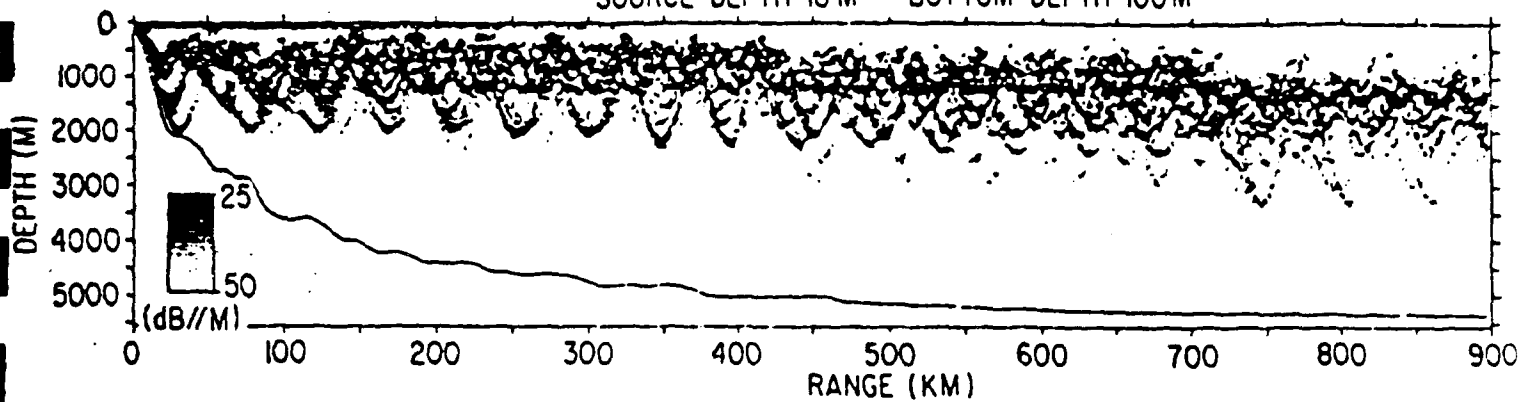


Figure 2. Conversion of high-angle raypaths to nearly horizontal by reflection off a sloping bottom [2].



SOURCE DEPTH 18 M — BOTTOM DEPTH 1000 M



SOURCE DEPTH 18 M — BOTTOM DEPTH 806 M

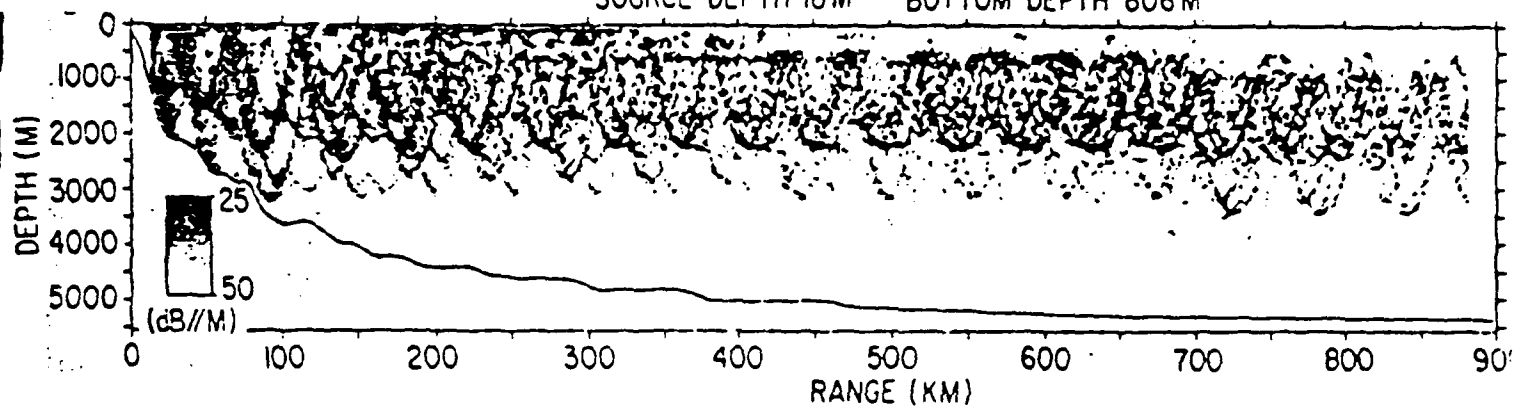


Figure 3. Intensity field plots for sound propagation from a shallow source over the continental slope to a deep ocean receiver [13].



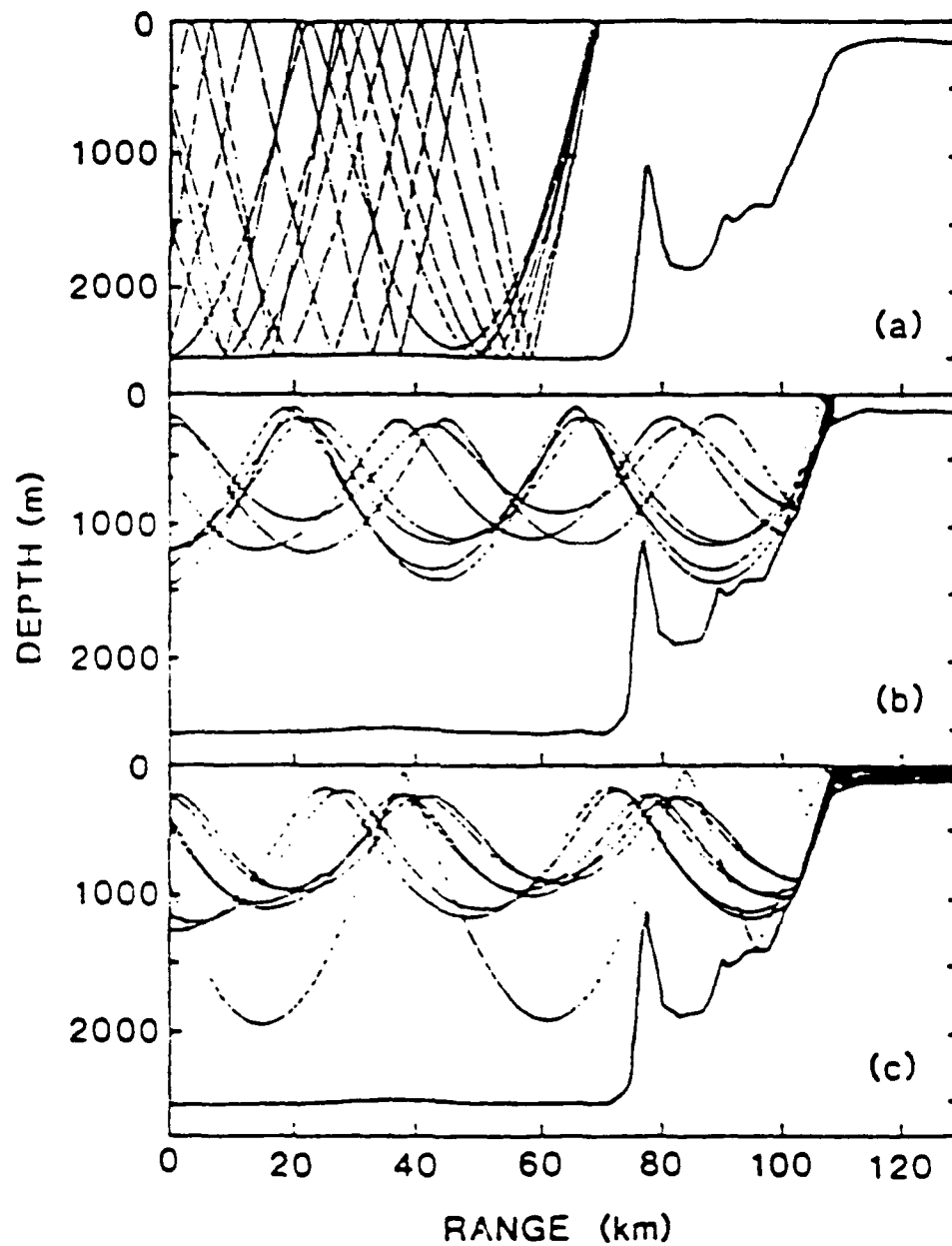


Figure 4. Propagation paths predicted by the numerical ray model GRASS for 22-m-deep sources at ranges of (a) 70 km, (b) 110 km, and (c) 130 km for source angles within  $\pm 10^\circ$  of the horizontal [14].



Array Response - 85010 Bin #5902  
f = 200 Hz, KB window (alpha = 1.5)

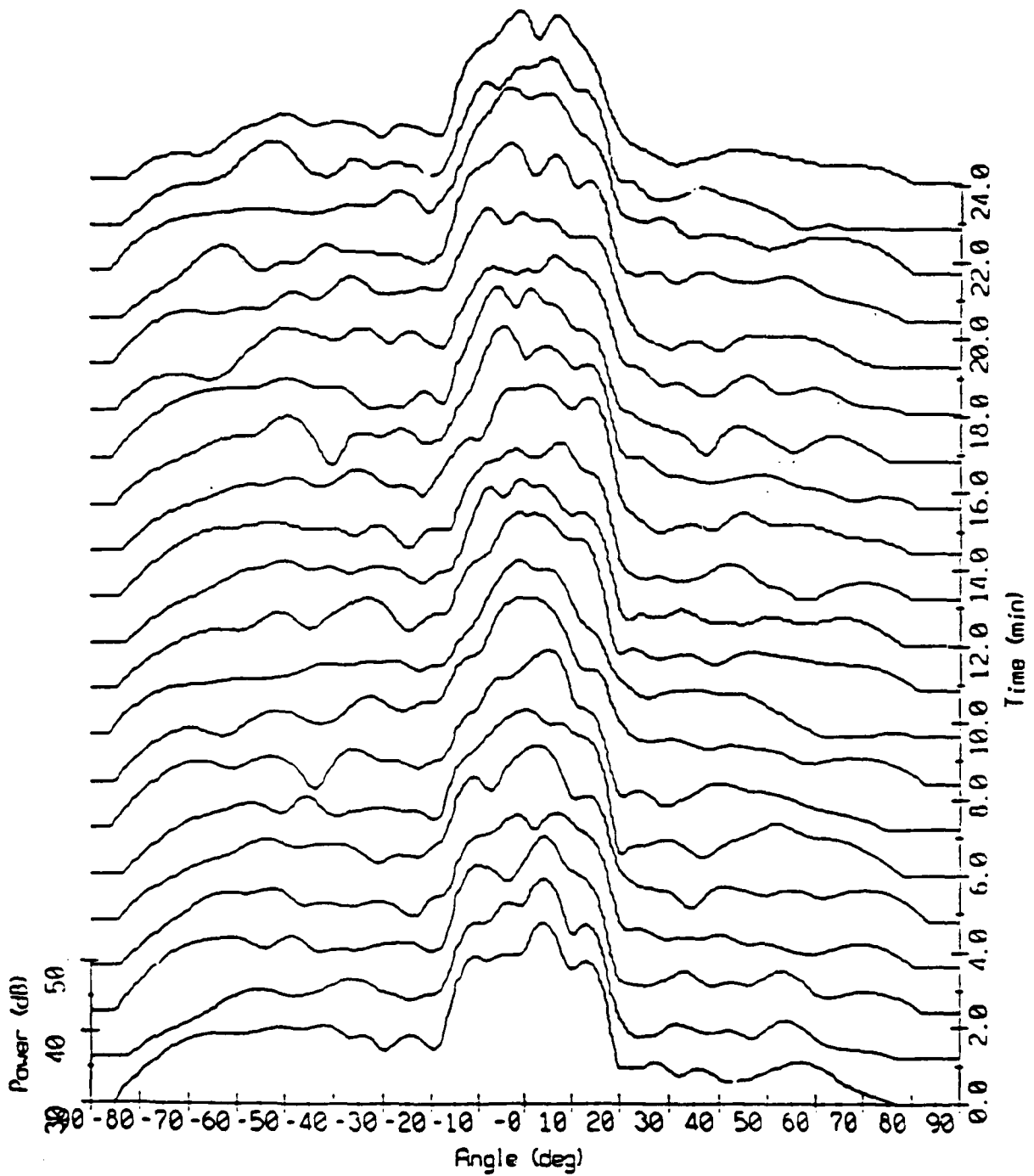
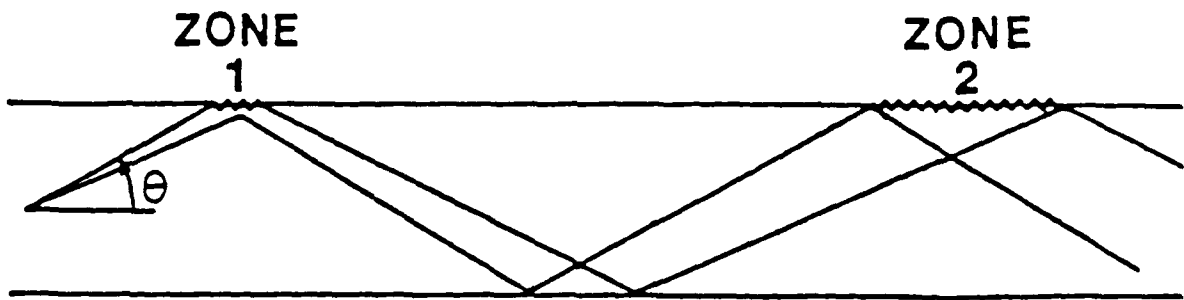


Figure 5. Ambient noise vertical directionality.  
32°N 124°W, wind speed 6 kts. Positive angles  
refer to downward looking beams [18].

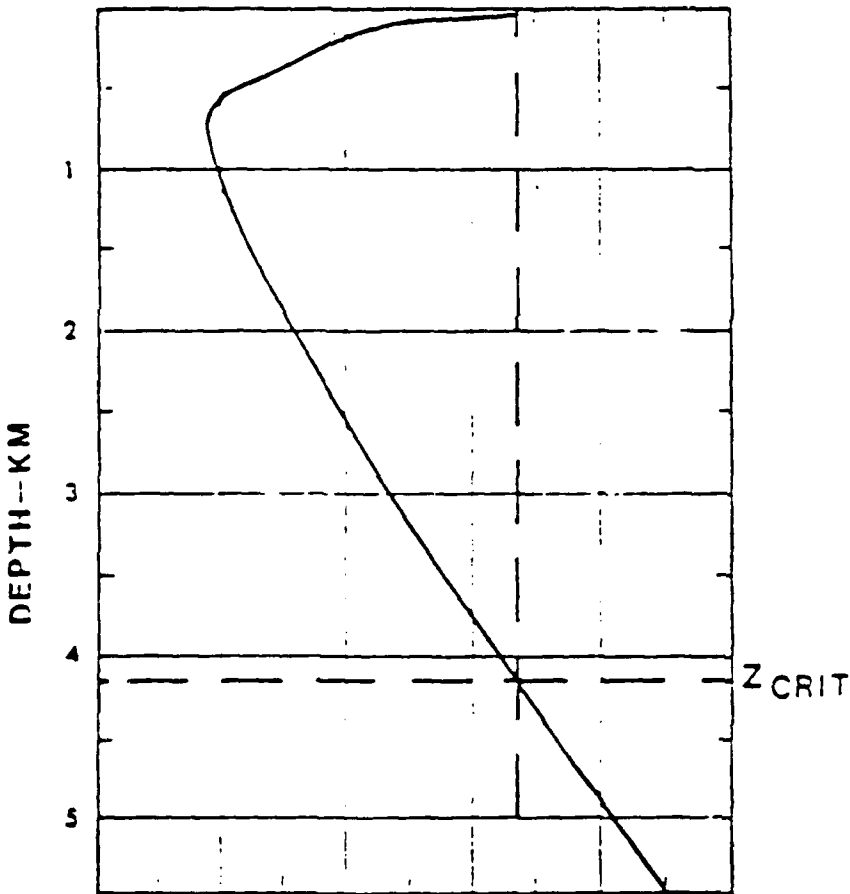




TYPICAL S.V.P.

SOUND SPEED M/S

1460 1480 1500 1520 1540 1560



DEEP-WATER  
VERTICAL ARRIVALS

$$C_0 < C_s < C_B$$

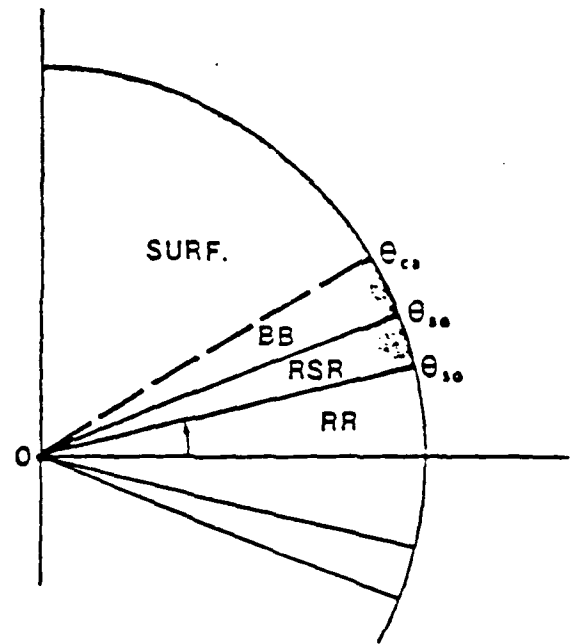


Figure 6. Deep-Water Vertical Arrival Structure [1].



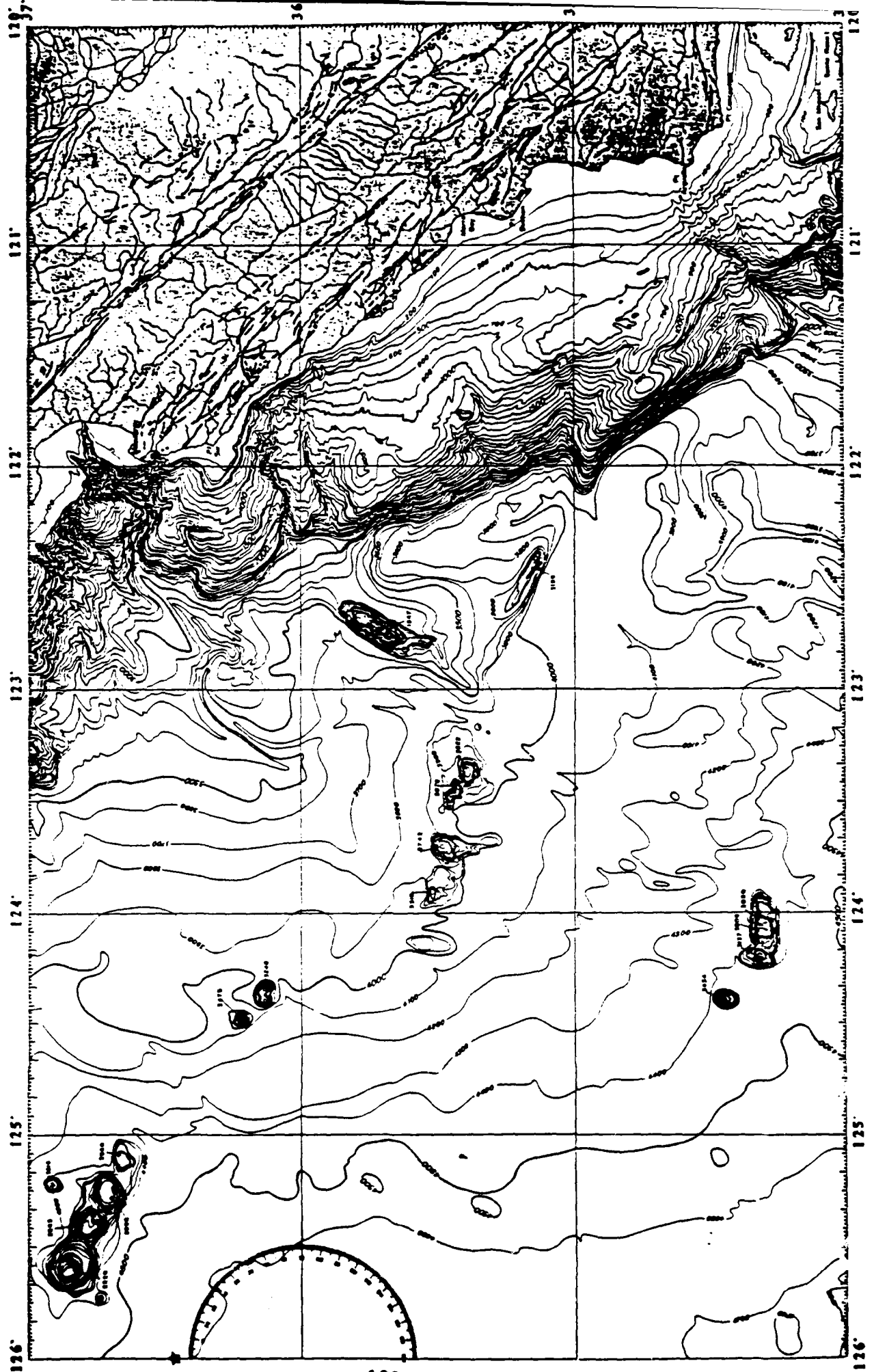


Figure 7. Proposed downslope conversion experiment area.



## References

- [1] D. Ross, "Role of Propagation in Ambient Noise," SACLANTCEN Conference Proceedings No. 32 (Underwater Ambient Noise), 15 June 1982, SACLANT ASW Research Centre, San Bartolomeo, Italy.
- [2] R.A. Wagstaff, "Low-frequency ambient noise in the deep sound channel - The missing component," *J. Acoust. Soc. Am.* 69(4): 1009-1014 (1981).
- [3] S.C. Wales and O.I. Diachok, "Ambient noise vertical directionality in the northwest Atlantic," *J. Acoust. Soc. Am.* 70: 577-582 (1981).
- [4] R. Dashen and W. Munk, "Three models of global ocean noise." *J. Acoust. Soc. Am.* 76: 540-554 (1984).
- [5] W.M. Carey and R.A. Wagstaff, "Low-frequency noise fields," *J. Acoust. Soc. Am.* 80(5): 1523-1526 (1986).
- [6] R.W. Bannister, "Deep sound channel noise from high-latitude winds," *J. Acoust. Soc. Am.* 79(1): 41-48 (1986).
- [7] J. Northrop, M.S. Loughridge, and E.W. Werner, "Effect of Near-Source Bottom Conditions on Long-Range Sound Propagation in the Ocean," *J. Geophys Res* 73: 3905-3908 (1968).
- [8] G.B. Morris, "Preliminary Results on Seamount and Continental Slope Reflection Enhancement of Shipping Noise," SIO Ref 75-34, Scripps Institution of Oceanography (1975).
- [9] G.R. Ebbeson and R.G. Turner, "Sound propagation over Dickins Seamount in the Northeast Pacific Ocean," *J. Acoust. Soc. Am.* 73: 143-152 (1983).
- [10] N.R. Chapman and G.R. Ebbeson, "Acoustic shadowing by an isolated seamount," *J. Acoust. Soc. Am.* 73: 1979-1984 (1983).
- [11] T.M. Brocher, B.T. Iwatake, and D.A. Lindwall, "Experimental studies of low-frequency waterborne and sediment borne acoustic wave propagation on a continental shelf," *J. Acoust. Soc. Am.* 74: 960-972 (1983).
- [12] W.M. Carey, R.A. Wagstaff, B.A. Brunson, and M.R. Bradley, "Low-Frequency Noise Fields and Signal Characteristics," pp. 753-766, appears in: T. Akalame and J.M. Berkson (eds). *Ocean Seismo-Acoustics*. NY: Plenum, 1985.
- [13] W.M. Carey, "Measurement of down-slope sound propagation from a shallow source to a deep ocean receiver." *J. Acoust. Soc. Am.* 79(1): 49-59 (1986).
- [14] S.E. Dosso and N.R. Chapman, "Measurement and modeling of downslope acoustic propagation loss over a continental slope," *J. Acoust. Soc. Am.* 81: 258-268 (1987).
- [15] W.M. Carey, I.B. Gereben, and B.A. Brunson, "Measurement of sound propagation downslope to a bottom-limited sound channel," *J. Acoust. Soc. Am.* 81(2): 244-257 (1987).
- [16] R. Doolittle, A. Tolstoy, and M. Buckingham, "Experimental confirmation of horizontal refraction of cw acoustic radiation from a point source in a wedge-shaped ocean environment," *J. Acoust. Soc. Am.* 83: 2117-2125 (1988).
- [17] S.A.L. Glegg and J.R. Yoon, "Experimental measurements of 3-dimensional propagation in a wedge-shaped ocean with pressure release boundary conditions, submitted *J. Acoust. Soc. Am.* (1988).
- [18] W.S. Hodgkiss and F.H. Fisher, "Vertical Directionality of Ambient Noise at 32°N as a Function of Longitude," TM-387, Marine Physical Laboratory, Scripps Institution of Oceanography (1987). Results summarized in: Y.T. Chan (ed). *Underwater Acoustic Data Processing*. Boston: D. Reidel, 1988.



# **NOISE FLOOR MECHANISMS**

**R.D. GAUL / A. WITTENBORN (BSC)**

### Noise Floor Mechanisms

This brief reviews an ambient noise measurement exercise that occurred in the Northeast Pacific in September and October 1975. A selection of about 20% of the acoustic data were analyzed and results are given in a report by A.F. Wittenborn published by Tracor in April 1976. The report has been declassified. Most of the viewgraphs in this presentation are taken or derived from that report; all are unclassified.

CHURCH OPAL EXERCISE (U)

ACODAC MEASUREMENTS (U)

AMBIENT NOISE AND ASSOCIATED PROPAGATION  
FACTORS AS A FUNCTION OF DEPTH AND  
WIND SPEED IN THE DEEP OCEAN (U)  
(PRELIMINARY REPORT)

(Preliminary Report)

by

A.F. Wittenborn  
Principal Investigator

Tracor, Inc.  
1601 Research Blvd.  
Rockville, Maryland 20850

1 April 1976

Prepared for  
LONG RANGE ACOUSTIC PROPAGATION PROJECT,  
NAVAL OCEAN RESEARCH AND DEVELOPMENT ACTIVITY

### Bathymetry for the Northeast Pacific

The bathymetry of the Northeast Pacific is dotted with widely dispersed seamounts, but otherwise devoid of major restrictions for long range acoustic propagation. The measurement area is about midway between the Hawaiian Islands (lower left corner) and San Diego. All the major transoceanic shipping lanes are well to the north and the region to the south is bottom limited for long range acoustic propagation.

BATHYMETRY FOR  
NORTHEAST PACIFIC  
1977

LEGEND	
DEPTH IN METERS	
—	2000
- - -	3000
· · ·	4000
· · ·	5000
· · ·	6000
· · ·	7000

CONTOUR INTERVAL - 1000 METERS  
(BASED ON SOUND SPEED IN WATER  
OF 1500 METERS/SECOND)



### Bathymetry in the Vicinity Measurement Site

Ambient noise measurements were made for two weeks at the "ACODAC Site." The location is on an abyssal plain with a characteristic depth variability of about 200 fathoms within a range of 100 miles from the site. To the north is an east-west range of scattered seamounts.

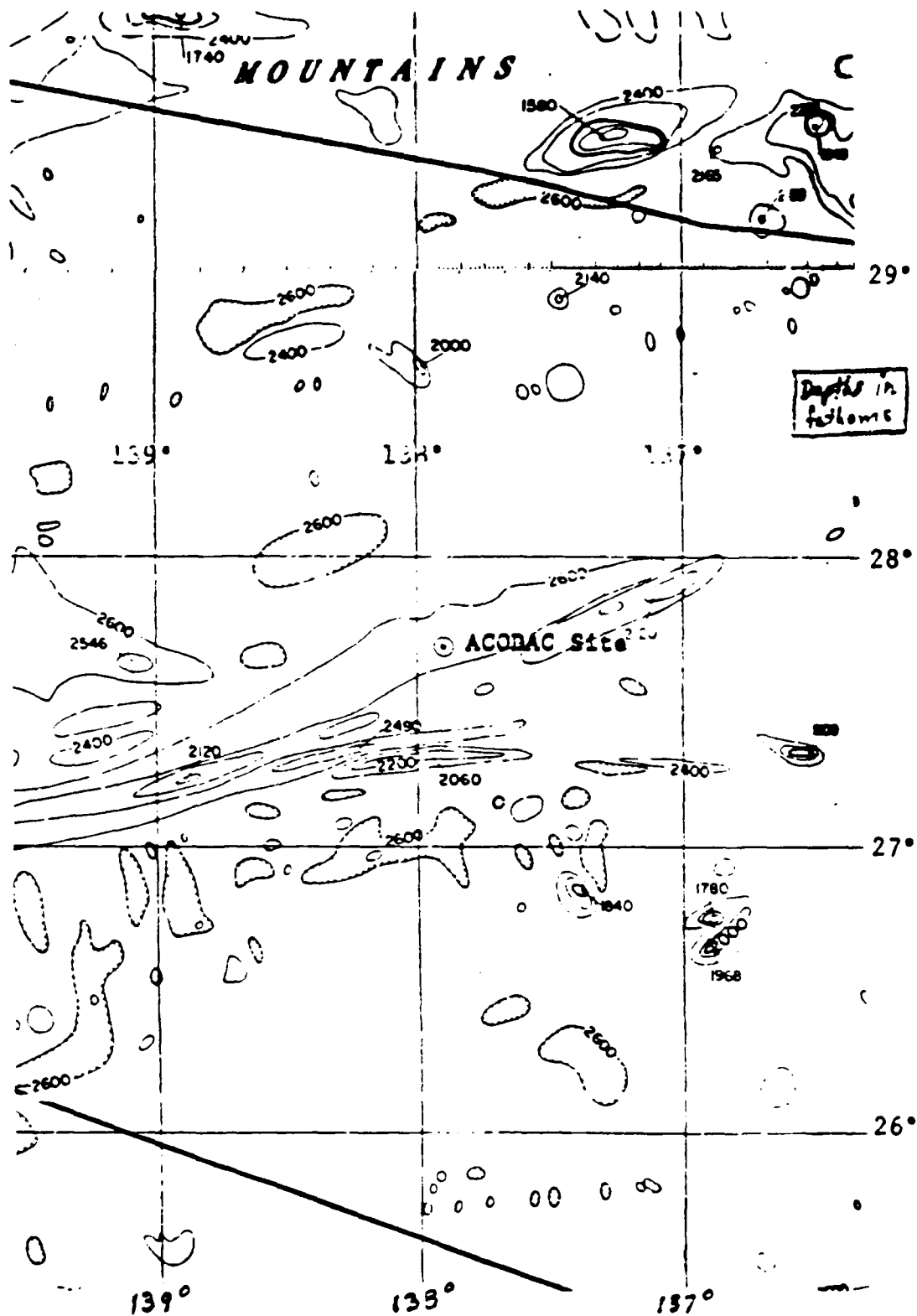


Figure 18(U). Bathymetry in the vicinity of the measurement site. The black lines are ship tracks discussed in text (U)

### Sound Speed Profile

The sound speed profile at the measurement site is devoid of irregular features. The base of the sound channel (critical depth) is at 4,060 meters which is slightly more than 600 meters above the ocean bottom.

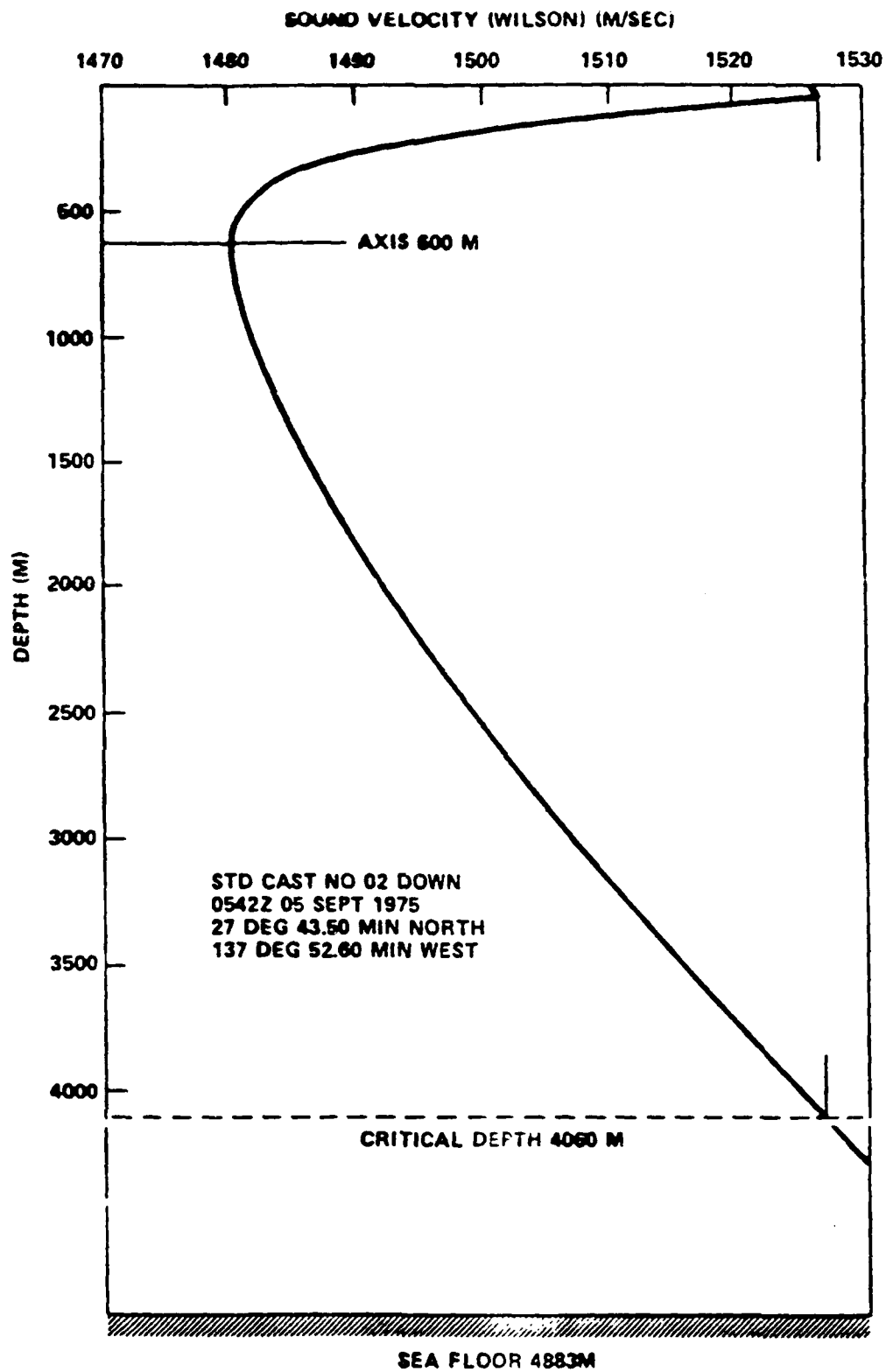


Figure 2(U). Sound speed profile at the measurement site (U)

### Hydrophone Locations as a Function of Depth

Single hydrophones were placed vertically in the depth range from 3,460 meters to 4,850 meters (10 meters above the ocean bottom). Data were analyzed from eight hydrophones, two of which were above the critical depth.

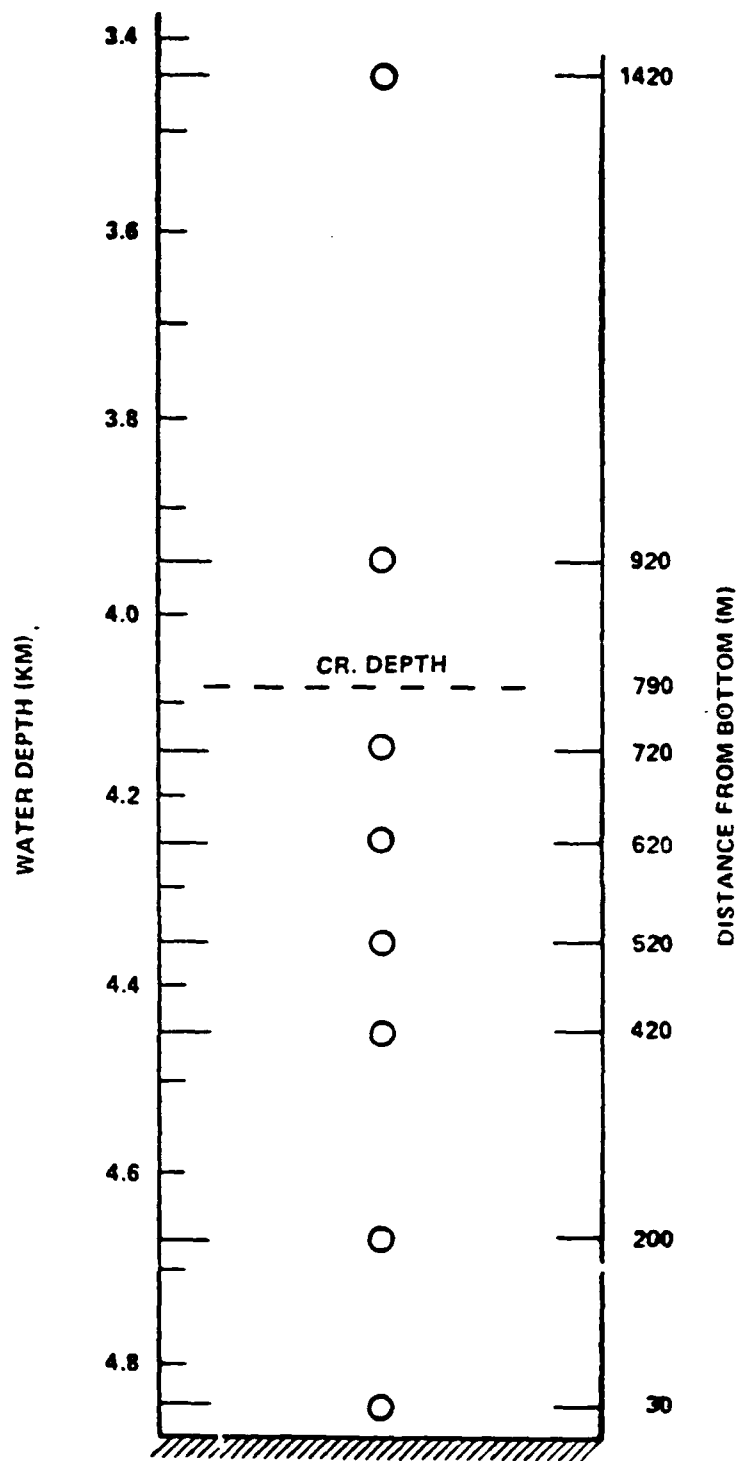


Figure 1(U). Hydrophone locations as a function of depth or distance from the bottom for the CHURCH OPAL data presented in this report (U)

#### Processing Technique

The data from selected hydrophone time segments were spectrally analyzed at a frequency resolution of 0.2 Hz. Spectra for evaluation of acoustic levels were based on an integration time of 10 minutes. Samples for ambient noise analysis were taken during periods when wind speed was judged to be steady for at least 12 hours.

# PROCESSING TECHNIQUE

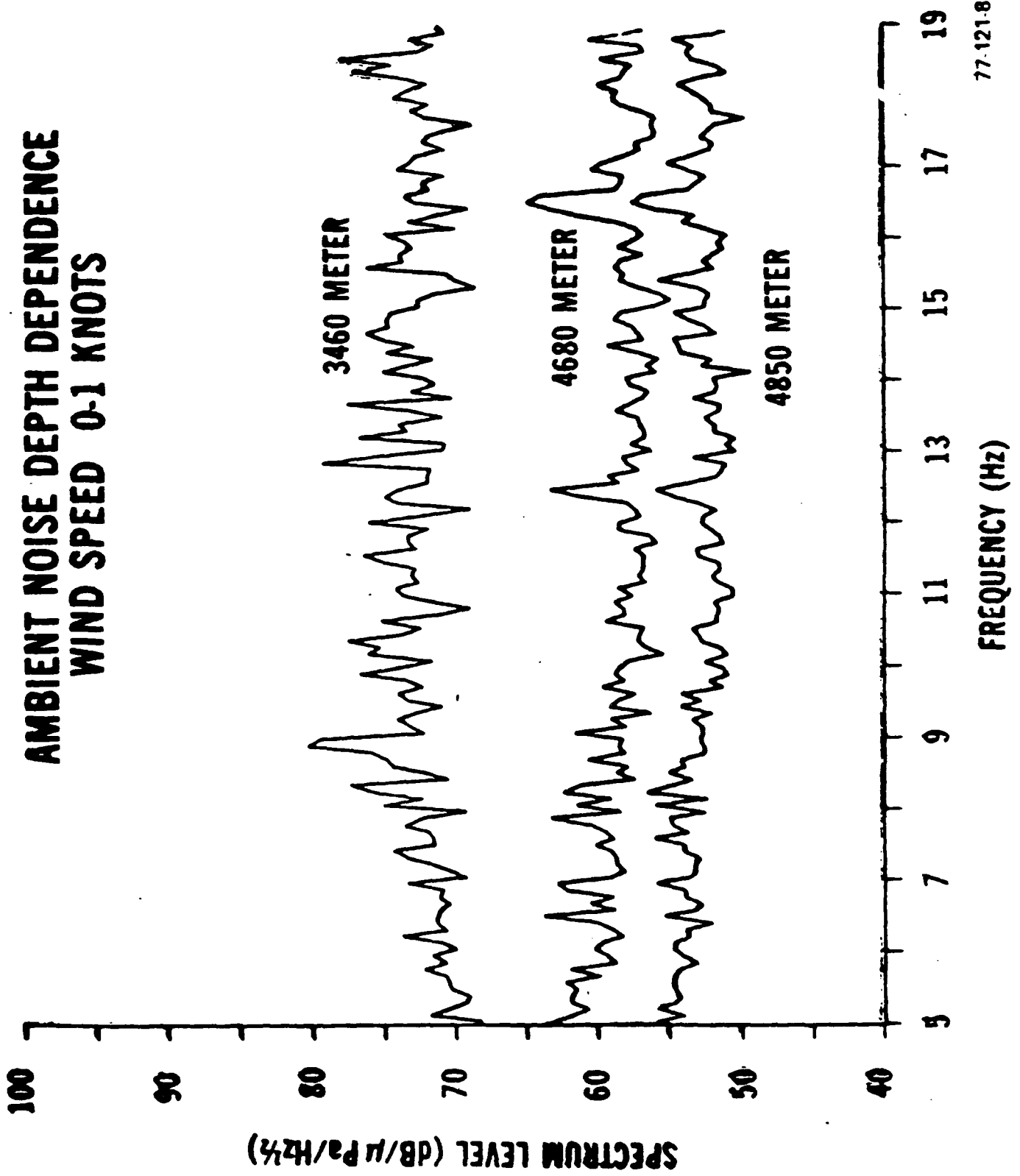
- NARROW BANDWIDTH
- "STATIONARY" SAMPLES

77-121-35

#### Ambient Noise Depth Dependence

The ambient noise spectrum in the frequency range of 5-19 Hz clearly shows a depth effect under calm conditions. The average level across the 5-19 Hz band is between 70-75 dB for the phone in the sound channel compared to 55-60 dB midway between the critical depth and the bottom, and 50-55 dB just above the bottom. It is noteworthy that the noise level in the channel tends to fade slightly below 10 Hz, whereas below the critical depth, noise below 10 Hz tends to rise slightly.

**AMBIENT NOISE DEPTH DEPENDENCE  
WIND SPEED 0.1 KNOTS**

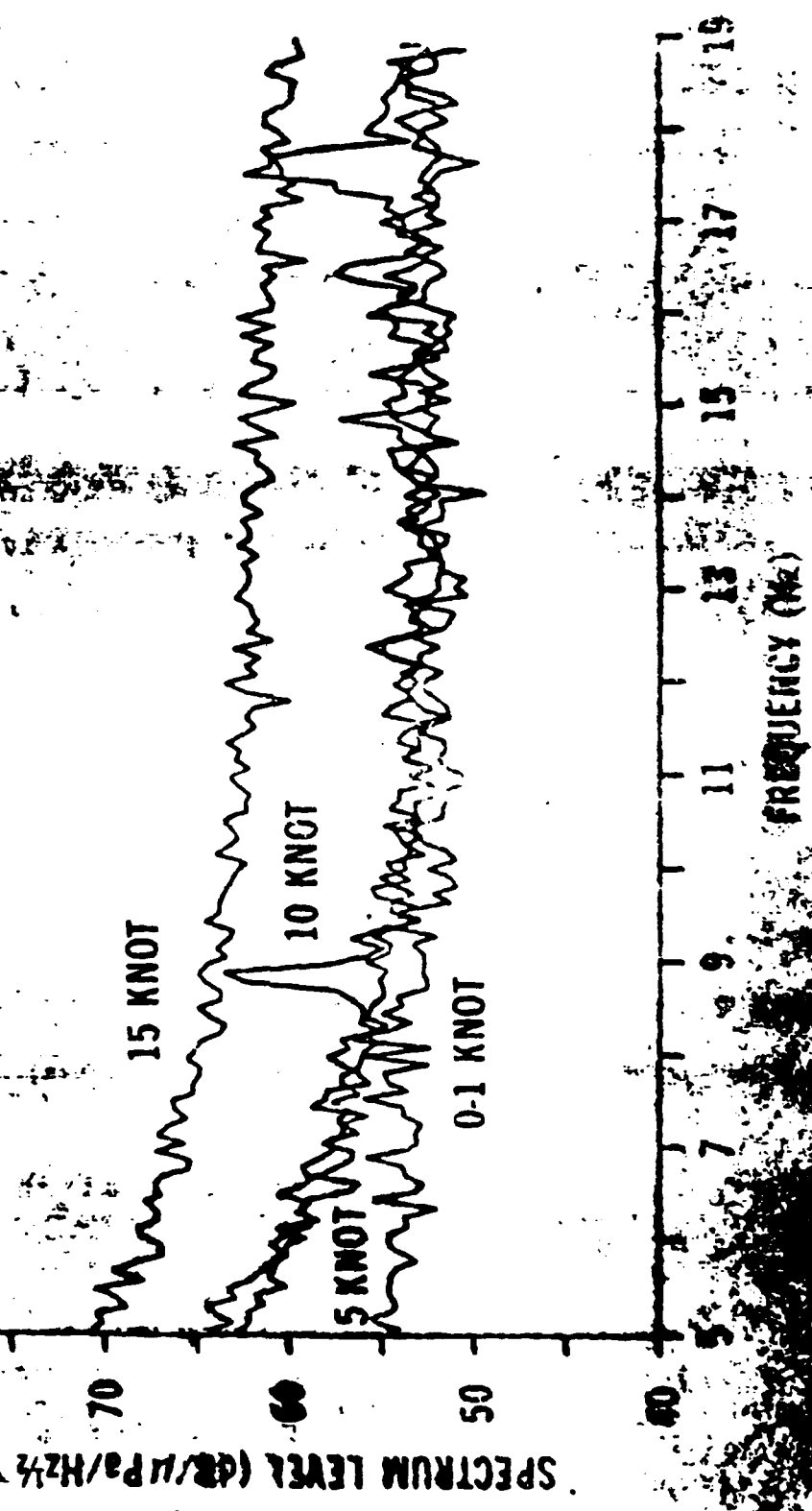


77-121-8

#### Ambient Noise Wind Speed Dependence

Some samples are shown for ambient noise at the maximum depth hydrophone at wind speeds up to 15 knots. The band is 5-19 Hz. Some of the data samples exhibit contamination by distant ship noise which also may account for the similarity of levels at zero, 5 and 10 knots. Note again that levels tend to rise below 10 Hz, but are flat up to 19 Hz.

AMBIENT NOISE  
DEPENDENCE AT 40 M



### Ambient Noise Levels

Ambient noise levels at 50 Hz within the sound channel show little depth effect and average about 75 dB. Near the ocean floor the levels range from about 50 dB at 5 knots wind speed to 60 dB at 15 knots. It is apparent that a distant source noise within the sound channel masks the locally generated wind noise. The containment of distant source noise in the channel allows the wind noise dependence to emerge at greater depths. However, the levels for 10 and 15 knot wind speeds likely are contaminated because the curves are not vertical at the bottom.

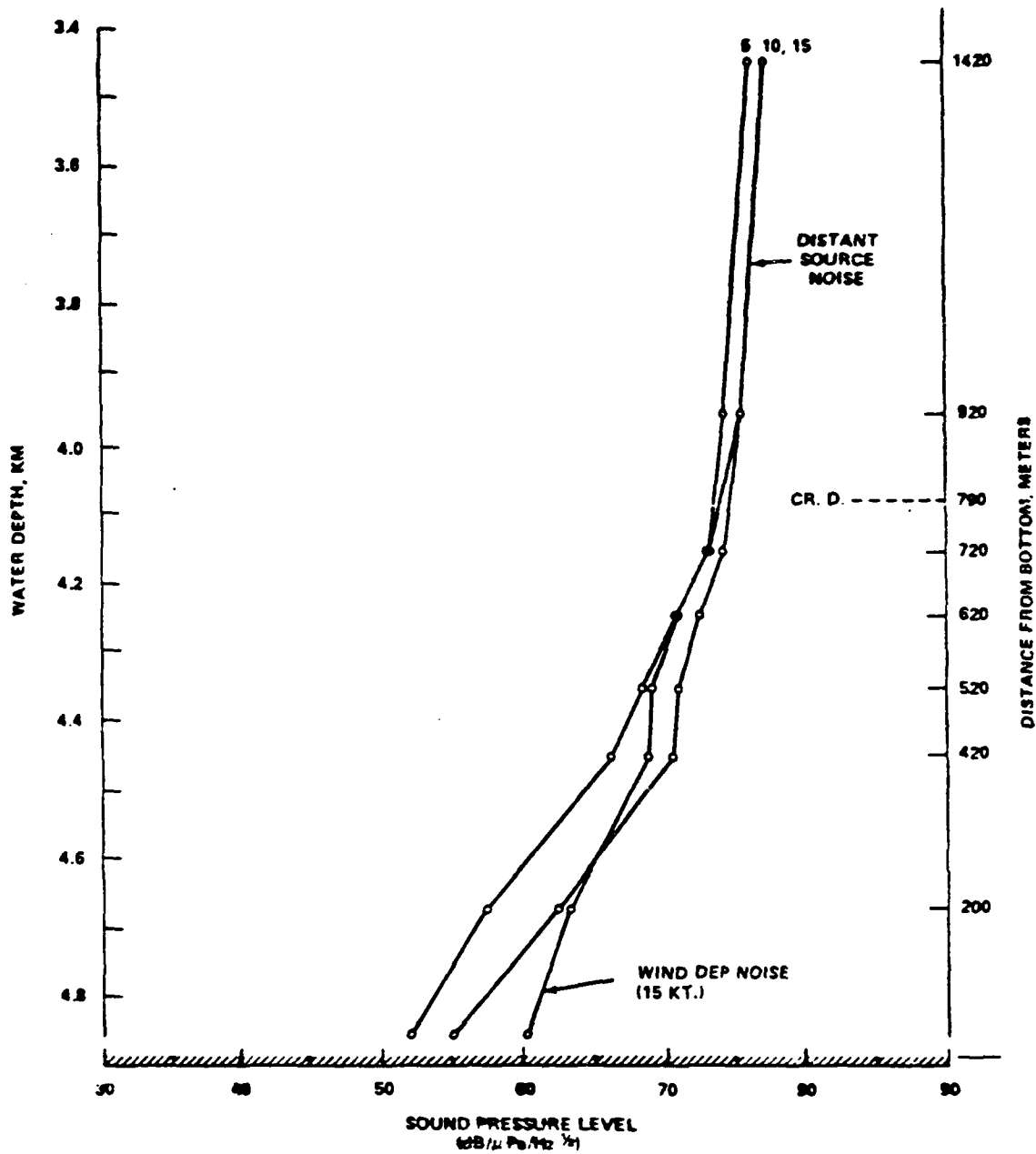


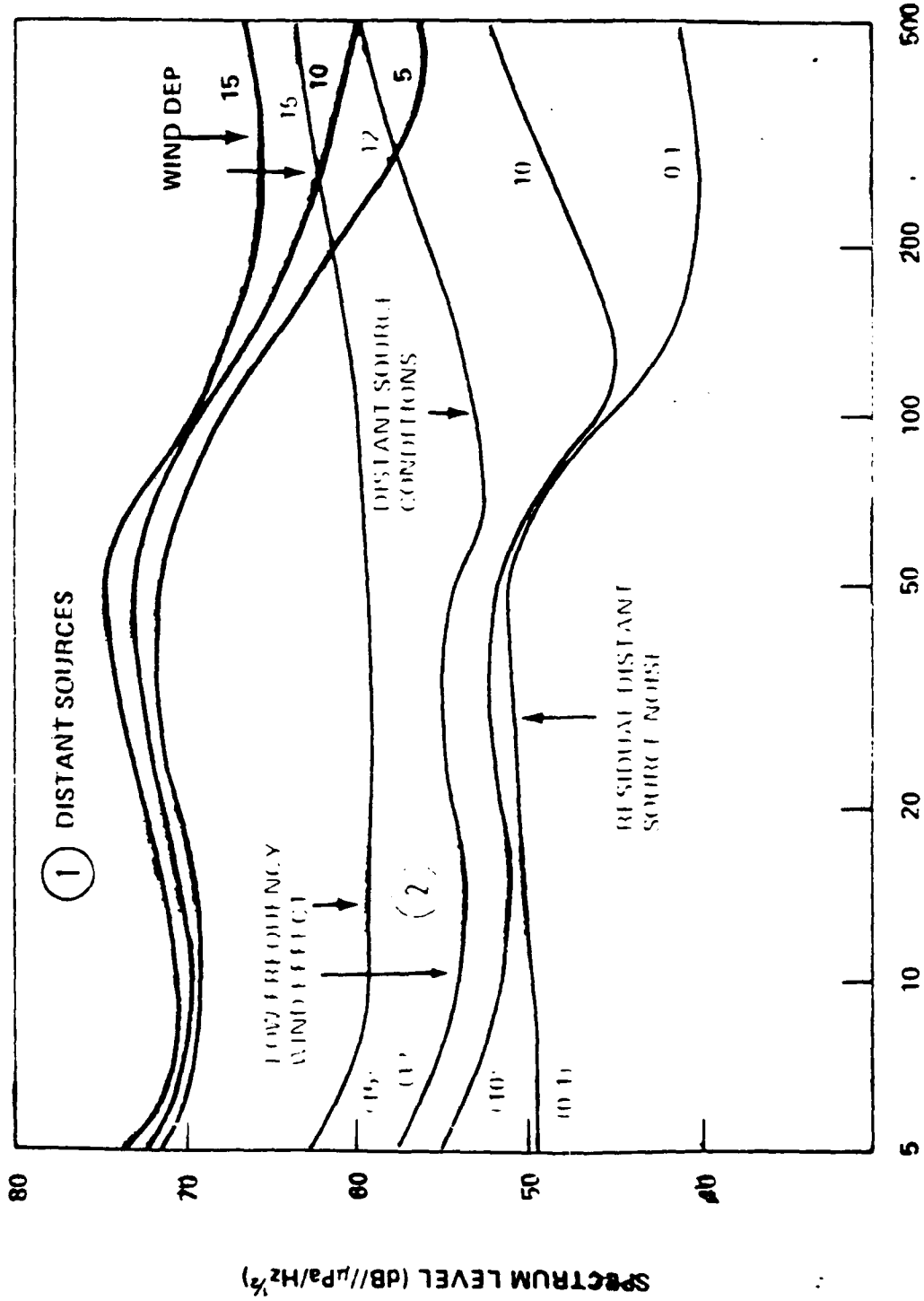
Figure 15(C). Ambient noise levels as a function of depth at 50 Hz for wind speeds of 5, 10, and 15 knots (U)

### Spectrum Level versus Frequency for 3960 and 4850 m

The curves based on data taken within the sound channel show that distant sources dominate at all frequencies up to at least 300 Hz. The curves for the near-bottom phone show contamination at frequencies below about 100 Hz for wind speeds below 12 knots. Therefore, levels solely dependent on these low wind speeds will be lower than shown. The curve for 15 knots appears to be a valid representation for wind dependence.

① 3960 M

② 4850 M

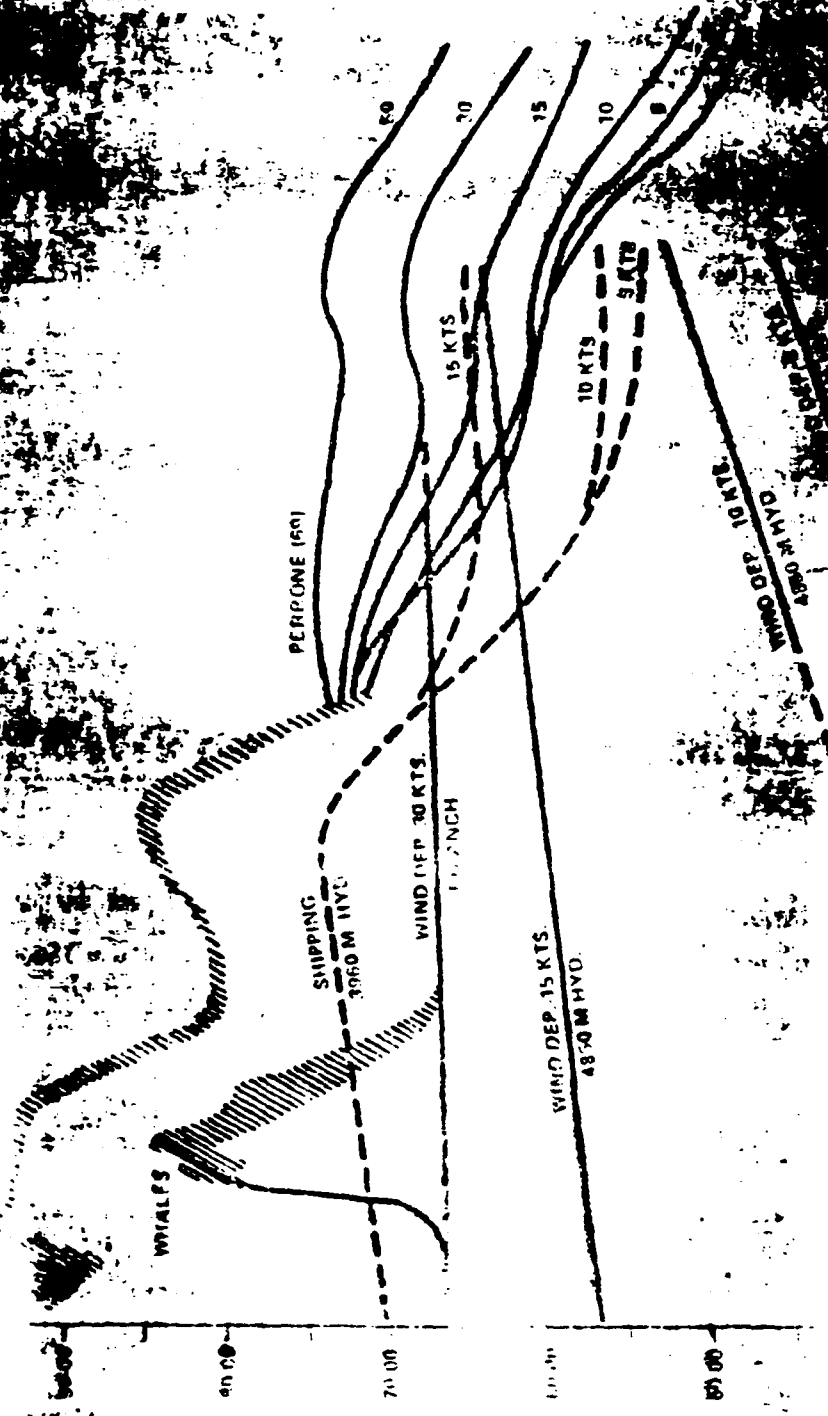


FREQUENCY (Hz)

77-121-12

#### Spectrum Level versus Frequency Relationships

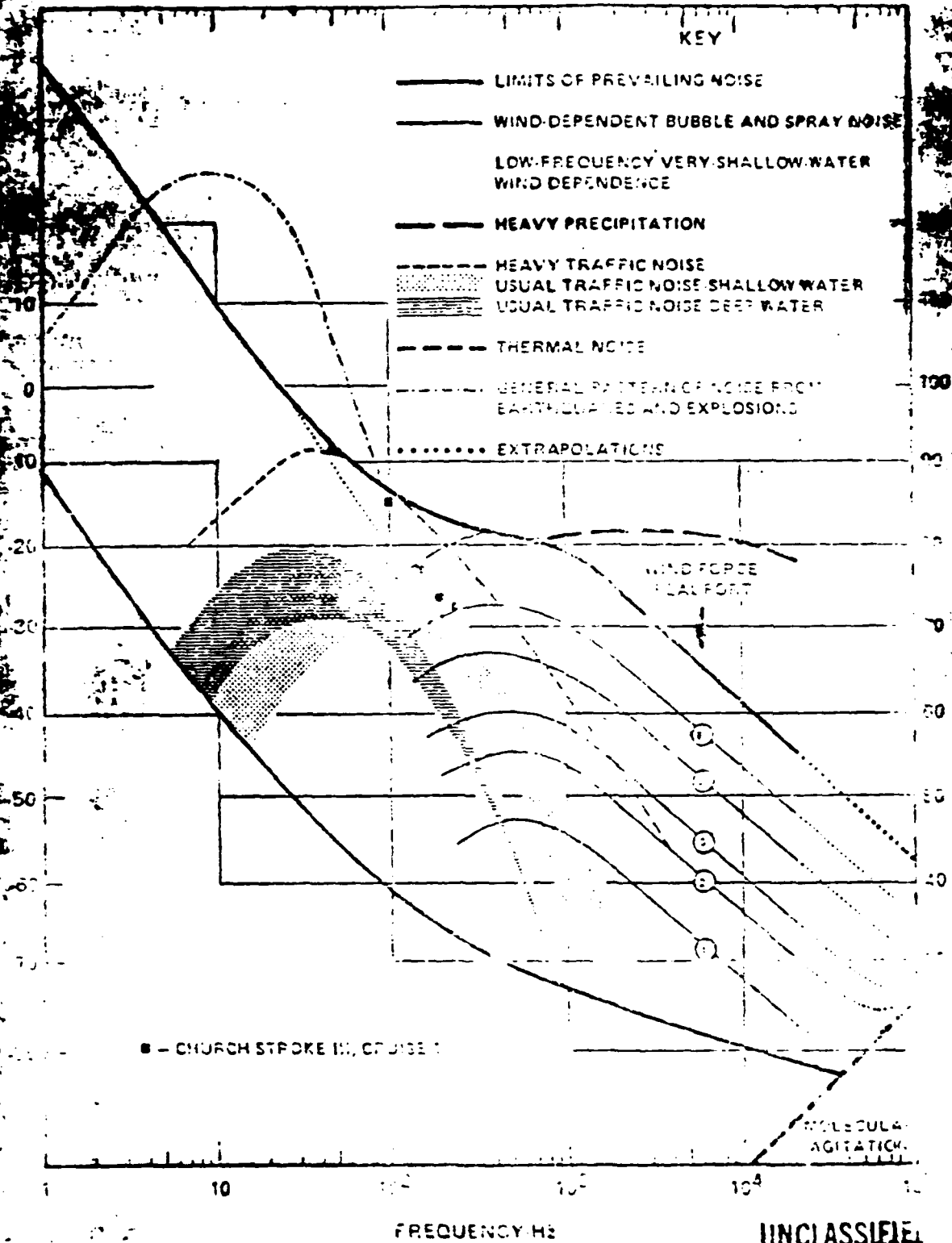
The composite curves show that the CHURCH OPAL data can be merged consistently with data from Bermuda as reported by Perrone. The hydrophones at Bermuda are within the sound channel so distant sources obscure the wind effect at low frequencies except during storms.



Sound Pressure Spectrum Level versus Frequency

The curves attributed mainly to Wenz are shown for reference. Note that the wind dependence curves show a maximum between 100 Hz and 1,000 Hz.

UNCLASSIFIED



UNCLASSIFIED

75-570-25

### Suggested Revision of the "Wenz Curves"

A set of curves are given that merge the CHURCH OPAL results with the Wenz curves for wind dependence. Levels below 40 dB at 10 Hz for up to 10 knot winds are inferred recognizing the effect of distant source contamination below 100 Hz.

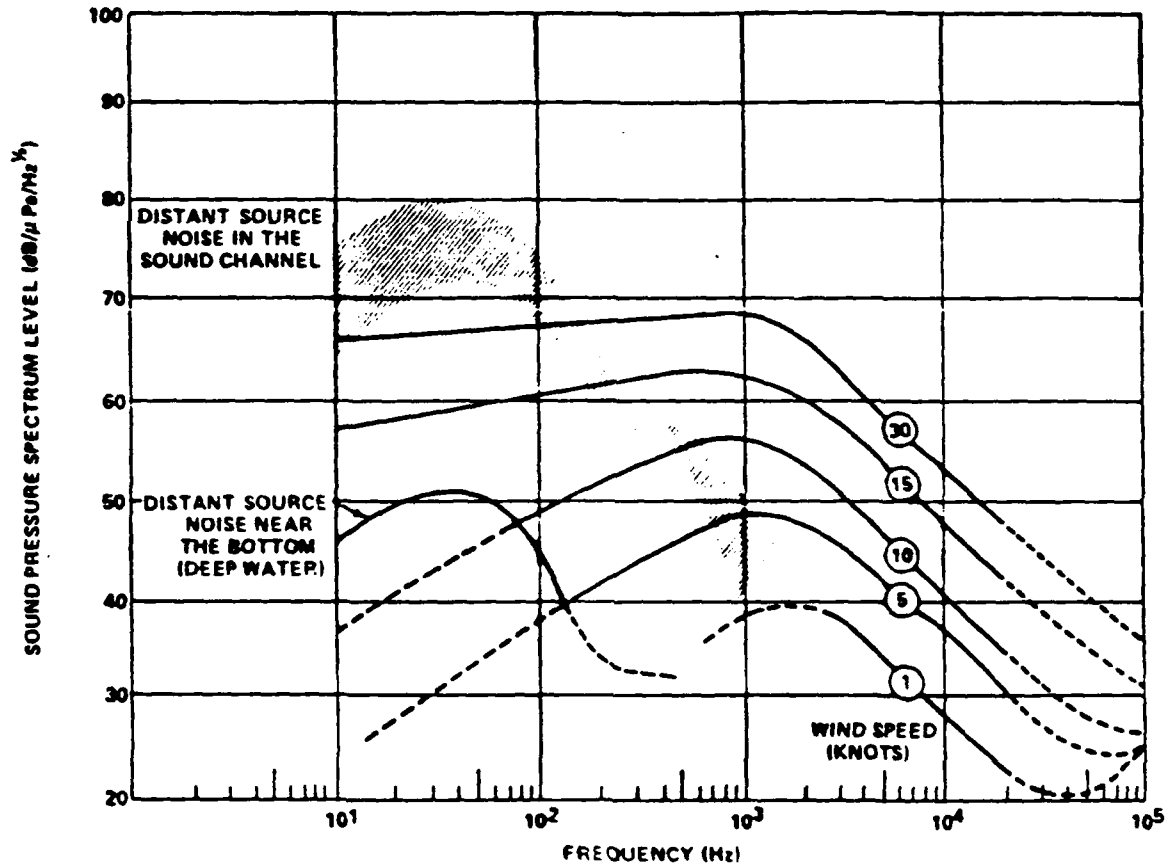


Figure S-1(U). Suggested revision of the "Wenz Curves" for locally generated wind dependent noise between 10 and 500 Hz (U)

### Measured Spectra

The spectra obtained during passage of a freighter 100 miles away show the effect of distant source masking in the sound channel. The 10-15 dB ambient noise reduction with depth makes the ship signature stand out against the background.

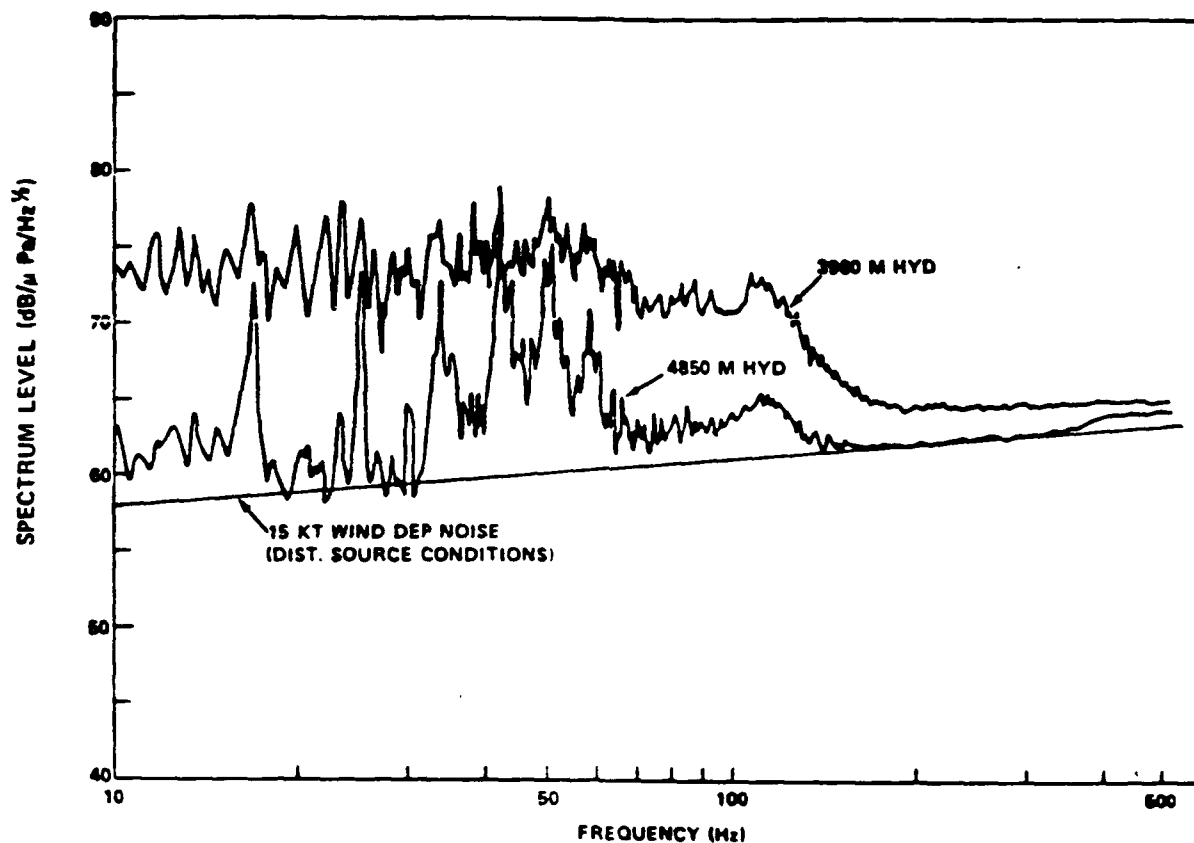
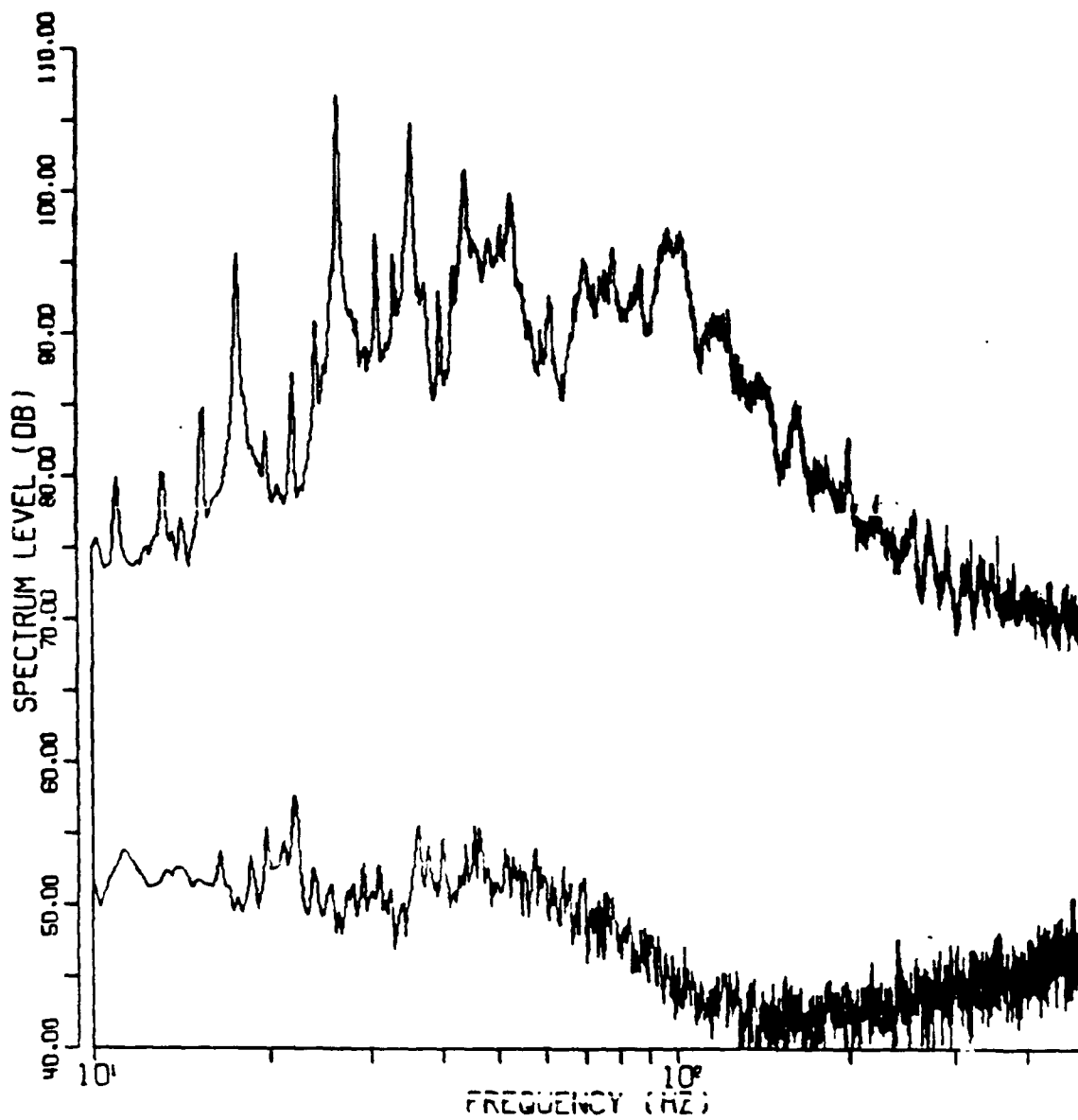


Figure S-2(U). Spectra measured with the 3960 meter (upper curve) and the 4850 meter (lower curve) hydrophones at the closest point of approach of a freighter (German, ADOLF LEONHARDT, bulk carrier, 22,000 tons, 10,600 bhp, 15 knots) 100 miles from the receivers, illustrating the lack of a significant depth effect for a "not distant" source. Local wind speed is 15 knots. (U)

### Two Examples of Processed Spectra

The example shows the changes in level and character of the spectrum when a freighter passed overhead. The lower spectrum was typical of the period just before arrival of the ship.



0013RUEE 253/13/35 - 253/13/45

Figure 6(U). Two examples of processed spectra as measured with the 4850 meter hydrophone. The upper curve corresponds to the CPA of a freighter passing overhead, 0.1 Hz frequency resolution 10 minute integration time. The lower curve corresponds to distant shipping (as defined in the text), 5 knot wind speed, 0.2 Hz frequency resolution, 10 minute integration time (U)

### Estimated Source Level a Function of Frequency

The spectrum is the signature for a ship that passed within one mile of the ACODAC site. The CHURCH OPAL database is a reservoir of single ship passages that can be fully documented for signature characterization.

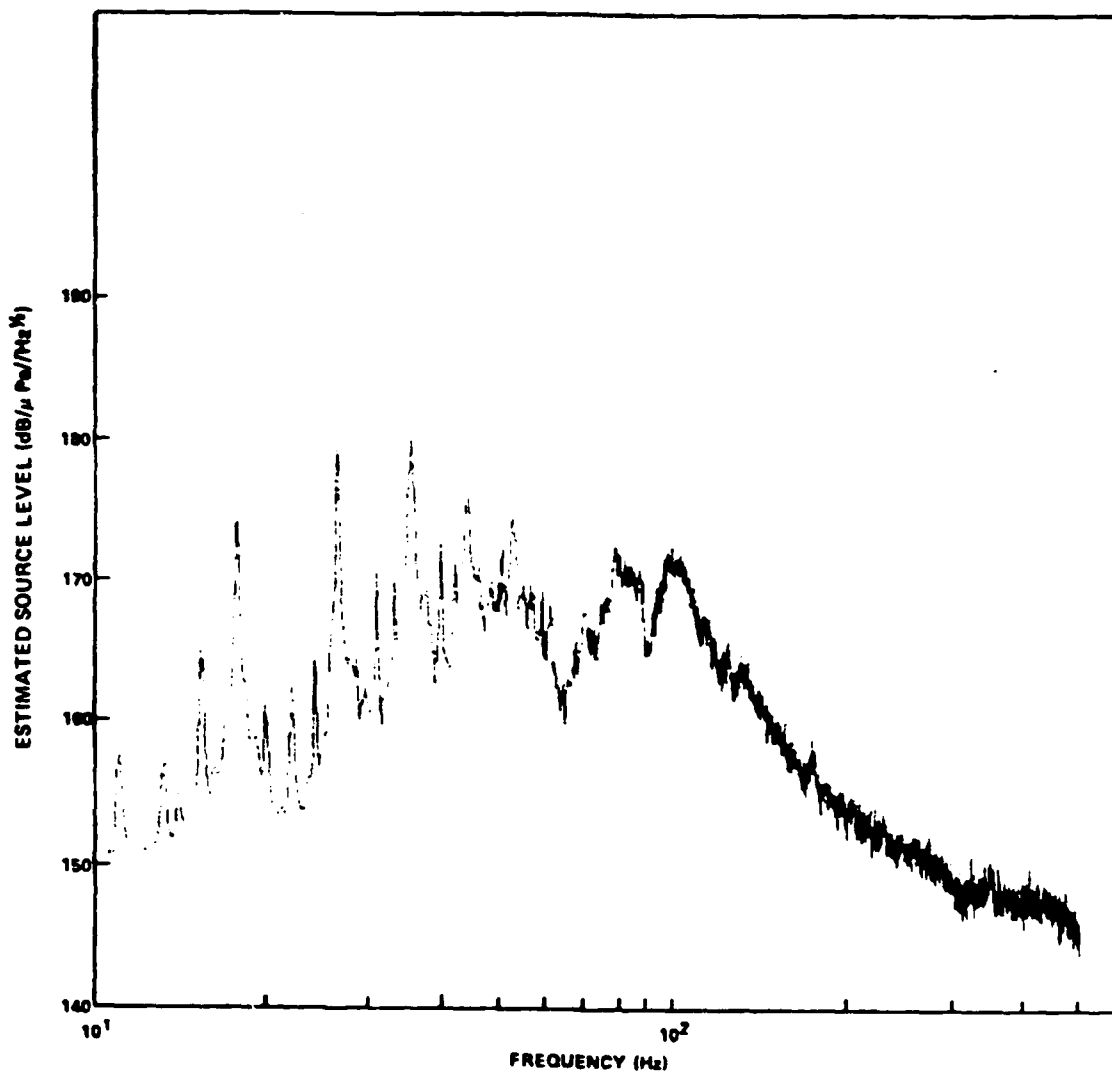


Figure 21(U). Estimated source level as a function of frequency for a Japanese bulk carrier (KANESHIZER MARU, 12,272 tons, 9400 brake horsepower, 14.75 knots) (U)



**AEAS NOISE MODELING PROGRAM -  
DIRECTIONS / NEEDS**

**E. CHAIKA (ONR)**



**VLF Ambient Noise Modeling**

**in the  
AEAS Program**



**Ed Chaika**

**September 1988**





# NOISE MODELS

## Type 1: System Design And Detailed Analysis

**Features:** Detailed source and propagation treatment,  
beamforming, discrete and distributed  
sources, statistics

**Example:** RANDI

## Type 2: Performance Assessment

**Features:** High speed, efficient, fleet tested, beamforming,  
discrete and distributed sources

**Example:** ANDES II



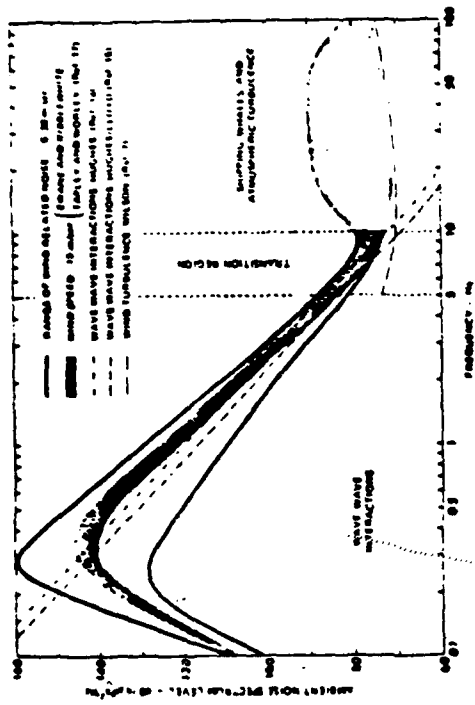


# VLF AMBIENT NOISE SOURCES

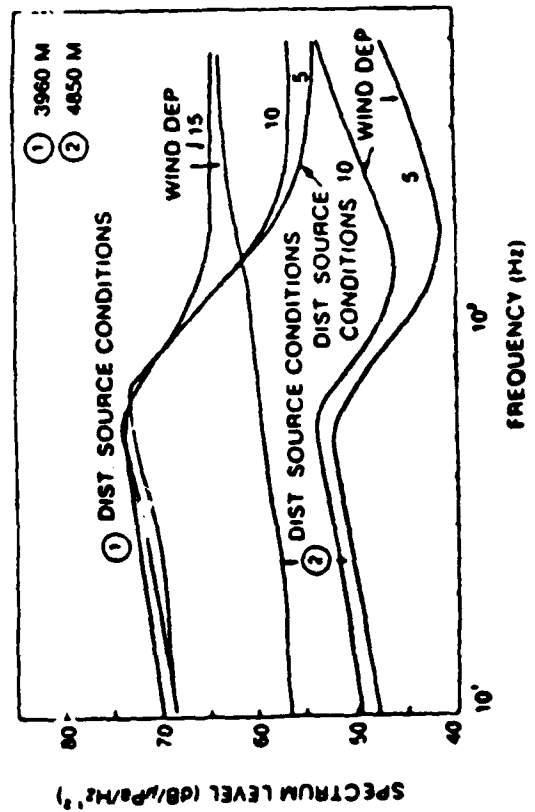
## MAJOR PERSISTENT SOURCES

- WAVE/WAVE
- WIND
- SHIPPING

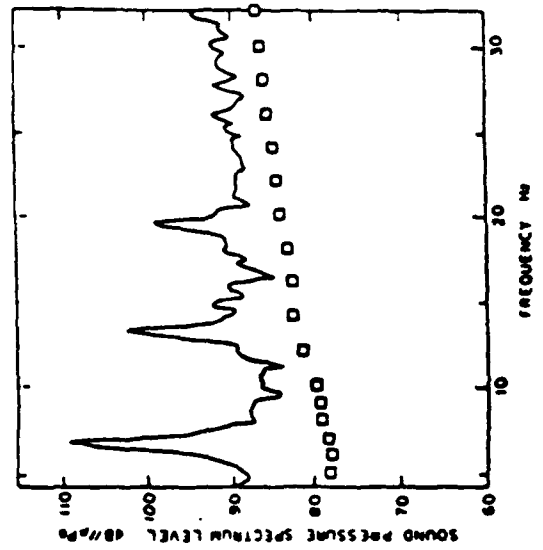
## WAVE/WAVE INTERACTION



## WIND



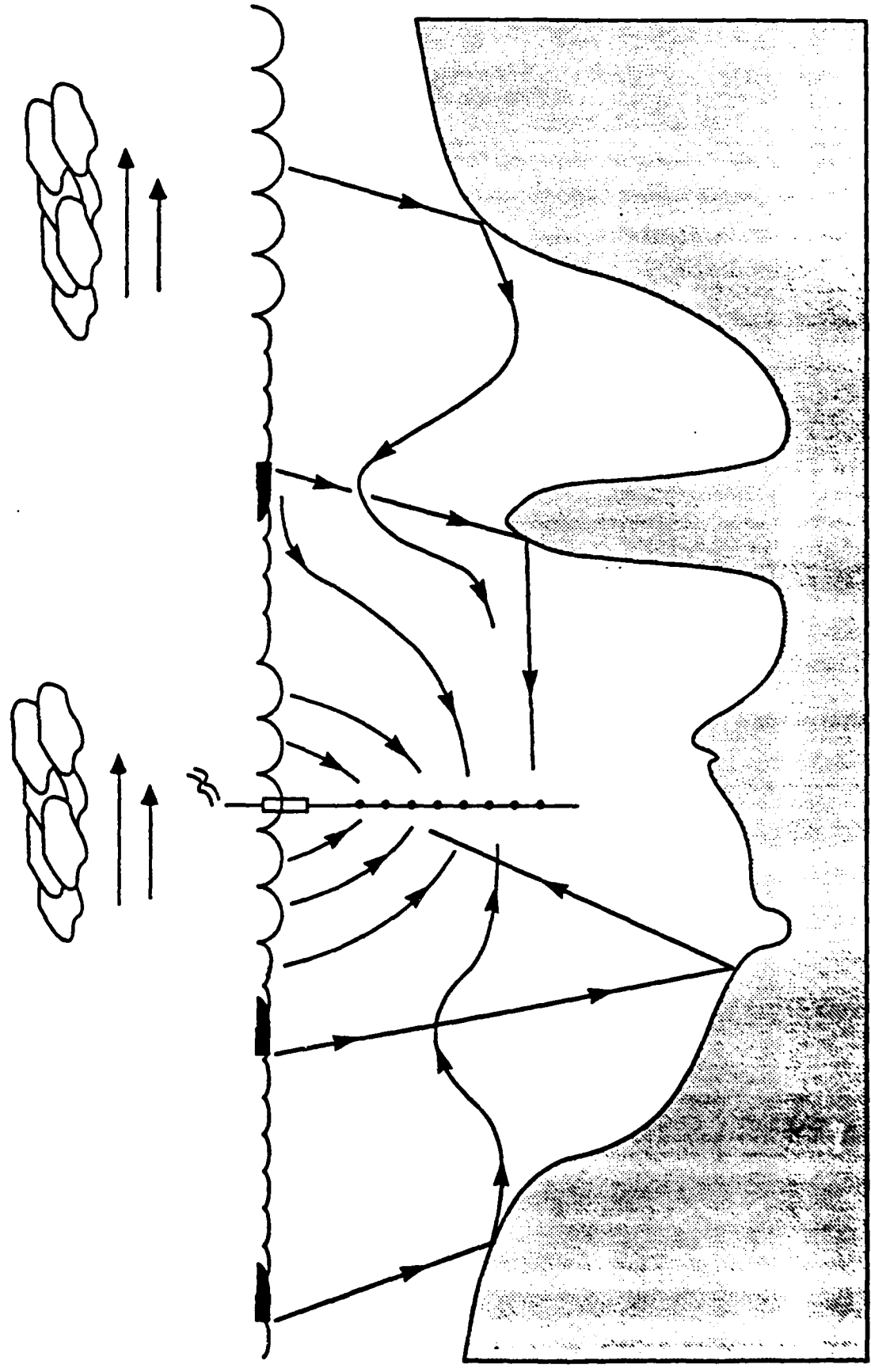
## SHIPS







# LOW FREQUENCY NOISE MODELING







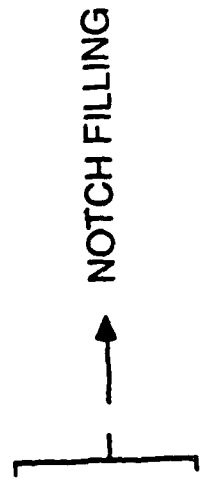
# GENERIC LOW FREQUENCY NOISE MODEL STRUCTURE

## 1. NOISE SOURCE DESCRIPTION

- TYPES (SHIPPING, LOCAL WIND, DISTANT WIND,...)
- SPATIAL DISTRIBUTION
- SOURCE SPECTRA (LEVEL vs FREQUENCY)
- RADIATION CHARACTERISTICS

## 2. TRANSMISSION LOSS MODEL

- FAST AND RANGE DEPENDENT
  - BASIN WIDE PROPAGATION CALCULATIONS REQUIRED
- MAJOR PROPAGATION EFFECTS ADEQUATELY TREATED
  - DOWNSLOPE ENHANCEMENT
  - LOW TO HIGH LATITUDE  
SOUND CHANNEL AXIS SHOALING
- VERTICAL ARRIVAL STRUCTURE AND TL DEPTH  
DEPENDENCE AVAILABLE







# GENERIC LOW FREQUENCY NOISE MODEL STRUCTURE

## 3. DETAILED OCEANOGRAPHIC DATA BASES

- BATHYMETRY
- WIND SPEED
- BOTTOM LOSS
- SHIPPING
- SOUND VELOCITY

## 4. EXECUTIVE

- EFFICIENT ACCUMULATOR
- OMNI
- HORIZONTAL AND VERTICAL DIRECTIONALITY
- STATISTICS

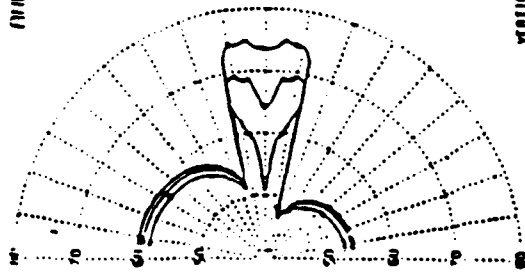




# ANDES NOISE PREDICTION SYSTEM

ANDES 2.2 Test Case - HLF Pac

500 Hz : 68.7 dB  
 1000 Hz : 73.3 dB  
 2000 Hz : 68.7 dB



500 Hz : 68.7 dB  
 1000 Hz : 73.3 dB  
 2000 Hz : 68.7 dB

ANDES VERSION 2.2 - HLF PAC  
 VERTICAL DIRECTIONALITY (1000 Hz)

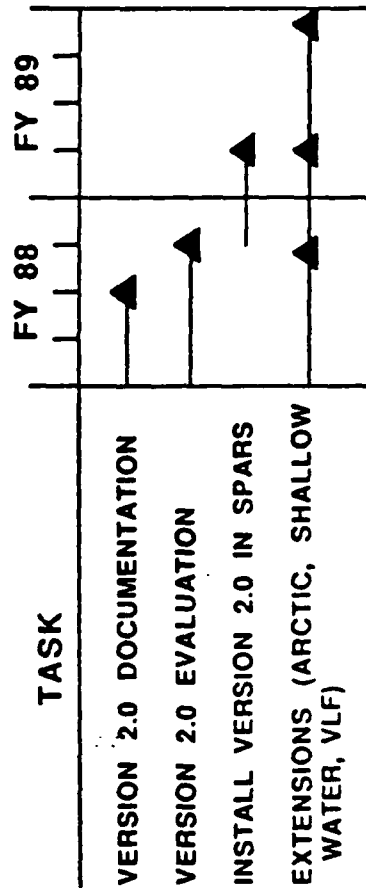
## MISSION

1. PROVIDE FAST, ACCURATE ESTIMATES OF THREE DIMENSIONAL NOISE DIRECTIONALITY
2. IMPLEMENT ON NAVY STANDARD DESK-TOP COMPUTER

## ACCOMPLISHMENTS

VERSION 1.0 COMPLETED WITH DOCUMENTATION FOR VAX AND NAVY STD DESK-TOP COMPUTER  
 USED EXTENSIVELY TO SUPPORT PMW 180  
 EVALUATED WITH ONR, SPAWAR AND NAVAIR DATA  
 VERSION 2.0 COMPLETED (INCLUDES ASTRAL 2.0 UPGRADES)  
 DELIVERED TO ARL/UT FOR INCLUSION IN SPARS

## SCHEDULE







## ANDES II NOISE MODEL

- LOCAL WIND SOURCE
- HITS DISTRIBUTED SHIPPING SOURCES
- DISTANT WIND SOURCE
  - COMPLEMENT OF LOCAL WIND SOURCE
  - DRIVEN BY SINGLE WIND SPEED
- DISCRETE SOURCES
  - USER SPECIFICS: RANGE, BEARING, SOURCE DEPTH, AND SOURCE LEVEL
  - DISCRETE HITS SOURCES
- CZ-ASTRAL TL MODEL
- EXECUTIVE DISPLAYS
  - ENVIRONMENTAL DATA
  - TRANSMISSION LOSS
  - SOURCE DENSITY
  - NOISE DIRECTIONALITY





# DISCRETE SHIPPING NOISE MODEL

- GENERATE BEAM TL (RANGE, BEARING) USING ASTRAL
- FROM HITS DETERMINE:
  - N, THE AVERAGE NUMBER OF SHIPS WITHIN A SPECIFIED RANGE OF THE RECEIVER
  - CUMULATIVE DISTRIBUTION FUNCTIONS (CDF) IN RANGE AND BEARING FOR SHIP LOCATIONS
- LOOP ON REALIZATIONS (MONTE CARLO)
  - DISTRIBUTE N SHIPS ACCORDING TO CDF'S
  - SUM BEAM NOISE FROM ALL SOURCES
- DISPLAY
  - BEAM NOISE CDF





**STATUS: ANDES EVALUATION**

---

- ANDES TESTING BY SAIC
  - SQUARE DEAL

- VLAM, TSVLA

- ANDES EVALUATION BY PSI

- CONTRACT SERIES

- RAMSDALE'S VEKA

- NRL VEKA





## NEW NOISE MODEL CAPABILITIES

- COMBINE LOCAL AND DISTANT WIND MODELS  
INTO SINGLE MODEL      FY 89
- VLF (5-20 Hz) NOISE MODELING      FY 89
  - CAN ASTRAL HANDLE THIS REGIME?
  - CAN WE IDENTIFY A MODEL FOR VLF  
SEA STATE NOISE?
  - HOW DO WE REPRESENT TONAL NATURE  
NOISE SPECTRUM?
- MODELING BEAM NOISE STATISTICS      FY 89
  - ESTIMATE TEMPORAL STATISTICS  
(CONDITIONAL PROBABILITIES)
  - USE WITH PSI BEAM INTERSECT MODEL





## ASTRAL UPGRADES

---

- ASTRAL SHALLOW WATER CAPABILITY  
(LOW FREQUENCY CUTOFF EFFECT) FY 88
- ACTIVATE ASTRAL SURFACE DUCT MODEL FY 88
- INVESTIGATE FEASIBILITY OF PROPERLY  
DOING PHASE INTEGRAL THROUGH SEDIMENT  
(IMPROVE SLOPE CONVERSION) FY 89





# DATA BASE UPGRADES

---

• BATHY: SYNBAPS → DBDBC -- FY 88

• GEO: BLUG → BLUG WITH SW -- FY 88

• SVP: WRIGHT/COLBURN → GDEM -- FY 88

• SHIPS: HITS → HITS WITH NOIC SW -- FY 89





# VLF AMBIENT NOISE MODEL EVALUATION

---

**APPROACH:** IDENTIFY KEY MECHANISMS/ISSUES AND VALIDATE  
TREATMENT IN INDIVIDUAL NOISE MODEL COMPONENTS

**REQUIREMENTS:** OCEANOGRAPHIC AND ACOUSTIC DATA FROM  
CAREFULLY PLANNED FIELD EXERCISES





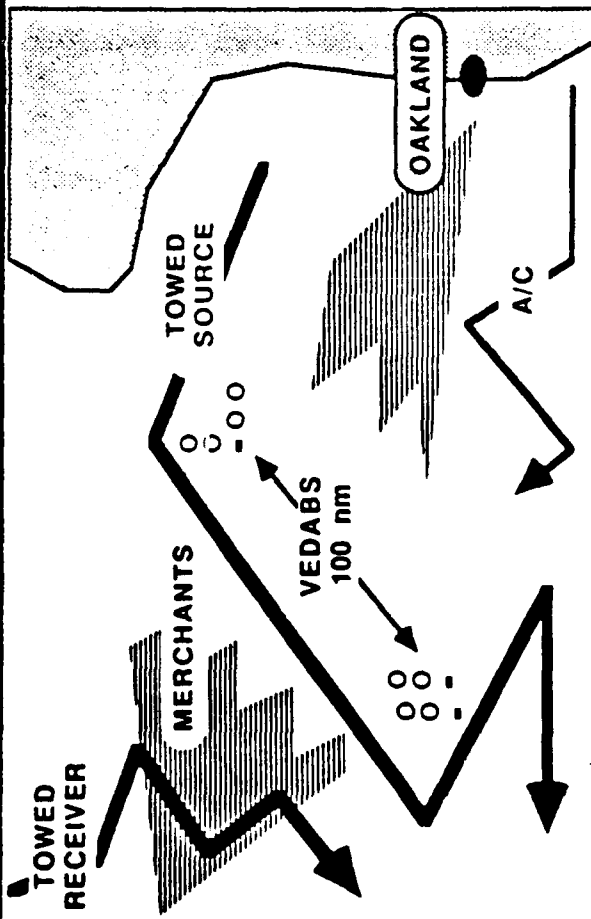
## MEASUREMENT REQUIREMENTS: ANDES II EVALUATION

- NEAR SHIPPING LANE
- RECEIVER DEPTH APPLICABLE TO SYSTEMS UNDER DEVELOPMENT
- BETTER CHARACTERIZATION OF WIND NOISE SOURCE PROPERTIES FROM 10-500 Hz FOR WIND SPEEDS UP TO AT LEAST 25 kts
- EXTENSIVE MONITORING OF SURFACE SHIP TRAFFIC (LOCATION, SPEED, TONNAGE/SOURCE LEVEL)
- MEASUREMENTS THAT ADEQUATELY SAMPLE SOUND SPEED AND TL FIELDS IN DIRECTION OF DISCRETE SOURCES





# OUTPOST SUNRISE AMBIENT NOISE MEASUREMENTS



## OBJECTIVES

1. PERFORM A DETAILED MEASUREMENT OF LOW-FREQUENCY, WIND-DRIVEN, AMBIENT NOISE MECHANISMS AND LEVELS IN THIN SEDIMENT AREA
2. SUPPORT VERTICAL ARRAY DESIGN AND DEVELOPMENT
3. EVALUATE DEPTH DEPENDENCE OF HORIZONTAL AND VERTICAL NOISE DIRECTIONALITY
4. VALIDATE ANDES MODEL

## APPROACH

1. USE VEDABS CONFIGURED IN VERTICAL AND HORIZONTAL ARRAYS
2. USE TOWED ARRAY FOR HORIZONTAL NOISE MEASUREMENT
3. TOW CW (AND POSSIBLY PRN) SOURCE
4. USE SUS FOR TRANSMISSION LOSS MEASUREMENTS

## STATUS

1. MEASUREMENT AT-SEA - 1st QTR FY 89
2. ANALYSIS OF DATA - FY 89
3. ANDES UPGRADE - FY 90





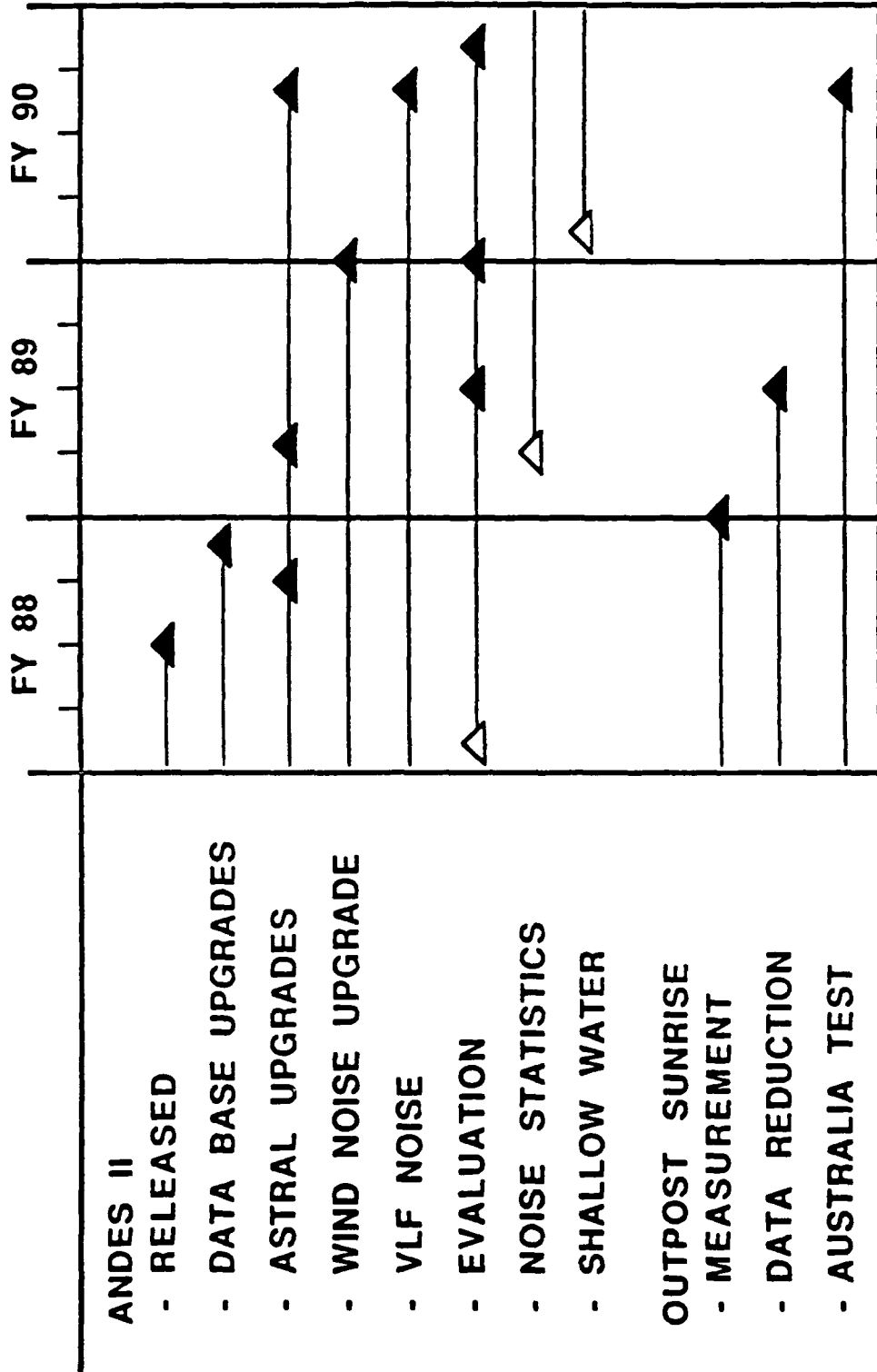
# VLF NOISE MODELING ISSUES

NEED	ISSUE
H	SHIPPING SOURCE LEVEL
H	SHALLOW WATER SOURCE COUPLING TO DEEP WATER RECEIVERS
H	NEAR-BOTTOM NOISE DEPTH DEPENDENCE
H	BROADBAND CROSS CORRELATION PROPERTIES OF NEAR-BOTTOM VERTICAL AND HORIZONTAL ARRAYS
H	HIGH GAIN POTENTIAL FOR NEAR-BOTTOM VOLUMETRIC ARRAYS
M	IMPORTANCE OF DISTANT STORM NOISE
M	WIND NOISE SOURCE LEVEL
M	TRANSMISSION LOSS MODEL
L	SOUND SPEED DATA BASE RESOLUTION
L	GEOPHYSICAL PROSPECTING
L	BIOLOGICS





# AEAS NOISE PROGRAM



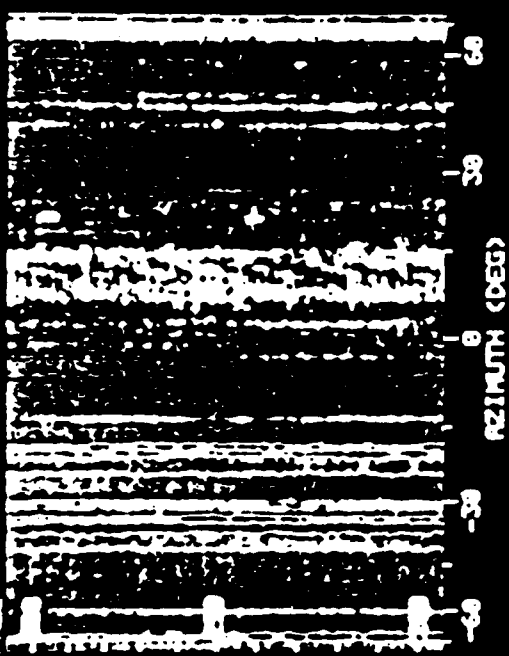


**NOISE HOLES -  
MEASURED AND MODELED**

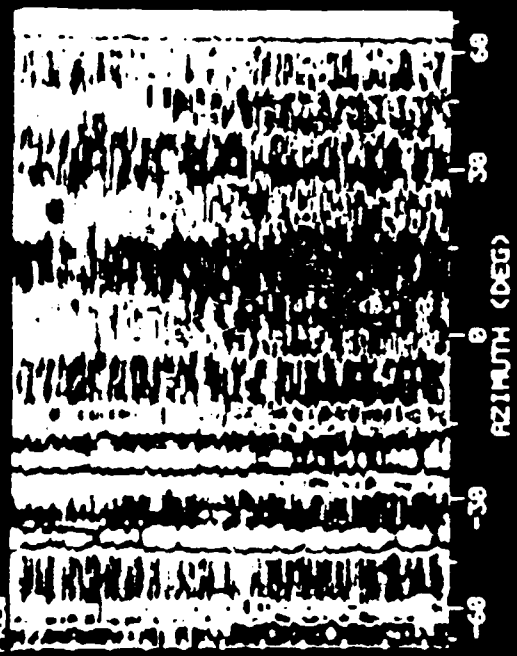
**R. HEITMEYER (NRL)**

Figure 1 illustrates the effect of aperture length on the frequency-azimuth and the azimuth-time noise surfaces obtained on a towed array in a ship-induced noise field. It is seen that, for the full aperture array (left-hand-side surfaces), there are a number of broadband components visible in the frequency-azimuth surface and a number of low level tracks visible in the azimuth-time surface that are not visible in the corresponding surfaces for the quarter length subaperture shown on the right-hand side.

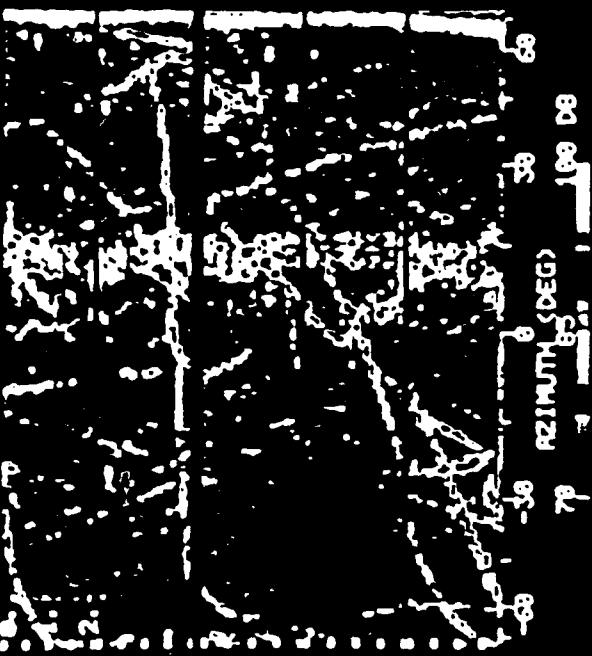
FR09 FULL APERTURE: TAPE/FRAME = 287/14



FR09 QTR APERTURE: TAPE/FRAME = 287/14



FR09 FULL APERTURE: 300 HZ



FR09 QTR APERTURE: 300 HZ

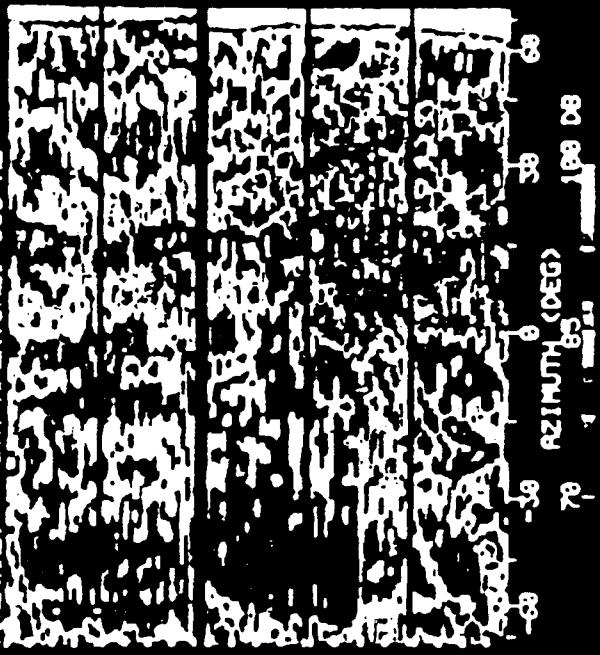


Figure 2 shows an estimate of the shipping distribution (HITS) for the Northeast Pacific (top) and the Mediterranean (bottom) along with a towed array measurement site in each area. Although the spatial shipping distributions clearly indicate more shipping in the Mediterranean than in the Northeast Pacific on a per unit area basis, the angular shipping distribution (mean number of ships per degree bearing relative to the site) for Northeast Pacific is greater than that for the Mediterranean.

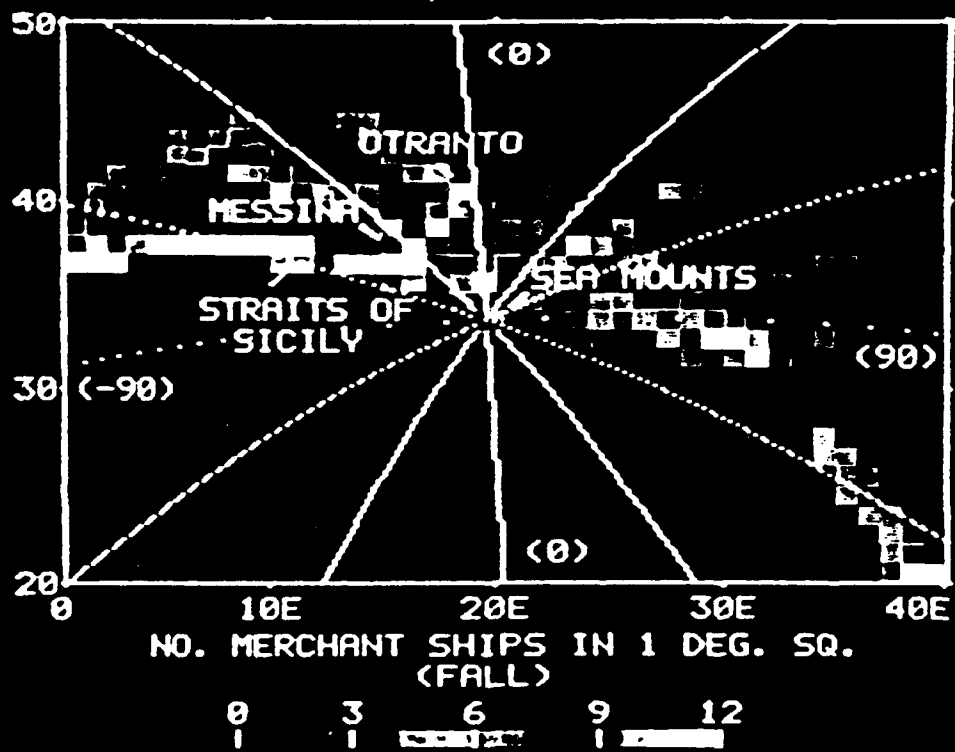
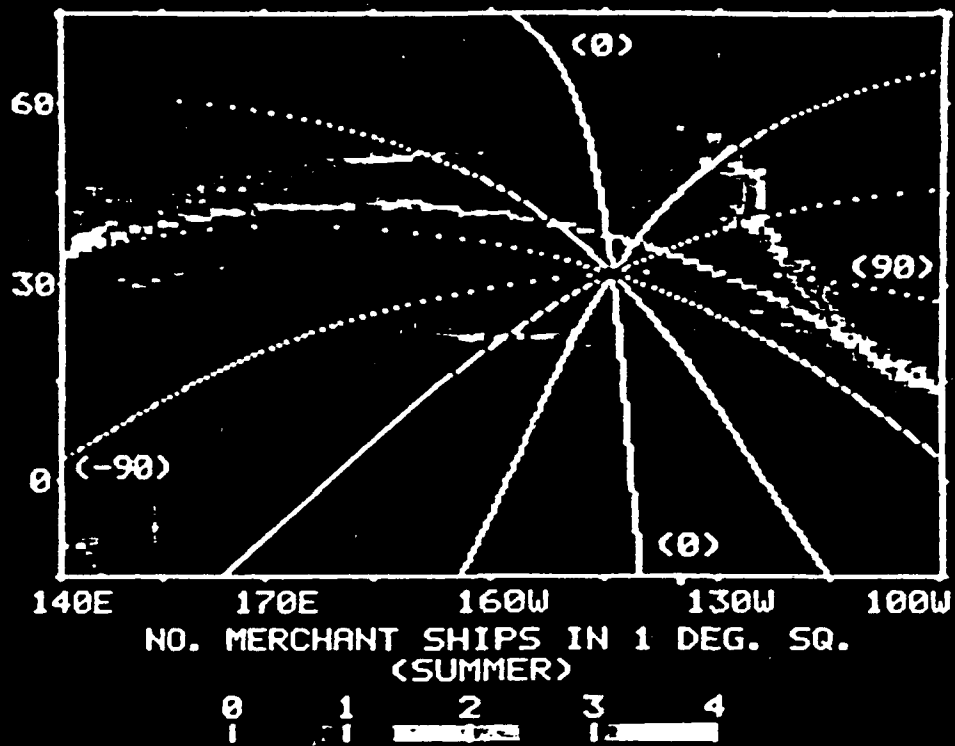


Figure 3 shows a measured beam noise cumulative distribution function for each of the two areas along with computed distribution functions obtained from the NRL/SACLANTCEN noise model. The interpretation of the measured results using the model suggests that the larger spread in the Mediterranean distribution function is primarily due to the smaller values of the angular shipping distribution. The modeled distribution functions were obtained using an assumed source level distribution function and hence, the close agreement shown in the figure does not constitute a validation of the model. The model itself is obtained under the assumption that the ship positions are distributed as a non-homogeneous Poisson process. From this assumption an explicit expression for the beam noise distribution function is obtained in terms of the array beam pattern, the transmission loss function, the source-level distribution, and the spatial shipping distribution.

# BEAM DISTRIBUTION FUNCTION

MEASURED  
COMPUTED

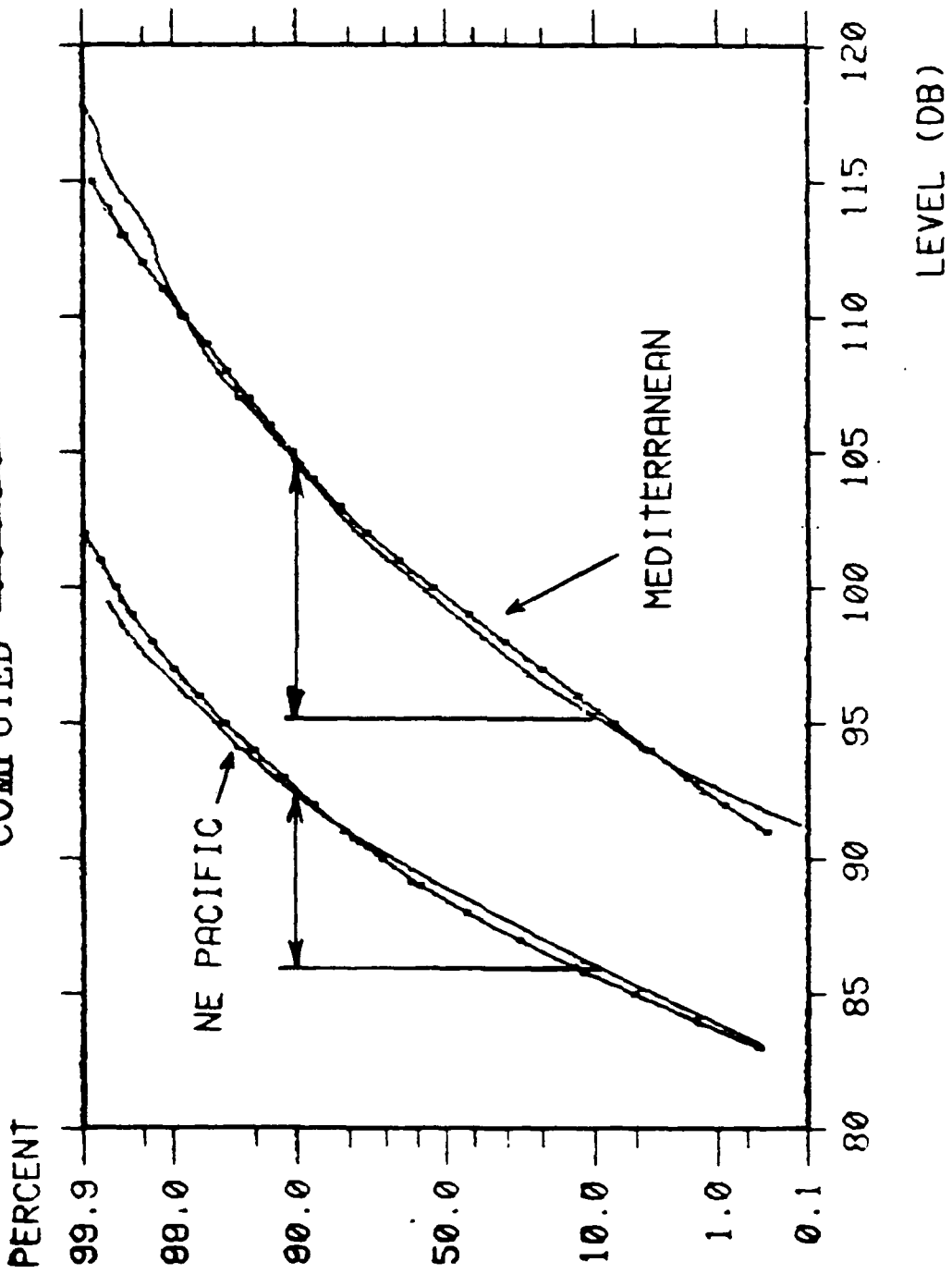


Figure 4 illustrates the salient properties of the modeled beam noise distribution function. The family of distribution functions shown are obtained for the broadside beam at the design frequency of an array operating in a fixed noise environment. Thus, the distribution functions illustrate the effect of array length as described by the directivity index. It is noted that the distributions functions exhibit two forms: a near-normal form which occurs for low directivities and is referred to here as the weakly-resolved form; and, a form consisting of a sharp rise at low beam noise values followed by a tail that extends to very large beam noise values. This form is referred to as the highly-resolved form. Finally note that there is a "noise floor" in the sense that, no matter how large the directivity, noise values less than the noise floor occur only rarely. Approximations of the noise model equations yield simple expressions which determine: (1) whether the distribution function is highly resolved or weakly resolved in terms of the beamwidth and the angular shipping distribution, and (2) the value of the noise floor in terms of the sidelobe degradation and the noise anisotropy. According to the resolution conditions, the distribution functions shown in the previous figure are weakly resolved. To obtain a highly resolved distribution function for the Northeast Pacific site would require an array with a directivity index of 26 dB (approximately 400 phones at the design frequency).

# BEAM DISTRIBUTION FUNCTION

AVE SHIPS PER DEG : 1  
SIDELOBE DEGRADATION : 15 dB  
ANISOTROPY : 0 dB

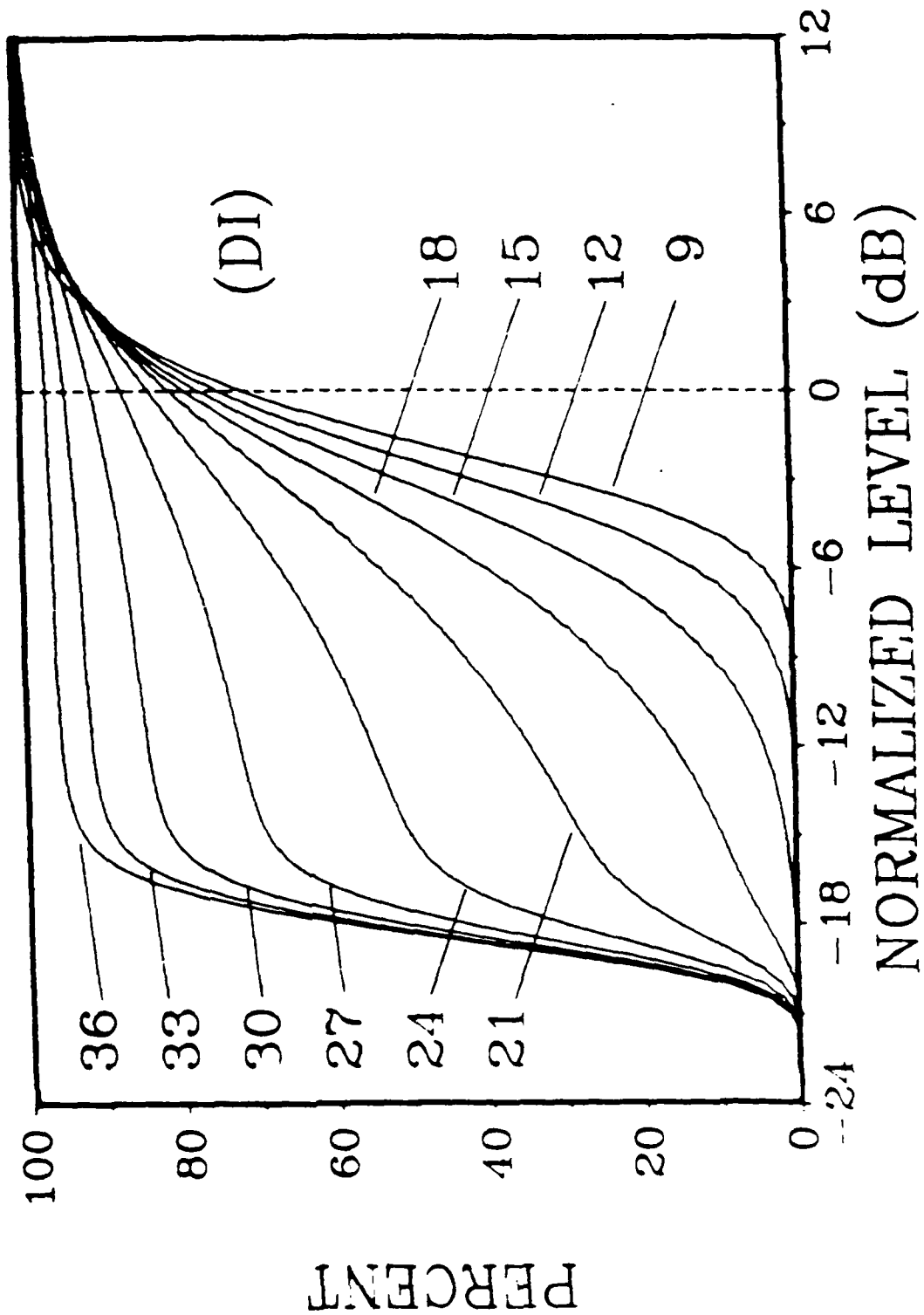


Figure 5 shows a second comparison of measured beam noise distributions at tow sites with the corresponding modeled distributions. The angular shipping distribution for the S. Sardegna distribution is significantly smaller than that for the S. Ionian distribution largely because of the fact that the S. Sardegna site is located closer to the primary Mediterranean shipping lane. The model interpretation suggests that the lower values of the angular shipping distribution at the S. Sardegna site are the major cause of the increased spread in the distribution function. According to the resolution conditions, both distribution functions are weakly resolved.

# BEAM DISTRIBUTION FUNCTION

402-412 HZ : 20 deg sector

MEASURED

COMPUTED

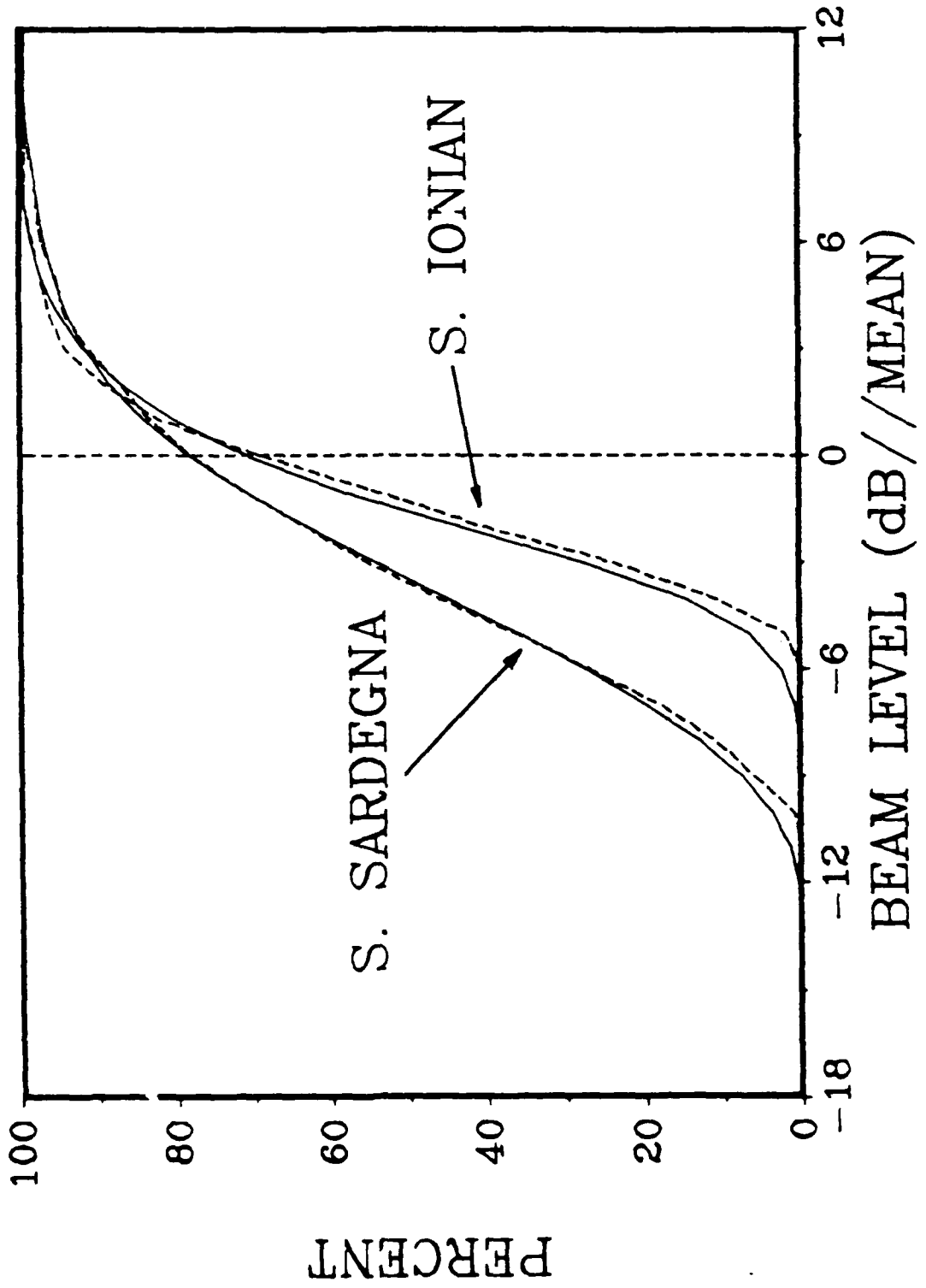


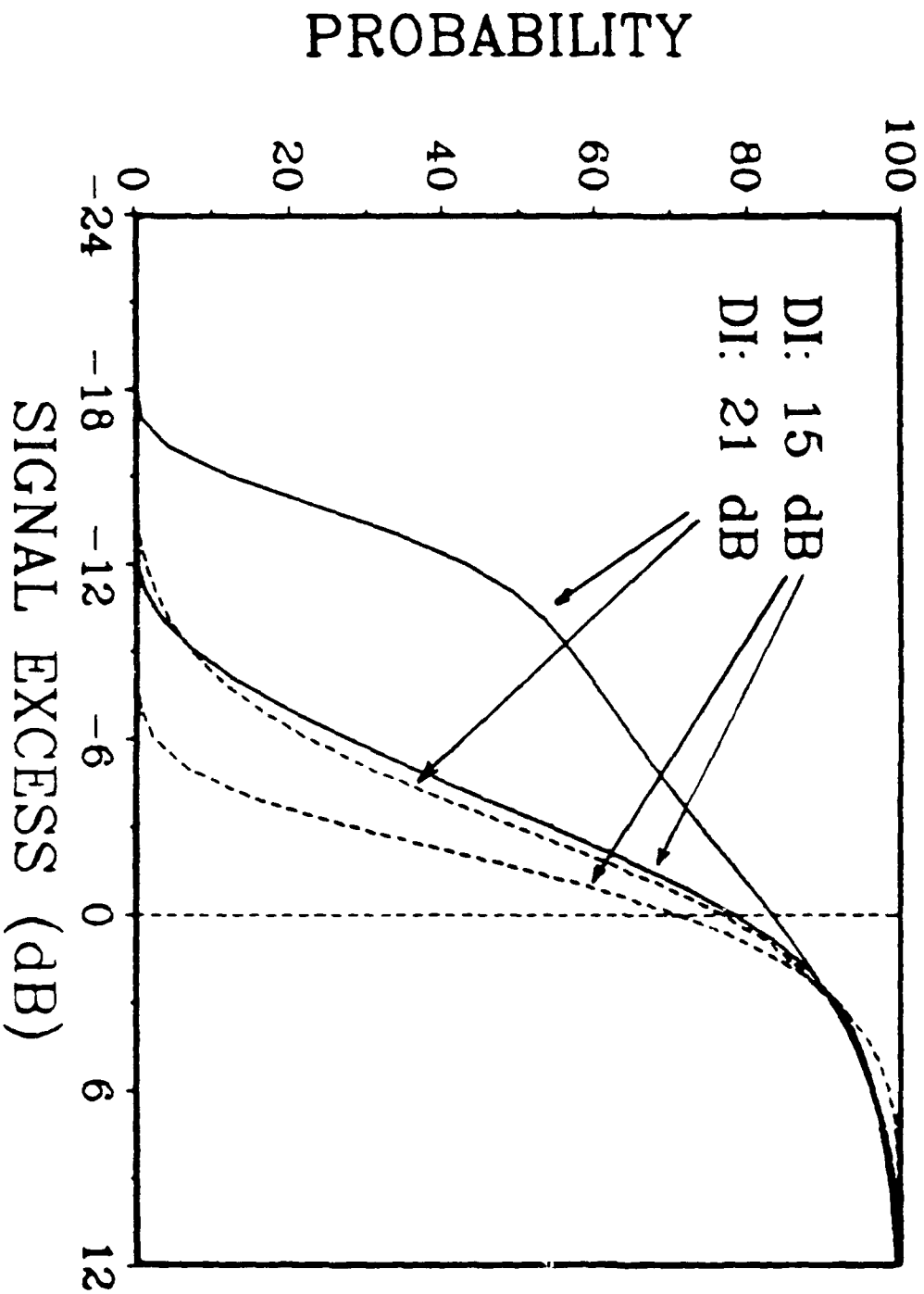
Figure 6 describes the implications of the beam noise distribution function on the detection performance for the two sites together with a prediction of the detection performance that would result using an array with four times the acoustical length of that used in the noise measurements. It is seen that, for the 15 dB directivity array, the increased spread in the beam noise distribution for the S. Sardegna site results in a significant improvement in the detection probability for a low level target, e.g., a target with signal excess of -6 dB is detected about 35% of the time at the S. Sardegna site and only about 2% of the time at the S. Ionian site. For the 21 dB directivity array, there is an even greater improvement in the detection performance of low level targets for the S. Sardegna site as can be seen by comparing the curves at a signal excess of -12 dB. This added increase in the detection performance results from the fact that for the 21 dB array, the noise has become highly resolved at the S. Sardegna site.

# DETECTION PROBABILITY

(False alarm = 10 % ; constant signal level)

S. IONIAN : - - - - -

S. SARDEGNA : \_\_\_\_\_



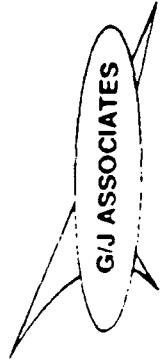


**SYSTEM / SELF / FLOW NOISE**

**J. GOTTWALD (J / G ASSOC.)**



# ARRAY NOISE





## NOISE MECHANISMS

- ELECTRONIC NOISE
- MECHANICALLY INDUCED NOISE
- TBL FLOW NOISE
- AMBIENT NOISE



## SOME DEFINITIONS

### ARRAY GAIN. AG

AG = TEN TIMES THE LOGARITHM TO THE BASE TEN OF  
THE RATIO OF THE SIGNAL-TO-NOISE RATIO AT  
THE ARRAY OUTPUT TO THE SIGNAL-TO-NOISE  
RATIO AT THE OUTPUT OF ONE ARRAY ELEMENT

IF: ALL ELEMENTS SENSE THE SAME SIGNAL FIELD, AND  
THE SIGNAL FIELD IS PERFECTLY COHERENT, AND  
ALL ELEMENTS SENSE THE SAME NOISE FIELD, AND  
THE NOISE FIELD IS ISOTROPIC, AND  
ALL ELEMENTS ARE SEPARATED BY AT LEAST ONEHALF  
WAVELENGTH, AND  
ALL ELEMENTS ARE GIVEN THE SAME WEIGHT.

THEN THE ARRAY GAIN REDUCES TO THE QUANTITY WHICH IS  
CLASSICALLY REFERRED TO AS THE DIRECTIVITY INDEX, DI.

IF ANY OF THESE CONDITIONS IS VIOLATED, THEN THE ARRAY  
GAIN CAN BE GREATER THAN, LESS THAN, OR POSSIBLY THE  
SAME AS THE DIRECTIVITY INDEX. WITHOUT DETAILED  
KNOWLEDGE OF THE SIGNAL AND NOISE FIELDS IT IS NOT  
POSSIBLE TO ACCURATELY PREDICT THE ARRAY GAIN.

NOTE: BOTH THE SIGNAL AND THE NOISE FIELD  
CHARACTERISTICS ARE REQUIRED - NOT JUST THE NOISE FIELD



## SOME DEFINITIONS

### COHERENCE

THE MAGNITUDE SQUARED COHERENCE FUNCTION IS A REAL VALUED QUANTITY DEFINED BY THE RATIO OF THE SQUARE OF THE ABSOLUTE VALUE OF THE POWER CROSS SPECTRAL DENSITY TO THE PRODUCT OF THE POWER SPECTRAL DENSITY FUNCTIONS OF THE TWO PROCESSES AT EACH FREQUENCY IN THE SPECTRUM.

THE NORMALIZED CROSSCORRELATION COEFFICIENT IS A REAL VALUED QUANTITY DEFINED BY THE RATIO OF THE CROSSCORRELATION FUNCTION TO THE SQUARE ROOT OF THE PRODUCT OF THE AUTOCORRELATION FUNCTIONS OF THE TWO PROCESSES AT ZERO TIME DELAY.

WHEN THE MAGNITUDE SQUARED COHERENCE FUNCTION IS INTEGRATED OVER A BANDWIDTH EQUAL TO THAT USED TO COMPUTE THE NORMALIZED CROSSCORRELATION COEFFICIENT, THE SQUARE OF THE NORMALIZED CROSSCORRELATION COEFFICIENT WILL EQUAL THE INTEGRATED MAGNITUDE SQUARED COHERENCE FUNCTION.



## SOME DEFINITIONS

### ARRAY

AN ARRAY. FOR THE PURPOSES OF COMPUTING ARRAY GAIN, INCLUDES

- 0 THE ACOUSTIC SENSOR OUTPUTS AVAILABLE FOR BEAMFORMING
- 0 THE MECHANICAL STRUCTURE TO WHICH THE ACOUSTIC SENSORS ARE ATTACHED OR IN WHICH THEY ARE MOUNTED
- 0 THE ATTACHMENT OF THE ARRAY STRUCTURE TO A SUPPORT STRUCTURE, TOW VESSEL OR THE OCEAN BOTTOM
- 0 THE INTERACTION BETWEEN THE ARRAY STRUCTURE AND THE ENVIRONMENT

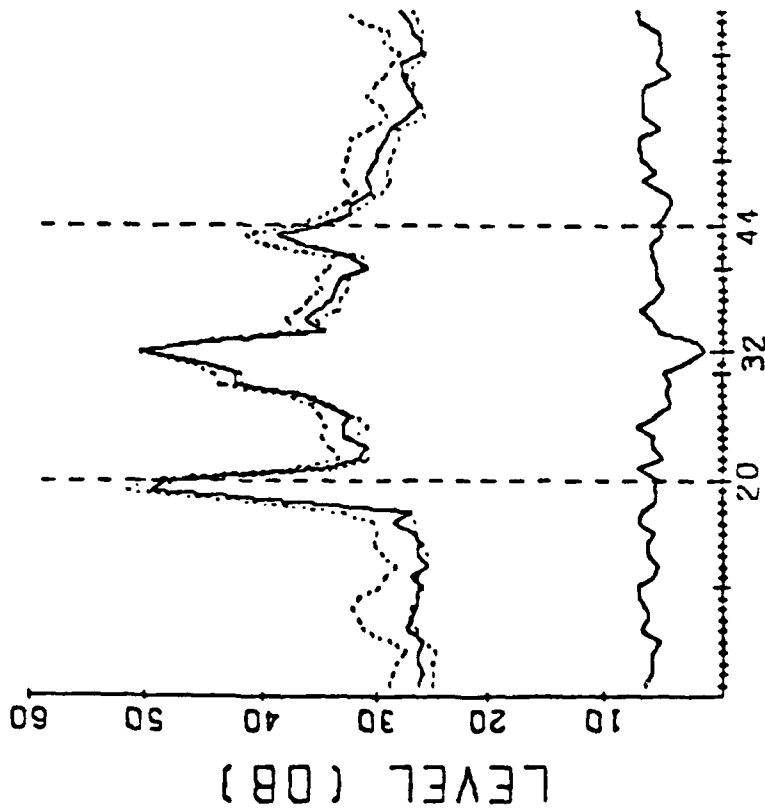
### HYDROPHONE GROUP

THE TERM HYDROPHONE GROUP REFERS TO N INTERCONNECTED OMNIDIRECTIONAL ACOUSTIC SENSORS WHICH ACT AS ONE ACOUSTIC SENSOR IN AN ARRAY

The 5th harmonic (300 Hz) of the power supply (60 Hz) is evident in these polar and rectangular plots on the broadside beam. The small standard deviation of the electrical noise is evident in the bottom curve of the rectangular plot.

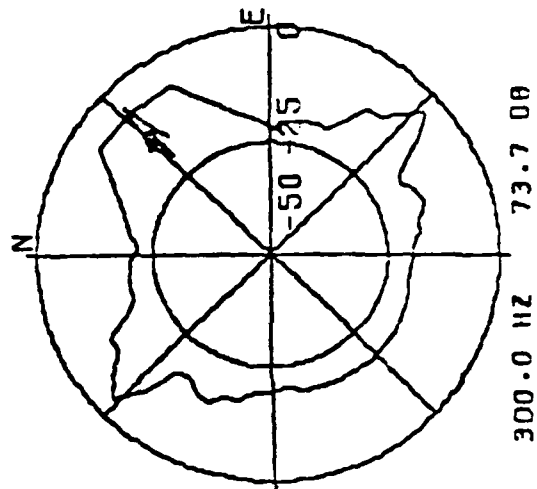
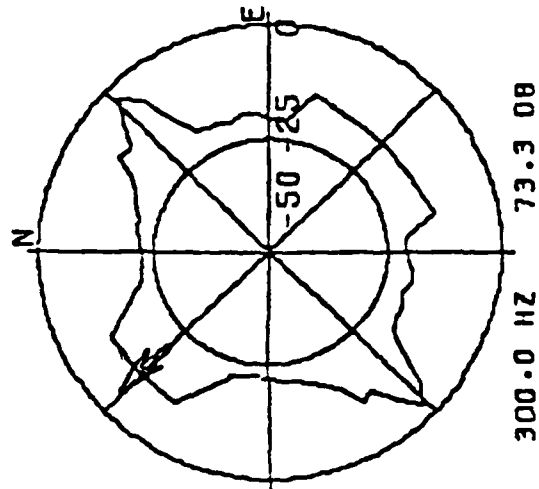


# COMMON MODE NOISE



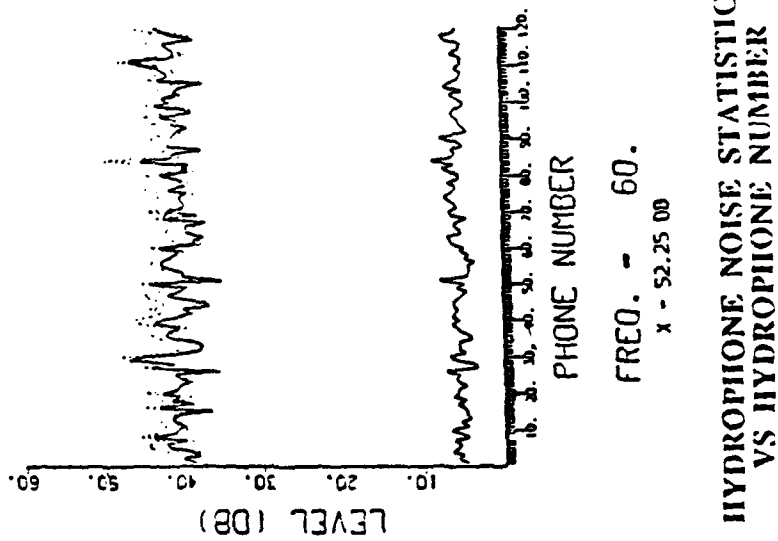
BEAM NUMBER

FREQ. = 300.0

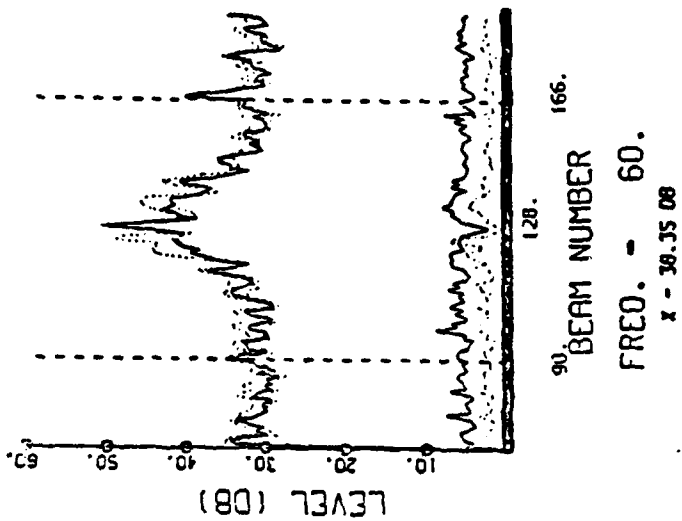


The 60 Hz power supply artifact is evident in these vertical directionality results at broadside as a high level noise (top current) with a very small standard deviation (bottom curve).

# ARRAY PERFORMANCE AT 60 Hz

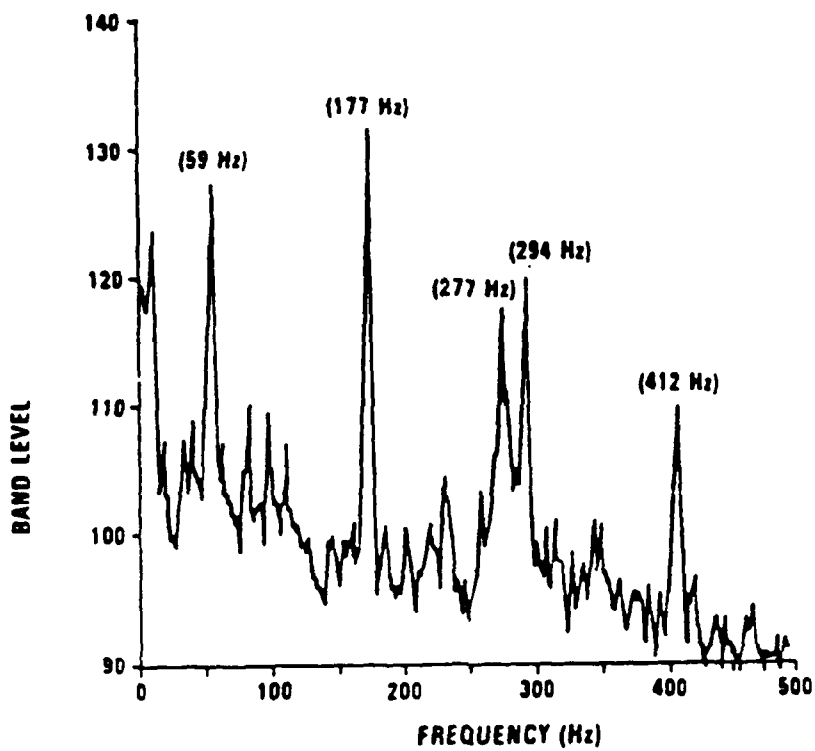


HYDROPHONE NOISE STATISTICS  
VS HYDROPHONE NUMBER



90 BEAM NUMBER STATISTICS  
VS BEAM NUMBER

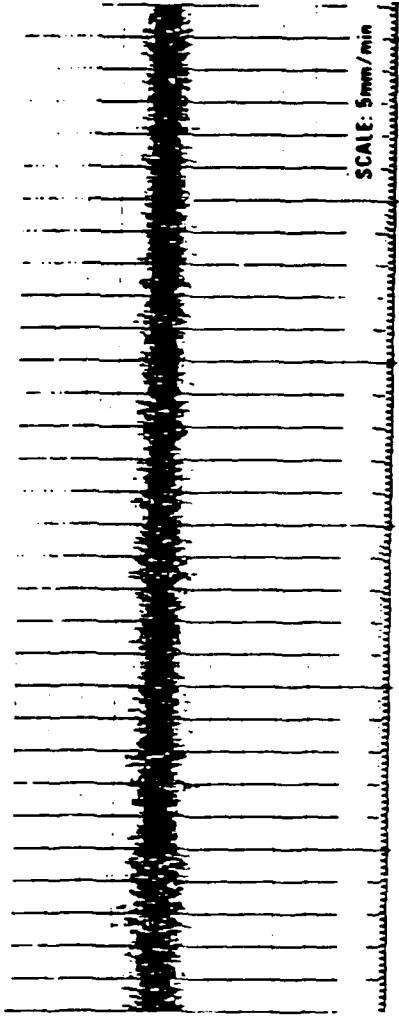




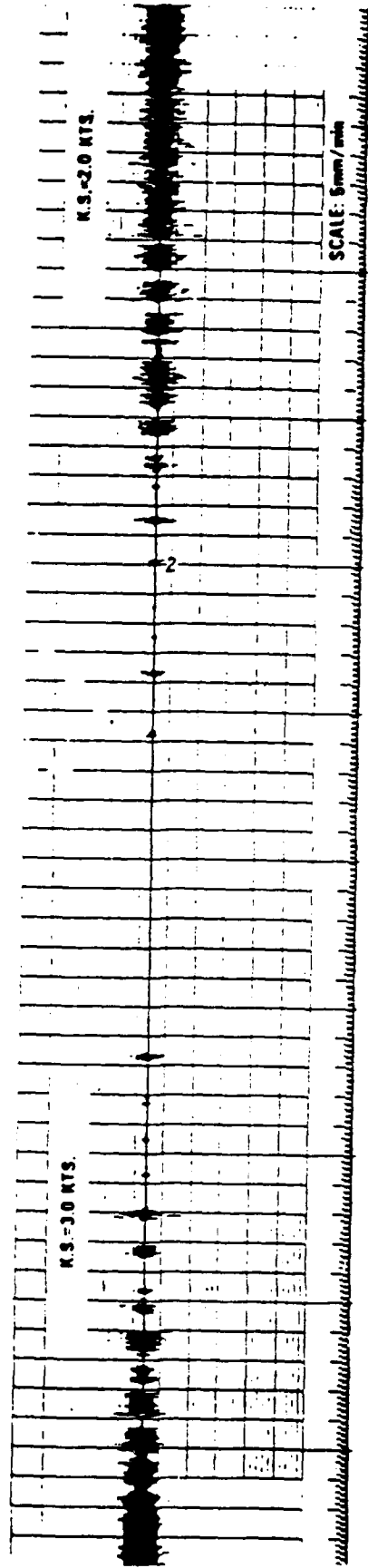
EXAMPLE OF THE EFFECT OF 60 HERTZ NOISE  
ON LOW FREQUENCY NOISE SPECTRA



NORMAL AND SATURATED HYDROPHONE CHANNEL OUTPUTS

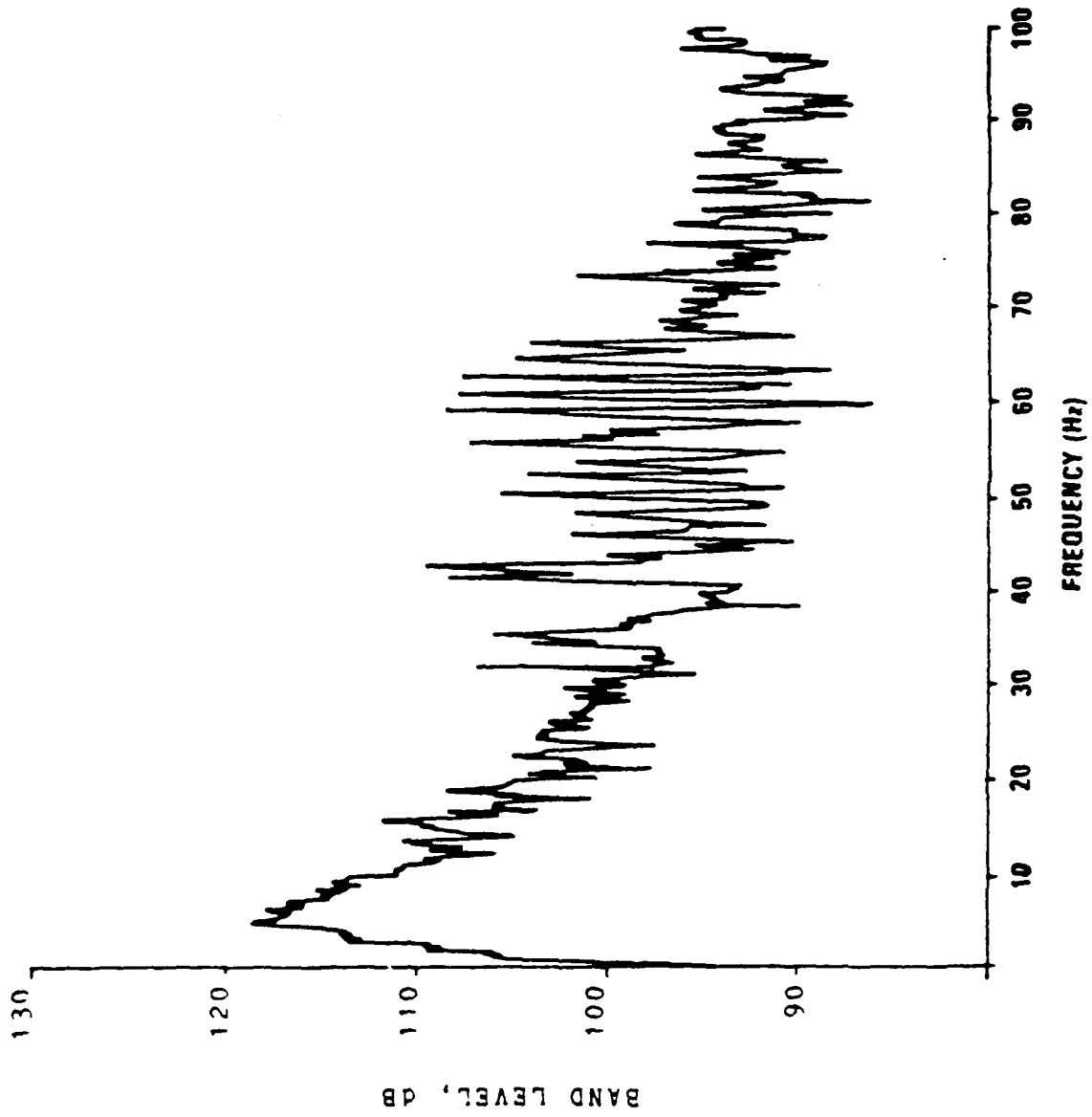


NORMAL OSCILLOGRAM

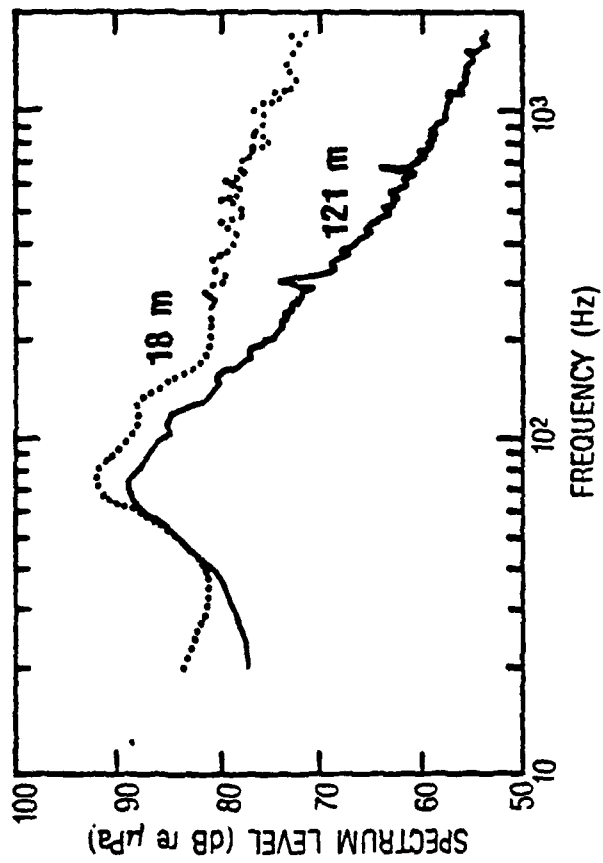


AMPLIFIER SATURATION





Spectral contamination due to clipping is illustrated by the difference in these two spectra. These data were measured by sonobuoys at two different depths in a shallow sea, i.e., maximum depth of about 125 m.





ELECTRONIC NOISE COHERENCE

60 HERTZ - COHERENCE = 1.0 WHEN ASSOCIATED WITH GROUNDING PROBLEMS

0 < COH < 1 WHEN ASSOCIATED WITH LEAKAGE OR INDIVIDUAL CIRCUIT PROBLEMS

DYNAMIC OVERLOAD - COHERENCE UNCHANGED OR DEGRADED DEPENDENT ON CAUSE AND NOISE-TO-NOISE RATIO



## MECHANICALLY INDUCED NOISE

### MECHANISMS

- HYDROPHONE ACCELERATION SENSIVITY(3D)
- STRUCTURAL RADIATION
- TURBULENCE
- ARRAY STRUCTURE
- TENSION INDUCED VIBRATIONS

### DESCRIPTIVE TERMS

- VORTEX SHEDDING
- STRUM
- TBL FLOW
- BULGE WAVES
- EXTENSIONAL WAVES



## HYDROPHONE ACCELERATION SENSITIVITY

- WHEN STRUCTURAL VIBRATIONS MAY BE INDUCED IN AN ARRAY THE SENSITIVITY OF THE INDIVIDUAL HYDROPHONES MUST BE KNOWN IN THREE DIMENSIONS
- THE INABILITY TO OR UNDESIRABILITY OF REDESIGNING A HYDROPHONE TO REDUCE OR ELIMINATE THE ACCELERATION SENSITIVITY IN A SPECIFIC DIRECTION MAY REQUIRE CHANGES IN THE ARRAY STRUCTURAL DESIGN



## STRUCTURAL RADIATION

- VORTEX SHEDDING CAN CAUSE STRUCTURAL VIBRATIONS WHICH IN TURN GENERATE OBSERVABLE ACOUSTIC RADIATION
- TOWED ARRAY SYSTEMS AND SHIP HULL MOUNTED ARRAY SYSTEMS ARE PARTICULARLY SUSCEPTIBLE TO STRUCTURAL RADIATION INDUCED BY VORTEX SHEDDING



## TURBULENCE

- NATURAL TURBULENCE CAN GENERATE PRESSURE GRADIENTS ALONG AN ARRAY AT VERY LOW FREQUENCIES
- STRUCTURALLY INDUCED TURBULENCE WILL GENERATE PRESSURE GRADIENTS JUST AS NATURAL TURBULENCE
- THE COHERENCE OF EITHER NATURAL OR INDUCED TURBULENCE DEPENDS ON THE PROPAGATION VELOCITY OF THE TURBULENCE



## ARRAY STRUCTURE

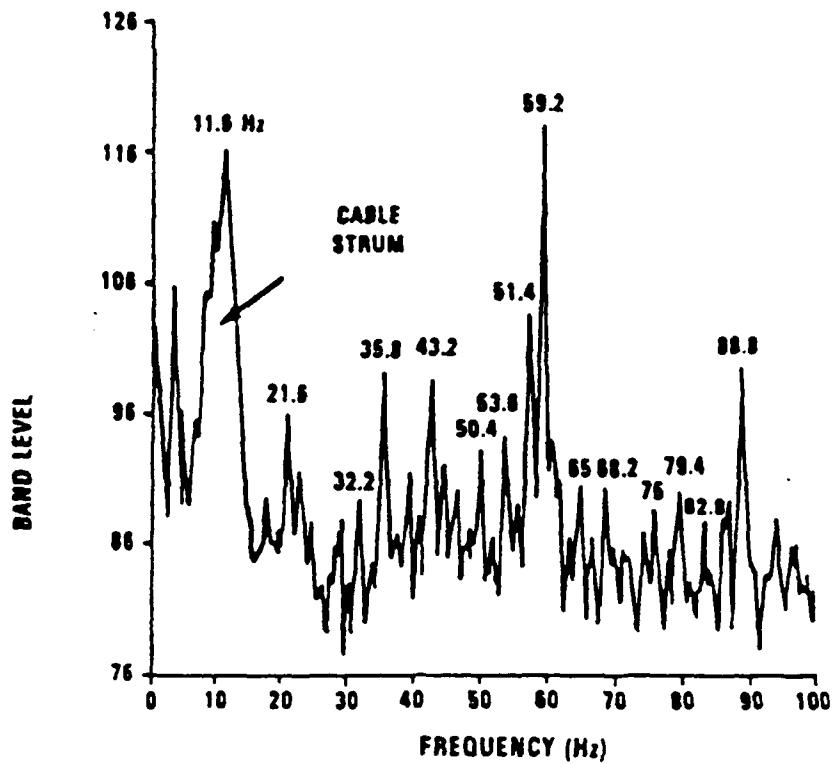
- UNEXPECTED ARRAY NOISE CAN BE GENERATED BY THE CONSTRUCTION OF THE ARRAY
- MATERIALS
- CONFIGURATION
- ENVIRONMENT
- INSTALLATION



## TENSION INDUCED VIBRATIONS

- VORTEX SHEDDING
- MECHANICAL VIBRATIONS OF ATTACHED MACHINERY
- WAVE INDUCED FORCES
- WIND INDUCED FORCES

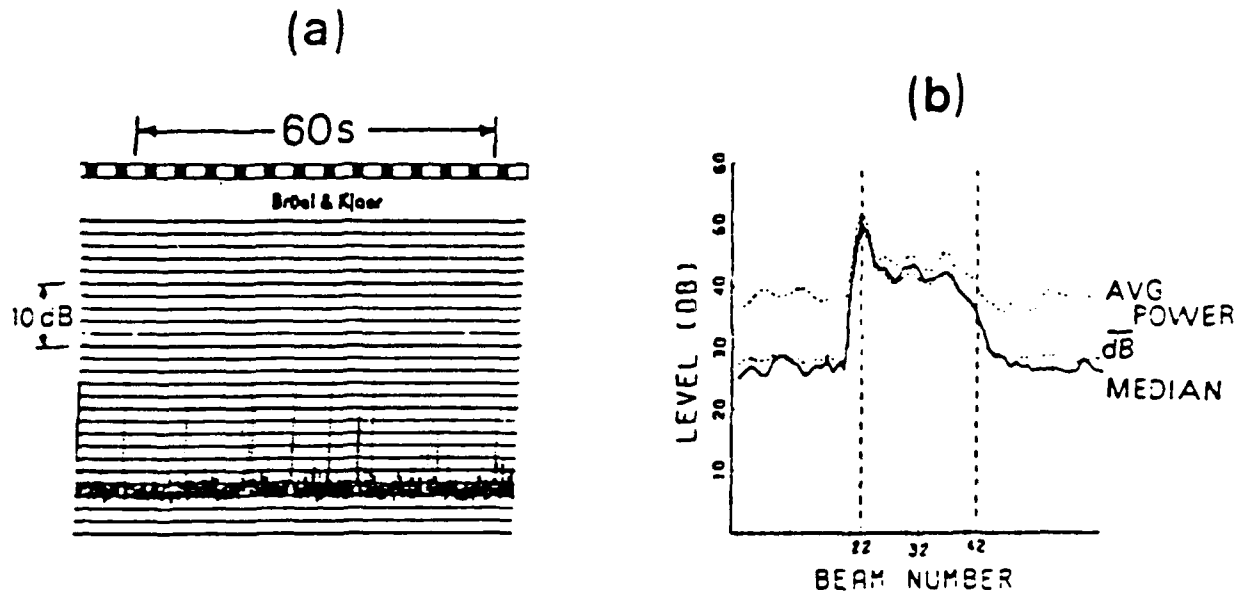




EXAMPLE OF THE EFFECT OF CABLE STRUM ON LOW FREQUENCY NOISE SPECTRA

The effects of "pops" observed aurally on the hydrophones of a towed array. The condition was caused by the oil-deficient hose forcing the strength members to make random contact with the hydrophones. The "pops" disappeared when fill-fluid was added to the array.

# MECHANICAL NOISE



STRIP-CHART RECORDING OF NOISES ON ONE HYDROPHONE CHANNEL (4a) AND THE EFFECTS ON THE BEAMFORMED OUTPUT (4b). POWER AVERAGE (top dashed curve), MEDIAN (solid curve), AND dB AVERAGE (bottom dashed curve)

This example shows the differences in performance at 10 Hz in a vertical array near the Gulf Stream. The left column is when the array is over powered by a strong source, and the effects of uniform shading are evident. The correlation matrix shows that all beams are correlated. This is proof that the source dominates and the sidelobe structure is evident. The right column is for no source, but strong current flow past the array. The ambient noise is marked by the flow noise as evidenced by the high level virtual beams. The light area below the main diagonal of the correlation matrix is evidence of noncorrelation as expected with flow noise.



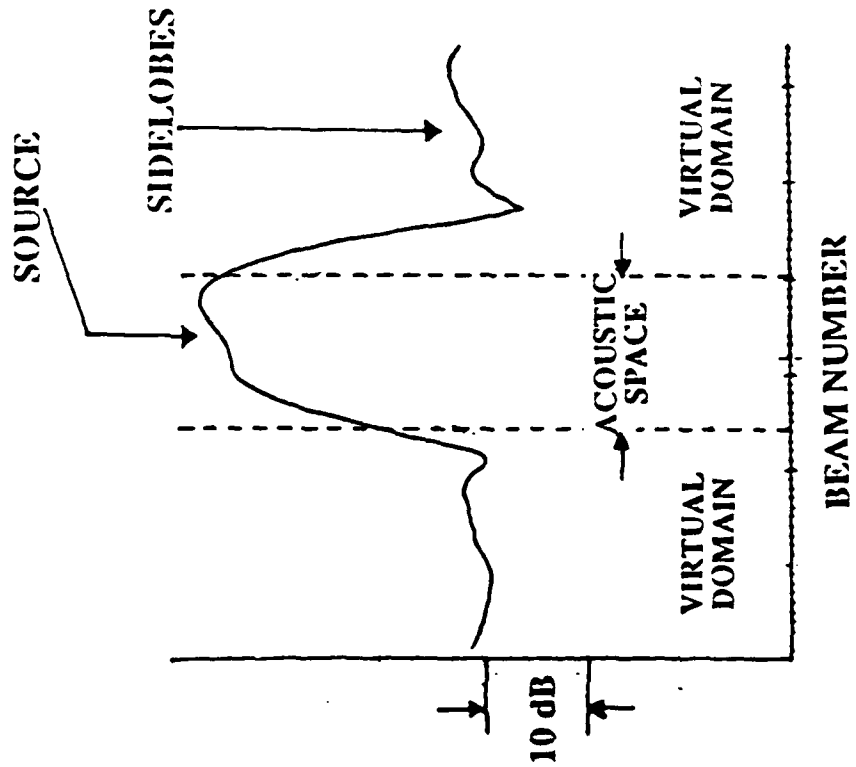
This example is similar to the previous one, but the shading is Hann and the current flow past the array was less.



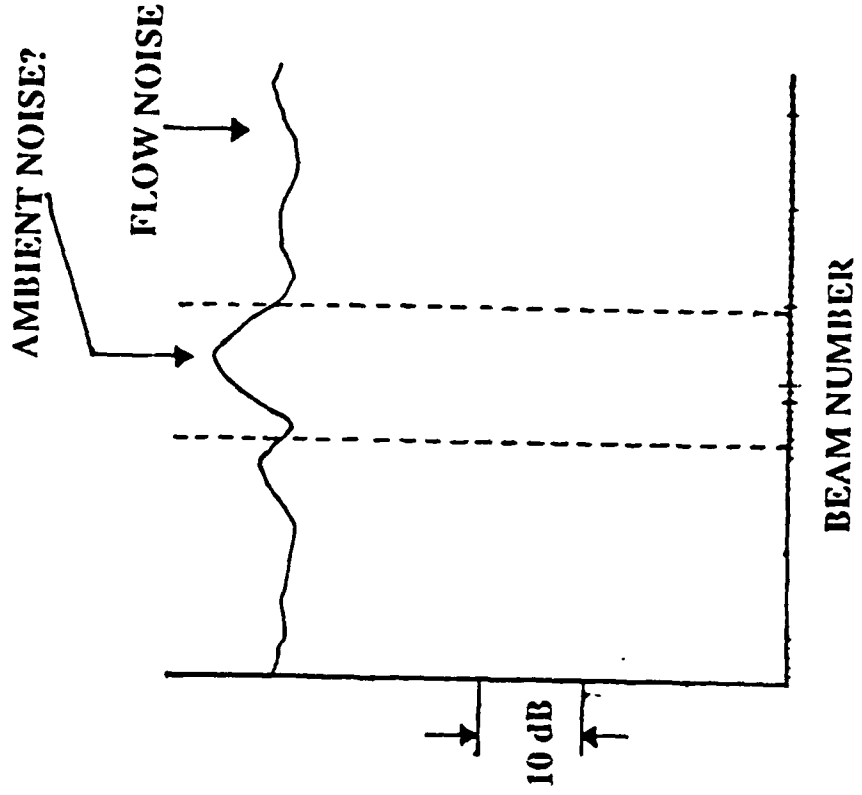


# SYSTEM NOISE: FLOW NOISE EFFECTS

## SIGNAL MEASUREMENT



## NOISE MEASUREMENT





# LONGITUDINAL VIBRATION NOISE



# BULGE WAVE EQUATION

$$p = \rho_i c_b v_{x_0} \exp i(k_1 x - \omega t) \exp (-k_2 x)$$

- where  $\rho_i$  = internal fluid density
- $c_b$  =  $\omega/k_b$  = bulge wave velocity  
=  $[Eh/\rho_i D]^{1/2}$
- $v_{x_0}$  = end cap longitudinal velocity amplitude
- $k_1$  = real part of the wave number
- $k_2$  = imaginary part of the wave number
- $\omega$  = angular frequency
- $k_b$  =  $k_1 + ik_2$
- $E$  = Young's modulus for the hose wall material
- $h$  = hose wall thickness, and
- $D$  = diameter of hose.



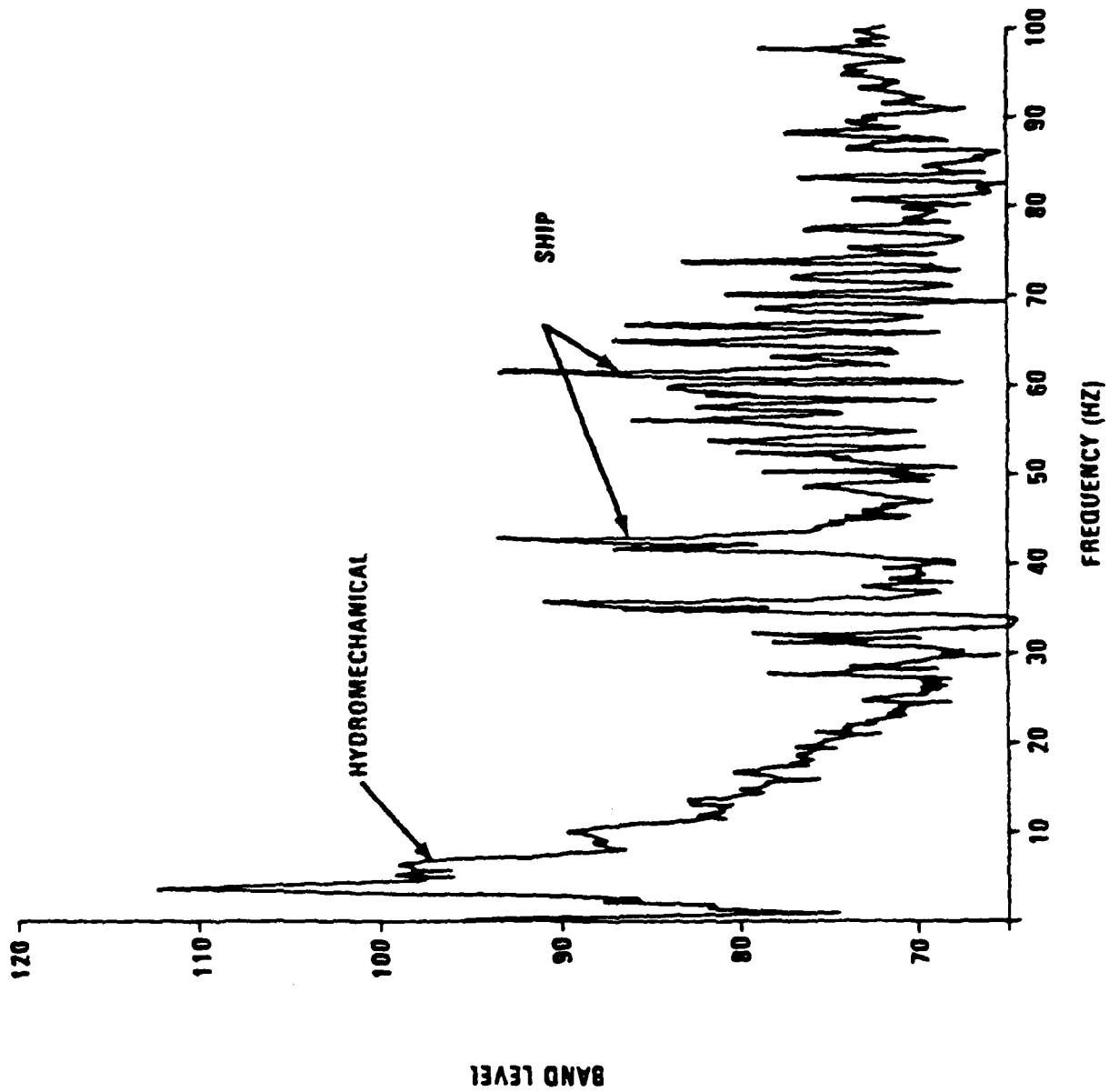
# EXTENSIONAL WAVE EQUATION

$$p_E = - \frac{2v^2}{1-v^2} \frac{c_b^2}{c_p} \rho_i v_{x_0} \exp i(k_1'x - \omega t) \exp(-k_2'x)$$

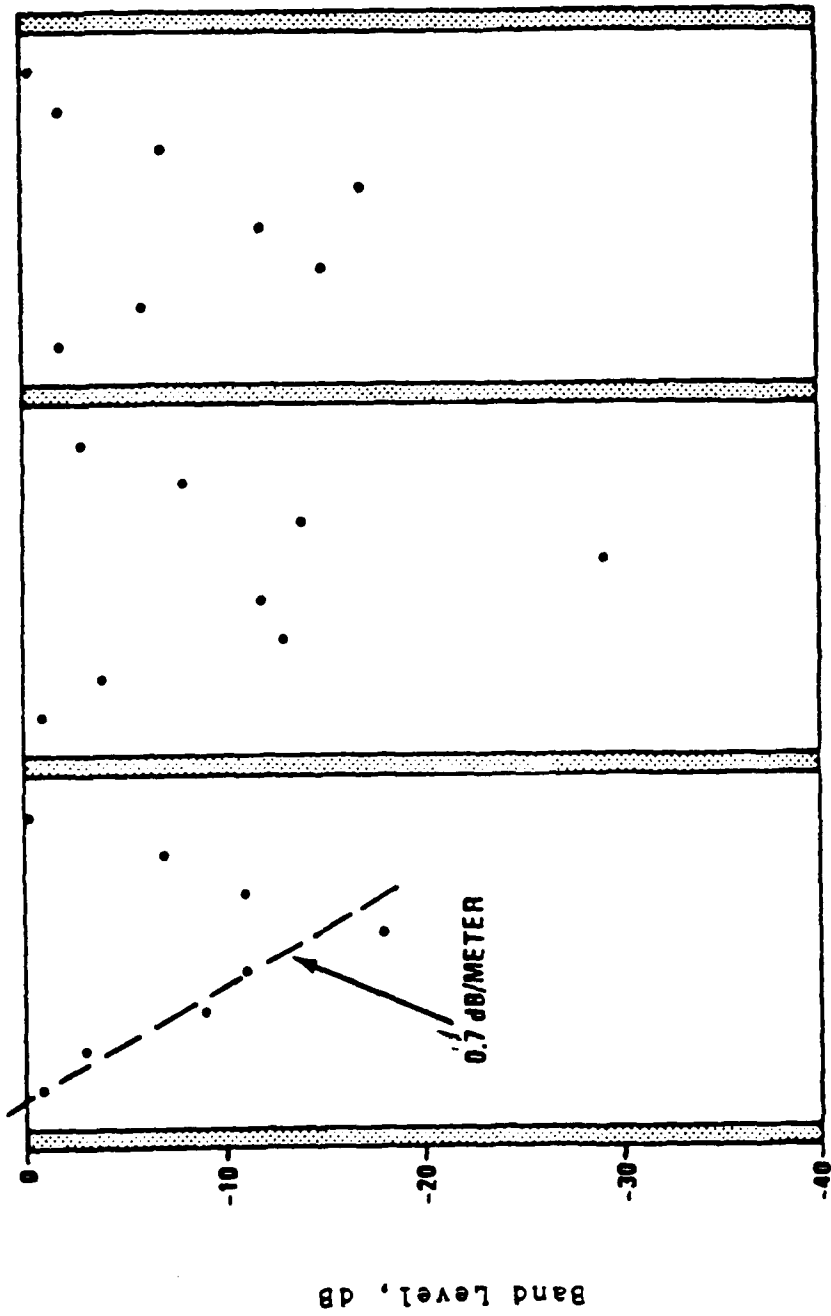
where

- $v$  = Poisson's ratio ( $\approx 0.45$ ) for the hose material
- $c_p^2 = E/\rho_s(1-v^2)$
- $\rho_s$  = density of hose material ( $\approx 1.196 \text{ g/cm}^3$ )
- $c_E$  = extensional wave velocity  $\approx c_p$
- $k_E = k_1' + ik_2'$
- $|k_E| = \omega/c_E$



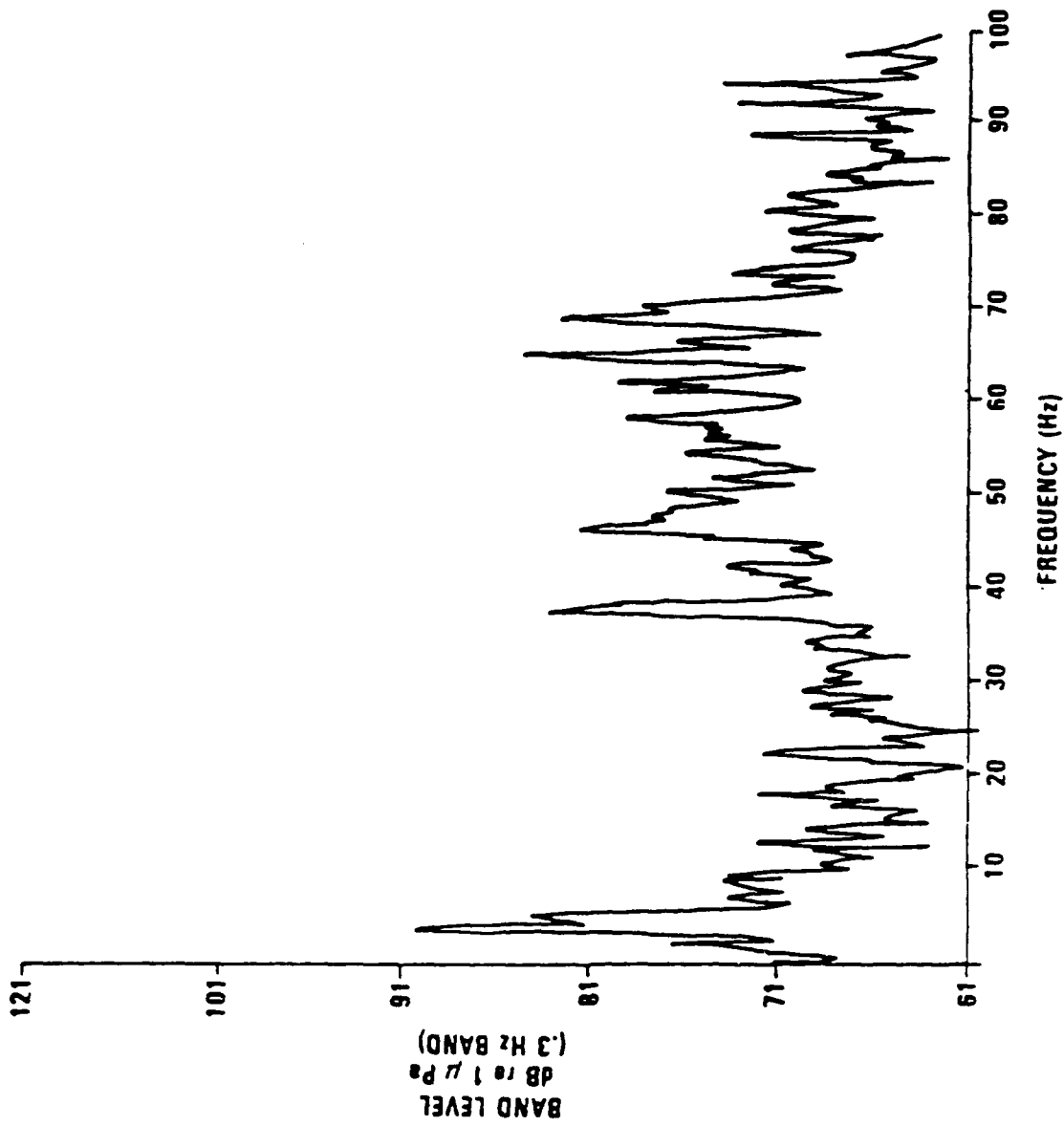






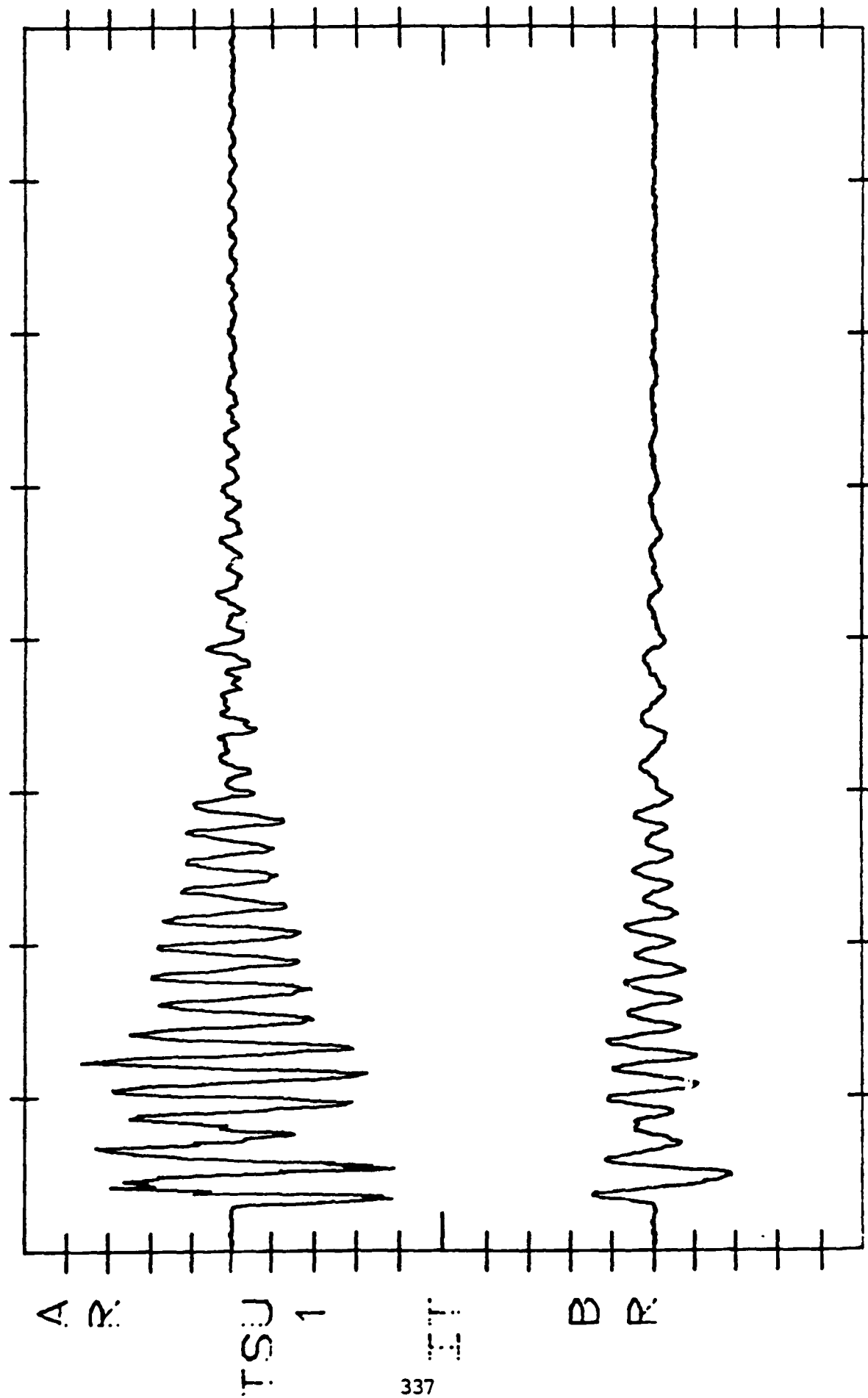
EXAMPLE OF BULGE WAVE ATTENUATION WITH DISTANCE







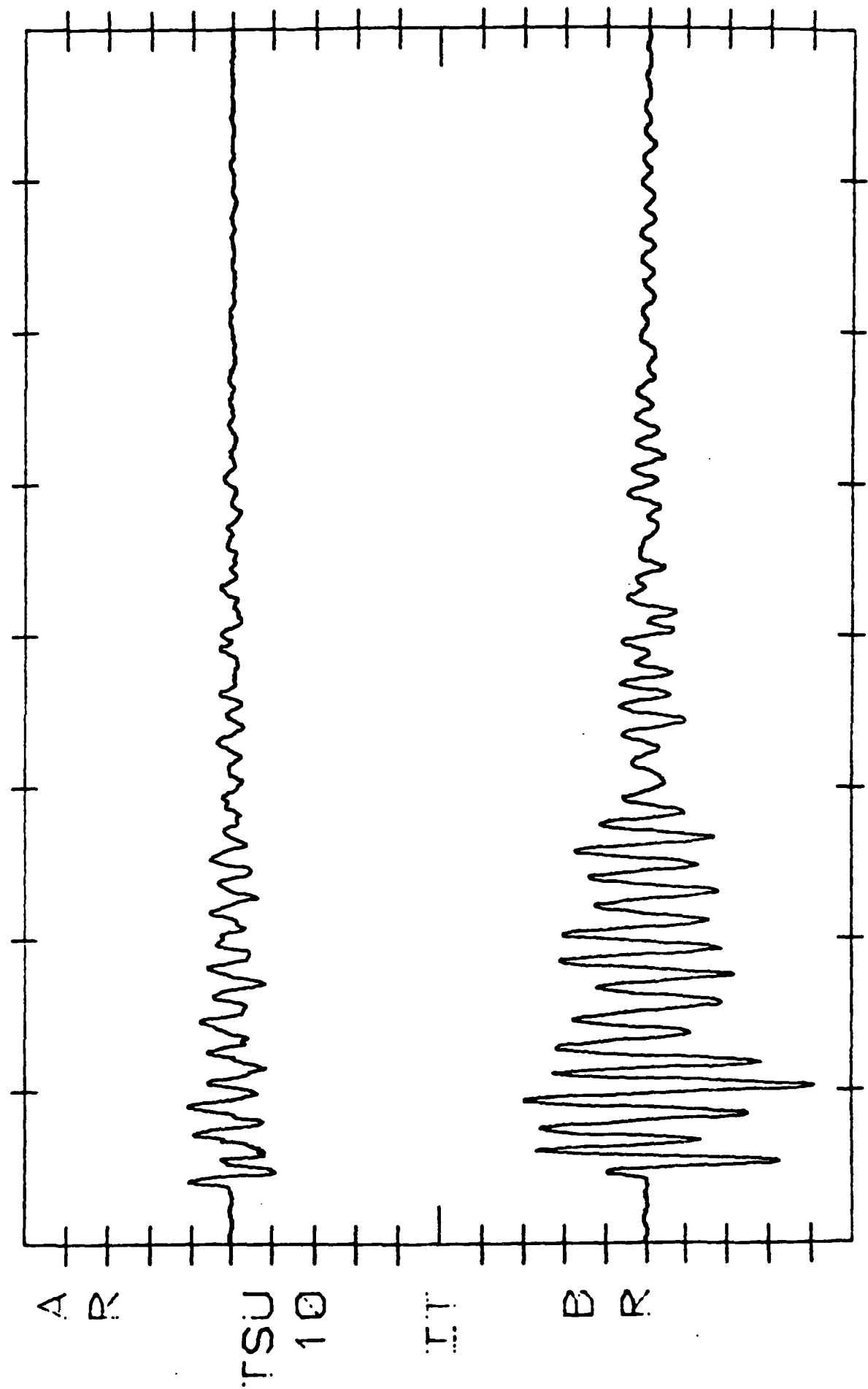
400. --03 V VL,  
400. --03 V T



0.5A 0.2A A/4 SEC 2



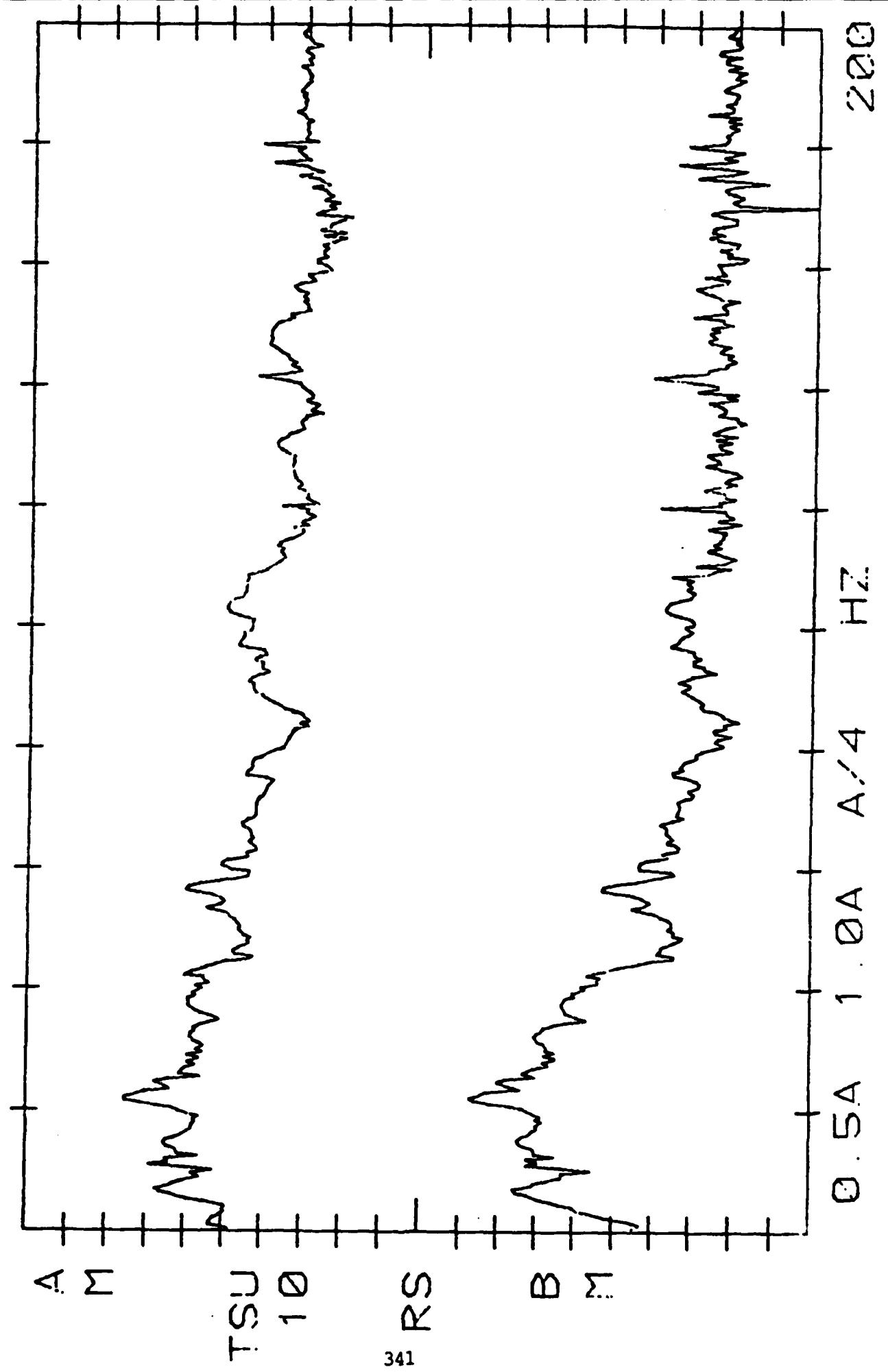
602. -03 V VLN  
600. -03 V T



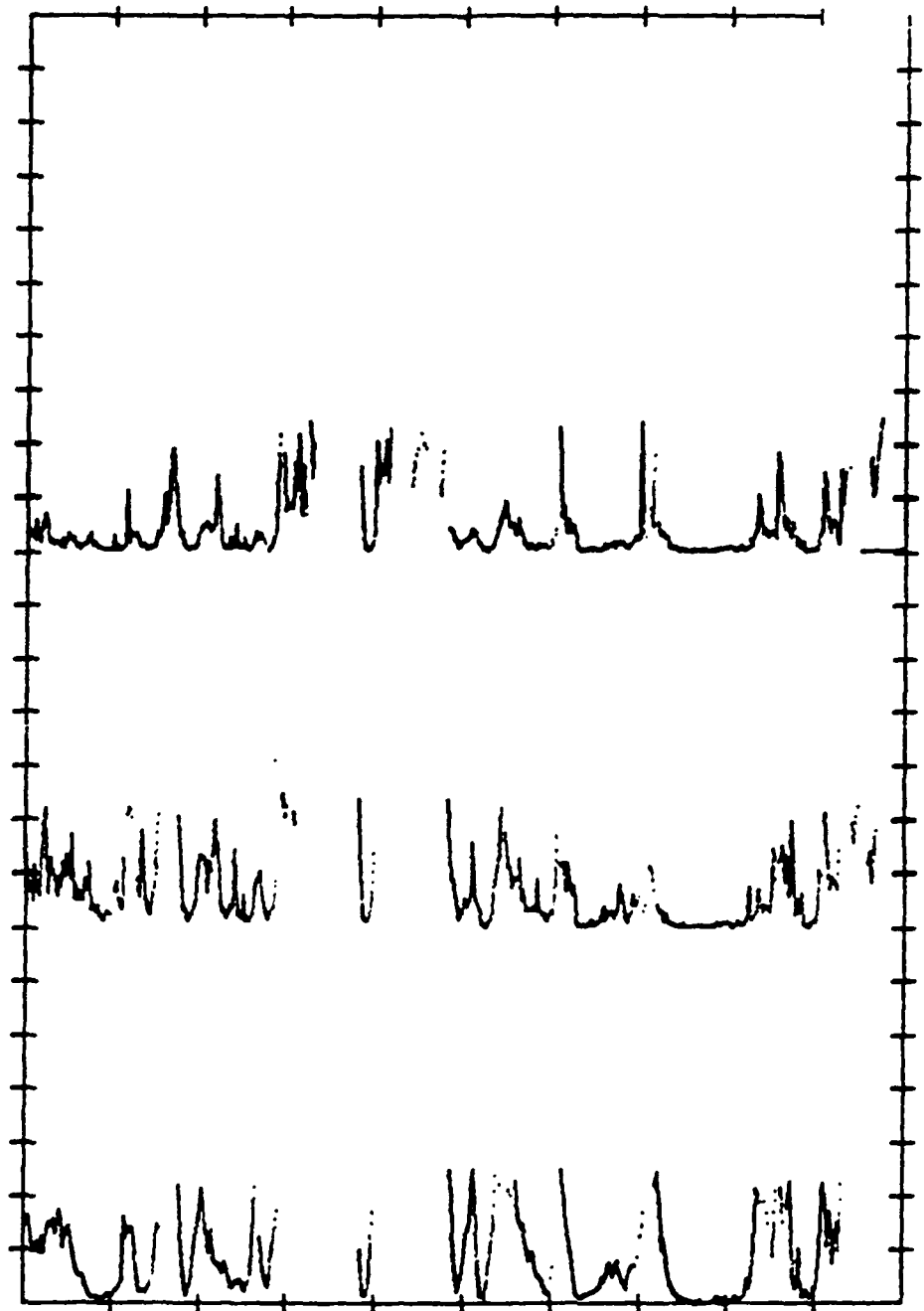
0.5A 1.0A A/4 SEC 2



--10.0 dBV  
--10.0 dBV  
V.L.C  
T

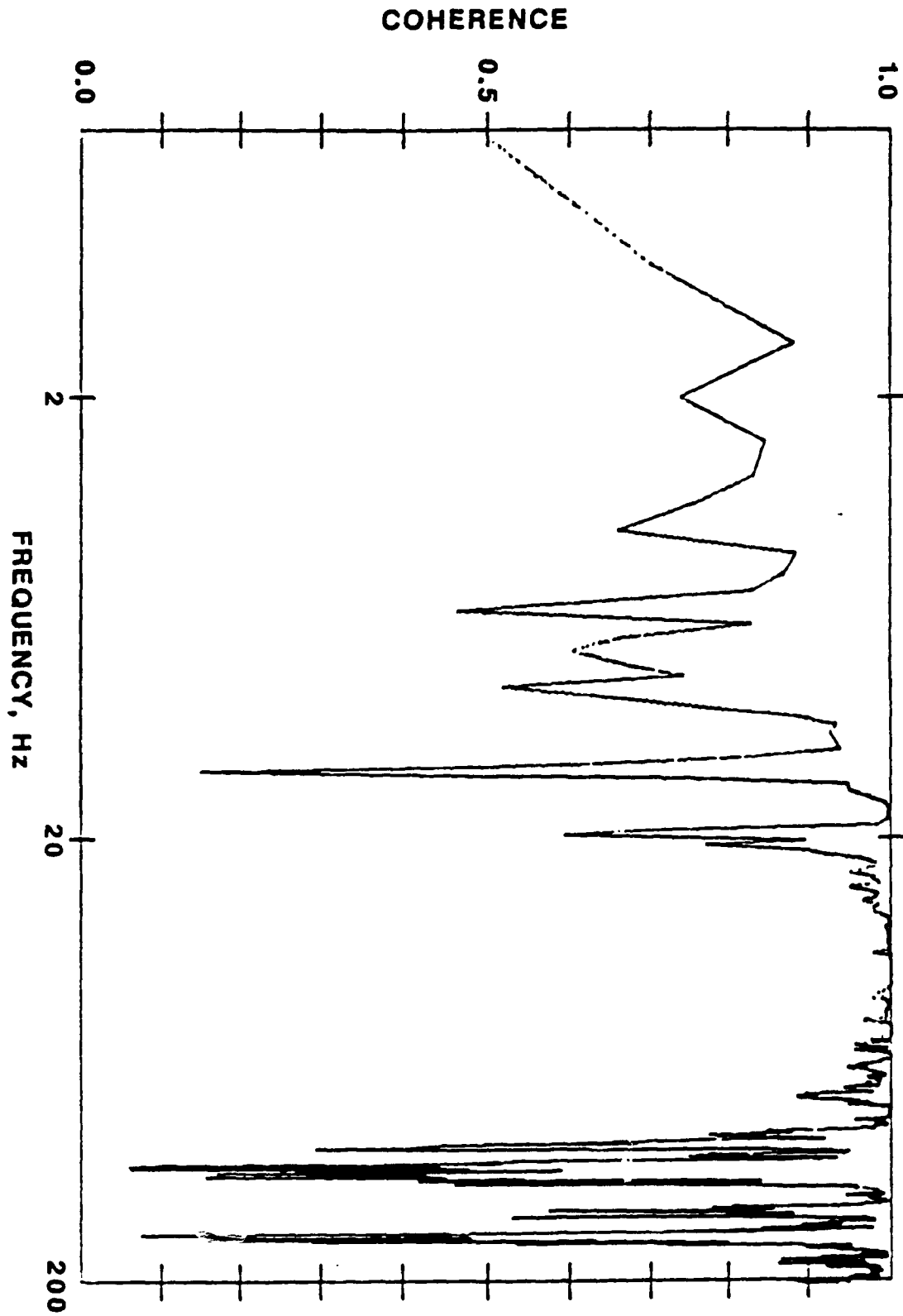








HYDROPHONE SEPARATION - 3.12 meters





## HYDROMECHANICAL WAVE COHERENCE

COHERENCE OF BULGE AND EXTENSIONAL WAVES IN OIL FILLED ARRAY STRUCTURES IS ESSENTIALLY UNITY WHEN IT IS THE DOMINATE NOISE SOURCE.

LEVELS ARE DEPENDENT ON DRIVING FORCES AND THE DETAILS OF THE ARRAY STRUCTURE

RUBBER-BOOTED, OIL FILLED HYDROPHONES CAN SUFFER FROM A FORM OF HYDROMECHANICAL WAVE GENERATION WHICH CAN LIMIT THEIR LOW FREQUENCY DYNAMIC RANGE



**TURBULENT BOUNDARY**

**LAYER FLOW NOISE**



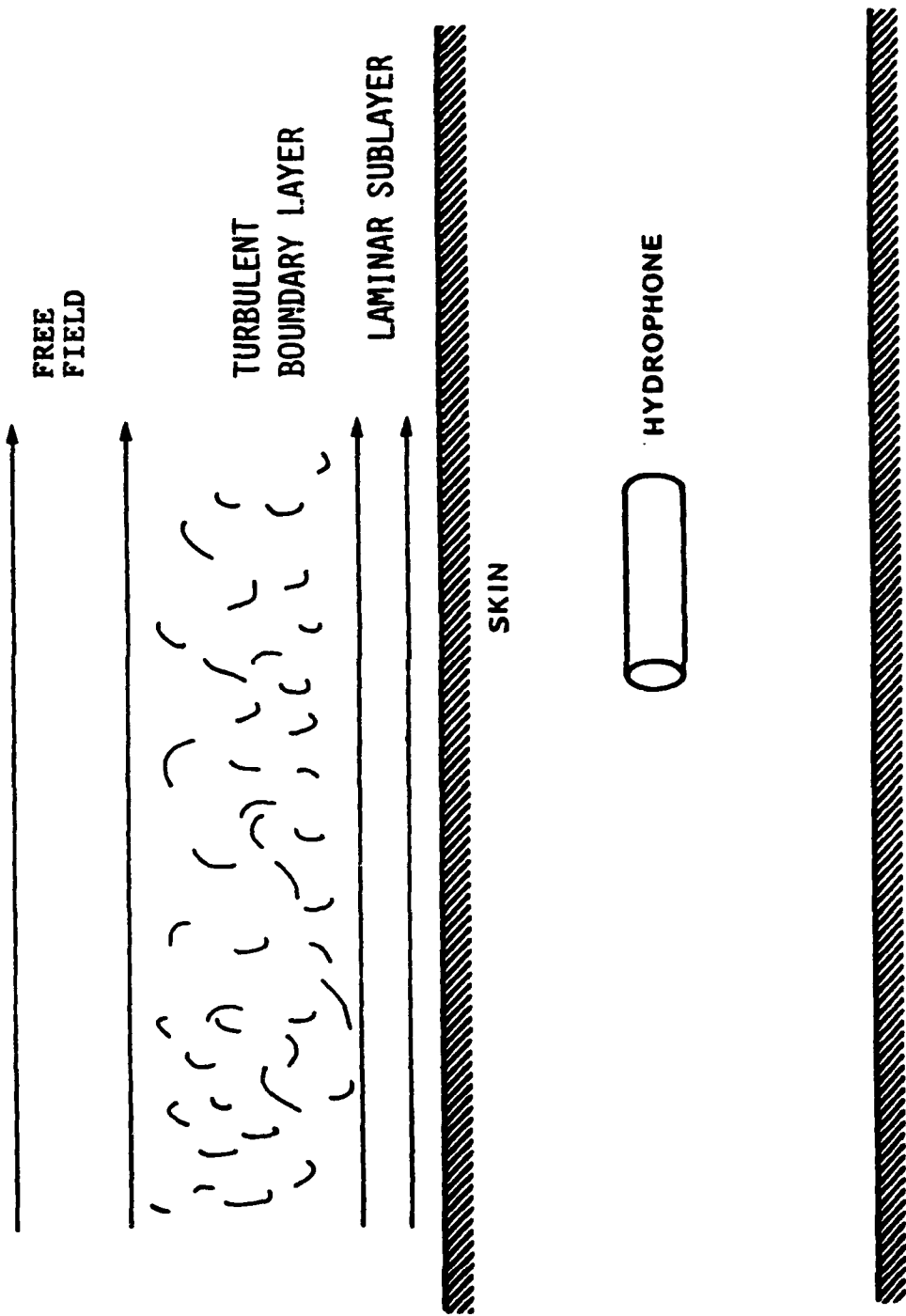
FREE  
FIELD

TURBULENT  
BOUNDARY LAYER

LAMINAR  
SUBLAYER

SKIN

HYDROPHONE





$$P(\omega) = 0.75 \times 10^{-5} \partial_r^2 \rho^2 u^3 \delta^* \quad \omega \leq \omega_0$$

$$P(\omega) = 1.5 \times 10^{-5} \partial_r^2 \rho^2 u^6 / (w^3 \delta^{*2}) \quad \omega \geq \omega_0$$

$$\delta^*(x) = 0.704 \frac{x}{\left(\frac{Ux}{\nu}\right)^{1/5}}; \quad \omega_0 = 2\pi \frac{U}{5\delta^*}$$

- $\omega$  Angular Frequency
- $\partial_r$  Kraichnan constant
- $\rho$  Density
- $\delta^*$  Displacement thickness
- $\omega_0$  Characteristic frequency =  $2\pi \frac{U}{5\delta^*}$
- $x$  Distance from leading edge (or coupling)
- $U$  Velocity
- $\nu$  Kinematic viscosity
- $c$  Sound Speed



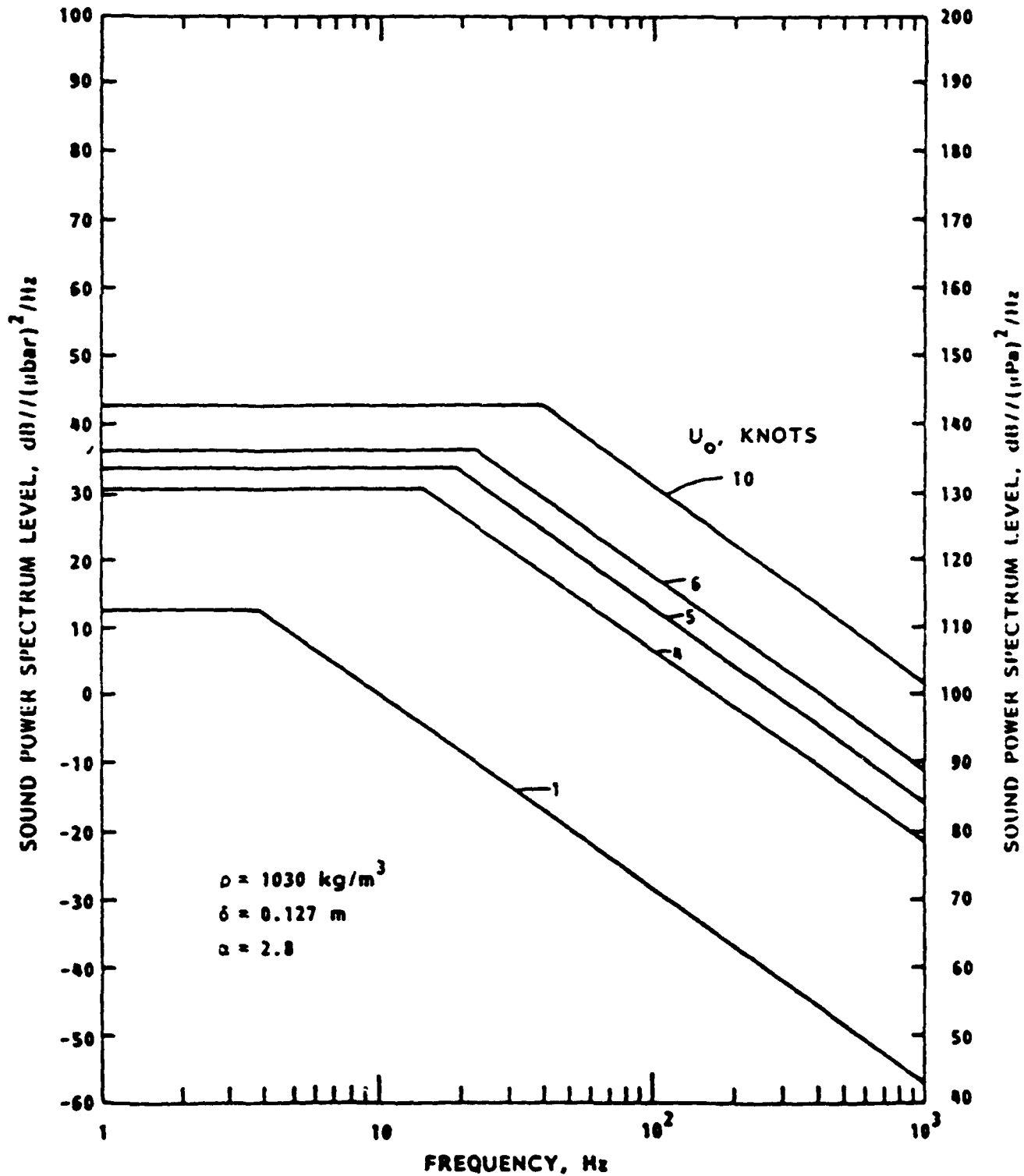


FIGURE 2 - POWER SPECTRAL DENSITY OF TURBULENT WALL PRESSURE FLUCTUATIONS FOR SPEEDS OF 1, 4, 5, 6 AND 10 KNOTS



CORCOS (1963)

DETERMINED THE RATIO OF THE MEASURED  
SPECTRAL DENSITY TO THE ACTUAL  
SPECTRAL DENSITY BASED ON AN EMPIRICAL  
MODEL EXTRACTED FROM DATA TAKEN BY  
CORCOS AND BY WILLMARTH



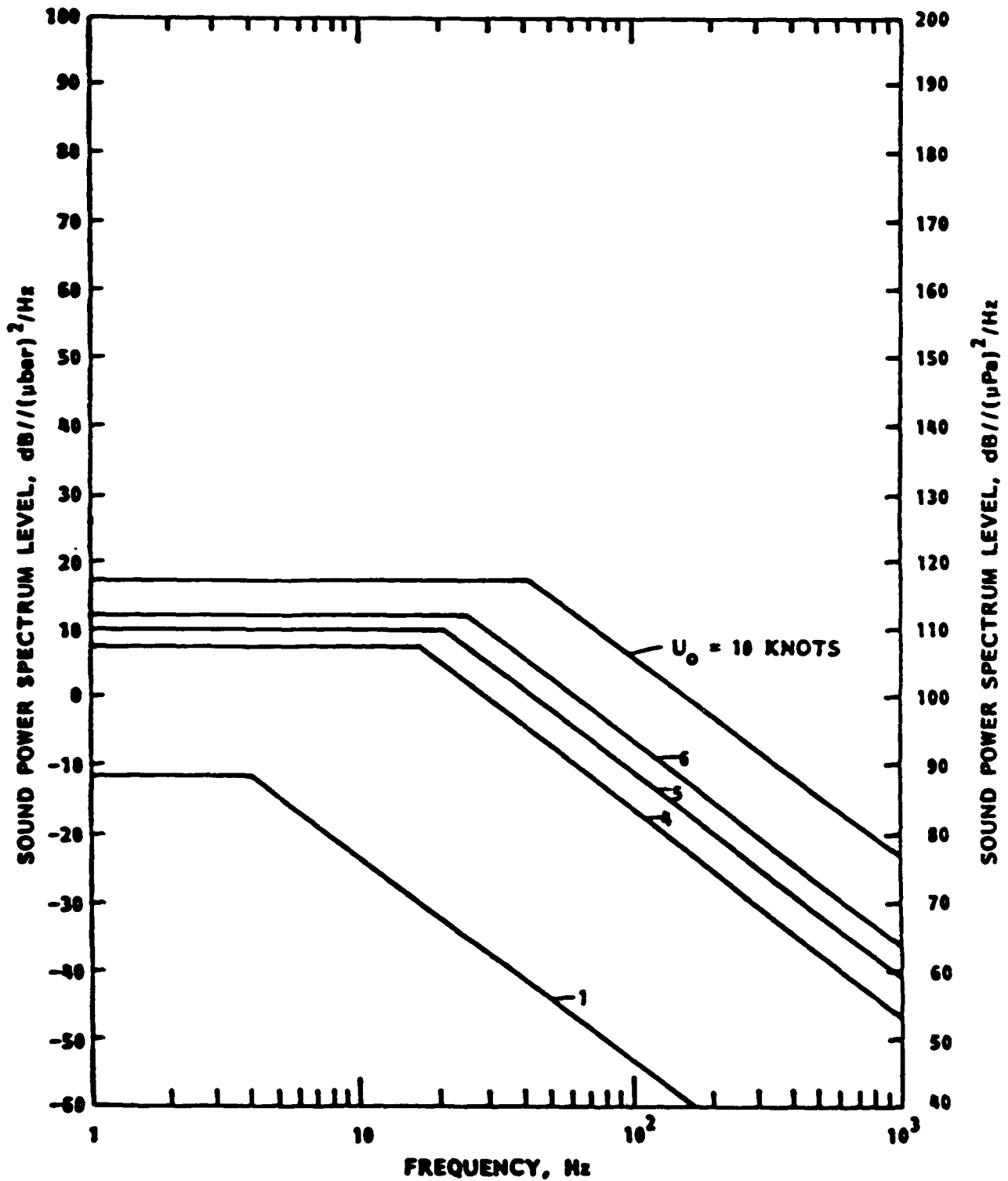
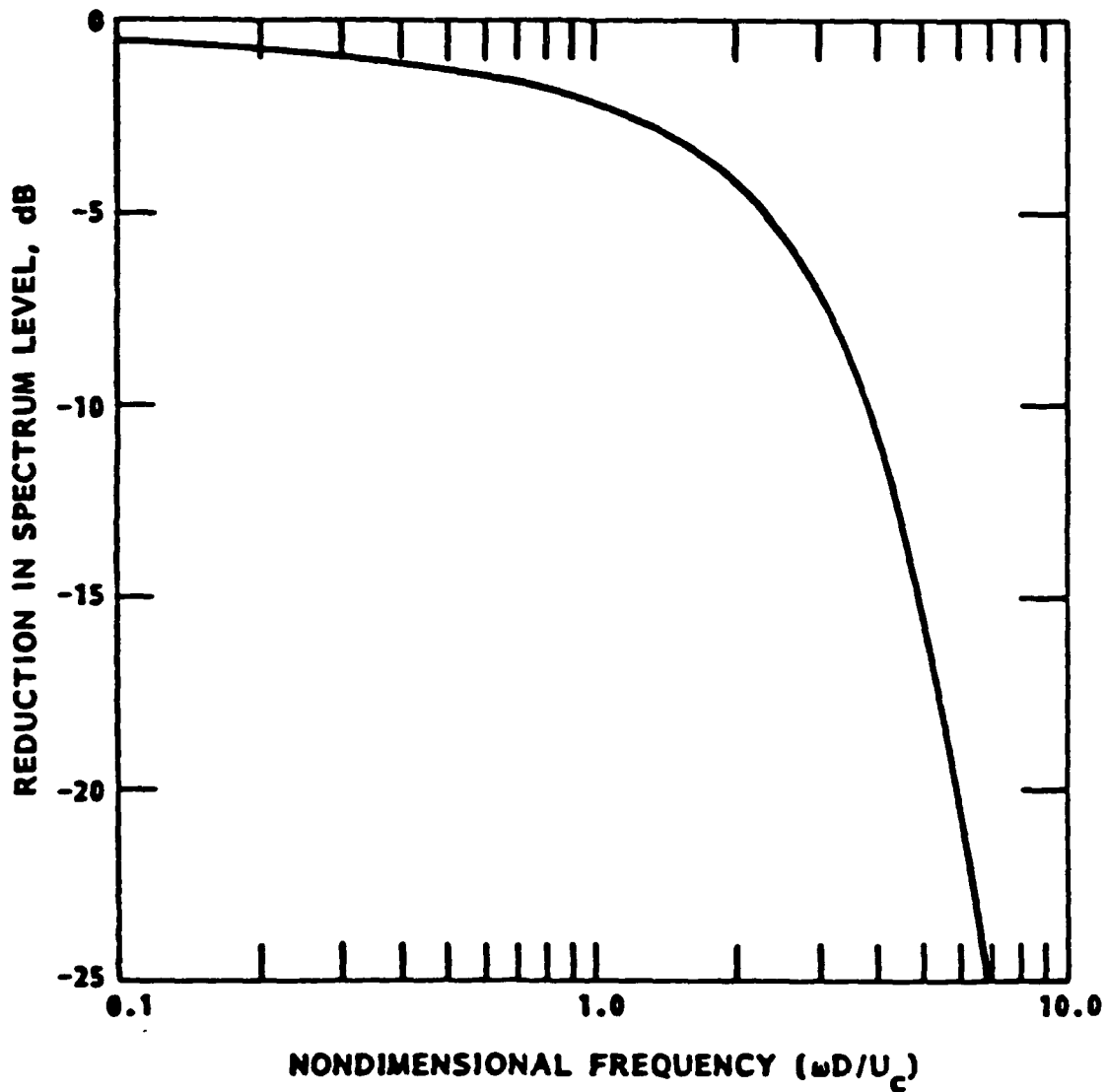


FIGURE 4 - ESTIMATED TURBULENT BOUNDARY LAYER NOISE SPECTRA FOR A PVC HOLED SEISMIC STREAMER AT SPEEDS OF 1, 4, 5, 6 AND 10 KNOTS





**FIGURE 5 - THEORETICAL REDUCTION IN WALL PRESSURE FLUCTUATION SPECTRAL DENSITY AS A FUNCTION OF NONDIMENSIONAL FREQUENCY FOR A RECTANGULAR HYDROPHONE OF DIMENSIONS  $D \times D$  WHERE  $D$  IS IN THE DIRECTION OF FLOW.**



# Tacor Hydraulics

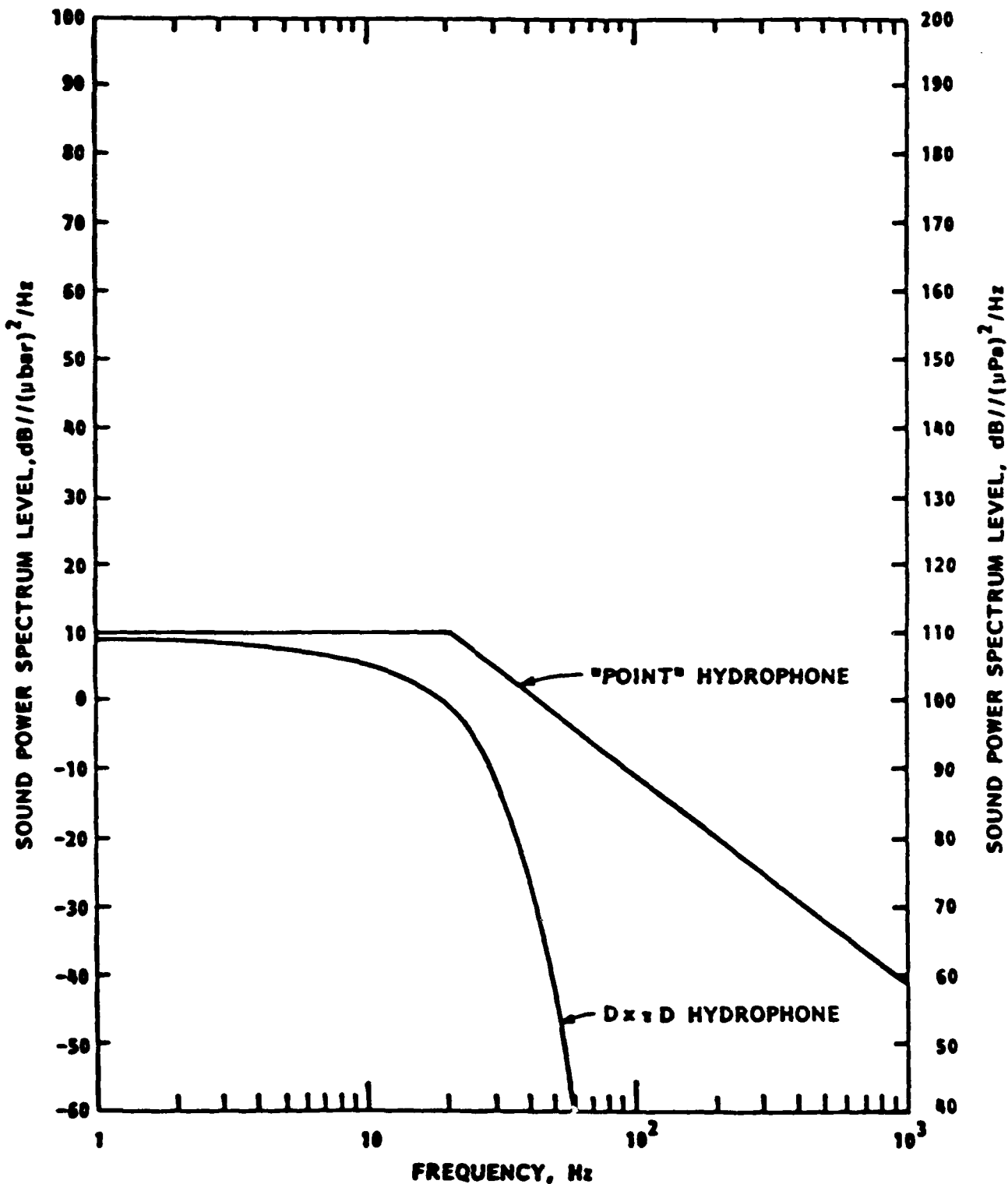
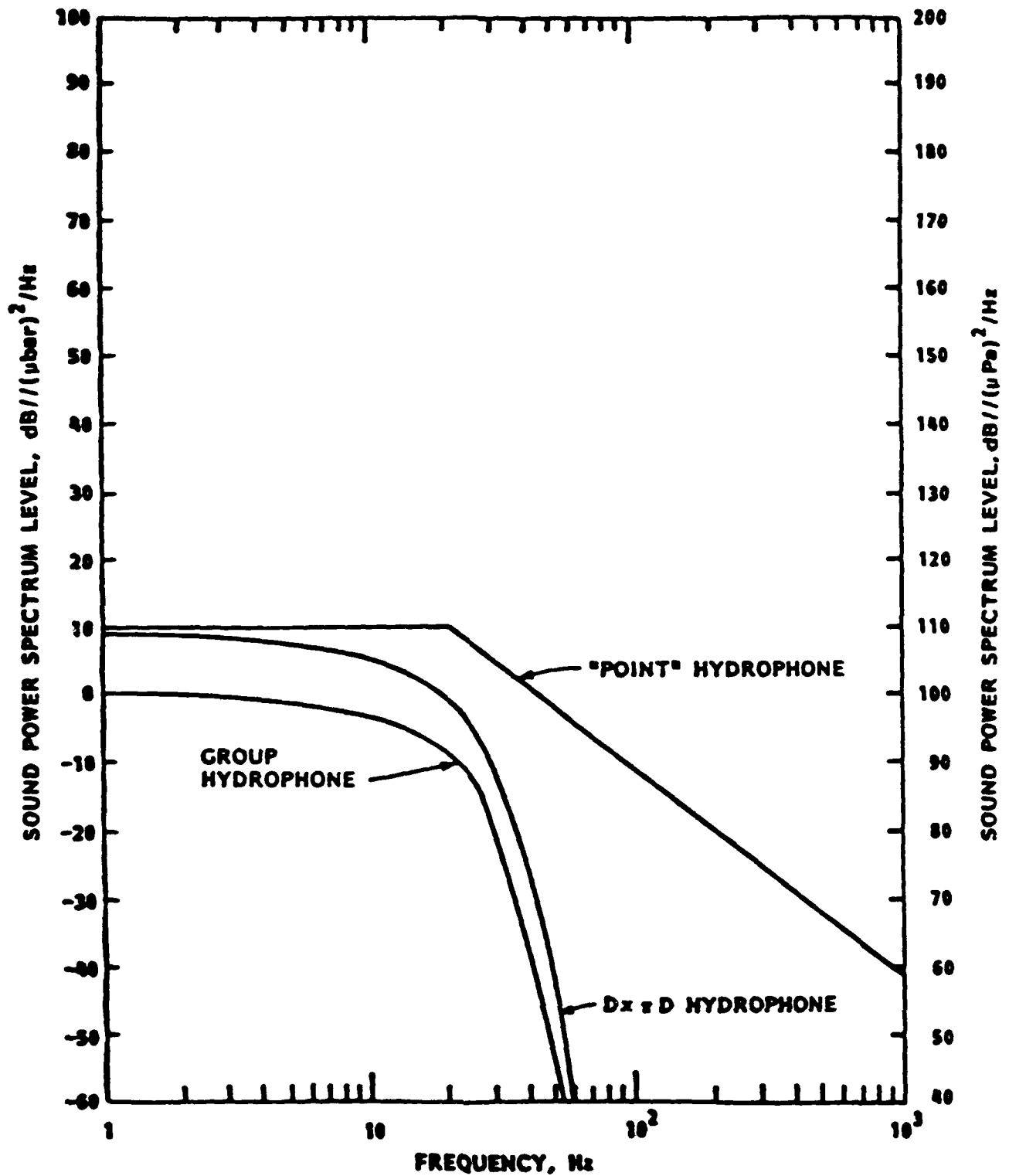


FIGURE 6 - WALL TURBULENT PRESSURE SPECTRAL DENSITY AS MEASURED USING A "POINT" HYDROPHONE IN THE WALL OF A TOWED ARRAY HOSED WITH PVC AND AS MEASURED BY A SMALL HYDROPHONE IN THE CENTER OF A HOSE OF DIAMETER 6.25 cm. TOW SPEED = 5 KNOTS



# Tow Hydrodynamics



**FIGURE 7 - WALL TURBULENT PRESSURE SPECTRAL DENSITY AS MEASURED USING A "POINT" HYDROPHONE IN THE WALL OF A TOWED ARRAY HOSED WITH PVC, AS MEASURED BY A SMALL HYDROPHONE IN THE CENTER OF A HOSE OF DIAMETER 6.25 cm AND AS MEASURED BY A GROUP OF SEVEN HYDROPHONES. TOW SPEED = 5 KNOTS**



FFT Power Spectra,  $dl = 0.002$ ,  $N = 5000$ ,  $l = 512$   
 Swell:13, File(s): 5, Traces: 91 x 90

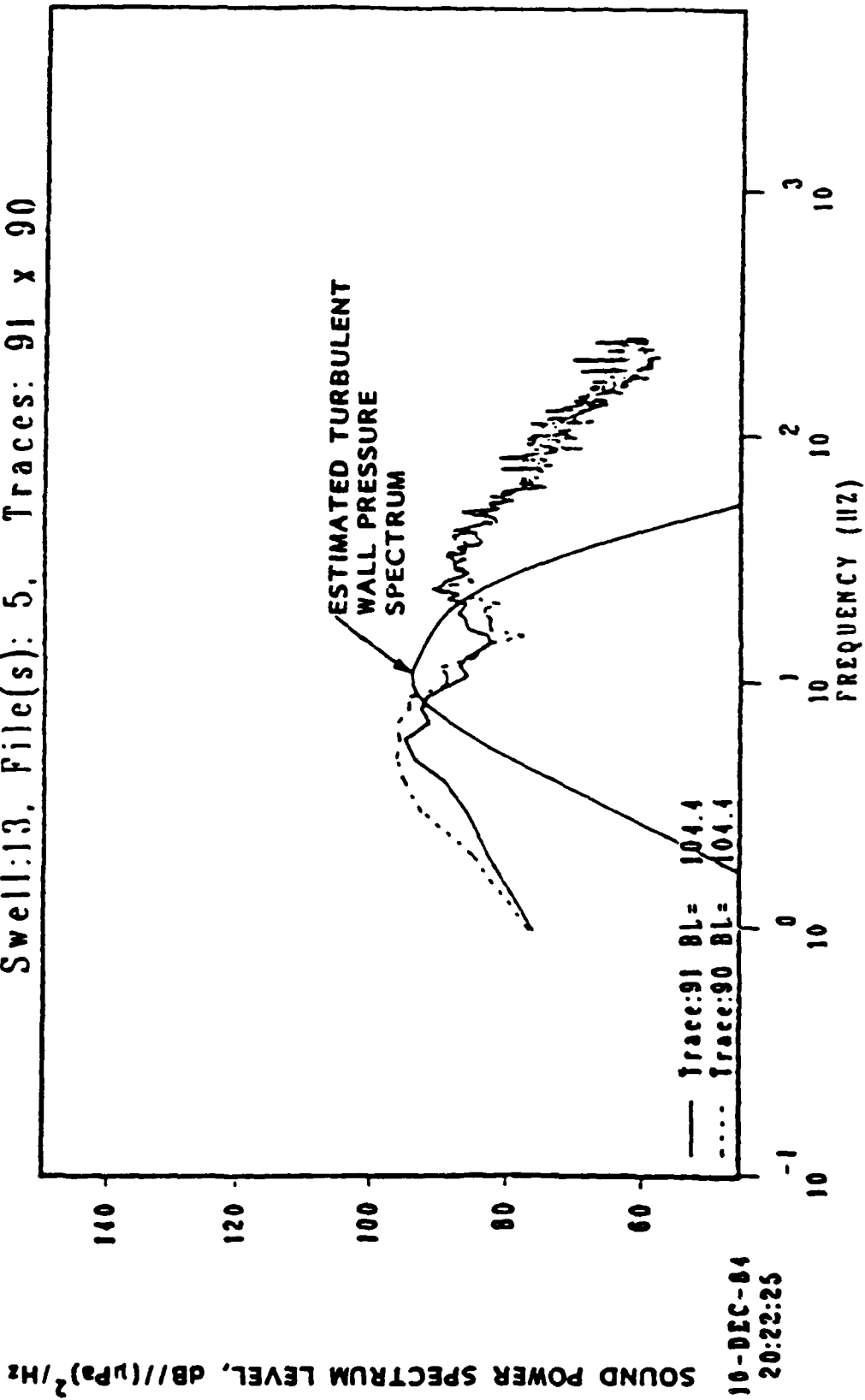


FIGURE 9 - COMPARISON OF SELECTED SPECTRA FOR HEAD SEA, LOW NOISE, CENTER SECTION WITH ESTIMATED TURBULENT WALL PRESSURE SPECTRUM FOR 3.7 KNOTS



FFT Power Spectra,  $dl = 0.002$ ,  $N = 5000$ ,  $L = 512$   
 Swell:13, File(s): 5, Traces: 15 x 14

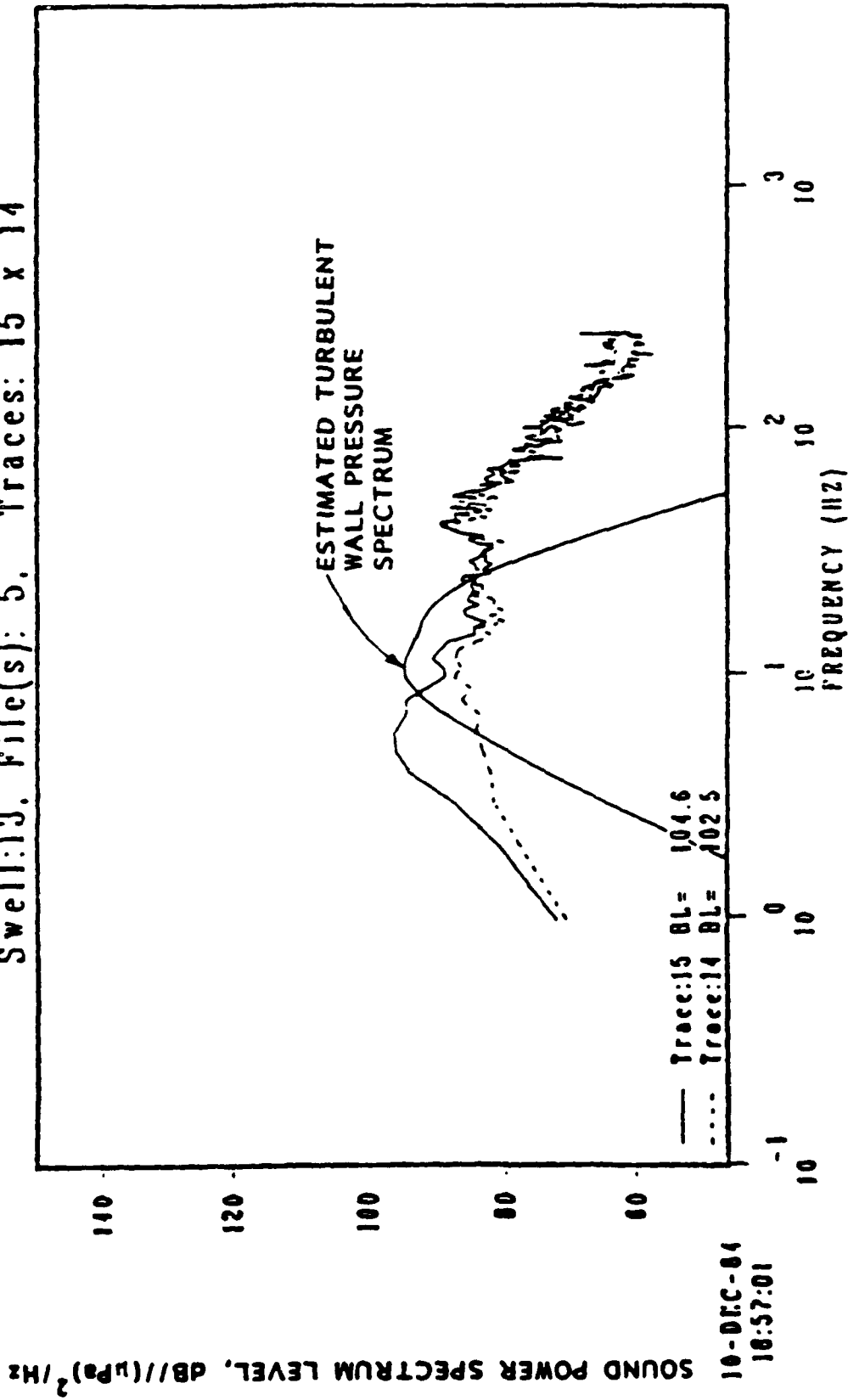


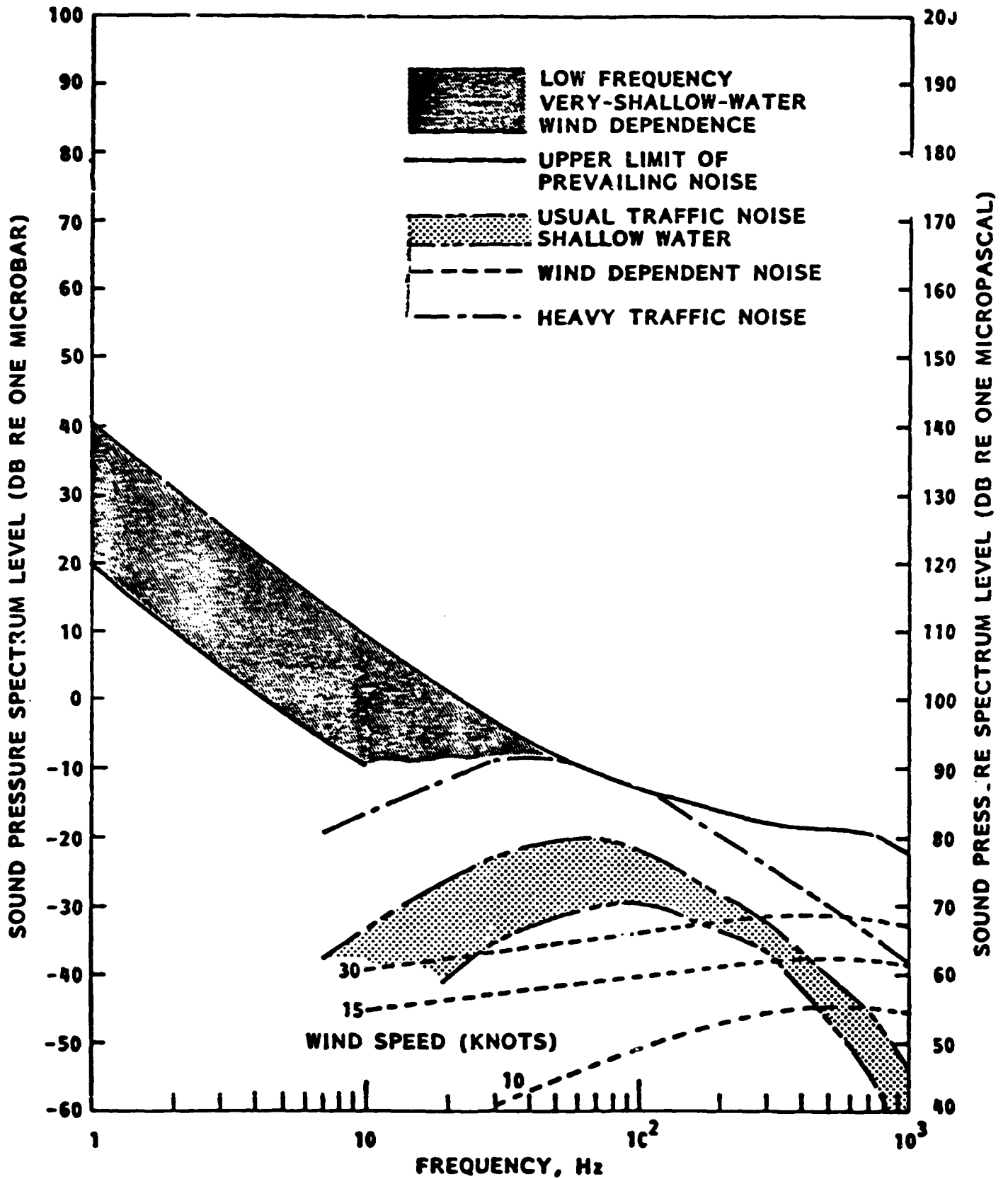
FIGURE 10 - COMPARISON OF SELECTED SPECTRA FOR HEAD SEA, LOW NOISE, AFT SECTION WITH ESTIMATED TURBULENT WALL PRESSURE SPECTRUM FOR 4.1 KNOTS



## **OCEAN AMBIENT NOISE**

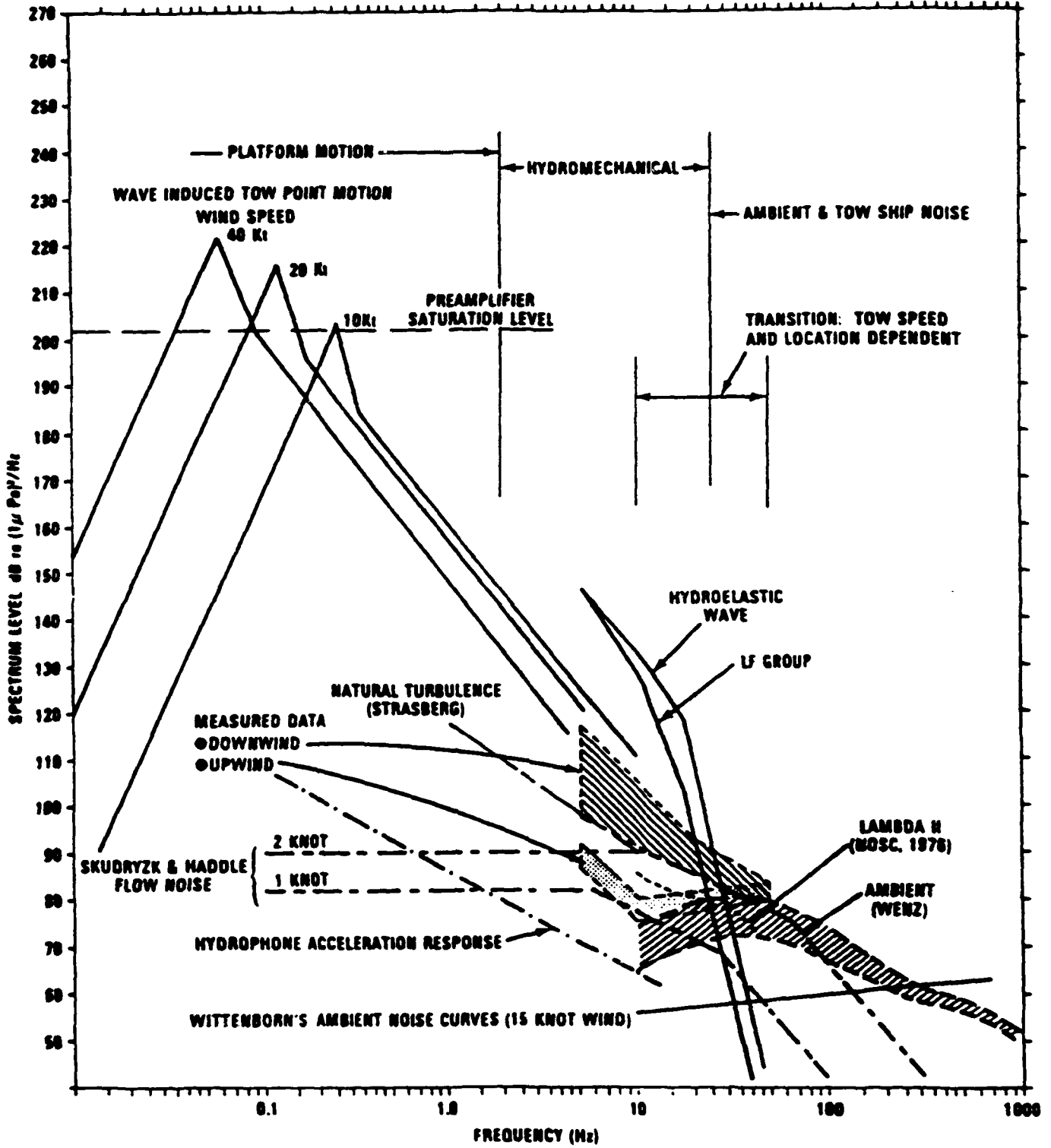
- **Shipping Noise**
- **Wind Generated**





OCEAN AMBIENT NOISE







**AMBIENT / PSEUDO / SELF NOISE ON VLA**

**P. MIKHALEVSKY / H. FREESE (SAIC)**



**ANALYSIS OF SVLA EXPERIMENT DATA**

**H. FREESE  
Y. LEE  
P. MIKHALEVSKY**

**SAIC  
MCLEAN, VA.**

**PRESENTED AT:  
HGI/AEAS VLF AMBIENT NOISE WORKSHOP  
NORDA, 20 SEPTEMBER 1988**



SVLA EXPERIMENT

DATA PROCESSING/BEAMFORMING

NOISE AND SIGNAL CHARACTERISTICS

ESTIMATES OF ARRAY GAIN

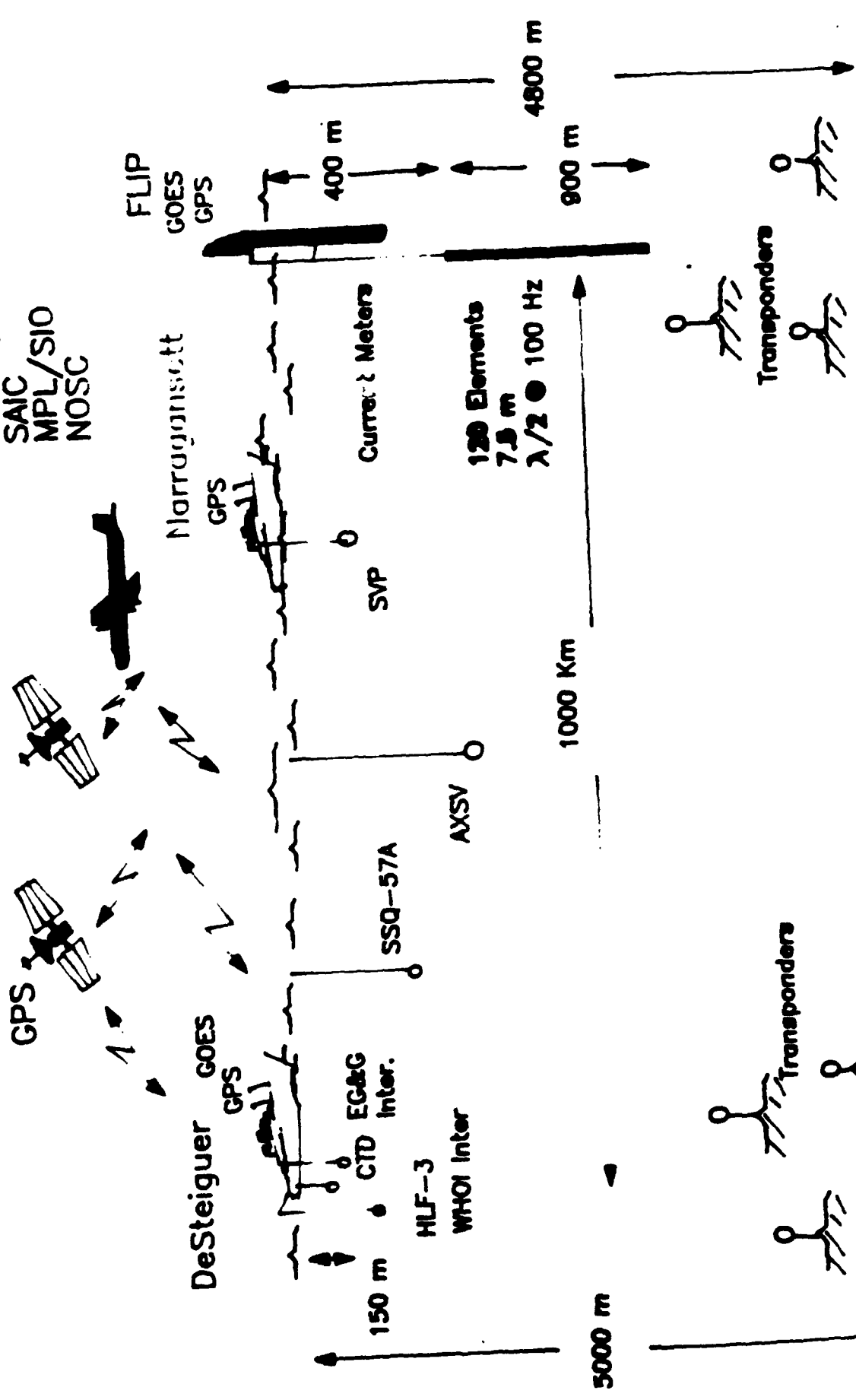
SUMMARY



# SVLA EXPERIMENT FALL 1987

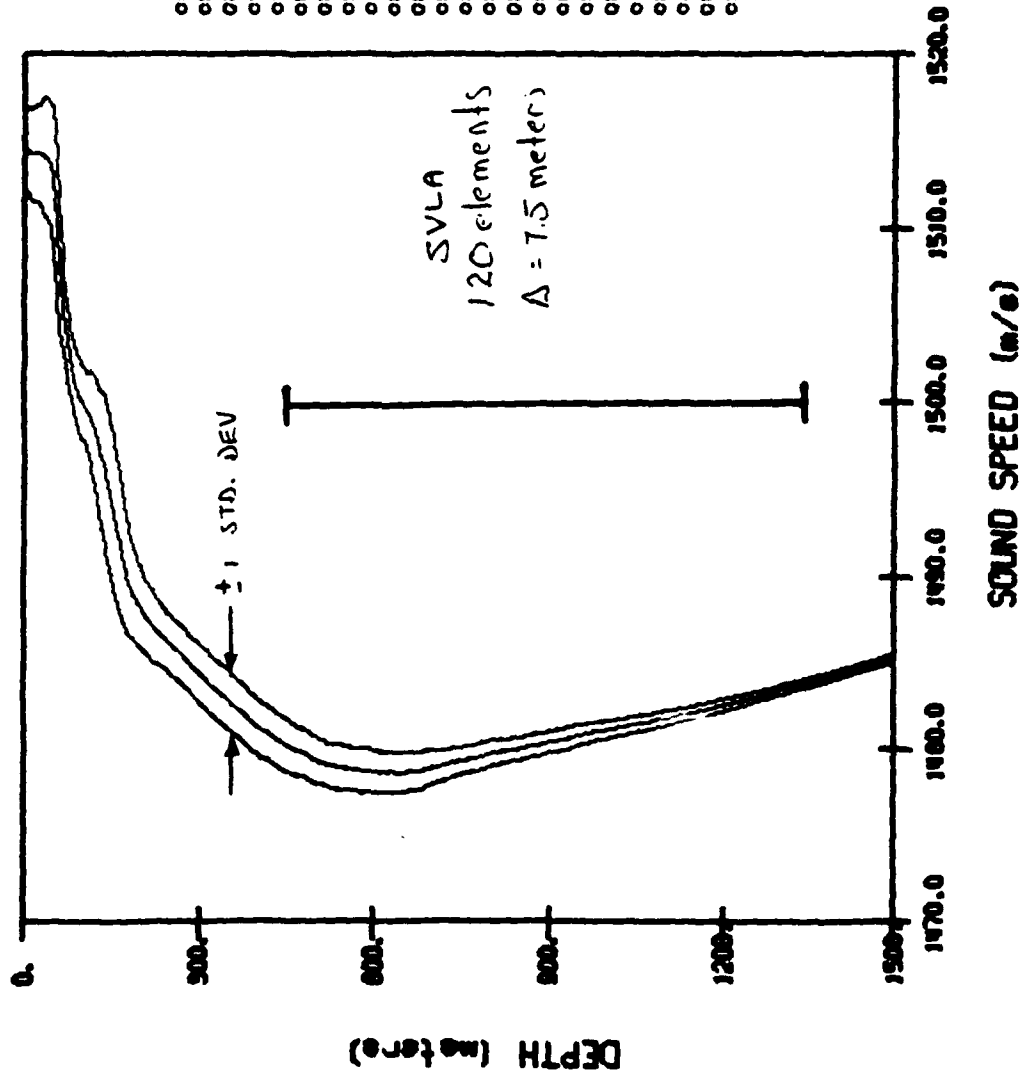
Participants:  
 SAIC  
 MPL/SIO  
 NOSC

GOES





# CTD PROFILES



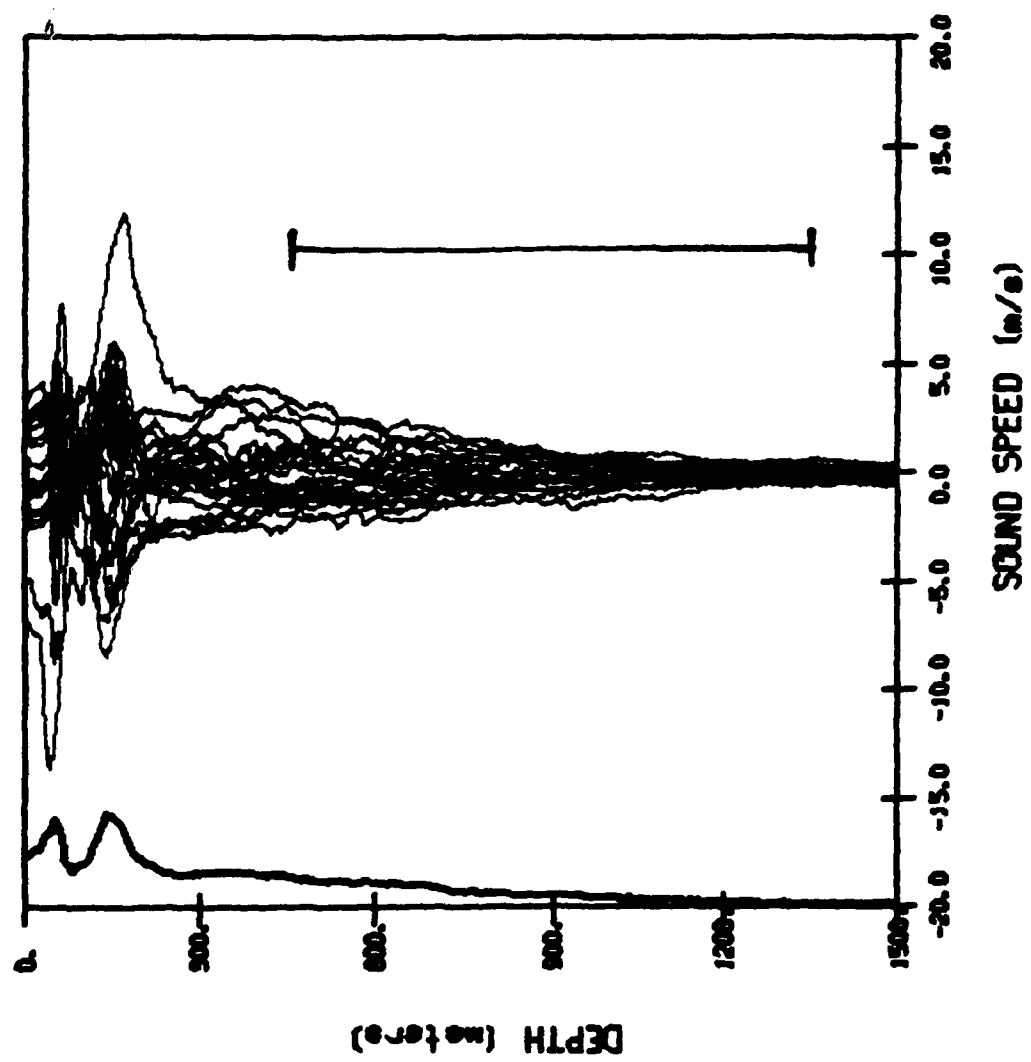
12:34:27.01  
09/15/88

01 \\hgl\env\otd\191530.dat  
 01 \\hgl\env\otd\211600.dat  
 01 \\hgl\env\otd\220430.dat  
 01 \\hgl\env\otd\220800.dat  
 01 \\hgl\env\otd\221130.dat  
 01 \\hgl\env\otd\221426.dat  
 01 \\hgl\env\otd\221707.dat  
 01 \\hgl\env\otd\222030.dat  
 01 \\hgl\env\otd\222330.dat  
 01 \\hgl\env\otd\230200.dat  
 01 \\hgl\env\otd\230500.dat  
 01 \\hgl\env\otd\230750.dat  
 01 \\hgl\env\otd\231046.dat  
 01 \\hgl\env\otd\231330.dat  
 01 \\hgl\env\otd\231640.dat  
 01 \\hgl\env\otd\232000.dat  
 01 \\hgl\env\otd\232230.dat  
 01 \\hgl\env\otd\240110.dat  
 01 \\hgl\env\otd\240355.dat  
 01 \\hgl\env\otd\240705.dat  
 01 \\hgl\env\otd\240930.dat  
 01 \\hgl\env\otd\241200.dat  
 01 \\hgl\env\otd\241500.dat  
 01 \\hgl\env\otd\242300.dat



# CTD PROFILES

12:35:00.07  
09/15/88





**ENVIRONMENT**

**WIND SPEED NIL TO 25 KNOTS**

**EASTERLY CURRENTS OF 8 CM/SEC @ 100 METERS**

**ARRAY SEEMS TO BEHAVE AS A STICK WITH THE POSSIBLE  
EXCEPTION OF TOP TWO SECTIONS.**

**ARRAY TILT OF UP TO A FEW DEGREES**

**ENVIRONMENT (SOUND SPEED) NOT UNUSUAL**



**SOURCES OF NOISE**

**OWN SHIP (MACHINERY, WAVE SLAP)**

**FLOW INDUCED (STRUM, TURBULENCE)**

**MEASUREMENT SYSTEM (ELECTRONIC)**

**ARRAY MOTION (COUPLING TO SURFACE SHIP)**

**OTHER POINT SOURCES**

**SURFACE WAVES**

**SEISMIC ACTIVITY RADIATED FROM BOTTOM**



**PARTITIONING OF NOISE ENERGY**

**OCEAN/MECHANICAL-ELECTRICAL**

**LOCAL/DISTANT**

**SHALLOW/DEEP**

**DISCRETE/CONTINUOUS**

**RESOVLEABLE/UNRESOLVEABLE**

**HOW IS NOISE ENERGY PARTITIONED AND WHAT ARE LEVELS?**

**HOW DOES THIS COMPARE TO SIGNAL ENERGY PARTIONING?**

**PROBLEM IS THE DETECTION OF M POINT TARGETS!**



**GENERAL NOISE CHARACTERISTICS**

**WHEN VIEWED BY PLANE WAVE BEAMFORMER:**

**LEVEL AS A FUNCTION OF:**

**DEPTH - TIME  
DEPTH - FREQUENCY  
WAVENUMBER - FREQUENCY  
k**

**STATISTICAL EIGENSTRUCTURE**

**WHEN VIEWED BY MATCHED FIELD BEAMFORMER:**

**LEVEL AS A FUNCTION OF:**

**RANGE - DEPTH - HORIZONTAL ANGLE**

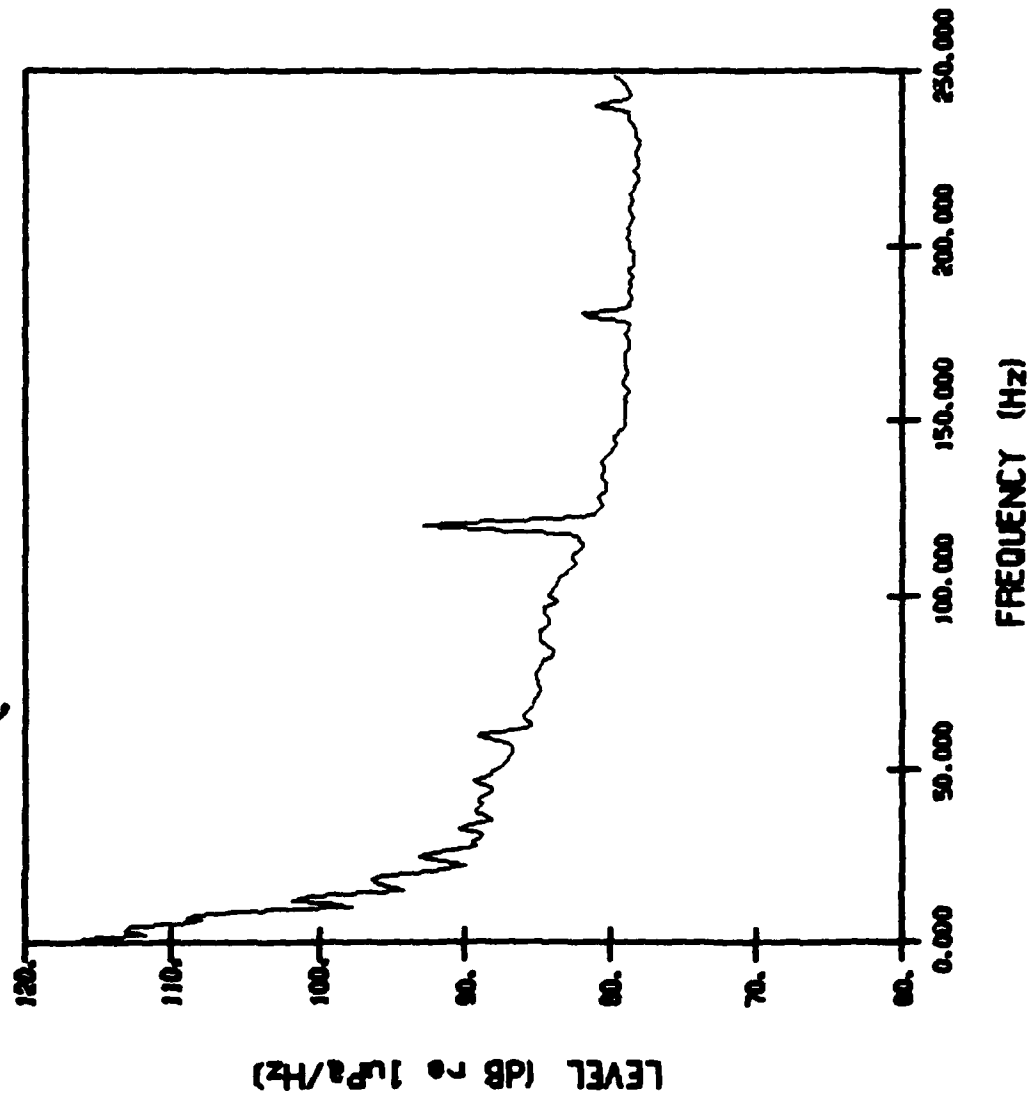
**ACOUSTIC MODE STRUCTURE**

**LEVEL AS A FUNCTION OF MODE NUMBER**

**COVARIANCE OF MODE AMPLITUDES**



SPECTRAL LEVEL  
(ARRAY AVERAGE)



10:21:25.40  
05/09/88  
chan power peak freq  
121. 123.0 116.7 0.977

tfirstr 0.002  
time= 9. 17.16.7. 42.  
file= oi\hgl\data\305000.out  
tape= 305,  
vergain= 38.1  
overlap= 50.  
window= 5.  
spectra= 37.  
npts= 512.

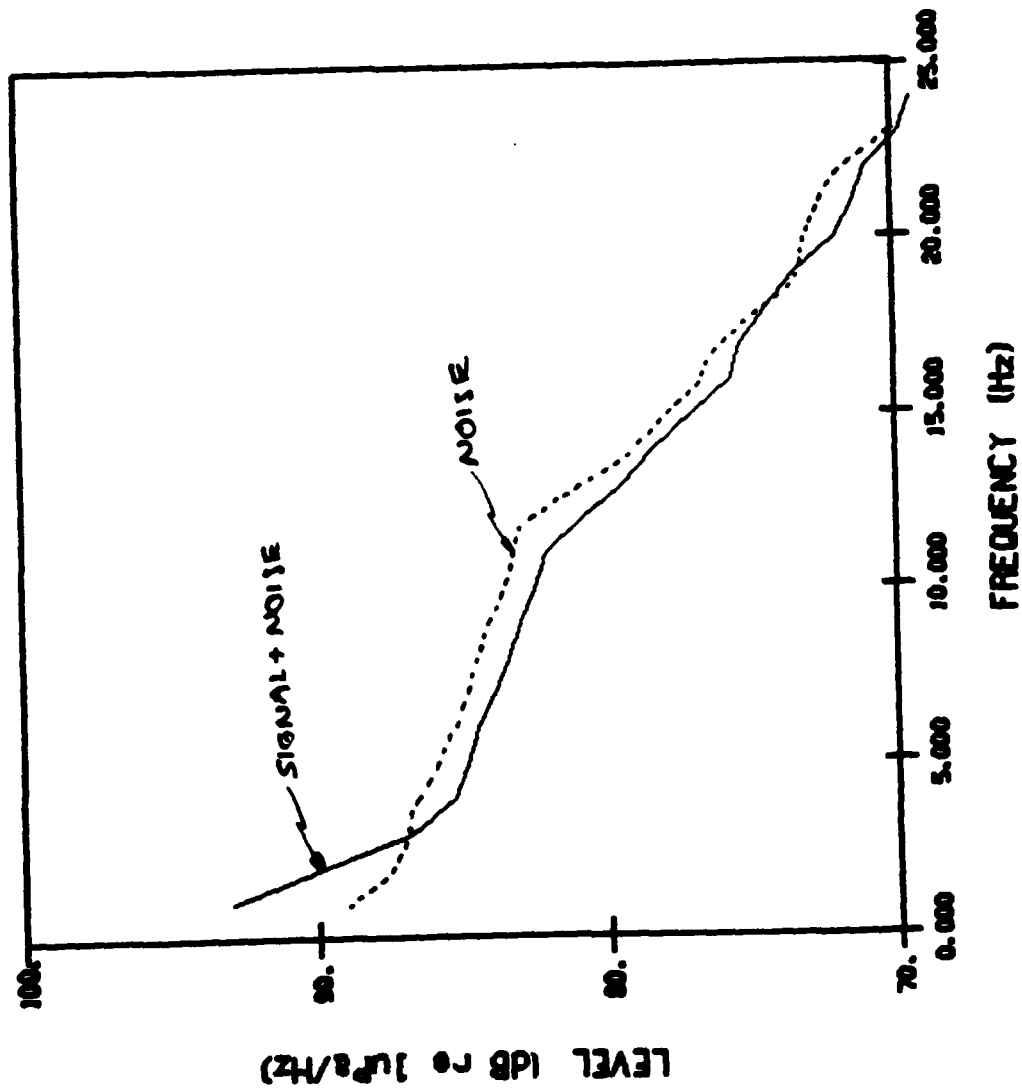


# EIGENVALUES (27 HZ SIGNAL PLUS NOISE)

## SPECTRAL LEVEL

14.19.47.  
7. 21.1988.  
chan power peak freq  
4. 97.7 99.0 1.0000

tfiret= 4.703  
time= 0. 0. 0. 0. 0.  
file= Vgl\data\580027e.out  
tape= 580  
varsize= 38.1  
overlap= 0.  
window= 0.  
spectre= 5.  
npt= 24.

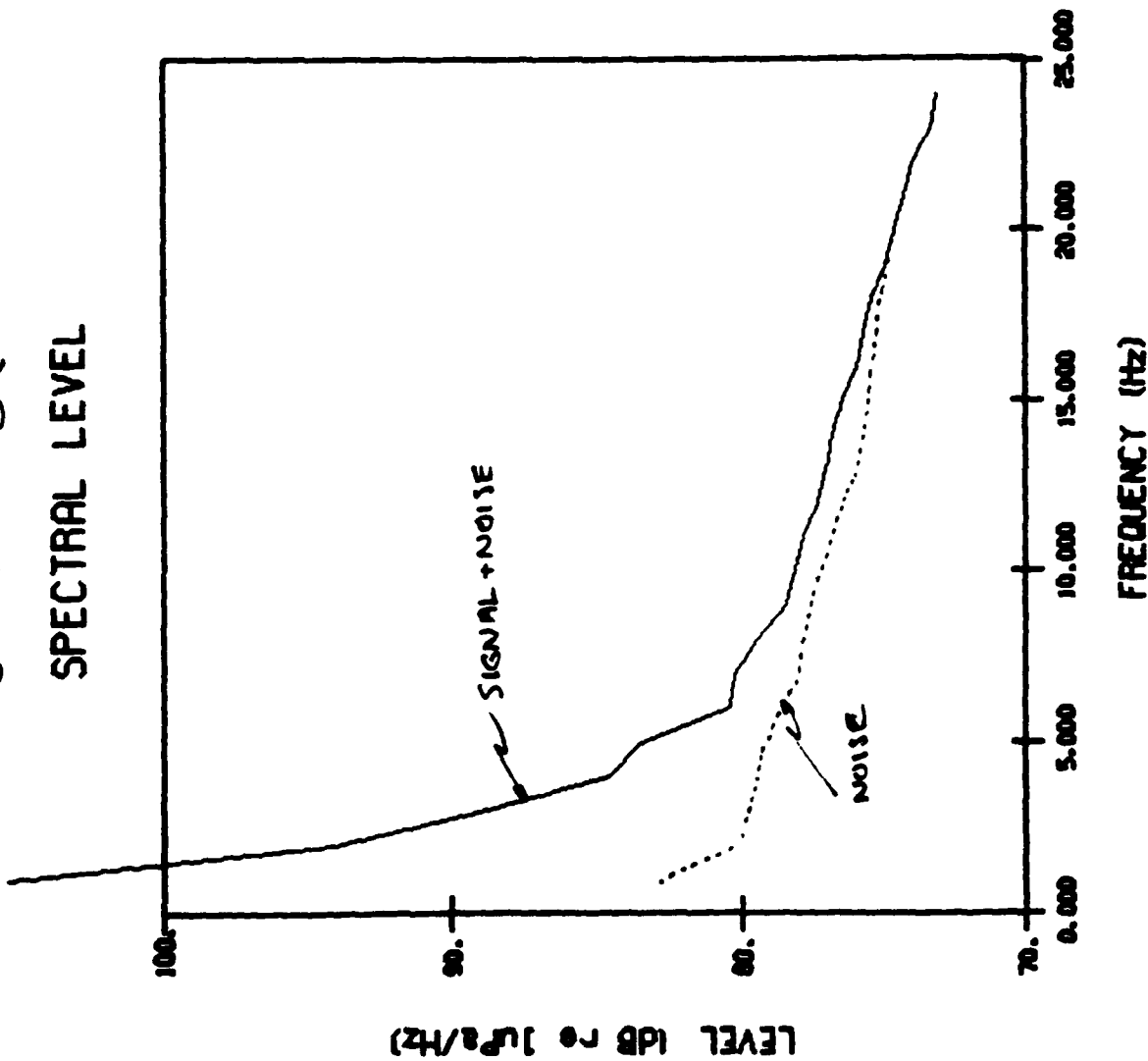




# EIGENVALUES (81 HZ SIGNAL PLUS NOISE)

## SPECTRAL LEVEL

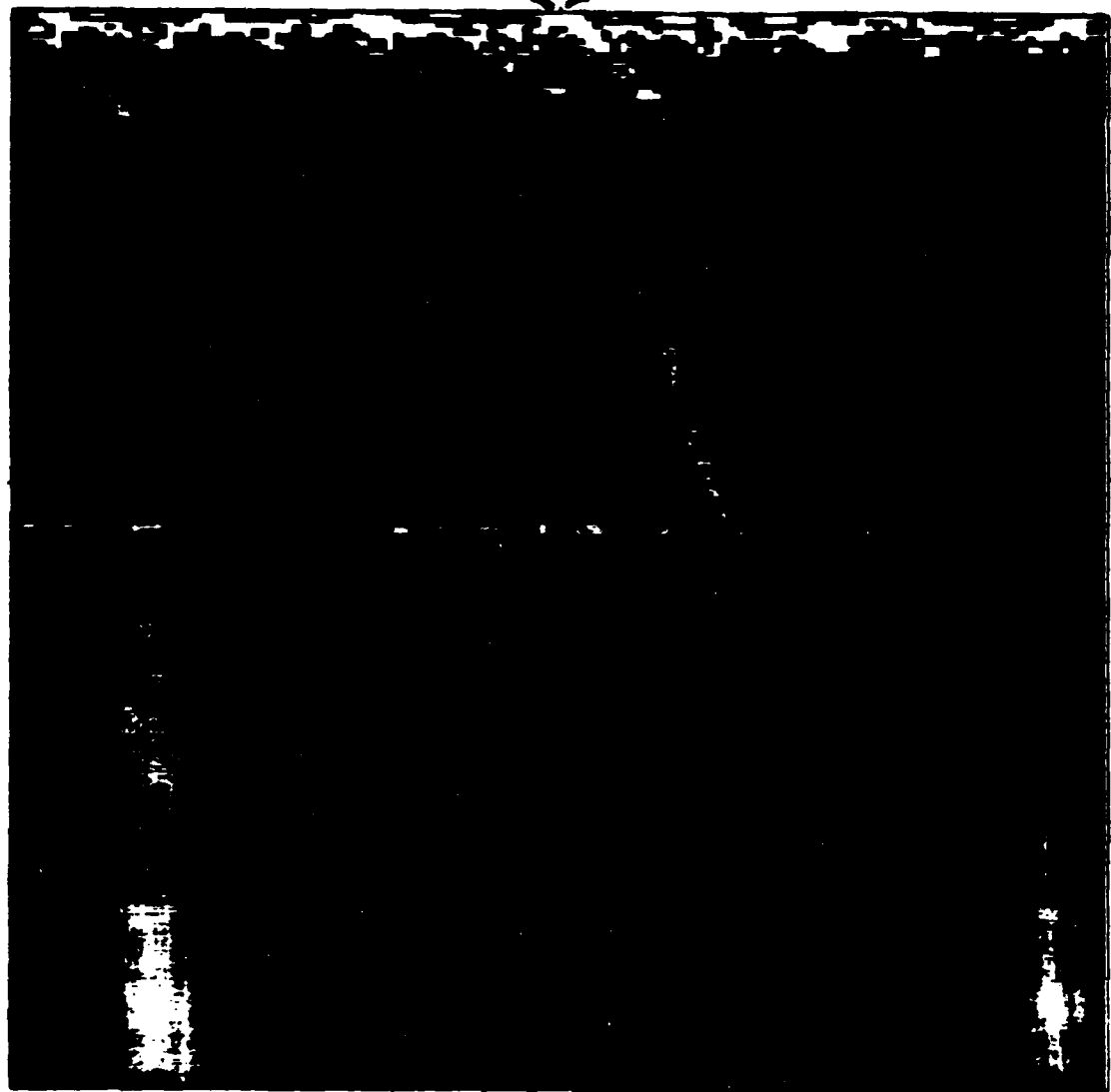
15.18.50.  
7. 21.1988.  
chan power peak freq  
4. 106.2 105.6 1.0000



tfir= 4.703  
tlim= 0. 0. 0. 0. 0.  
file= \hgl\data\579081e.out  
taps= 578  
vargain= 38.1  
overlap= 0.  
window= 0.  
spectra= 5.  
reps= 24.



ACOUSTIC  
REGION



FREQUENCY

20.5° 10.1° WAVENUMBER 9.4° 13.5° 20.5° 0 250

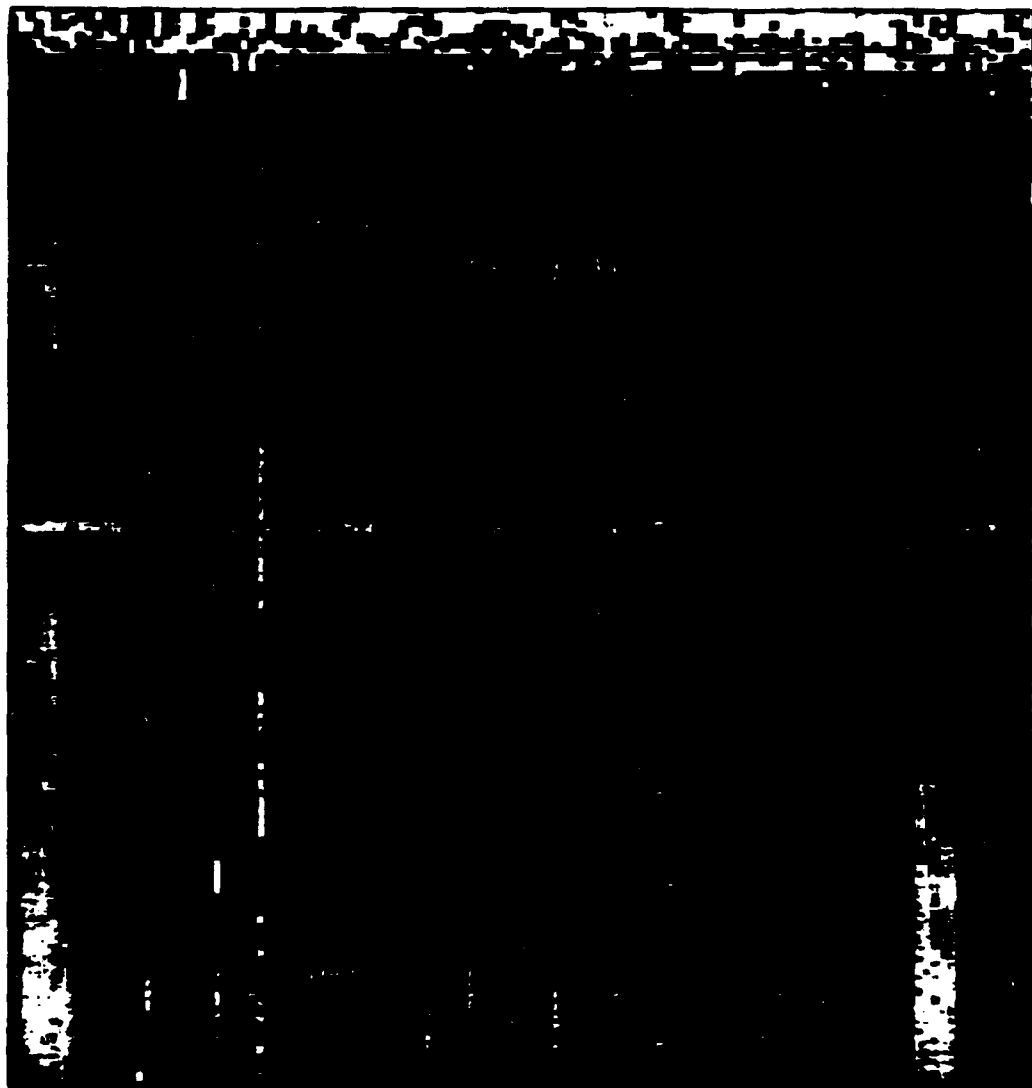
contour interval = 6. dB

385000sa.kf  
frequency = 0.  
tape = 365.

### WAVENUMBER - FREQUENCY SPECTRUM



# FREQUENCY - DEPTH SPECTRUM



0

FREQUENCY

250

1350

DEPTH

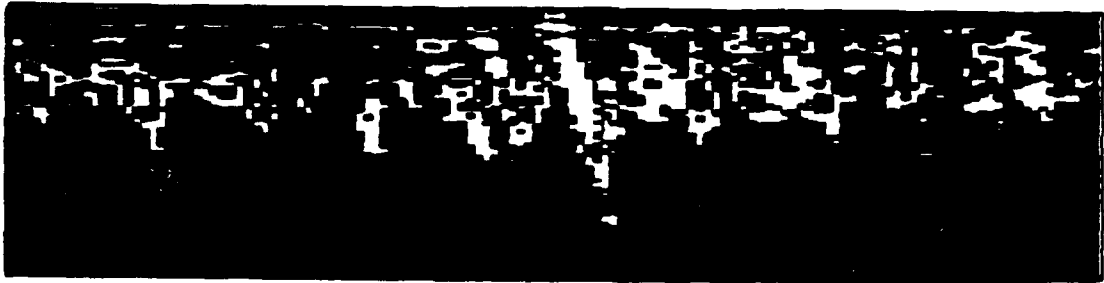
450



contour interval= 6. dB

385000sa.zf  
frequency= 0.  
tape= 385.





0  
FREQUENCY  
K-67

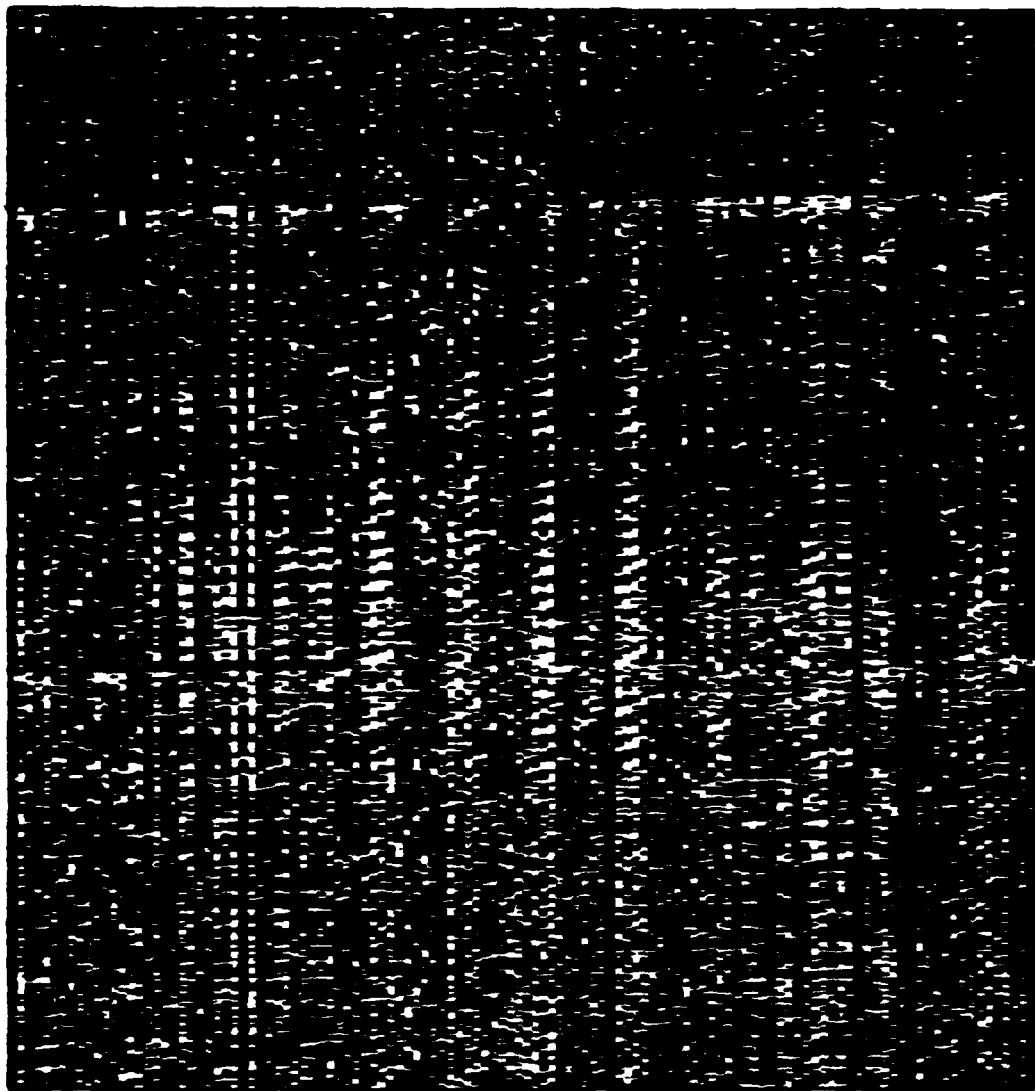
WAVENUMBER



contour interval= 6. dB

856000b.kf  
frequency= 0.  
tape= 856.





TIME

1350

DEPTH

450

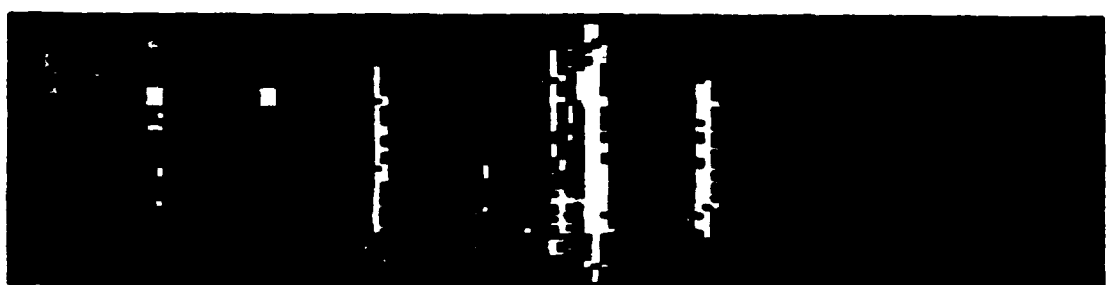
303



contour interval= 6. dB

385000sb.zt  
frequency= 0.  
tape= 385.





FREQUENCY

7 ± 1/3

WAVENUMBER



contour interval= 3. dB

385007n.kf  
frequency= 7.  
tape= 385.



FREQUENCY

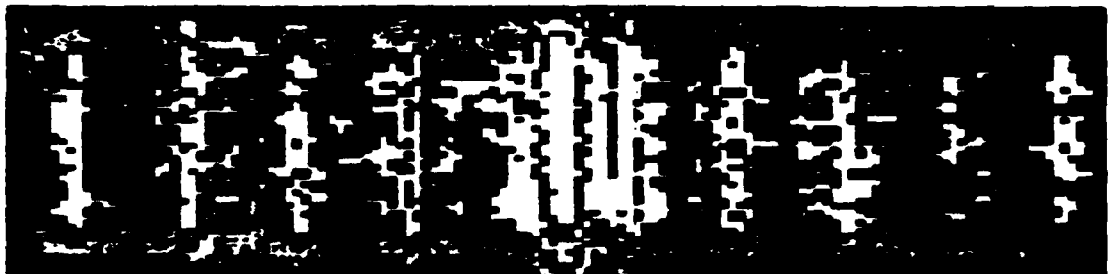
10 ± 1/3

WAVENUMBER



contour interval= 3. dB

385010n.kf  
frequency= 10.  
tape= 385.



FREQUENCY

14 ± 1/3

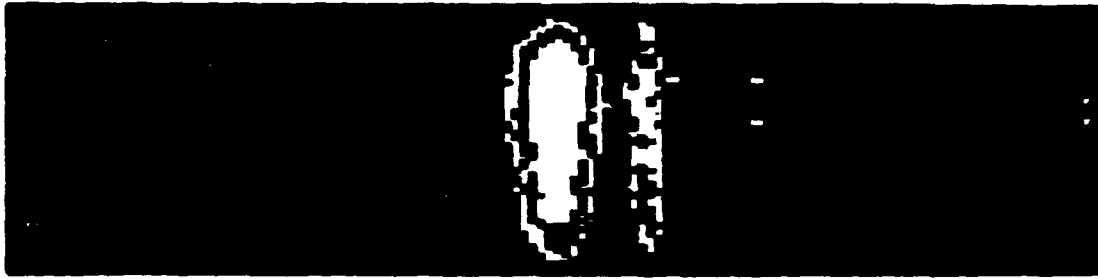
WAVENUMBER



contour interval= 3. dB

385014n.kf  
frequency= 14.  
tape= 385.





FREQUENCY

20 ± 1/3

WAVENUMBER



contour interval= 3. dB

385020n.kf  
frequency= 20.  
tape= 385.



FREQUENCY

29 ± 1/3

WAVENUMBER



contour interval= 3. dB

385029n.kf  
frequency= 29.  
tape= 385.



FREQUENCY

40 ± 1/3

WAVENUMBER



contour interval= 3. dB

385040n.kf  
frequency= 40.  
tape= 385.





FREQUENCY

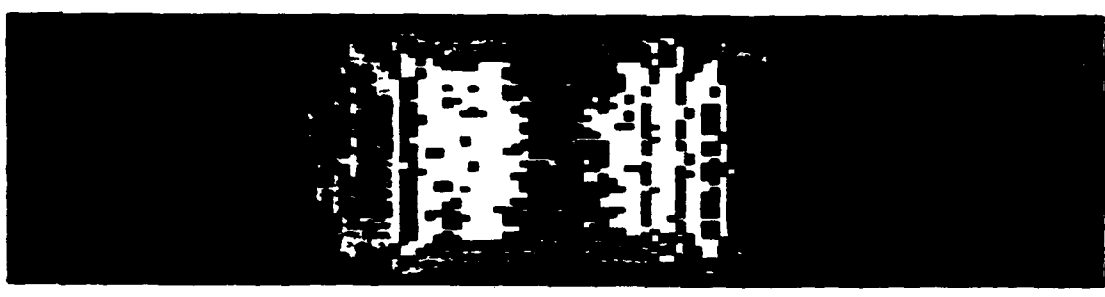
5 ± 1/3

WAVENUMBER



contour interval= 3. dB

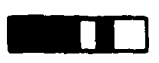
385005na.kf  
frequency= 5.  
tape= 385.



FREQUENCY

79 ± 1/3

WAVENUMBER



contour interval= 3. dB

385079n.kf  
frequency= 79.  
tape= 385.



FREQUENCY

27 ± 1/3



WAVENUMBER



contour interval= 3. dB

385027s.kf  
frequency= 27.  
tape= 385.

FREQUENCY

54 ± 1/3



WAVENUMBER



contour interval= 3. dB

385054ss.kf  
frequency= 54.  
tape= 385.

FREQUENCY

81 ± 1/3



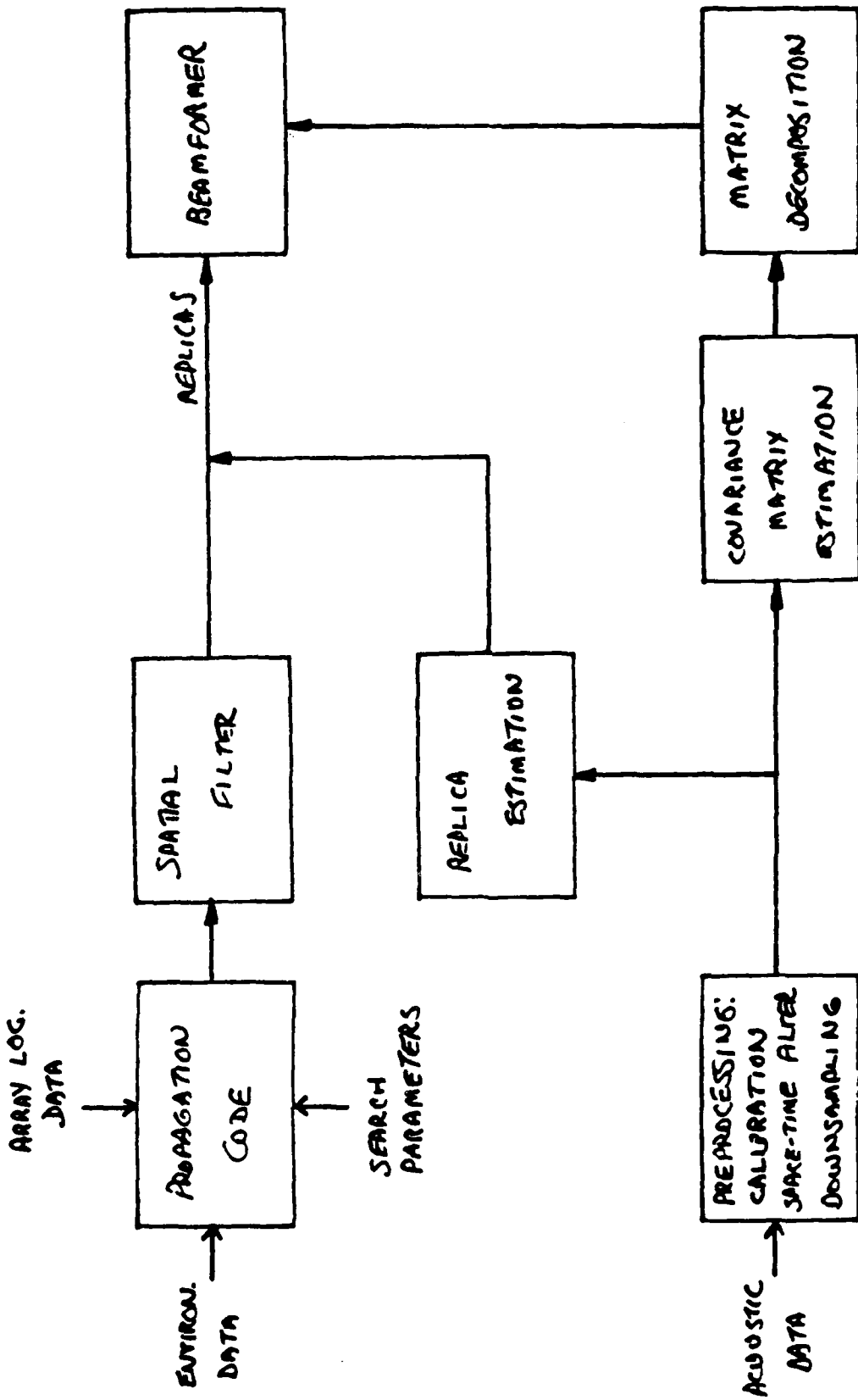
WAVENUMBER



contour interval= 3. dB

385081ss.kf  
frequency= 81.  
tape= 385.







## • PRE-PROCESSING

• System and sensor calibration

• Narrow-band-pass filtering  
+/- 0.4 Hz band  
down sample to 2/3 Hz

• Smoothing: coherent integration  
to increase input SNR

• Covariance Matrix:  $R(i, j) = \sum_{n=1}^N p(i, n) * p^*(j, n)$

• Matrix inversion/diagonalization

• Self replica beamforming:  
independent of mismatches  
upper limit of the beamforming



(MATCHED FIELD PROCESSING Cont.)

- o Range-dependent normal mode method with the adiabatic approximation.
- o Bartlett, MLM  
SVD, EMLM, MUSIC, MCM, etc.



• BEAMFORMING

R = Covariance Matrix  
A = Predicted Replica

BARTLETT       $A^H R A$   
MLM             $1/A^H R^{-1} A$

Constrained Methods: Replacing A by C

$$C = [CA1.A2.....]CA1.A2.....J^H A$$



(BEAMFORMING Cont.)

$$R = \sum \lambda_i V_i V_i^{\dagger}$$

$$R_S = \sum \lambda_s V_s V_s^{\dagger}$$

$$R_n^{-1} = \sum \frac{1}{\lambda_n} V_n V_n^{\dagger}$$

$$(R_n^{-1})_m = \sum V_n V_n^{\dagger}$$

SVD  $A^H R_S A$

Eigenvector  $1/A^H R_n^{-1} A$

MUSIC  $1/A^H (R_n^{-1})_m A$



o MISMATCH

$$\text{Let } R = \sigma_s^2 V_s V_s^t + \sigma_n^2 Q, \quad \cos^2 \theta = |V_s^t A|^2 / |V_s^t A|^2$$

Bartlett

$$AG = N \cos^2 \theta$$

MLM

$$AG = \frac{N \cos^2 \theta}{1 + N \frac{\sigma_s^2}{\sigma_n^2} (1 - \cos^2 \theta)}$$

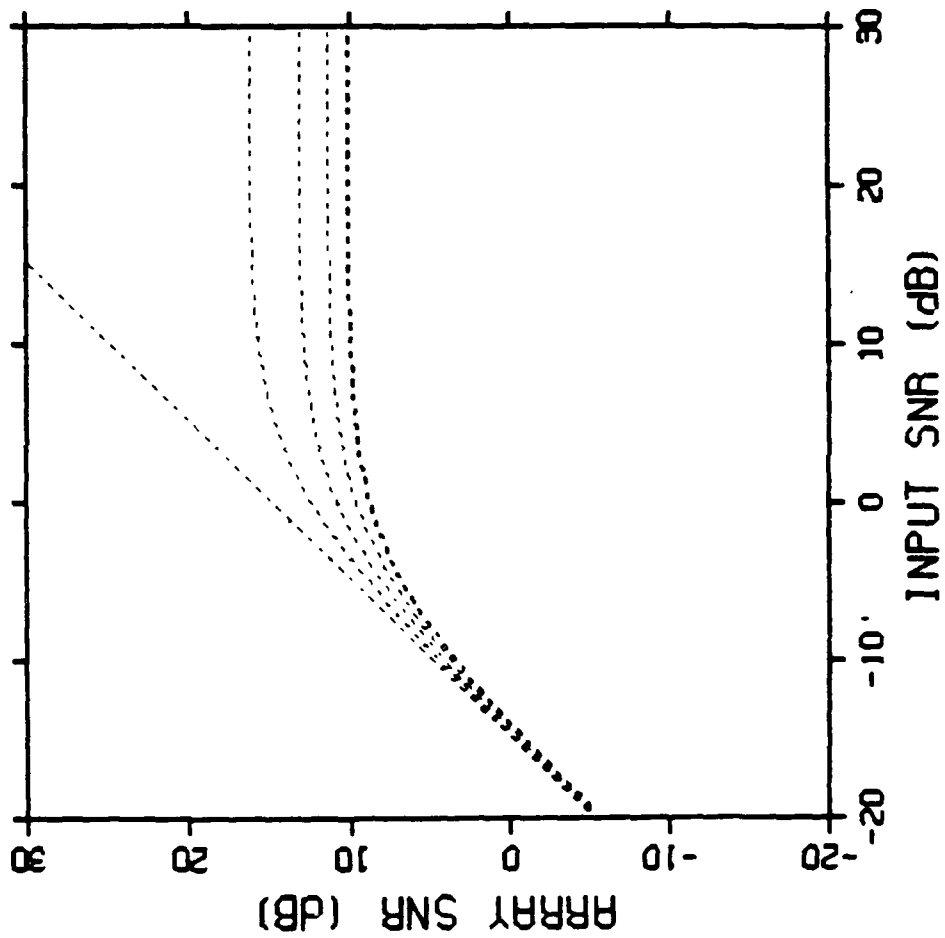


30 ELEMENT ARRAY WITH WHITE NOISE

MLM

AGMAX = 14.8

MISMATCH STEP = 0.1 dB





### ARRAY GEOMETRY

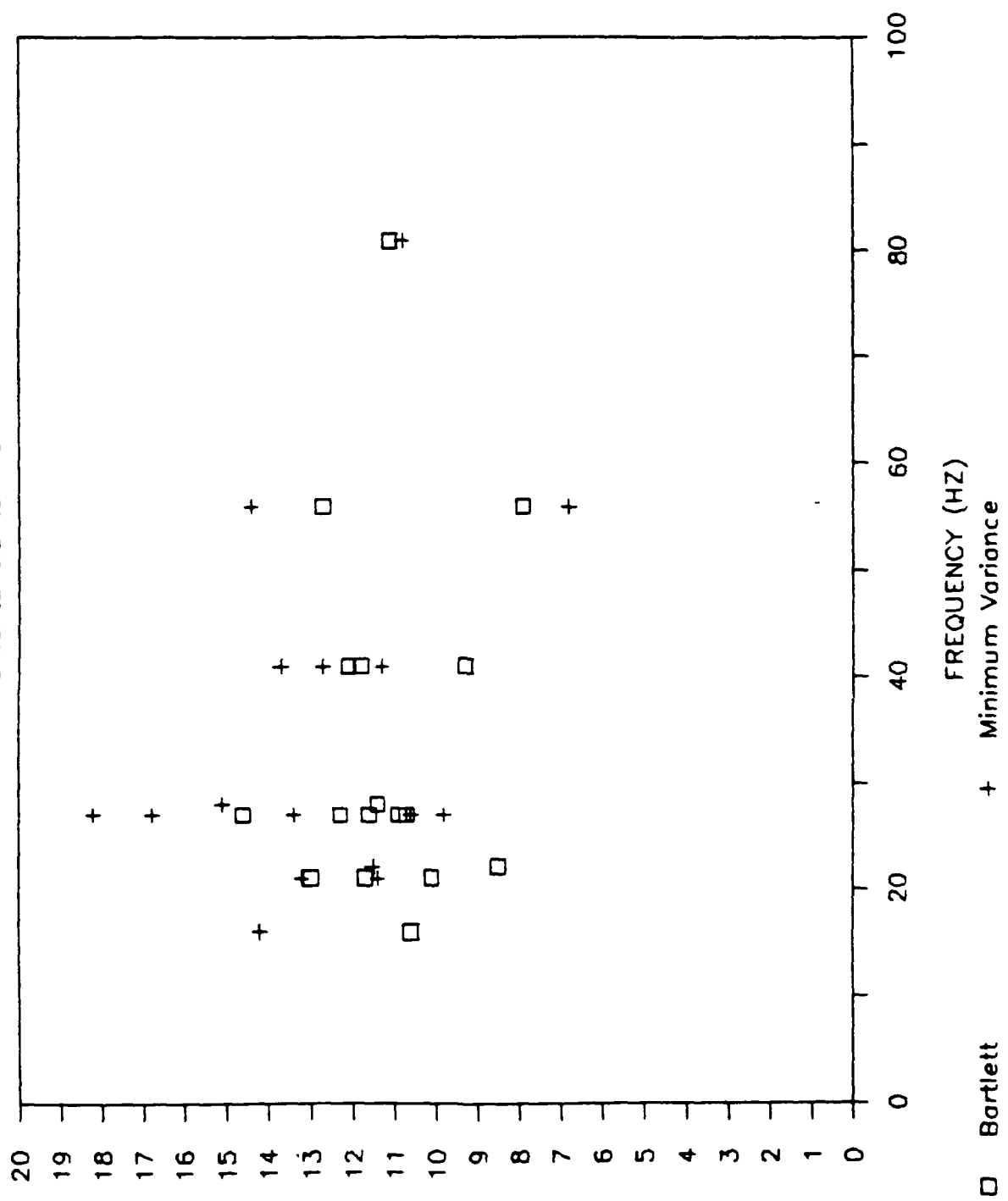
FREQUENCY	SPACING (WAVELENGTHS)	APERTURE (WAVELENGTHS)
16	.4	7.6
21	.53	10.0
27	.68	12.8
41	1.03	19.5
56	1.40	26.6
81	2.00	38.5

\* ONLY BOTTOM TEN ARRAY SECTIONS (OUT OF 12) HAVE BEEN USED IN CURRENT ANALYSIS



# ARRAY GAIN

20 Elements @ 37.5 meters

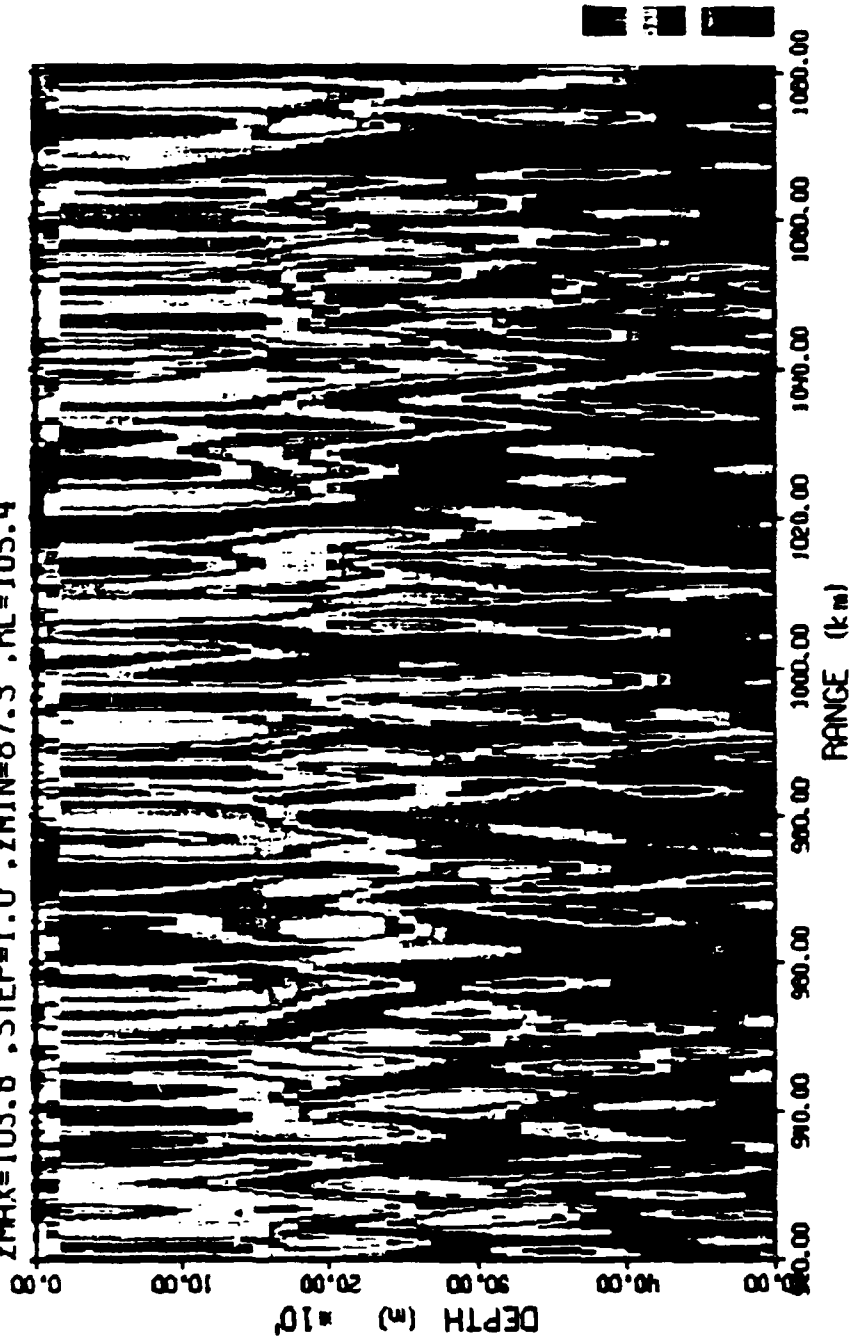


(80) N1AG  
435



# RANGE-DEPTH AMBIGUITY SURFACE

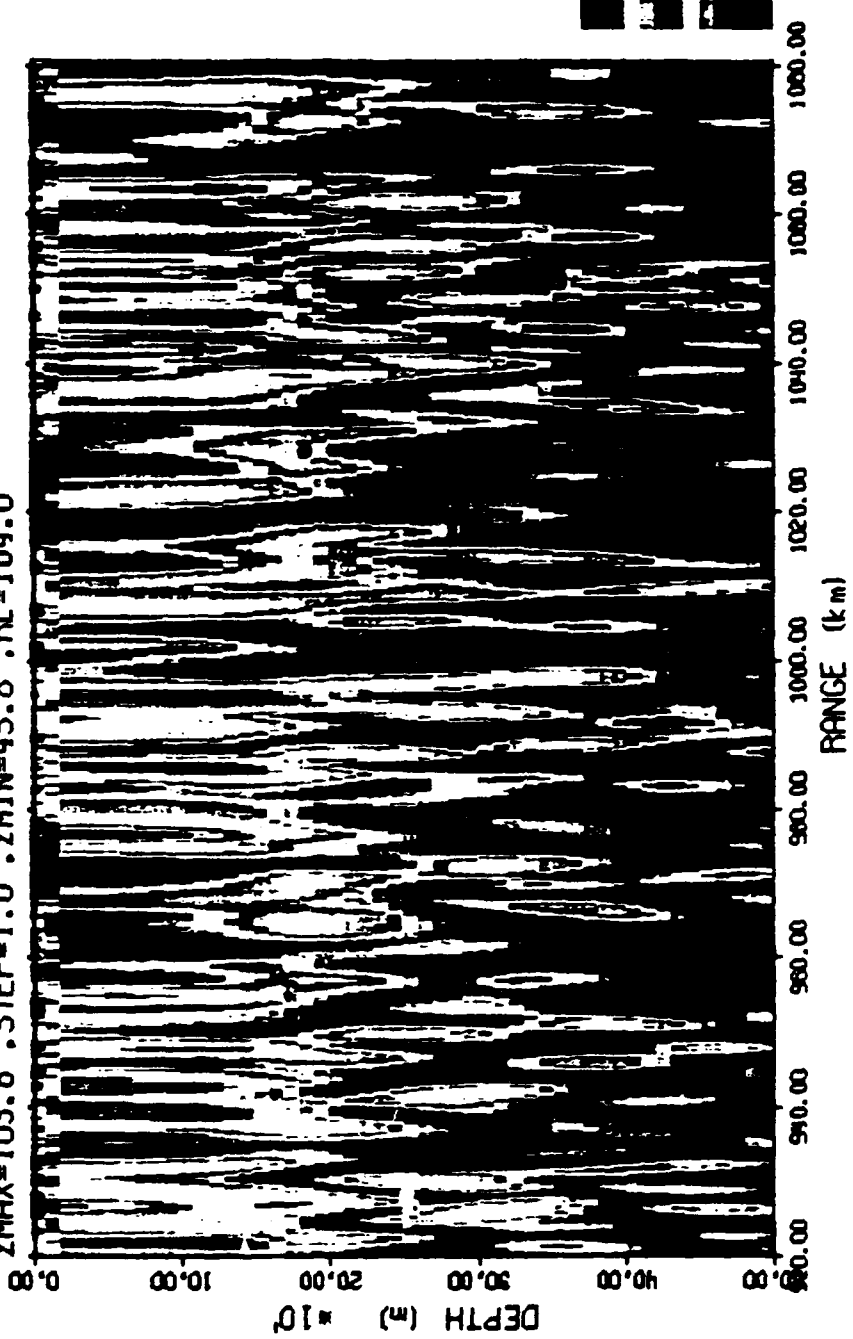
BARTLETT, CTD (I) PROFILE SOURCE  
F=27 Hz. TAPE 385. CHAN=4.100.5. 914 SAMPLES  
ZMAX=103.8 .STEP=1.0 .ZMIN=87.3 .RL=105.4





# RANGE-DEPTH AMBIGUITY SURFACE

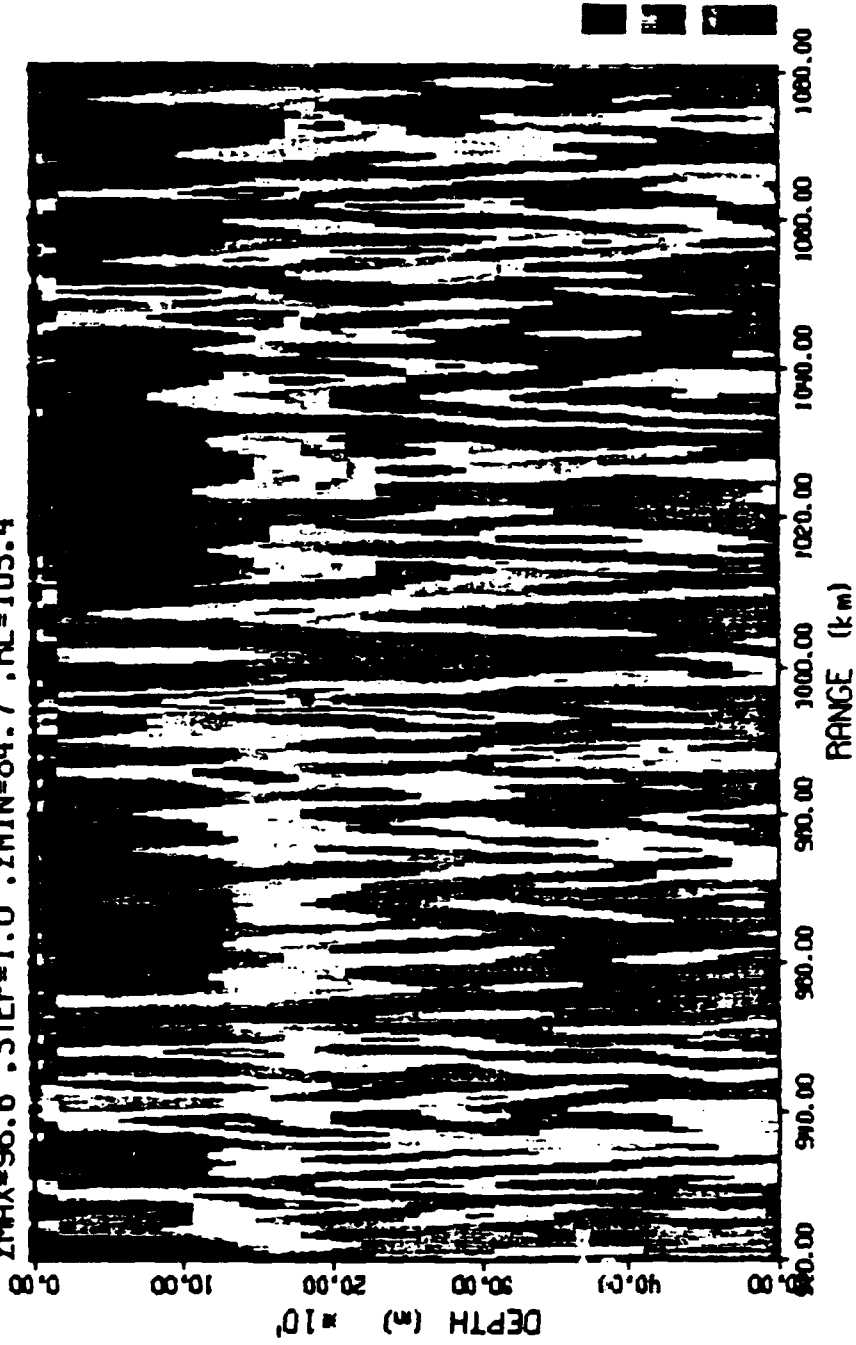
SVD, CTD(1) PROFILE SOURCE  
F=27 Hz, TAPE 385, CHAN=4.100.5, 914 SAMPLES  
ZMAX=103.8 .STEP=1.0 .ZMIN=45.8 .RL=104.0





# RANGE-DEPTH AMBIGUITY SURFACE

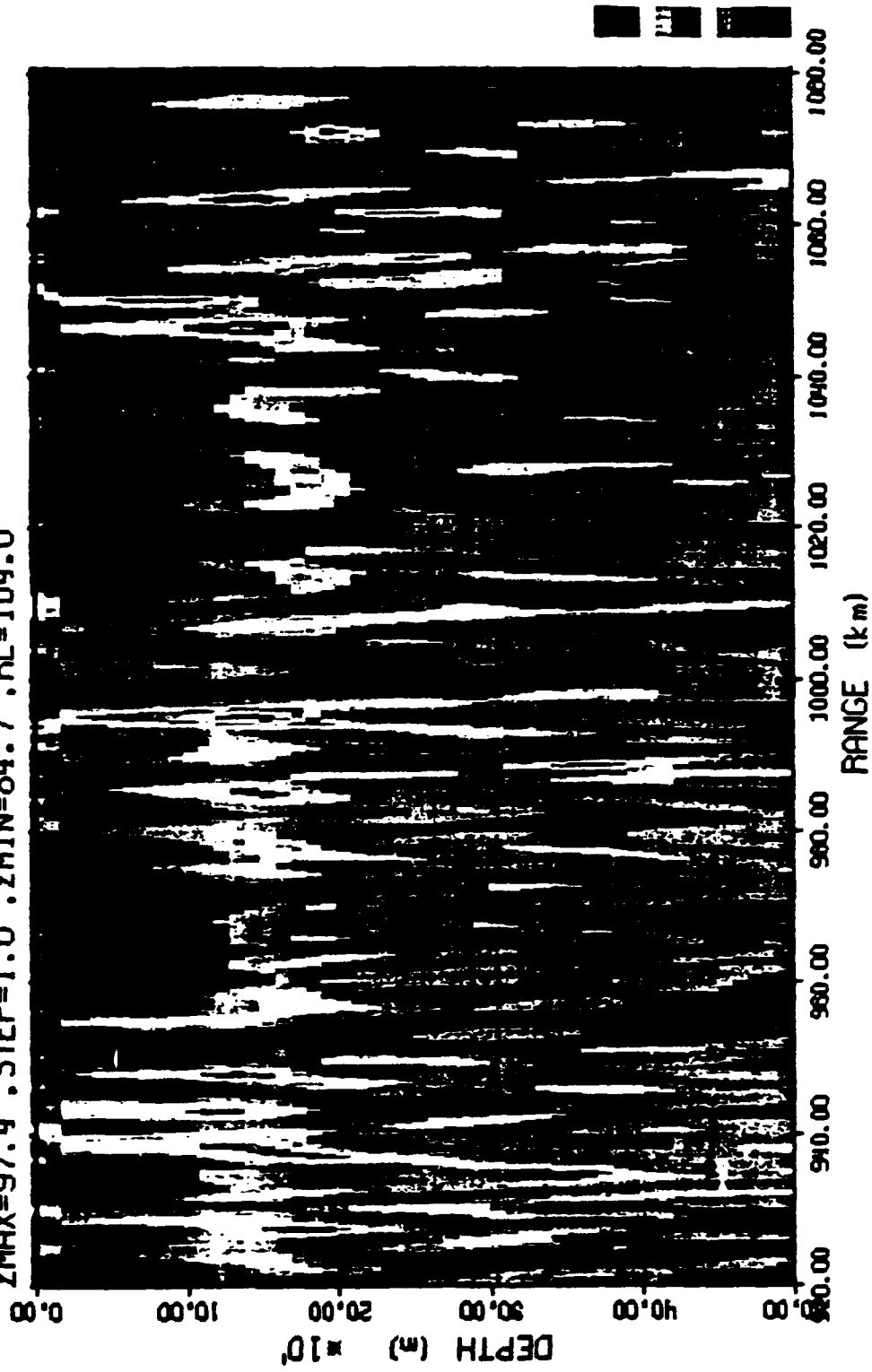
MLM, CTD(1) PROFILE SOURCE  
F=27 Hz. TAPE 385. CHAN=4.100.5. 914 SAMPLES  
ZMAX=96.6 .STEP=1.0 .ZMIN=84.7 .RL=105.4





# RANGE-DEPTH AMBIGUITY SURFACE

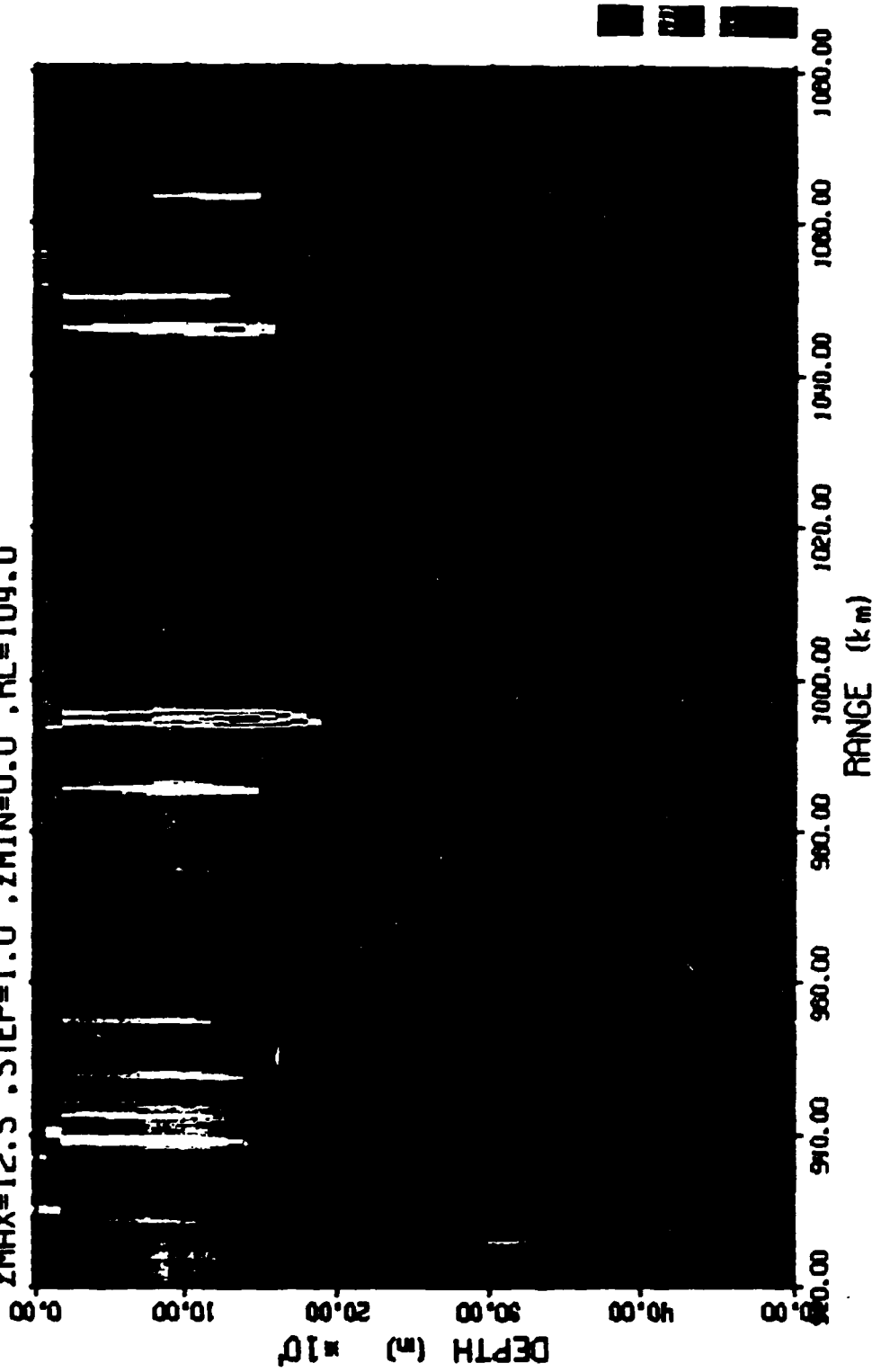
EMLM, CTD (1) PROFILE SOURCE  
F=27 Hz. TAPE 385. CHAN=4.100.5. 914 SAMPLES  
ZMAX=97.4 .STEP=1.0 .ZMIN=84.7 .RL=104.0





# RANGE-DEPTH AMBIGUITY SURFACE

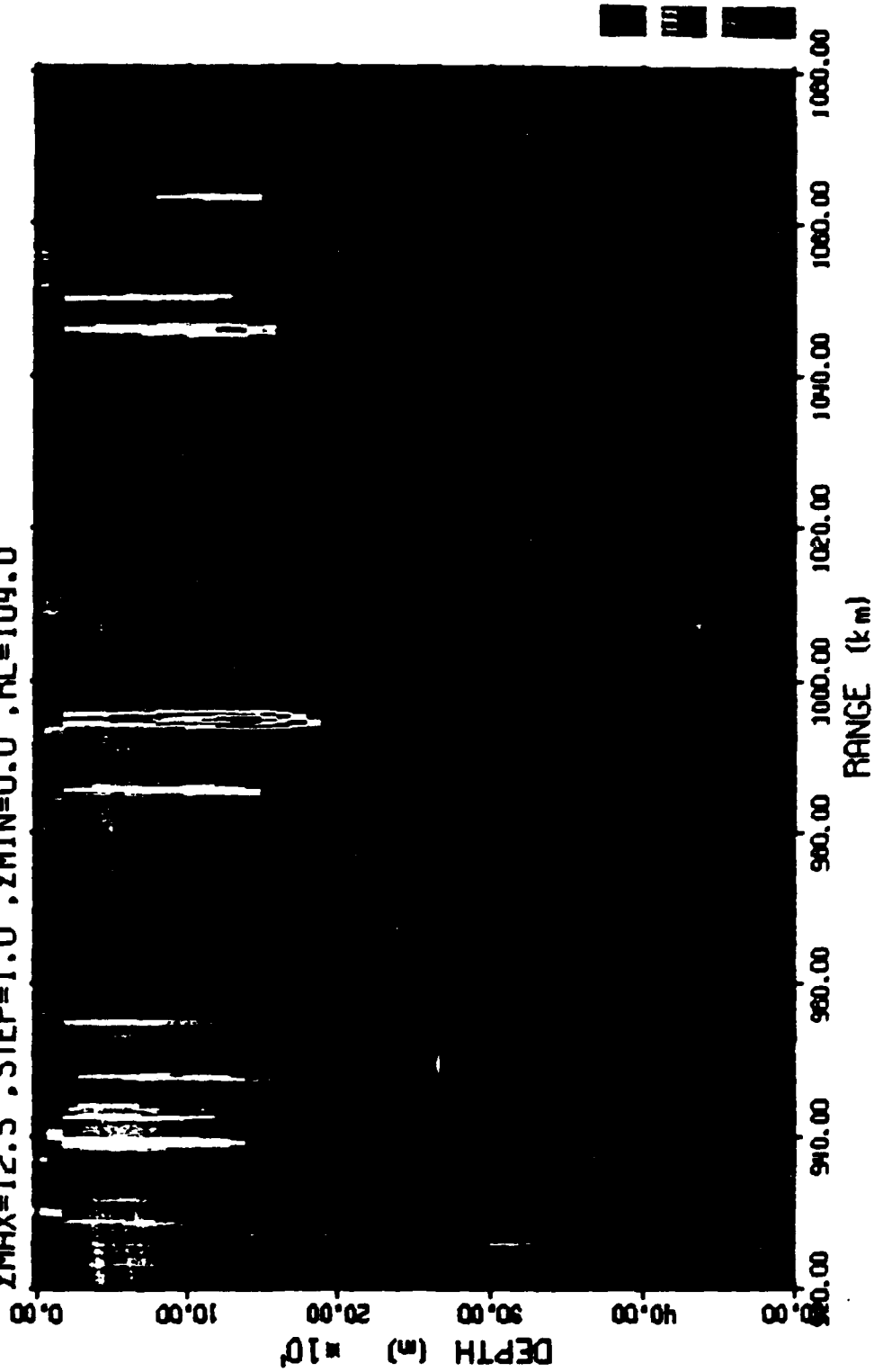
MUSIC, CTD(1) PROFILE SOURCE  
F=27 Hz. TAPE 385. CHAN=4,100.5. 914 SAMPLES  
ZMAX=12.5 .STEP=1.0 .ZMIN=0.0 .RL=104.0





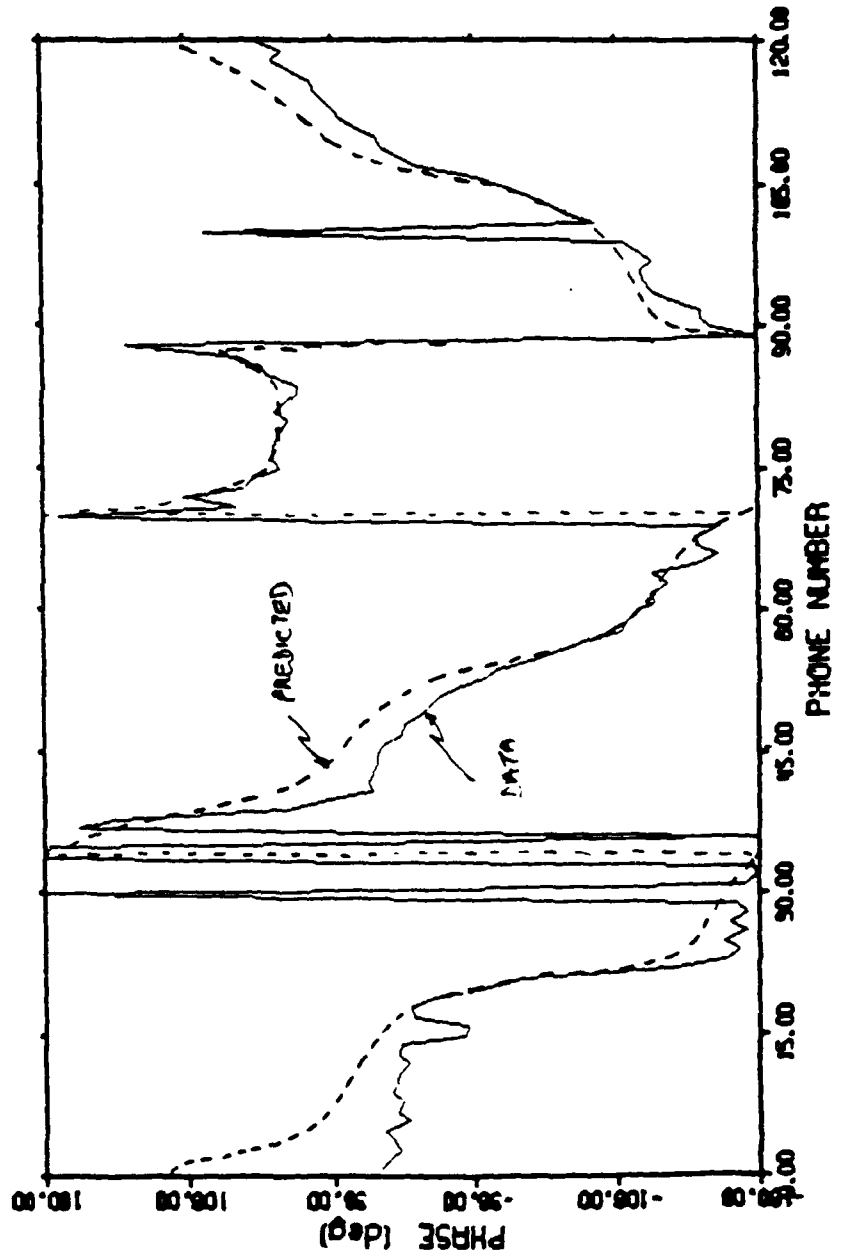
# RANGE-DEPTH AMBIGUITY SURFACE

MUSIC, CTD(1) PROFILE SOURCE  
F=27 Hz. TAPE 385. CHAN=4.100.5. 914 SAMPLES  
ZMAX=12.5 .STEP=1.0 .ZMIN=0.0 .RL=104.0



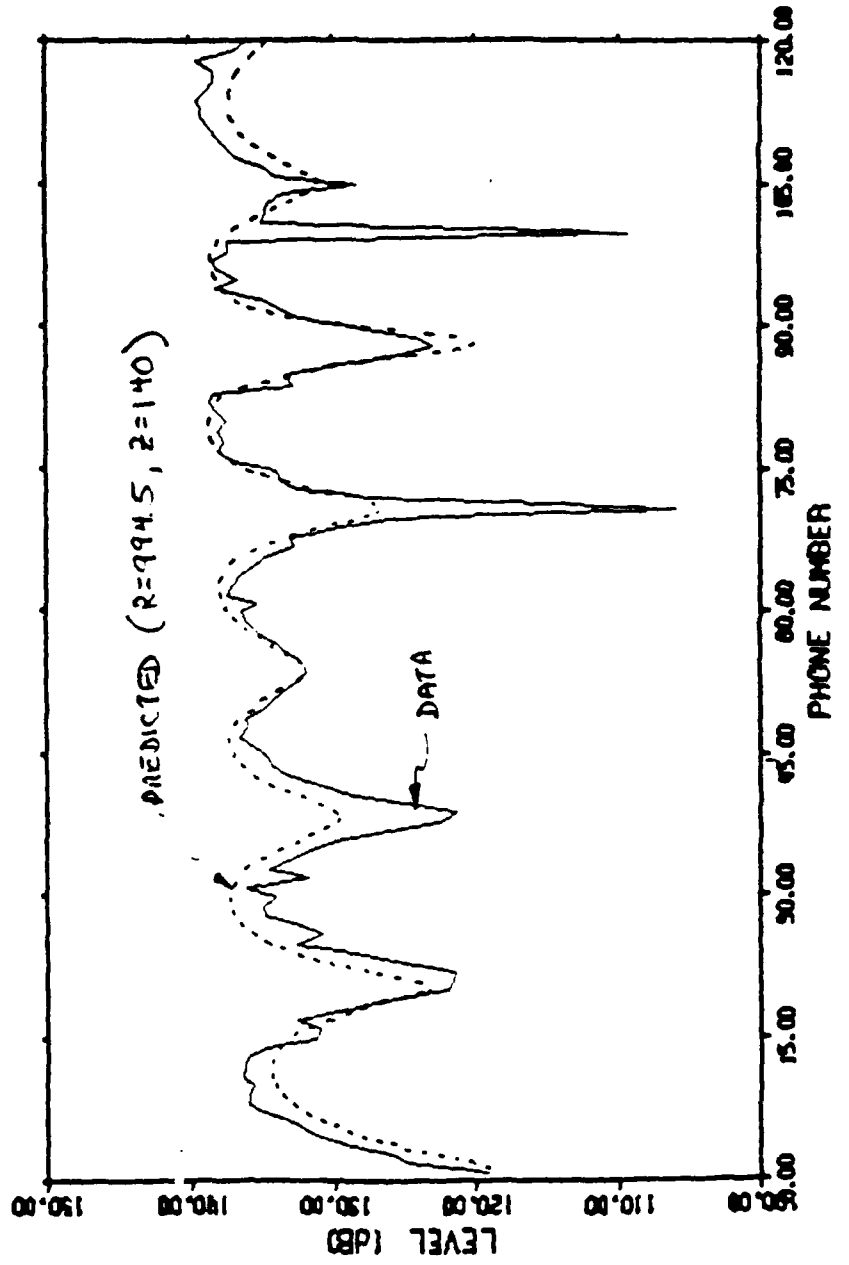


# TAPE 385, 512-PT FFT





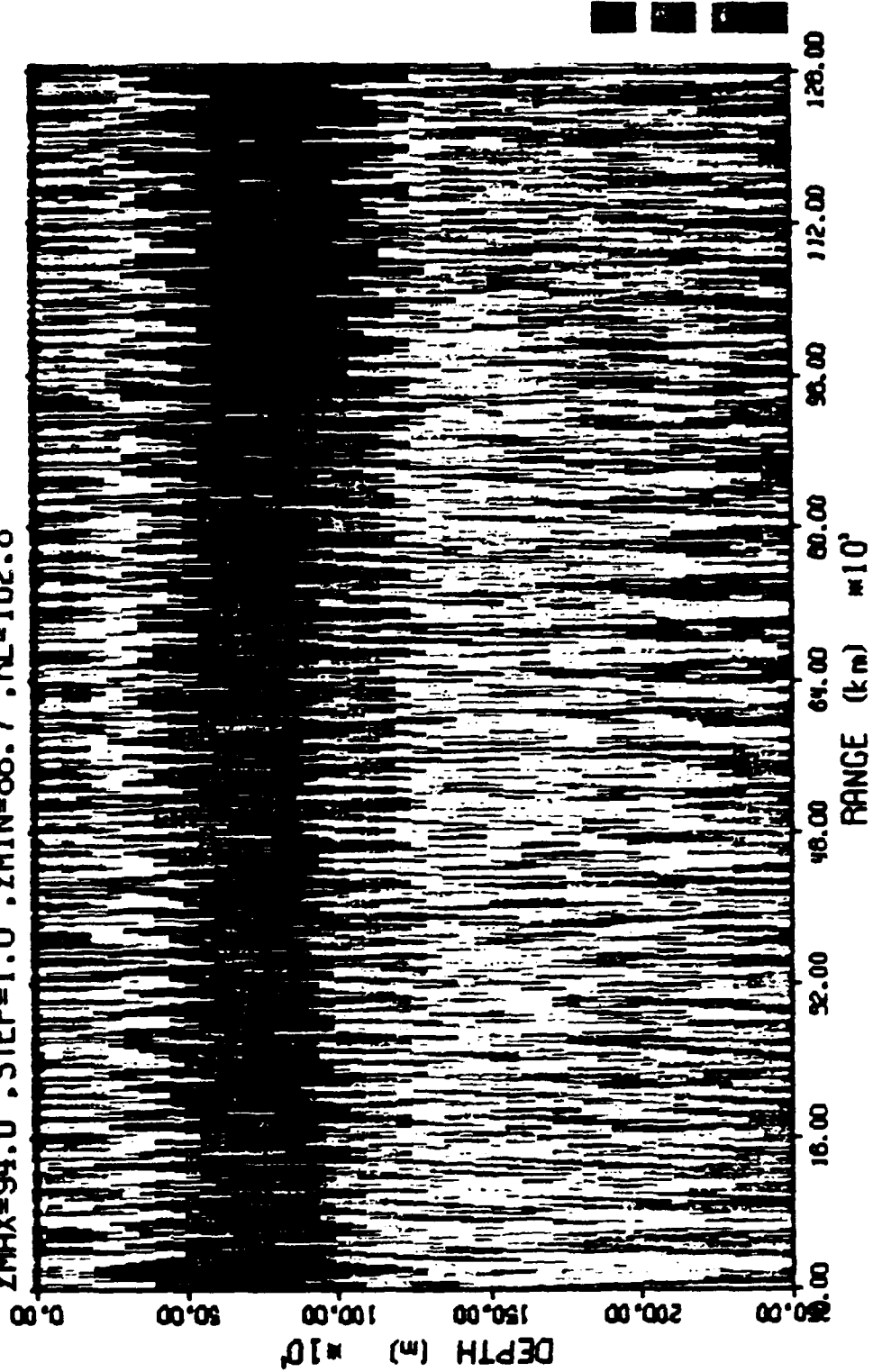
# TAPE 385, 512-PT FFT





# RANGE-DEPTH AMBIGUITY SURFACE

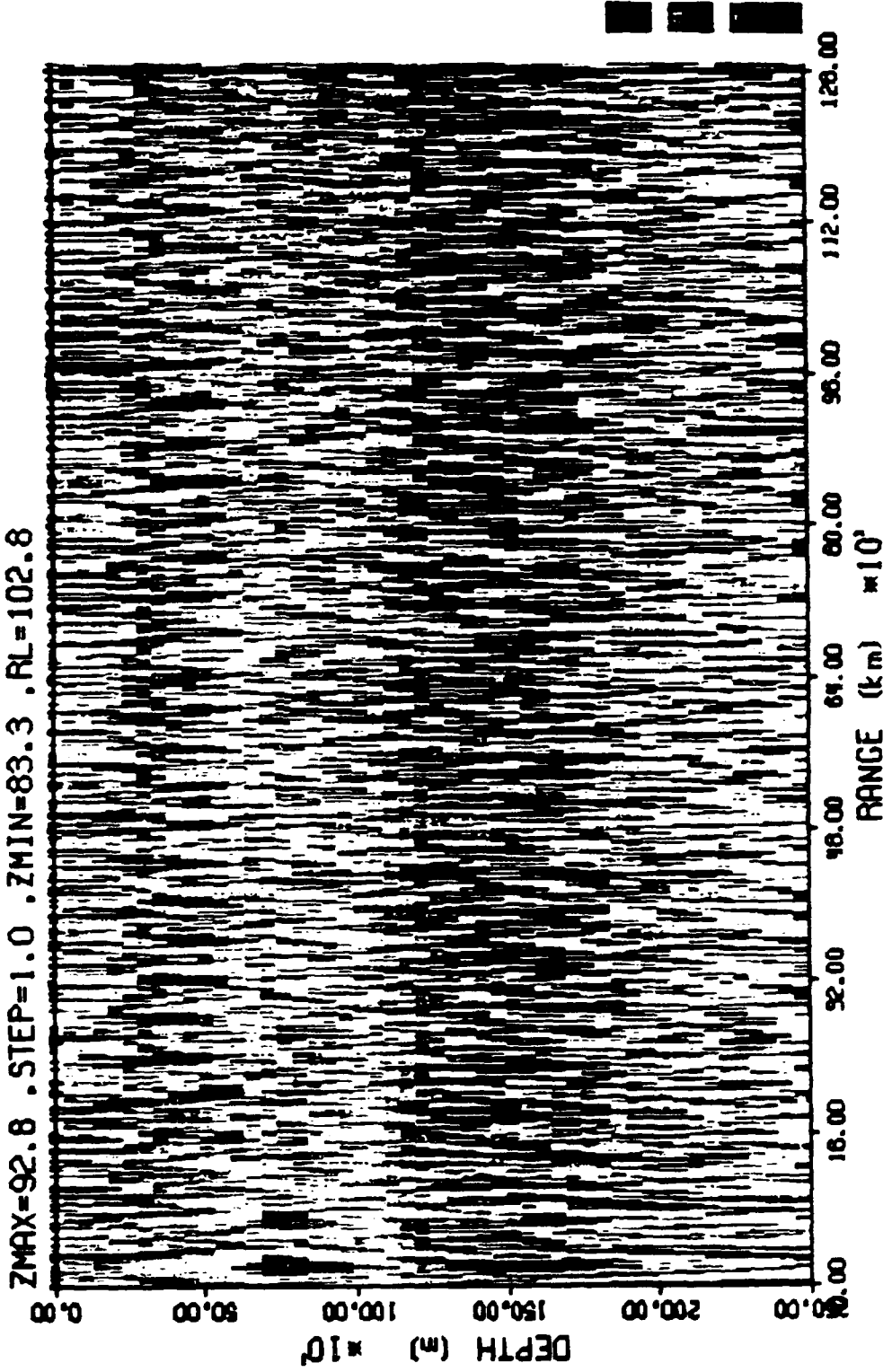
BARTLETT, CTID (1) PROFILE SOURCE  
F=10 HZ NOISE, TAPE 385, CHAN=4.100.5, 914 SAMPLES  
ZMAX=94.0 . STEP=1.0 . ZMIN=86.7 . RL=102.8





RANGE-DEPTH AMBIGUITY SURFACE

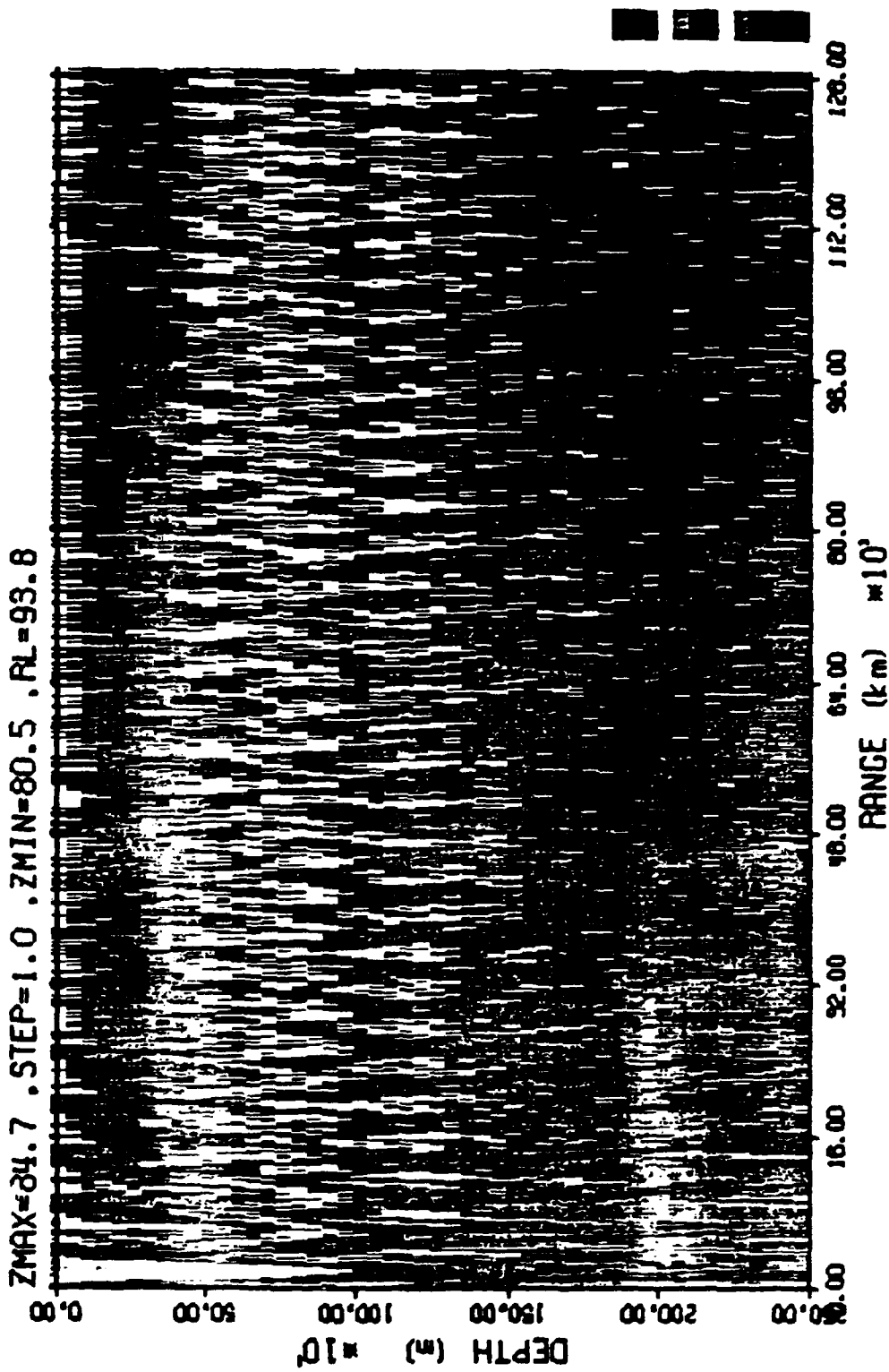
MLM, CTD(1) PROFILE SOURCE  
F=10 Hz NOISE, TAPE 385, CHAN=4, 100.5, 914 SAMPLES  
ZMAX=92.8 .STEP=1.0 .ZMIN=83.3 .RL=102.8





# RANGE-DEPTH AMBIGUITY SURFACE

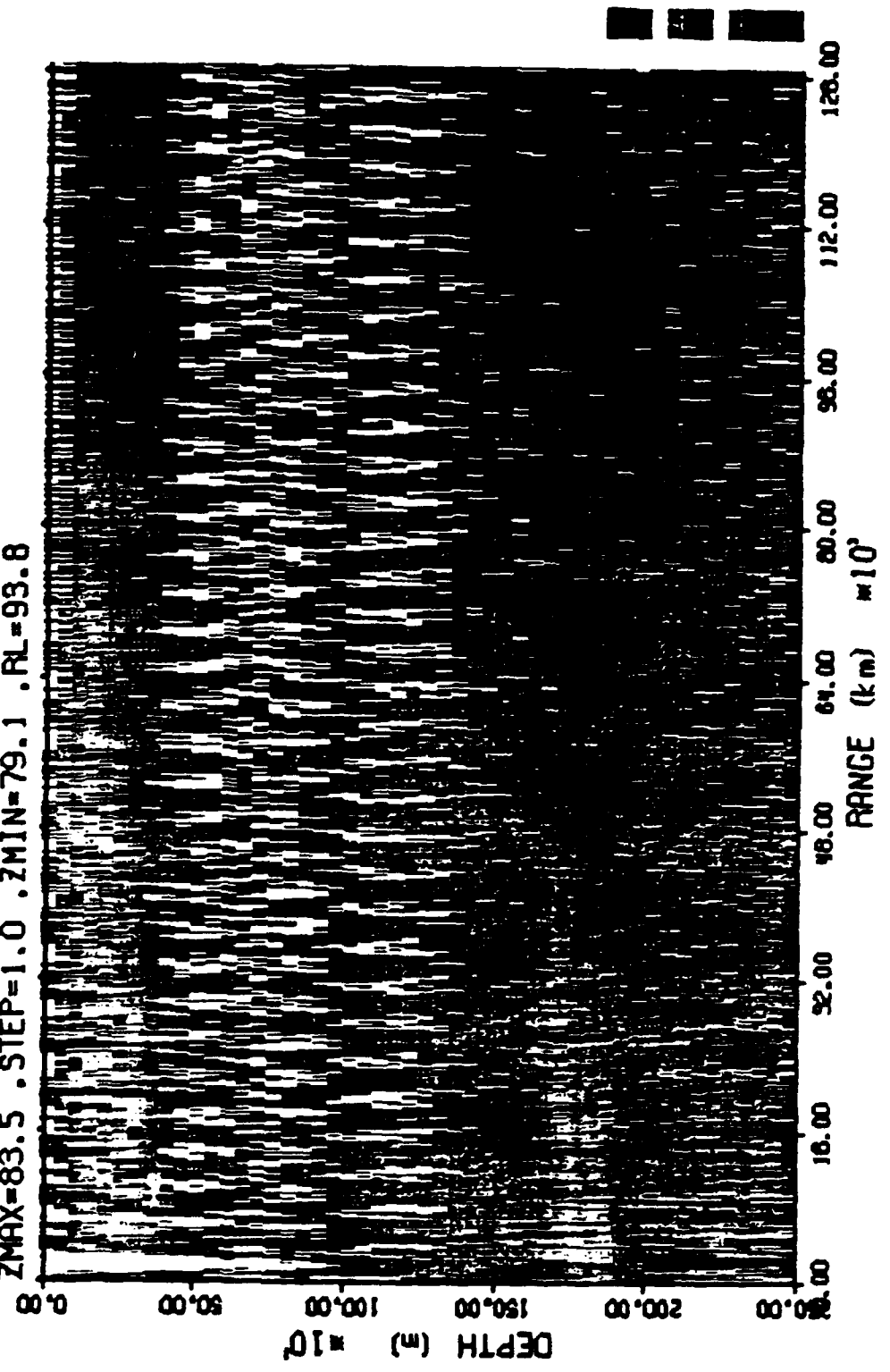
BARTLETT, CTD (1) PROFILE SOURCE  
F=29 Hz NOISE. TAPE 385. CHAN=4.100.5. 914 SAMPLES  
ZMAX=24.7 .STEP=1.0 .ZMIN=80.5 .RL=93.8





# RANGE-DEPTH AMBIGUITY SURFACE

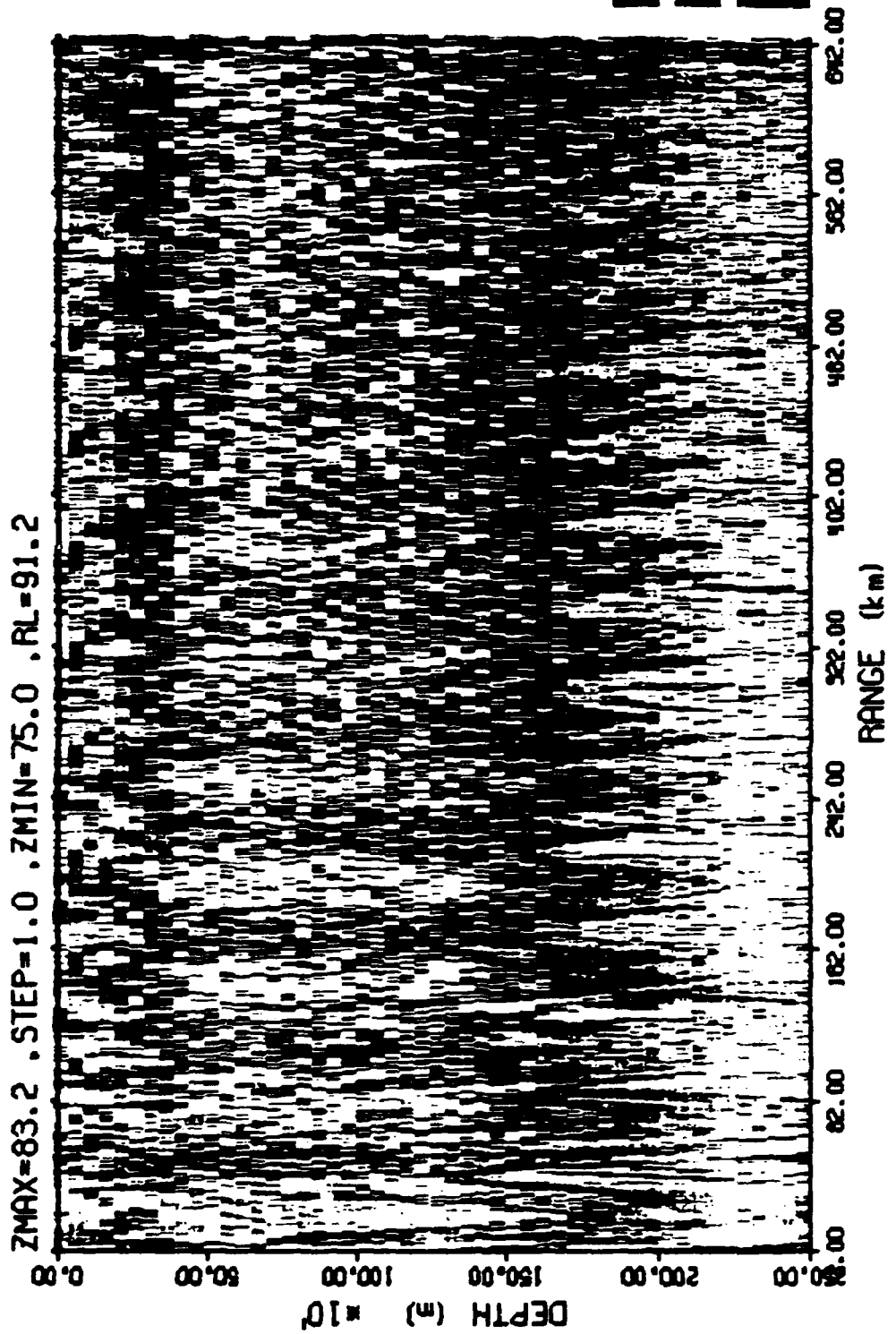
MLM, CTD(1) PROFILE SOURCE  
F=29 Hz NOISE, TAPE 385, CHAN=4,100.5, 914 SAMPLES  
ZMAX=83.5 .STEP=1.0 .ZMIN=79.1 .RL=93.8





# RANGE-DEPTH AMBIGUITY SURFACE

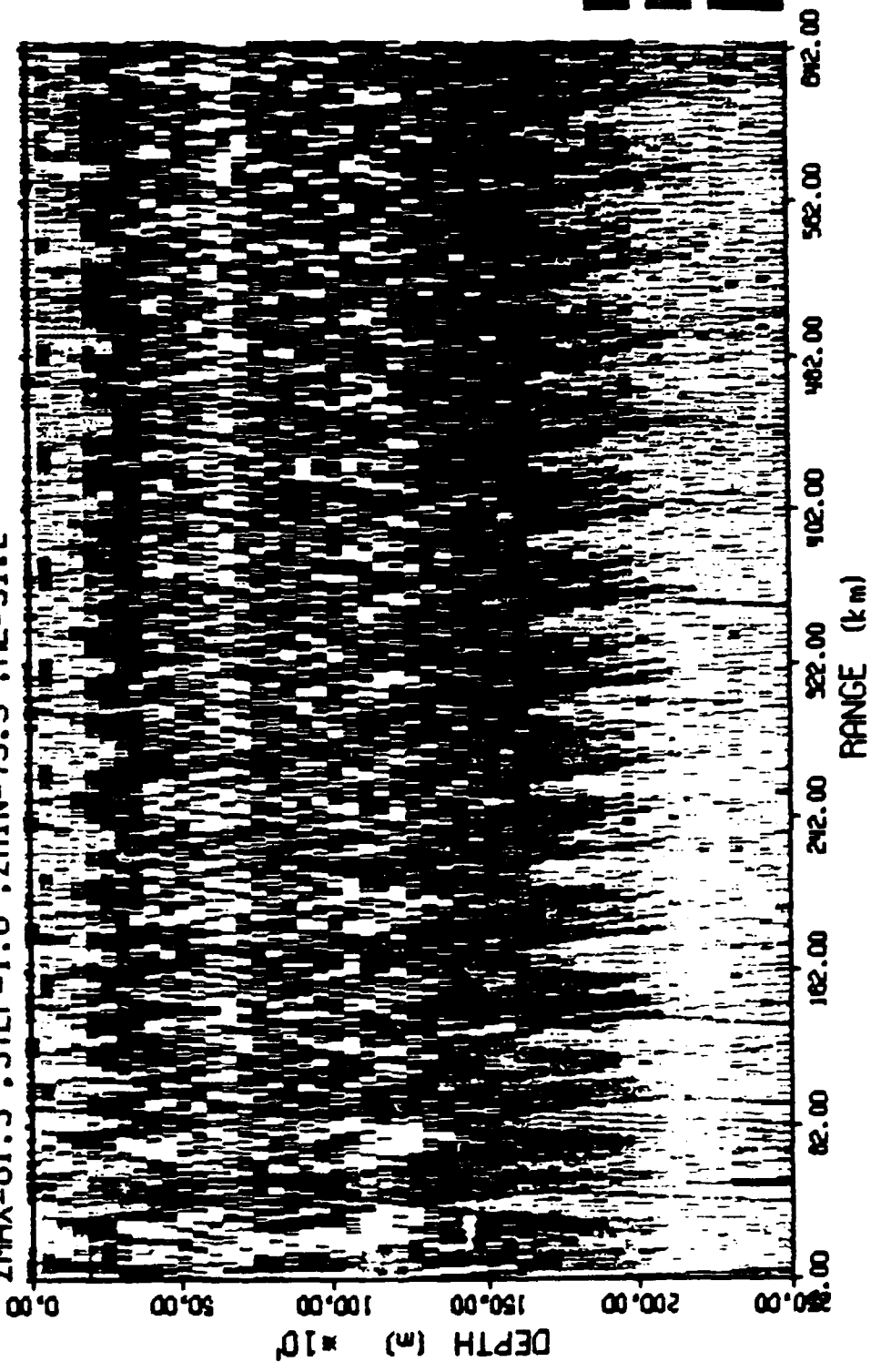
BARTLETT, CTID (I) PROFILE SOURCE  
F=79 Hz NOISE, TAPE 385. CHAN=4.100.5. 914 SAMPLES  
ZMAX=83.2 .STEP=1.0 .ZMIN=75.0 .RL=91.2





# RANGE-DEPTH AMBIGUITY SURFACE

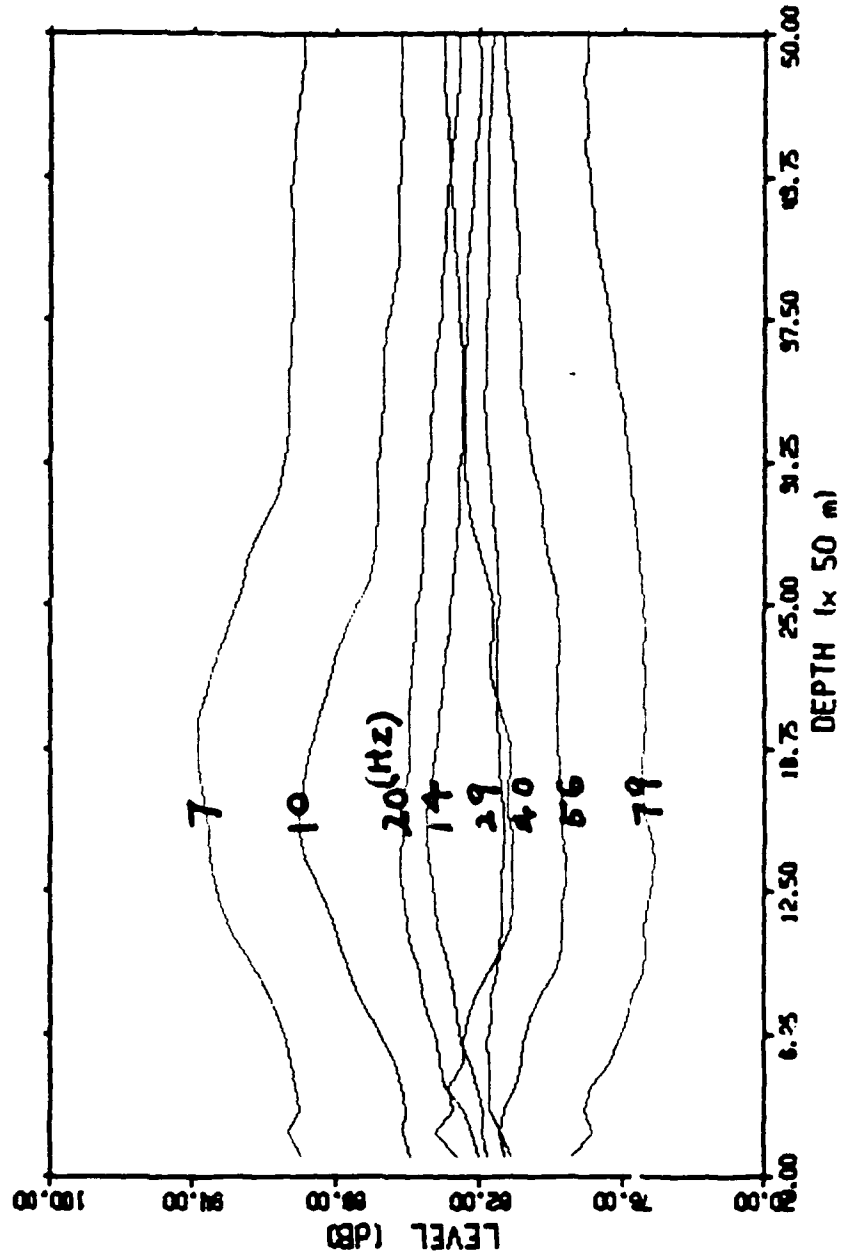
MLM, CTD(I) PROFILE SOURCE  
F=79 Hz NOISE. TAPE 385. CHAN=4.100.5. 914 SAMPLES  
ZMAX=81.5 .STEP=1.0 .ZMIN=73.9 .RL=91.2





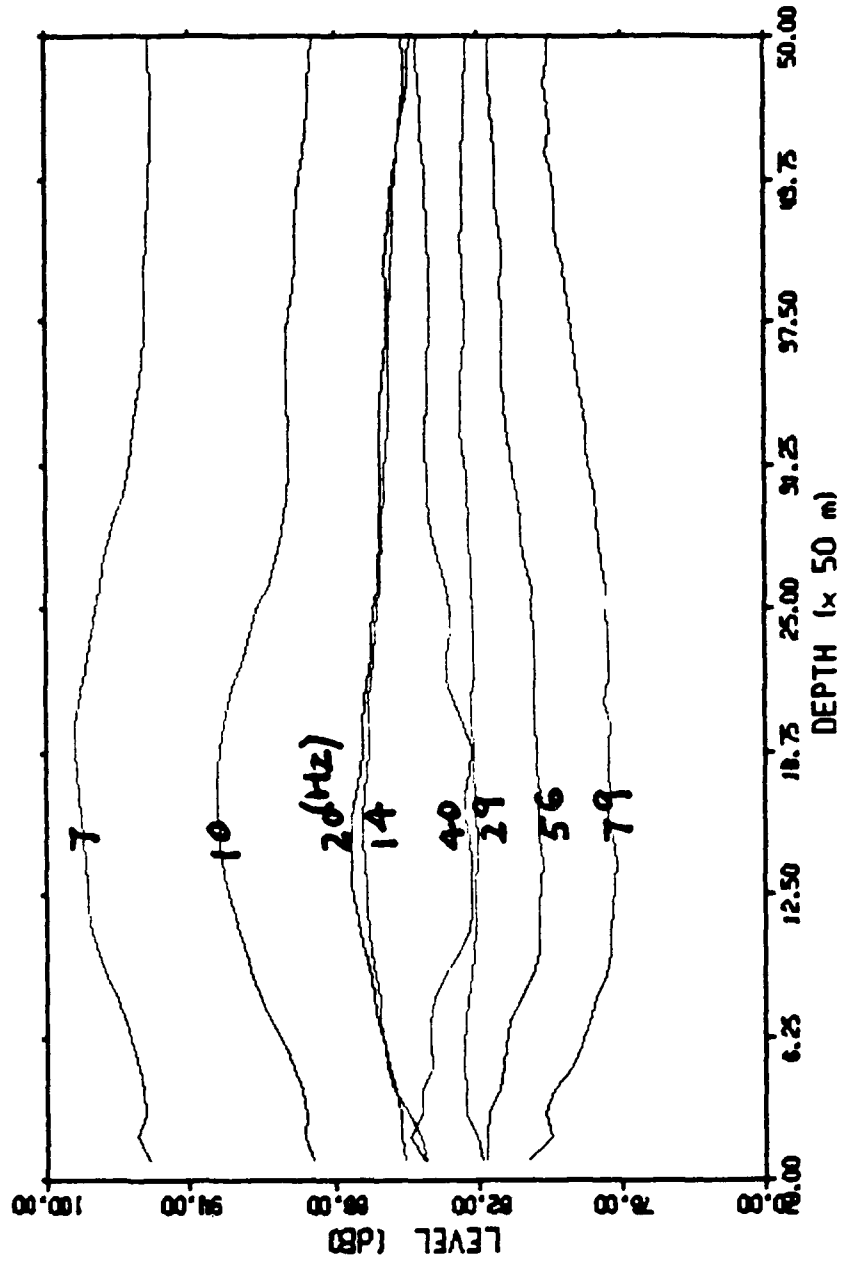
# NOISE DISTRIBUTION

## MLM, TAPE 385





NOISE DISTRIBUTION  
BARTLETT, TAPE 385





## SUMMARY OF PRELIMINARY RESULTS

### VLF NOISE

BELOW 15 HZ THE TOTAL NOISE IS DOMINATED BY:

NONACOUSTIC NOISE (STRUM AND TURBULENCE)  
ACOUSTIC NOISE FROM WAVE SLAP ON MOORING SHIP

MOST OF THIS NOISE (IF IT DOES NOT DRIVE FRONT END ELECTRONICS INTO SATURATION) CAN BE REMOVED WITH WAVENUMBER FREQUENCY FILTERING IF ARRAY IS LARGE ENOUGH.

SURGES IN MOORING SHIP CAN COUPLE TO ARRAY

TRANSITION REGION FROM HIGH ANGLE TO LOW ANGLE NOISE AT ABOUT 30 HZ IN THIS EXPERIMENT, CONFORMS WITH CURRENT NOTIONS ABOUT GENERATING MECHANISMS. THIS IS SUPPORTED WITH A RANGE - DEPTH ANALYSIS AS WELL.

NO EVIDENCE OF DISCRETENESS, BUT ARRAY DOES NOT HAVE ENOUGH D.O.F. TO ASSESS THIS ISSUE VERY WELL. THEREFORE RESULT IS NOT SURPRISING.

### ARRAY GAIN

ARRAY GAIN OF APPROXIMATELY  $10 \cdot \log(N)$  ACHIEVEABLE WITH THIS ARRAY

REGION OF MINIMUM GAIN @ TRANSITION FREQUENCY?

A FEW dB OF NOISE SUPPRESSION APPEARS POSSIBLE WHEN ARRAY IS FOCUSED ON TARGET. 6 dB APPEARS POSSIBLE AT LOW FREQUENCIES BUT RESULTS ARE BIASED BY NON-ACOUSTIC NOISE.



# **SURTASS NOISE FIELD MEASUREMENTS**

**E. HOLMSTROM (COSP) / S. KOONEY (NORDA) /  
M. BRADLEY (PSI)**





# SURTASS NOISE FIELD MEASUREMENTS

BY

LT. ERIK HOLMSTROM (COSP)  
S. F. KOONEY (NORDA)  
R. A. WAGSTAFF (NORDA)  
M. BRADLEY (PSI)  
R. TOWNSEN (SI)

The SURTASS array is the longest LF and VLF towed array that is currently available. SURTASS ships have made measurements in a number of ocean areas of interest to the HGF program. The data obtained can be of benefit to the program at very little cost or effort because AEAS has already initiated processing the data at NORDA. Details of that effort are included in this presentation.



# SURTASS DATA BASE

**PURPOSE:** PLANNING/ REAL TIME  
OPERATIONAL DECISIONS

COSP  
COSL  
CTF-66

ARCHIVAL

CNOC (NAVOCEANO)

FUTURE?

TACTICAL  
SUBMARINE

AIR

R & D COMMUNITY?

**PERFORMER:**  
**SPONSOR:**

NORDA/PSI  
AEAS

The SURTASS processing is being done at NORDA using the DANDE system. The ambient noise horizontal directionality data will be stored on optical disk and provided to COSP, COSL, CTF-66, and NAVO in formats that are compatible with their read capabilities.



# SURTASS DATA BASE SCHEDULE

---

SHIP DANDE: COSP TO NORDA - 4/88

DANDE OPERATIONAL: 9/88

COMPLETE DATA PROCESSING: 3/89

PRODUCTS TO FLEET/NAVO: 4/89





# SURTASS BEAM NOISE DATA

## AQUISITION

SYSTEM: SURTASS / RELEASE-9

STORAGE MEDIUM: CARTRIDGE MAGNETIC  
TAPE UNIT (CMTU)

## PROCESSING

SYSTEM: DATABASE OF AMBIENT NOISE  
DIRECTIONALITY EVALUATIONS  
(DANDE)

STORAGE MEDIUM: OPTICAL DISK

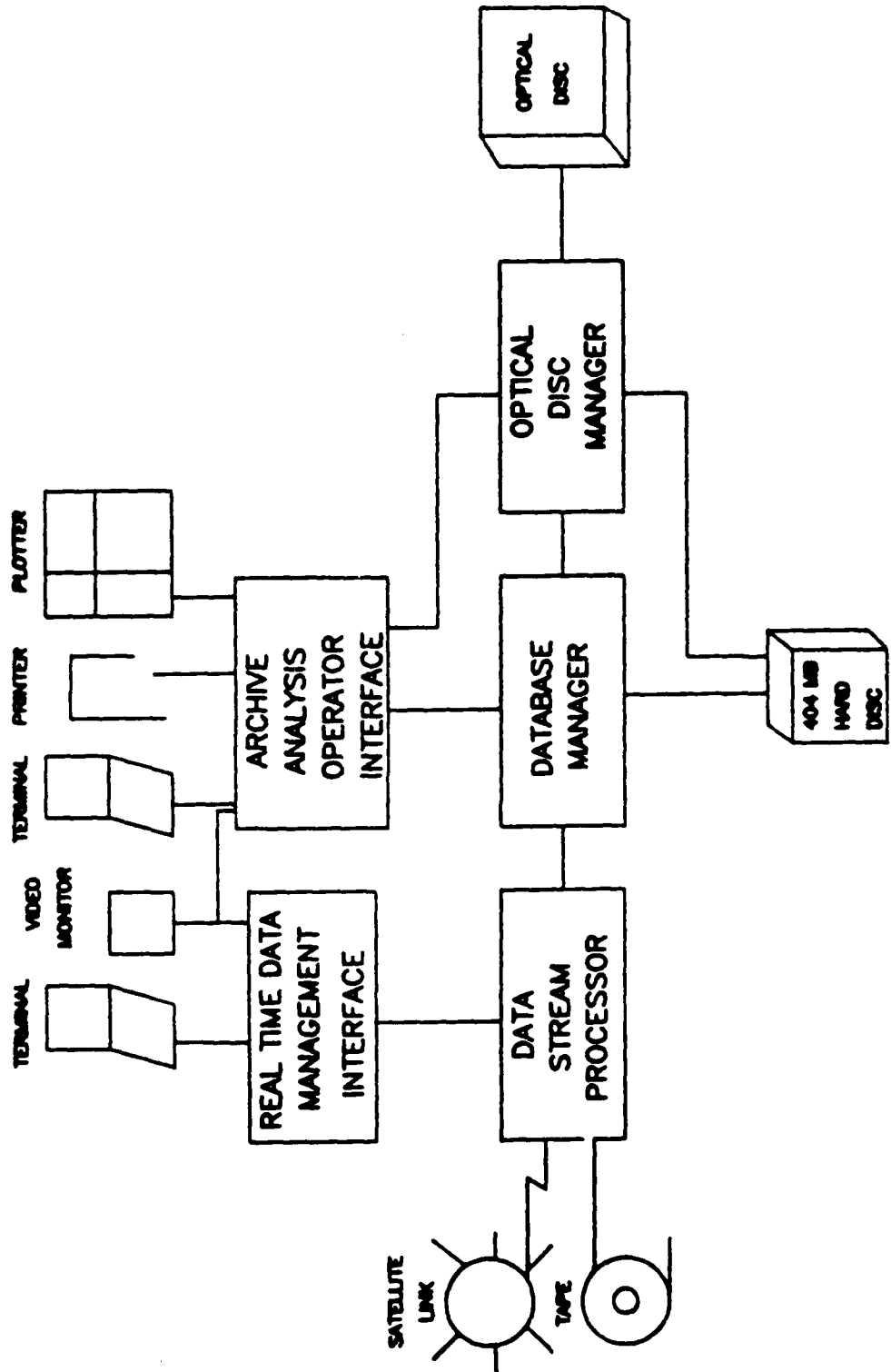
## DANDE LOCATION

PAST - COSP  
PRESENT - NORDA

This viewgraph presents a block diagram of DANDE.



# SURTASS R-9 DATA PROCESSING SYSTEM







# DATA AVAILABLE

- PACIFIC, ATLANTIC, AND MED.
- 11 SHIPS
- BIMONTHLY COVERAGE OVER TWO YEAR PERIOD
- APPROXIMATELY 3000 TAPES
- BEAM NOISE
- HYDROPHONE LEVELS





# SURTASS DATA ACQUISITION SYSTEM

- HORIZONTAL TOWED ARRAY
- FFT BEAMFORMER
- BAND WIDTH OF DATA    Hz
- ARRAY CONFIGURATION
- BEAM WIDTH





# DANDE DATA BASE

- HORIZONTAL DIRECTIONALITY AND STANDARD DEVIATION ARCHIVED ON OPTICAL DISK
  - HORIZONTAL DIRECTIONALITY OF 1 deg RESOLUTION
  - AVERAGED FOR A 5 deg lat X 5 deg lon
  - RUNNING AVERAGE
  - MONTHLY
- ARRAY HEADING ROSE GENERATED FORM ARCHIVED HORIZONTAL DIRECTIONALITIES





# PROCESSING SYSTEM

---

- DEDICATED SYSTEM (R-9 CONFIGURATION)
- CAN SET ACCEPTANCE PARAMETERS FOR READING LEGS
- STORES UPTO 3800 LEGS OF DATA
- 10 FREQUENCIES OF INTEREST
- CAN SET ACCEPTANCE PARAMETERS FOR POLYGON FORMATION
- FORMS POLYGONS OF 3-9 LEGS
- OUTPUTS:
  - STATISTICS TABLE
  - BEAM LEVEL PLOT
  - RANK CORRELATION MATRIX
  - HORIZONTAL DIRECTIONALITY
  - ARRAY HEADING ROSE
  - AZIMUTHAL ANISOTROPIC CUMMULATIVE DISTRIBUTION FUNCTION (AACDF)
- AUTOMATIC MODE AND MANUAL MODE CAPABILITY





# DANDE BEAM NOISE

## DATA QUALITY STATISTICS/PRODUCTS

- STDEV: STANDARD DEVIATION

- PRDIF: AVGPR - AVG

AVGPR = AVERAGE POWER LEVEL  
AVG = AVERAGE dB LEVEL

- SPEARMEAN RANK CORRELATION MATRIX  
BEAM X BEAM

- BEAM NOISE LEVEL VS BEAM NUMBER PLOT  
MEDIAN  
AVGPR  
PRDIF





# DANDE BEAM NOISE

## NOISE DIRECTIONALITY CHARACTERIZATION PRODUCTS

- DATA BASE COVERAGE/SUBCOVERAGE MAP
- BEAM NOISE TABULATION (All Beams)
  - ≡ 10, 25, 50, 75, 90 PERCENTILES
  - ≡ AVERAGE POWER LEVEL (AVGPW)
  - ≡ AVERAGE DECIBEL LEVEL (AVG)
  - ≡ STANDARD DEVIATION (STDEV)
- BEAM NOISE LEVEL (MEDIAN) vs BEAM NUMBER PLOT
- AZIMUTHAL ANISOTROPY CUMULATIVE DISTRIBUTION FUNCTION (AACDF) PLOT
- HORIZONTAL DIRECTIONALITY PLOT
- ARRAY HEADING ROSE PLOT

This is an example of noise field horizontal directionality plot "Noise rose" and corresponding Array Heading Rose for a search sector of  $22^\circ$  centered at  $315^\circ$ .







**DATA QUALITY  
STATISTICS / PRODUCTS**

**EXAMPLES**





# DATA QUALITY STATISTICS

## TRANSIENTS:

STDEV  
PRDIF

## POOR SIDELOBES:

CORRELATION MATRIX

## BEAMFORMER MALFUNCTION:

STDEV  
PRDIF  
CORRELATION MATRIX  
BEAM NOISE PLOT

## DATA TAPE/PROCESSOR PROBLEM:

STDEV  
PRDIF  
CORRELATION MATRIX  
BEAM NOISE PLOT

This is an example of processed SURTASS beam noise data.





# TOWED ARRAY STATISTICS

UNCLASSIFIED  
 SAMPLE SIZE 96  
 ST. TIME = 14 2: 0  
 LEG 1  
 ARRAY BEADING= 47

BEAM	RHDC	THDC	THDC	BW	10%	25%	MEDIAN	75%	90%	AVG	AVGPR	STDEV	UB	PROF
1	8.3	55.3	38.7	16.60	65.2	68.7	70.9	73.2	74.8	70.5	71.9	3.88	96	1.3
2	13.5	60.5	33.5	6.85	66.2	69.6	72.4	74.0	75.4	71.6	73.0	3.88	96	1.4
3	18.0	65.0	29.0	5.18	67.2	70.2	72.7	74.5	75.9	72.1	73.3	3.72	96	1.2
N-1	57.8	104.8	349.2	1.89	56.4	57.9	61.3	64.0	65.9	61.0	62.7	4.01	96	1.7
N	59.0	106.0	348.0	1.87	57.8	60.3	62.5	65.0	66.4	62.3	63.6	4.02	96	1.3





**DANDE: DATA QUALITY**

**EXAMPLE**

This correlation matrix indicates that nearly all beams are correlated with each other and corresponding beam noise plot. The curves in the beam noise plot are the beam noise power level (top), median level (middle), and the difference between the dB average and the average power level times 2 (bottom).

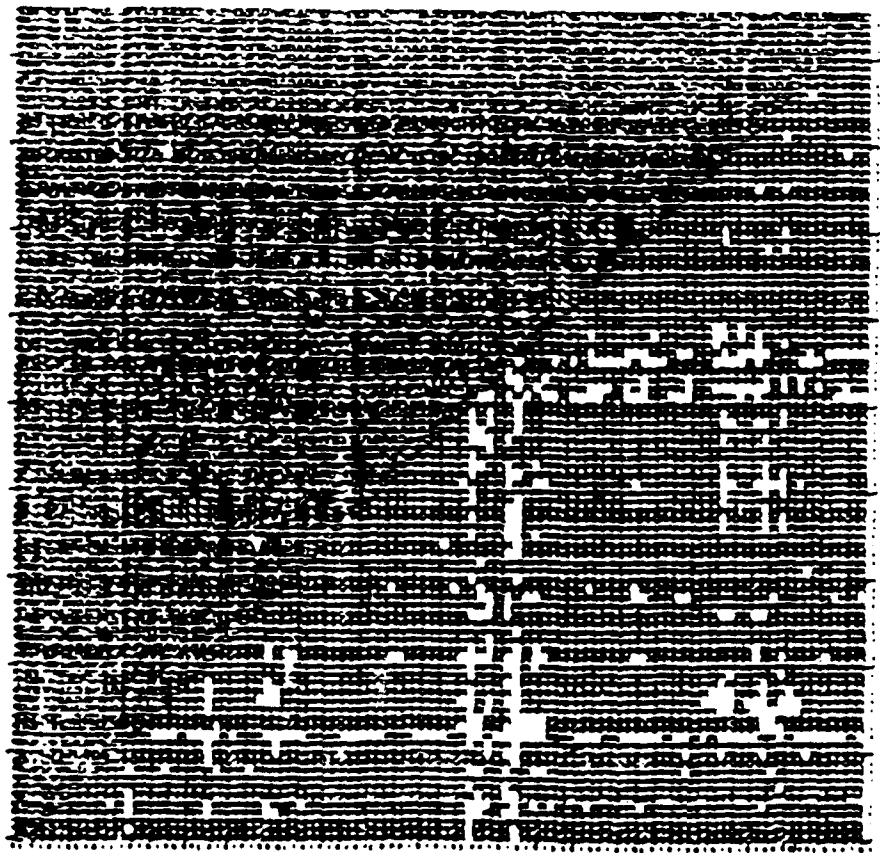
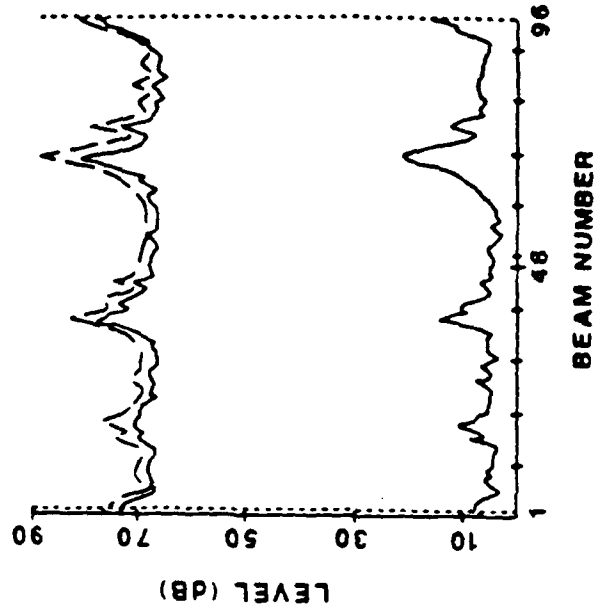
HEADING 55

TOP CURVES:

--- AVGPR  
— MEdIAN

BOTTOM CURVE:

2\*PRDIF(AVGPR-AVG)



COMPUTED OMNI LEVEL - 67.8

Example of poor quality beam noise data.

This example is similar to the previous one, but this one is for good data. Note the light area below the main diagonal of the correlation matrix.

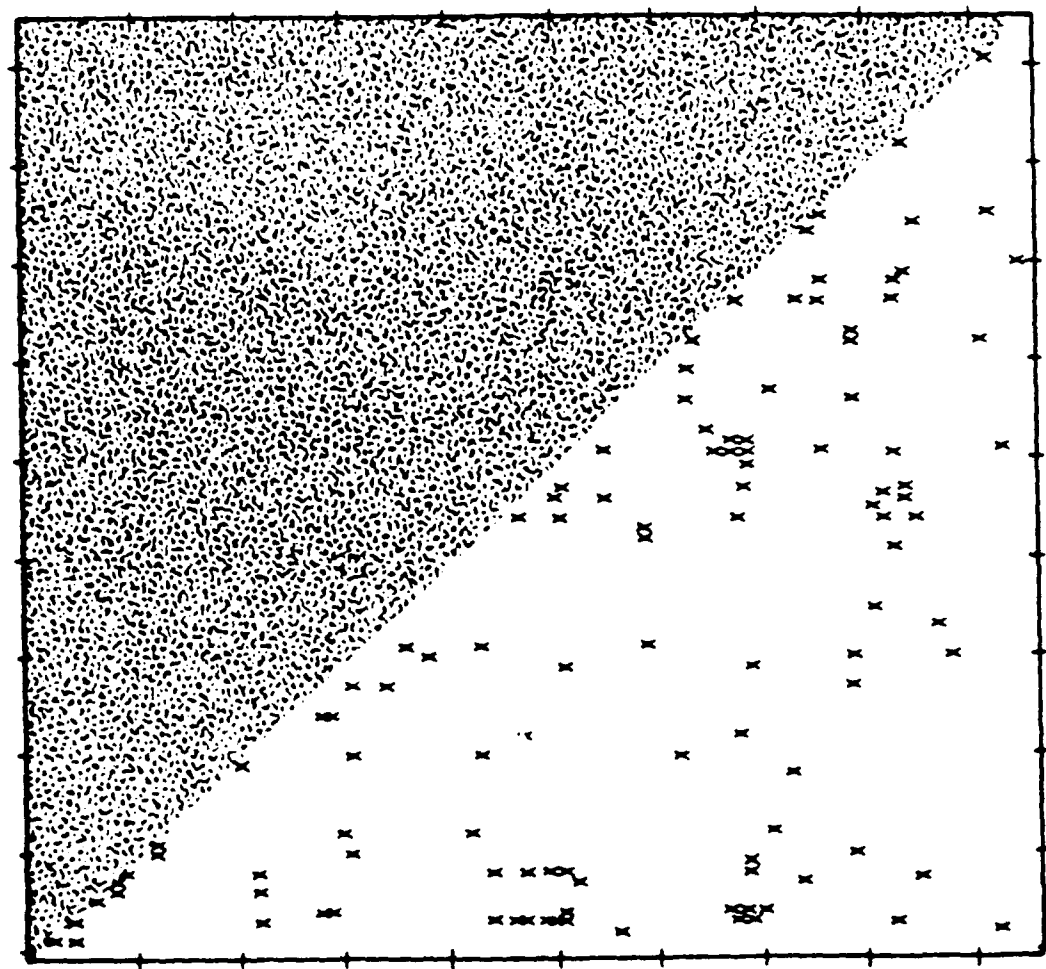
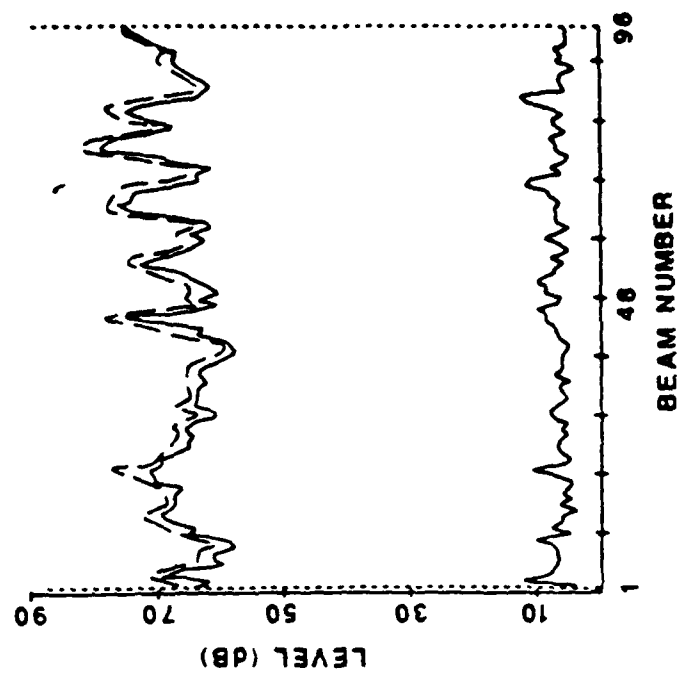
HEADING 276

TOP CURVES:

AVGPR - - - -  
MEDIAN - - - -

BOTTOM CURVE:

2\*PRDIF(AVGPR-AVG)



Example of high quality beam noise data.





# CURRENT STATUS

- 215 PACIFIC DATA TAPES PROCESSED  
(INCLUDING DATA QUALITY)
- HORIZONTAL DIRECTIONALITIES ARCHIVED
- PROCESSING FACILITY TRANSFERRED TO  
NORDA
- REPORT IN PREPARATION
- UPDATING TO STORE HORIZONTAL  
DIRECTIONALITIES FOR FINER RESOLUTION  
(1 deg lat x 1 deg lon)
- UPDATING TO STORE RAW LEG DATA ON  
OPTICAL DISC





# SUMMARY

- DANDE IS OPERATIONAL AT NORDA
- SURTASS BEAM NOISE DATA PRESENTLY BEING PROCESSED
- DATA QUALITY TESTS/STATISTICS PERFORMED
- NOISE FIELD PRODUCTS GENERATED
- HORIZONTAL DIRECTIONALITY ARCHIVED  
Although the Array Heading Rose is required, it is too specific to archive.
- ARCHIVED DATA TO BE PROVIDED TO FLEET/NA VOCEANO/TACTICAL UNITS?/SUBS?/AIR?  
Planning  
Real time operational decisions
- DATA AVAILABLE TO R/D COMMUNITY



# VLA MEASUREMENTS

W. HODGKISS (MPL)



# VLA Measurements

W. S. Hodgkiss

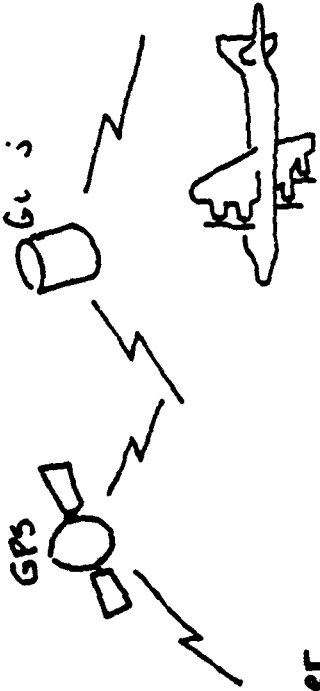
Marine Physical Laboratory  
Scripps Institution of Oceanography  
San Diego, CA 92152

HGI/AEAS VLF Ambient Noise Workshop

September 21, 1988

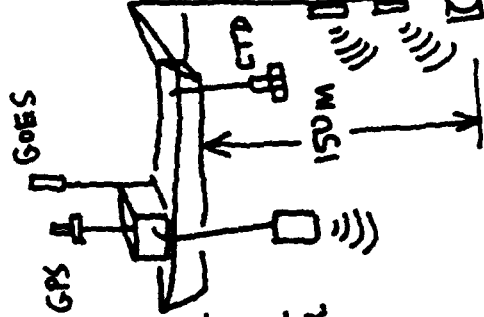


SVLA EXPERIMENT  
FALL 1987



USNS Destroyer

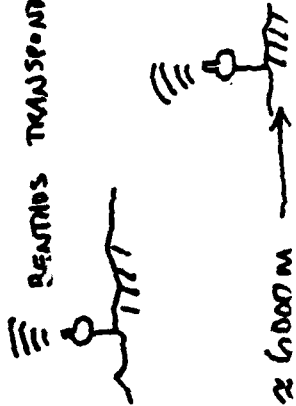
GPS



517

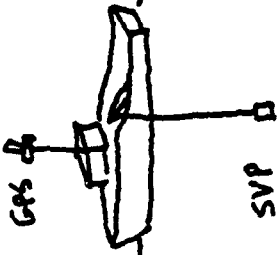
~5000 m

RENTAS TRANSPODERS



~6000 m

Naragansett



Flip

GOES

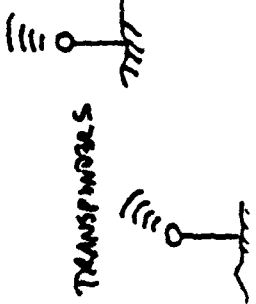


400 m

~480

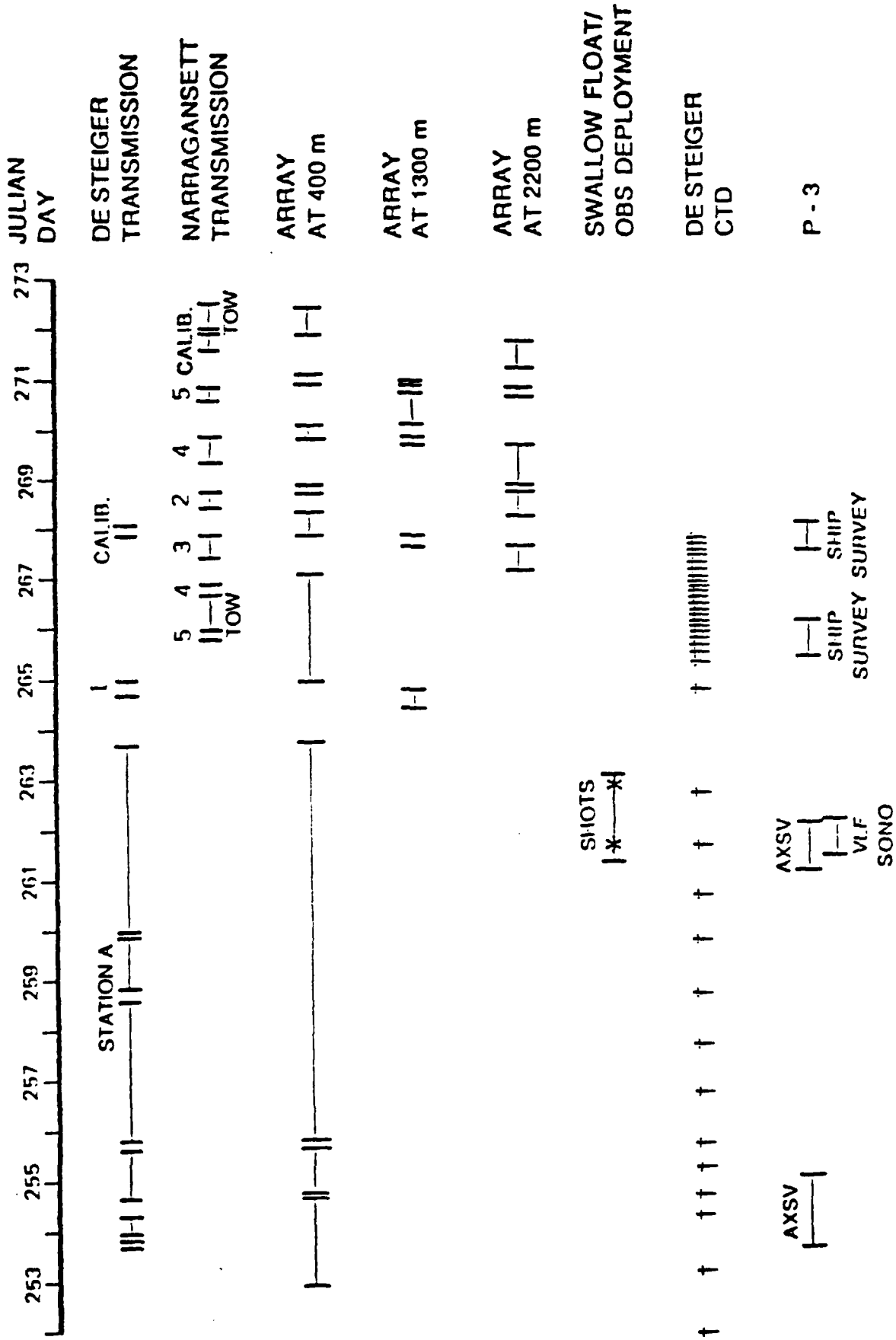
900 m

1000 KM

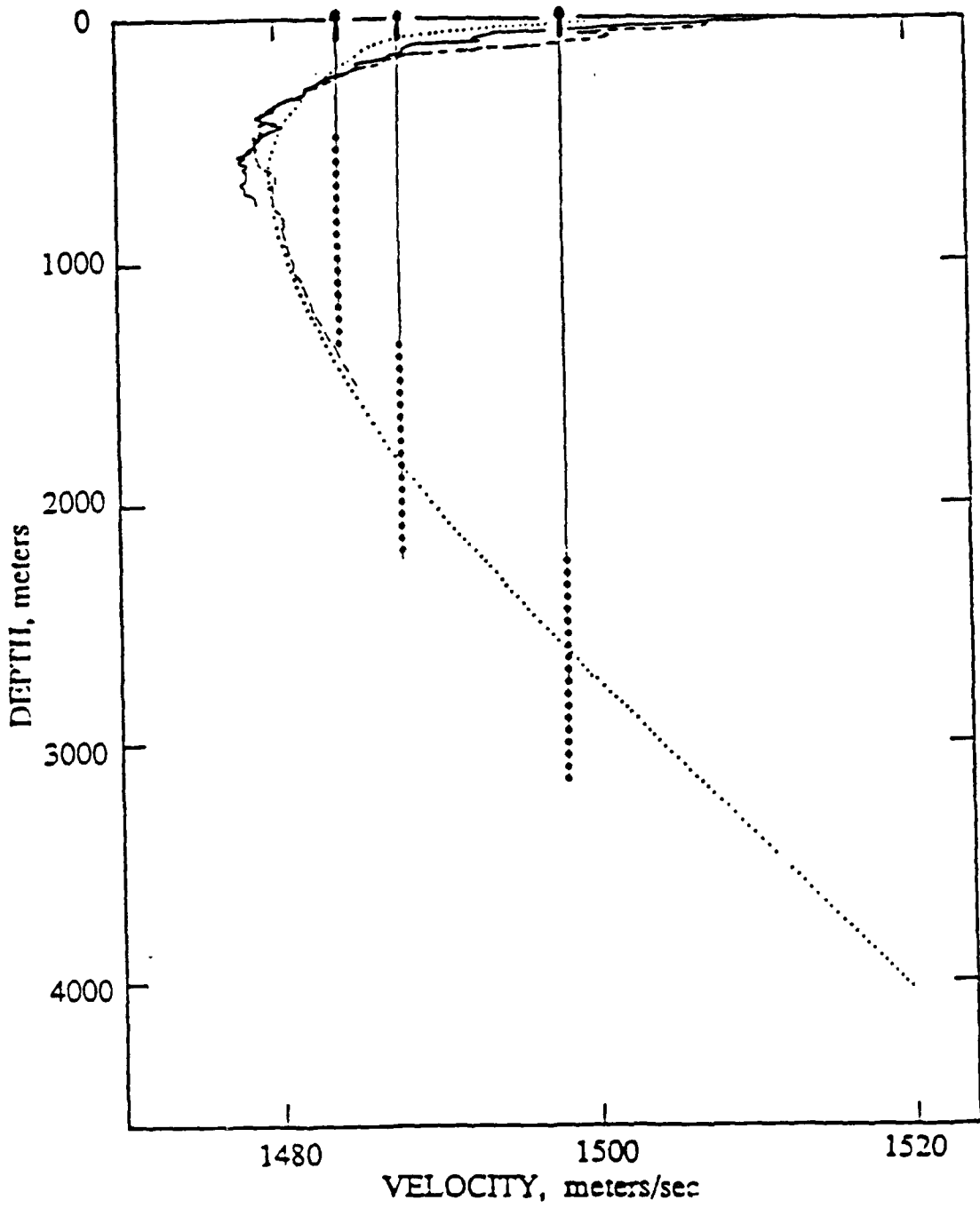




Time line for array, acoustic transmission and environmental data collected during the VLA Experiment, September 1987.







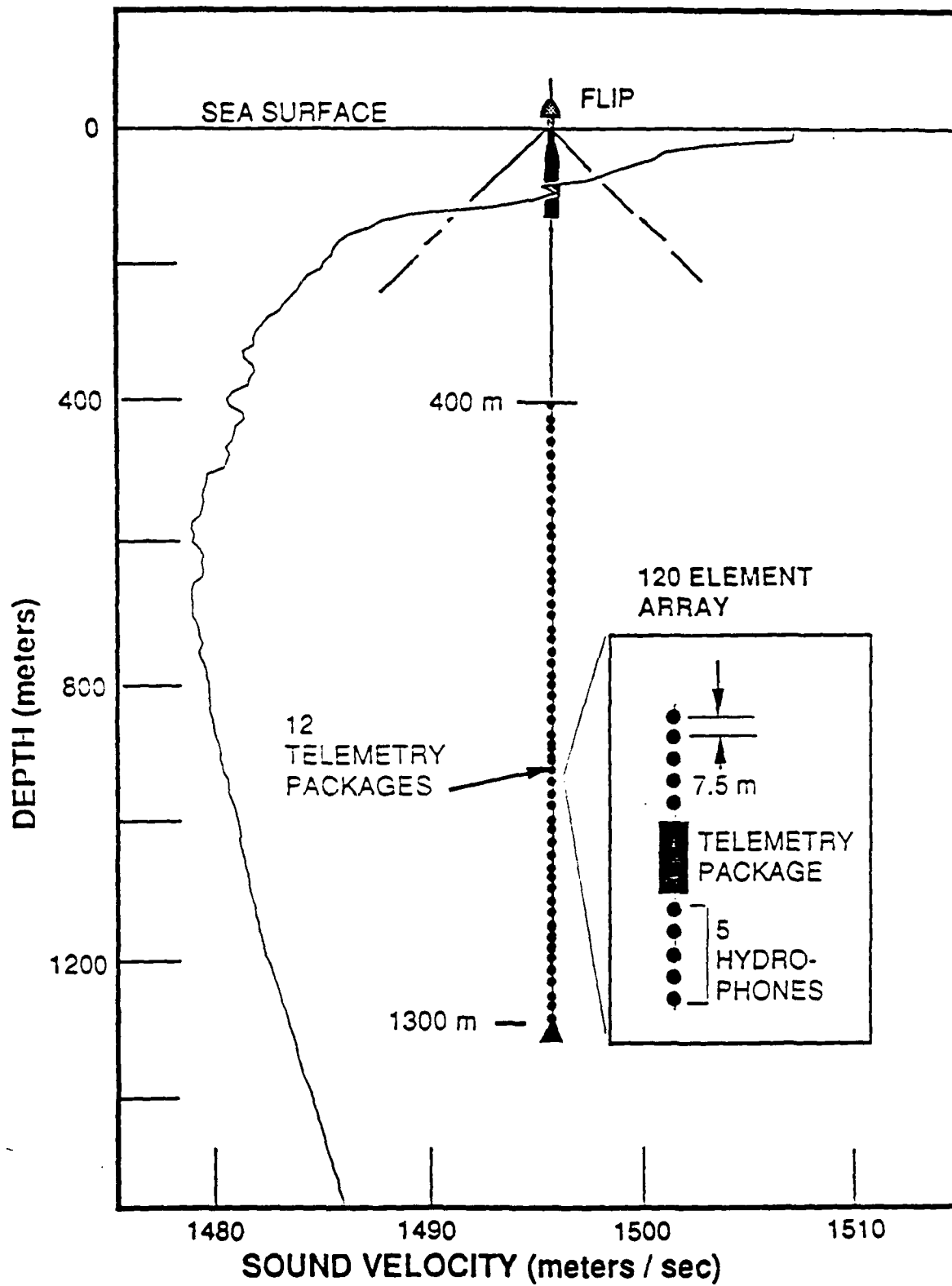


## Low Frequency Array

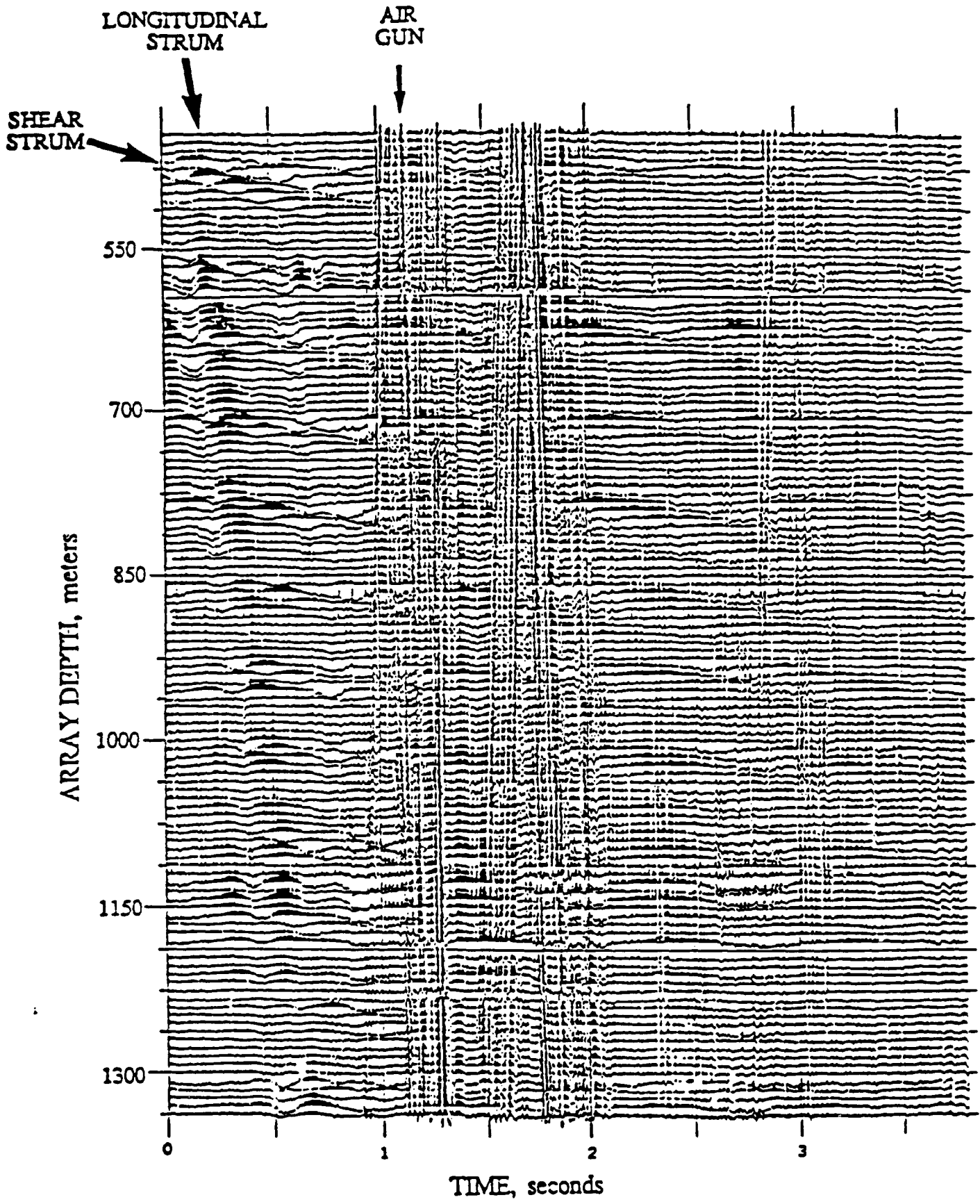
### Characteristics

- 10-200 Hz Frequency Region
- 200 Hydrophones (20 Sections with 10 Hydrophones/Section)
- 7.5 m Hydrophone Spacing ( $\lambda/2$  at 100 Hz)
- 500 Hz Data Sampling Rate (12 Bits/Sample)
- Additional Dynamic Range Provided by Programmable Gain Control Over Each Section
- 12 kHz Navigation of Each Array Section



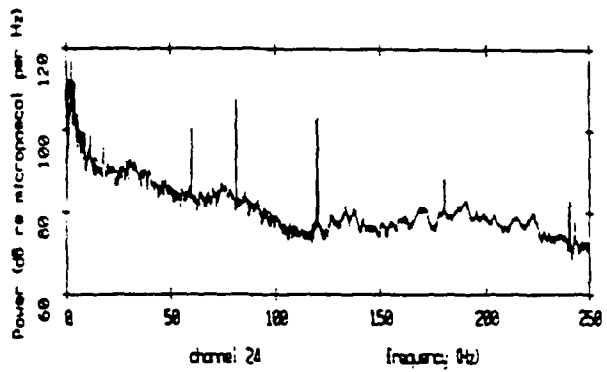




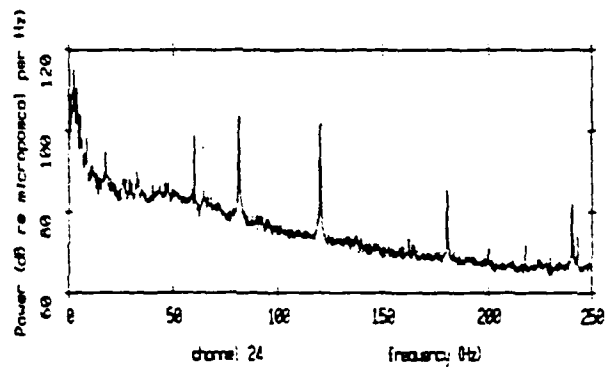


Time Series Display of Acoustic Channels. A graphic display of the acoustic channels shows an air gun source at a range of 300 miles as well as longitudinal and shear strum modes. The time record displayed is 3.5 seconds. The array hydrophone depths span 400 m to 1300 m.





TAPE: 235 GAIN: 42

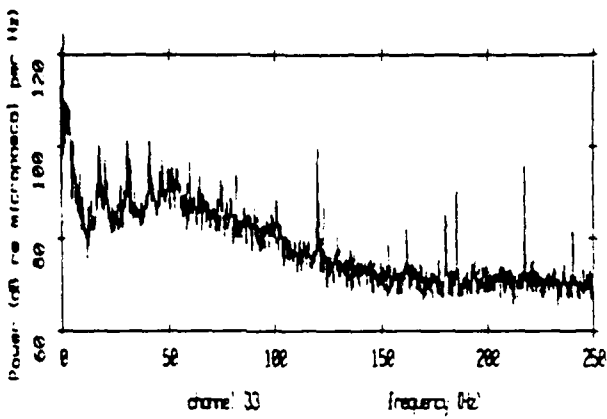


TAPE: 235 GAIN: 42 REMOVE PROFILER

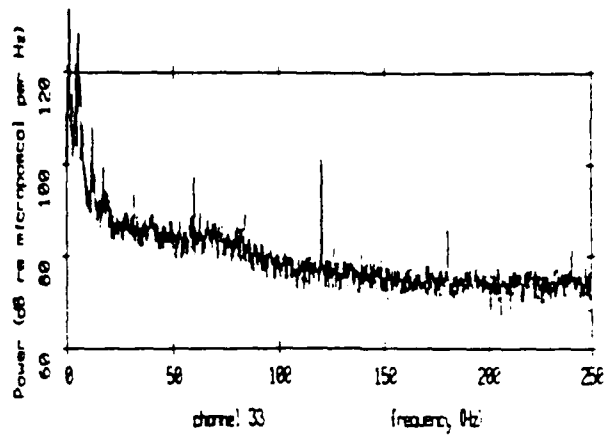


TAPE: 235 GAIN: 24 PROFILER

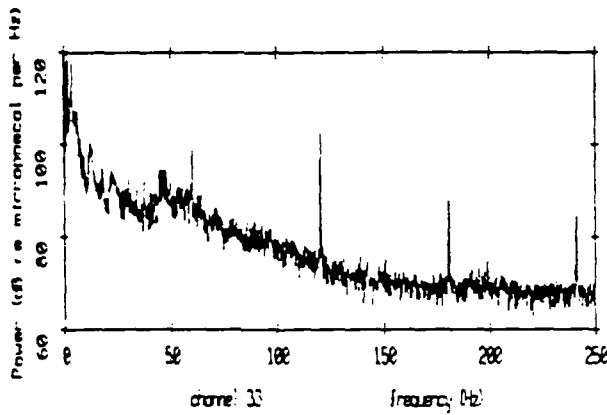




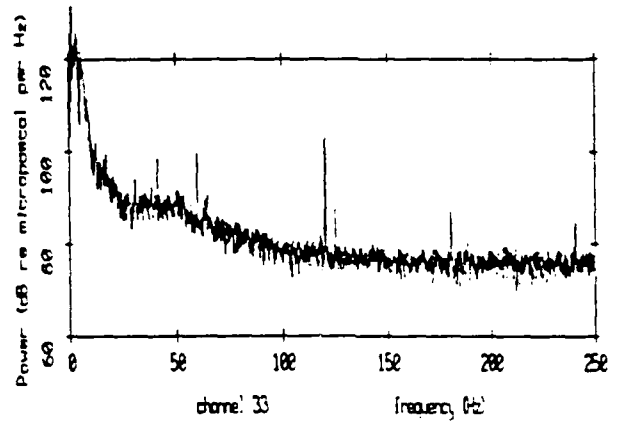
TAPE: 215 WIND: 4 kts DEPTH: 400 meters



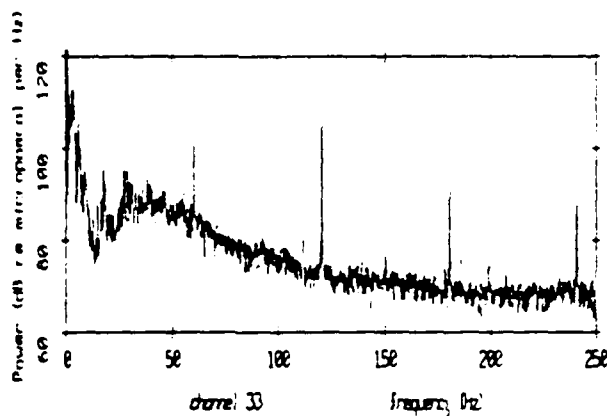
TAPE: 335 WIND: 23 kts DEPTH: 400 meters



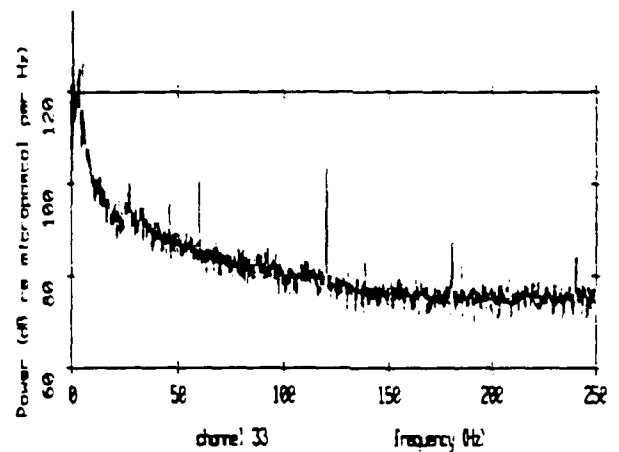
TAPE: 735 WIND: 6 kts DEPTH: 1300 meters



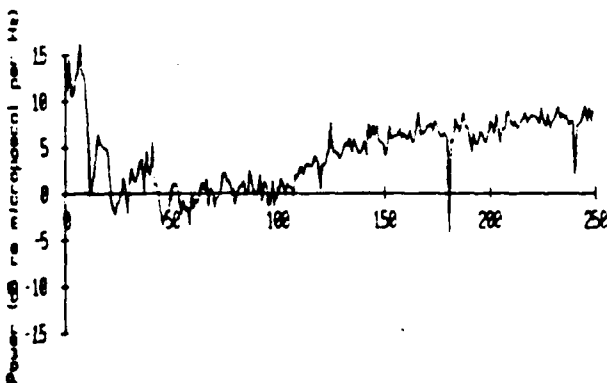
TAPE: 894 WIND: 26 kts DEPTH: 1300 meters



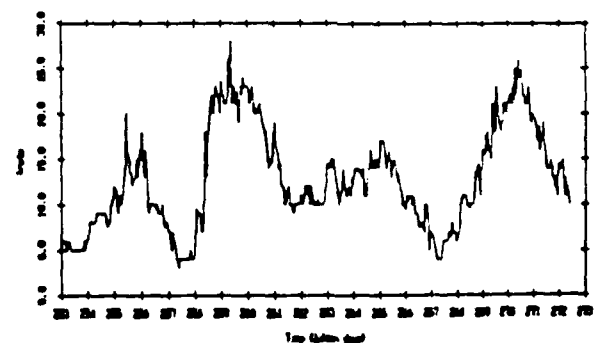
TAPE: 726 WIND: 4 kts DEPTH: 2200 meters



TAPE: 849 WIND: 22 kts DEPTH: 2200 meters

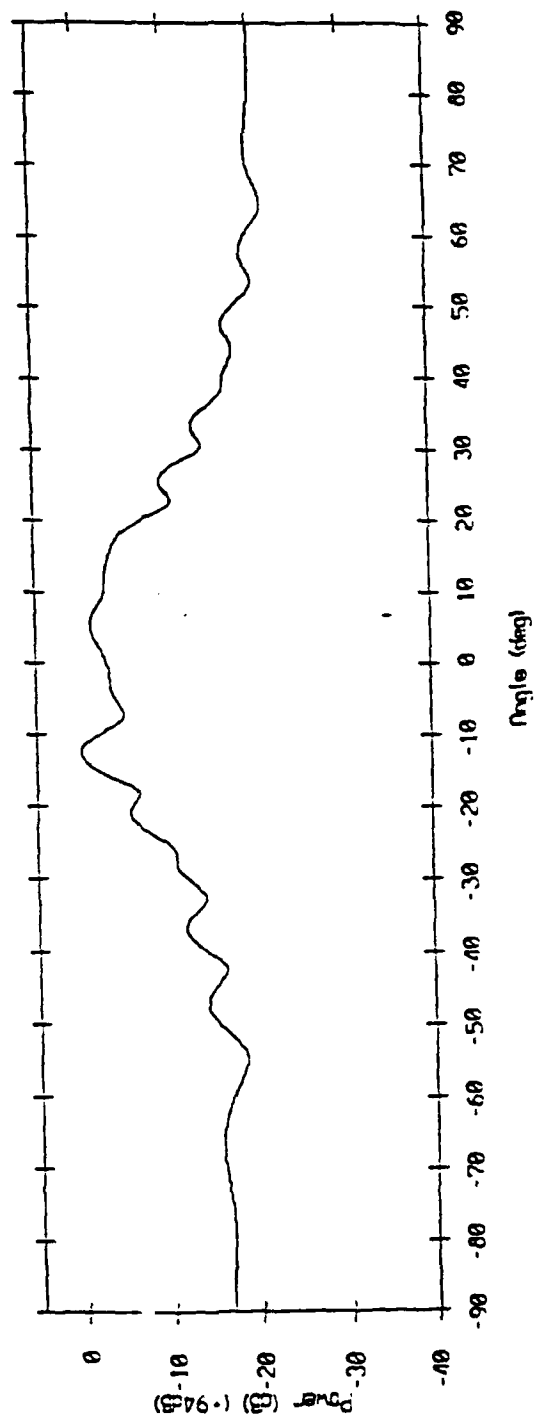
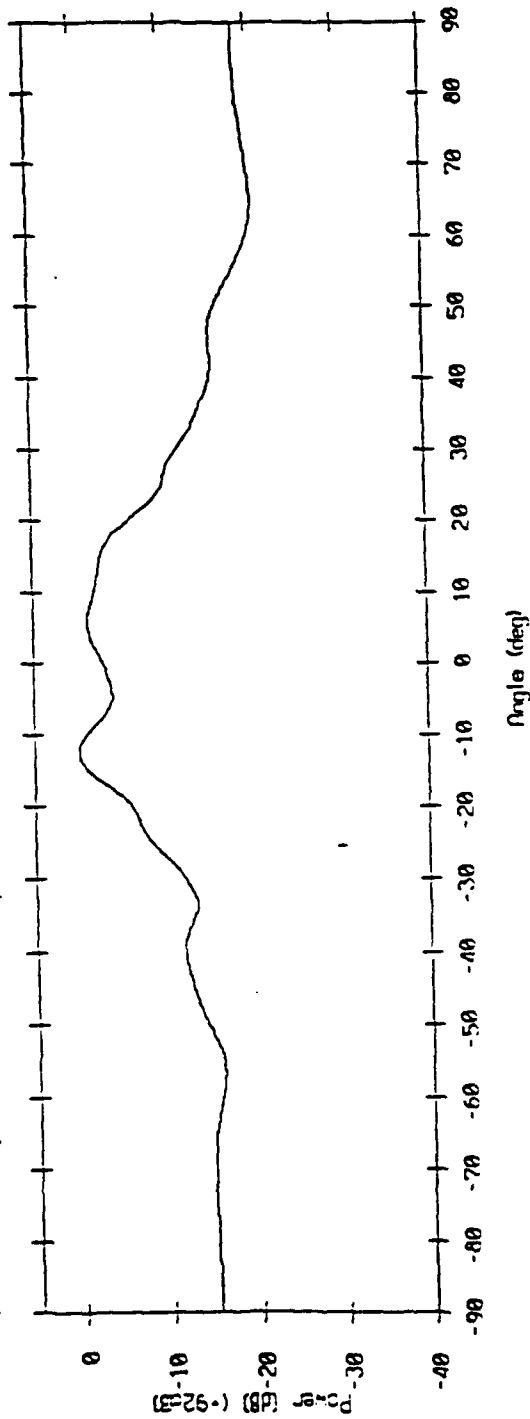


WIND SPEED days 25-27





Array Response - 39.1 Bin #1916  
 $f = 50$  Hz, KB window  $\alpha = 1.5$  (above), rect window (below)





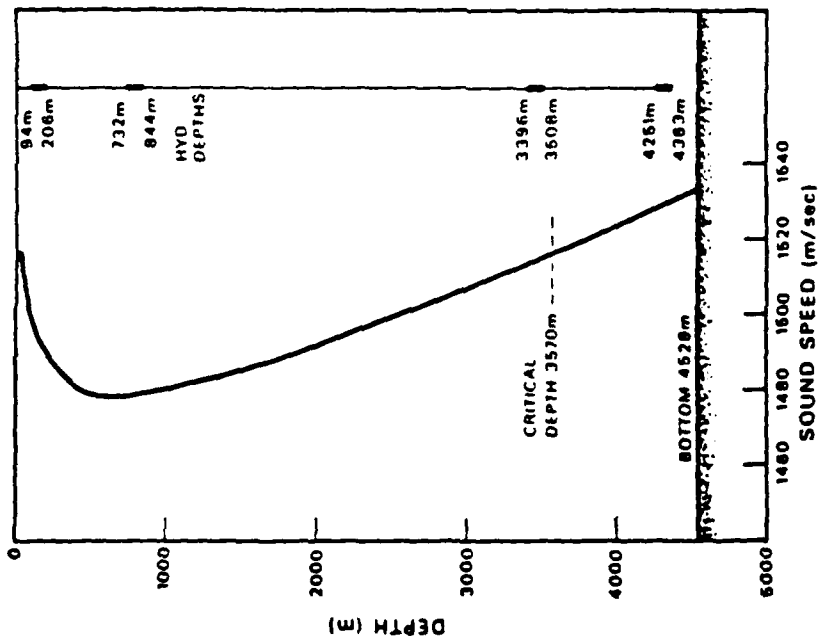


FIG. 6. Hydrophone depths relative to the sound speed profile during August 1974 ambient noise measurements.

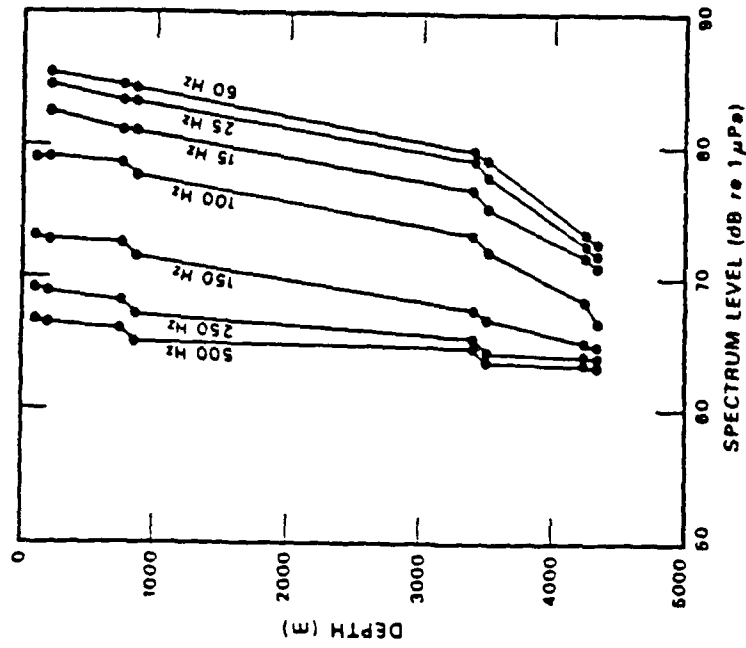


FIG. 9. Depth dependence of averaged uncontaminated ambient noise spectrum levels at August 1974 site.

G. B. Morris: Depth dependence of ambient sea noise



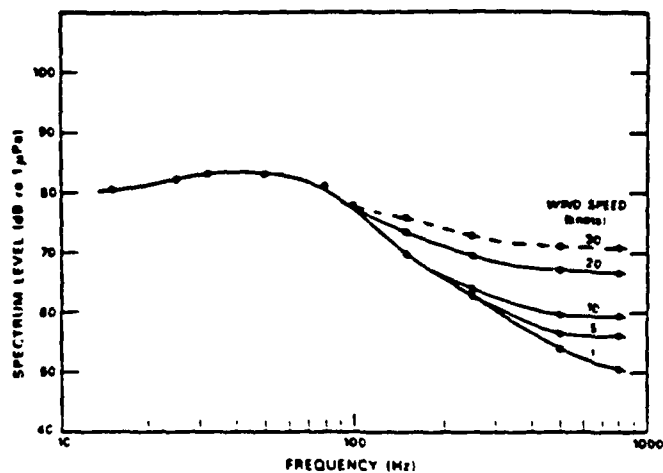


FIG. 11. Ambient noise spectra for five wind speeds at hydrophone depths near the sound channel axis.

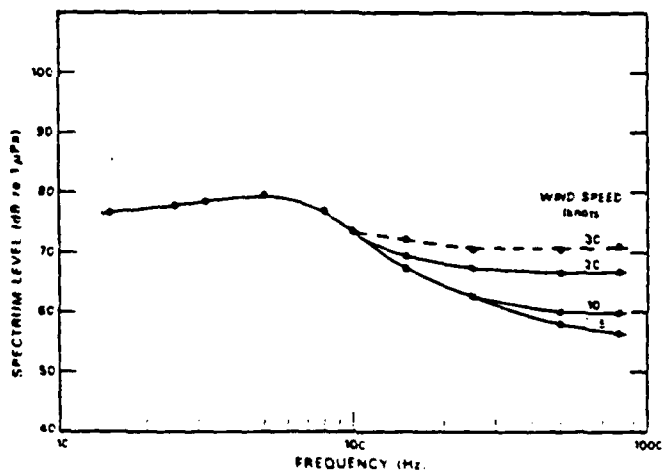


FIG. 12. Ambient noise spectra for five wind speeds at hydrophone depths approximately 170 m above the critical depth.

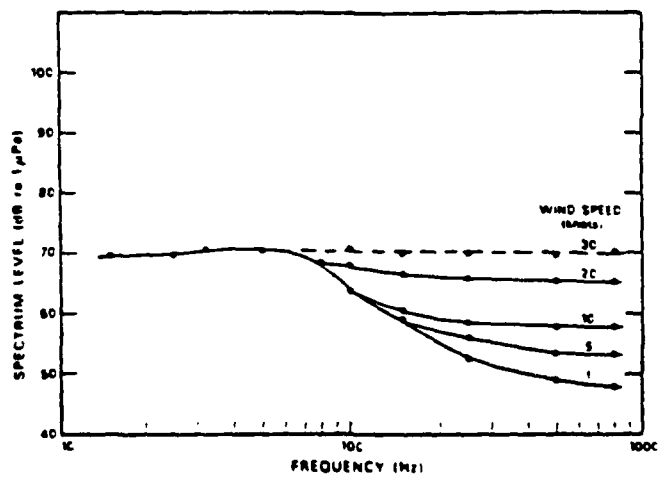


FIG. 13. Ambient noise spectra for five wind speeds at hydrophone depths about 150 m above the sea bottom.



## Mid-Frequency Data

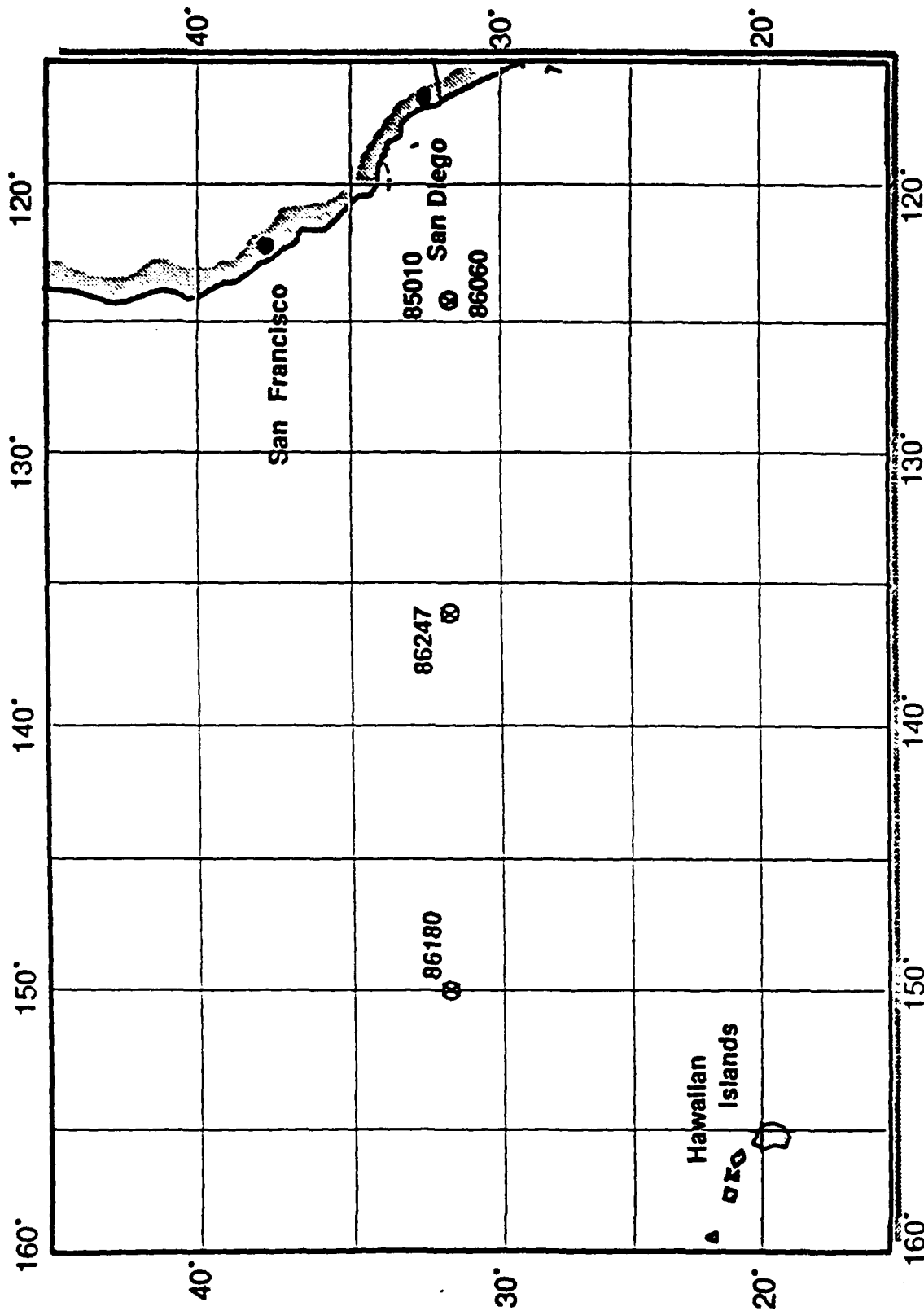
- October 1985 (NORDA VEKA 48-element vertical array)
  - 32° N, 124° W (Tape #85010, wind speed 6 kts)
- April/May 1986 (MPL 27-element vertical array)
  - 32° N, 124° W (Tape #86060, wind speed 22 kts)
  - 32° N, 136° W (Tape #86247, wind speed 17 kts)
  - 32° N, 150° W (Tape #86180, wind speed 10 kts)



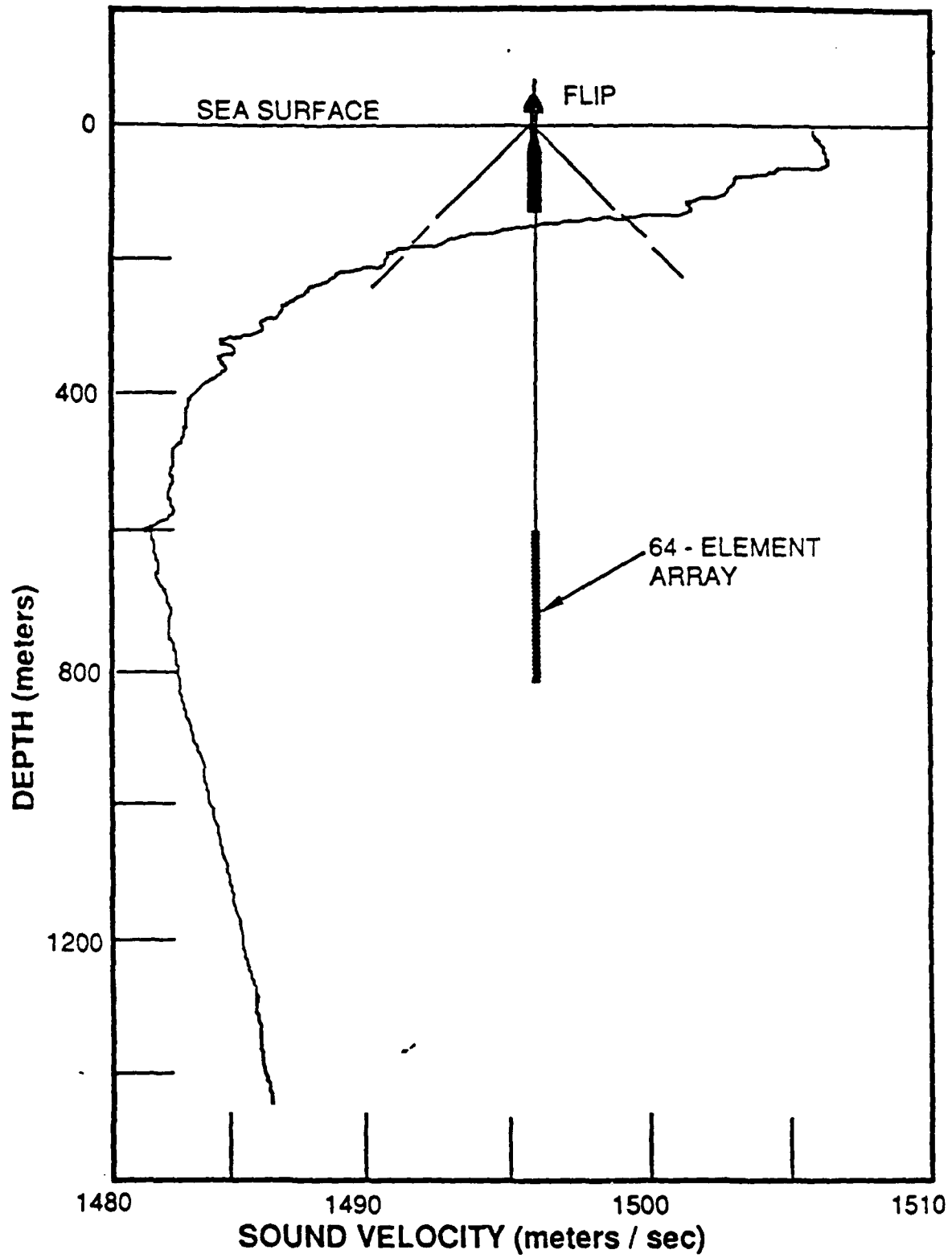


Marine Physical Laboratory

# Hawaii to California

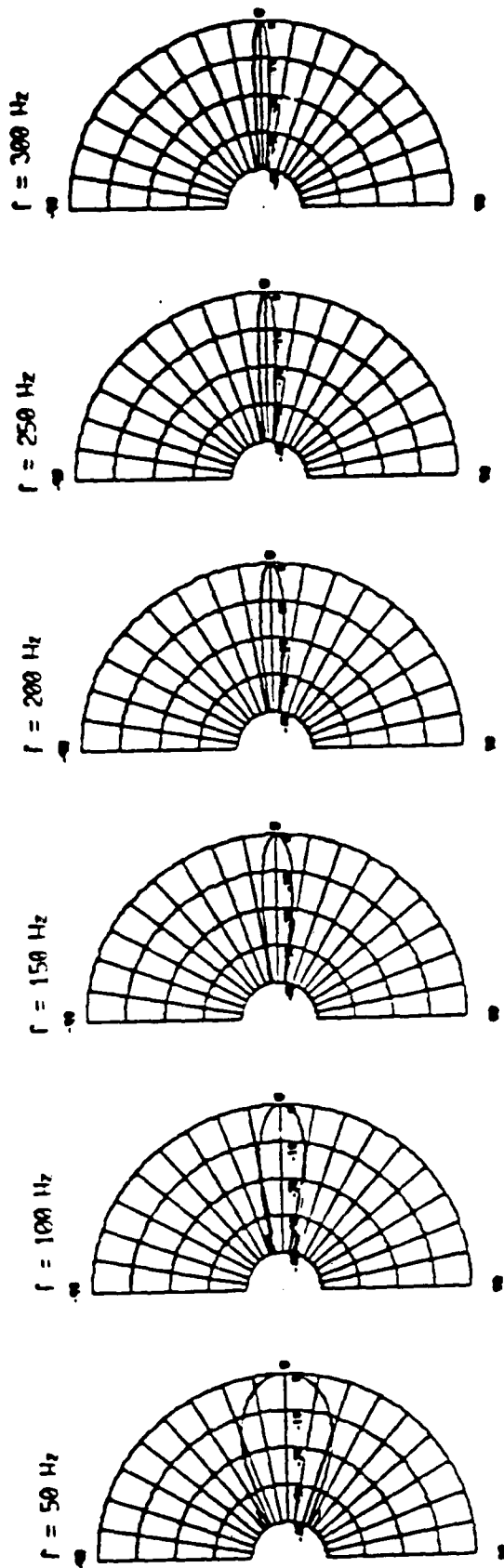








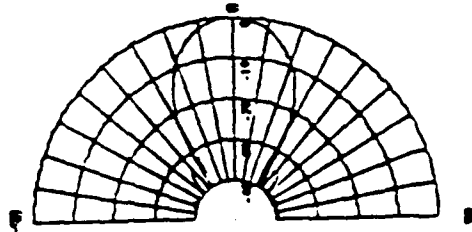
VEKA Array Beam Pattern: kb window ( $\alpha = 1.5$ )



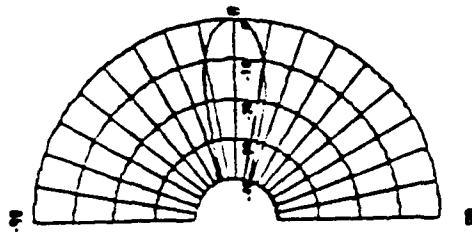


MPL Array Beam Pattern:  $k_0$  window ( $\alpha = 1.5$ )

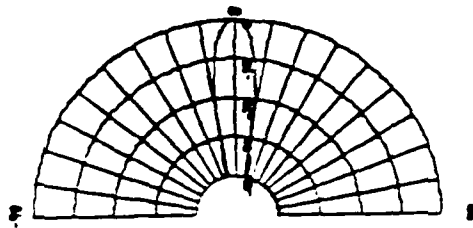
$f = 50$  Hz



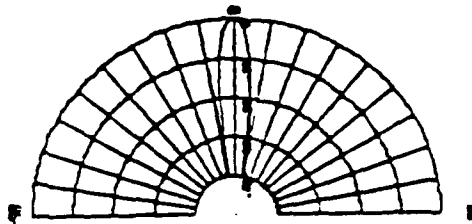
$f = 100$  Hz



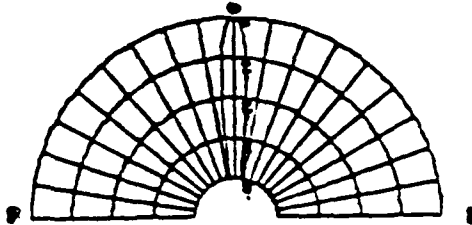
$f = 150$  Hz



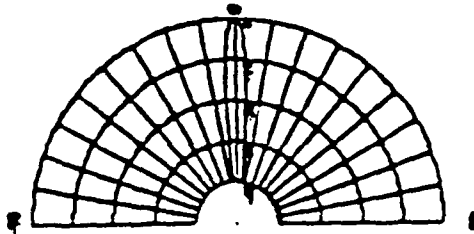
$f = 200$  Hz



$f = 250$  Hz

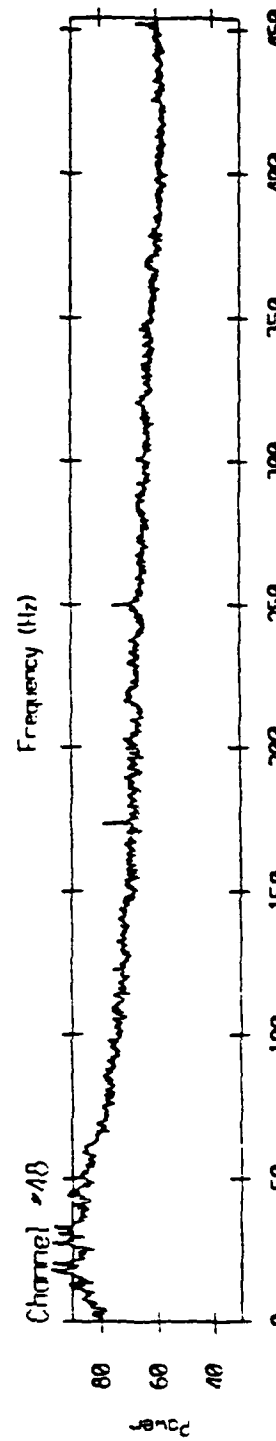
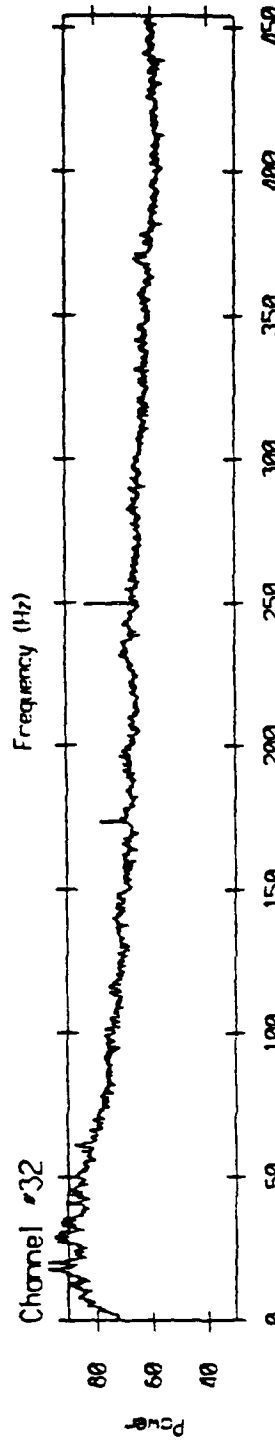
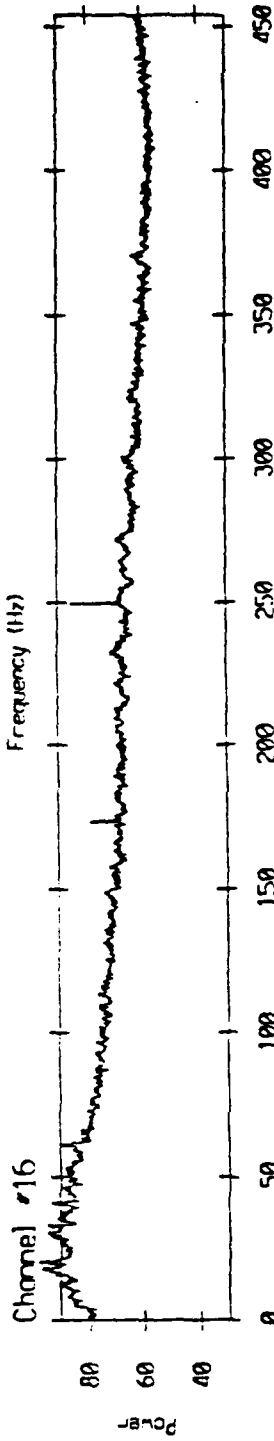
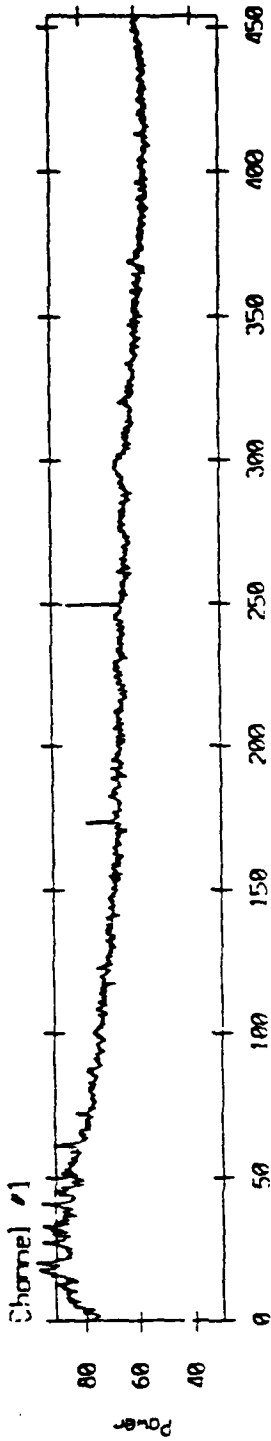


$f = 300$  Hz



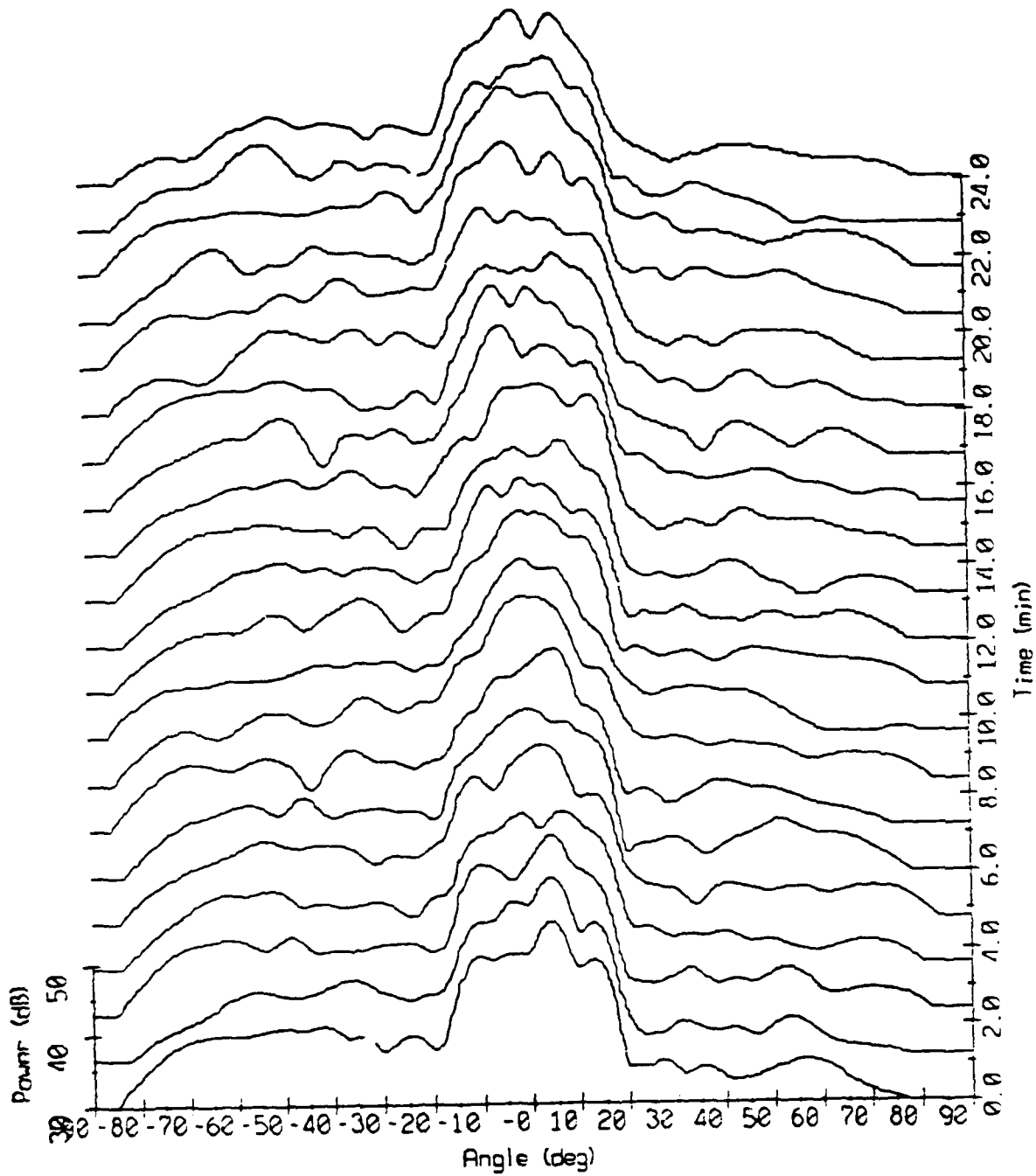


Power Spectrum - 85010.1



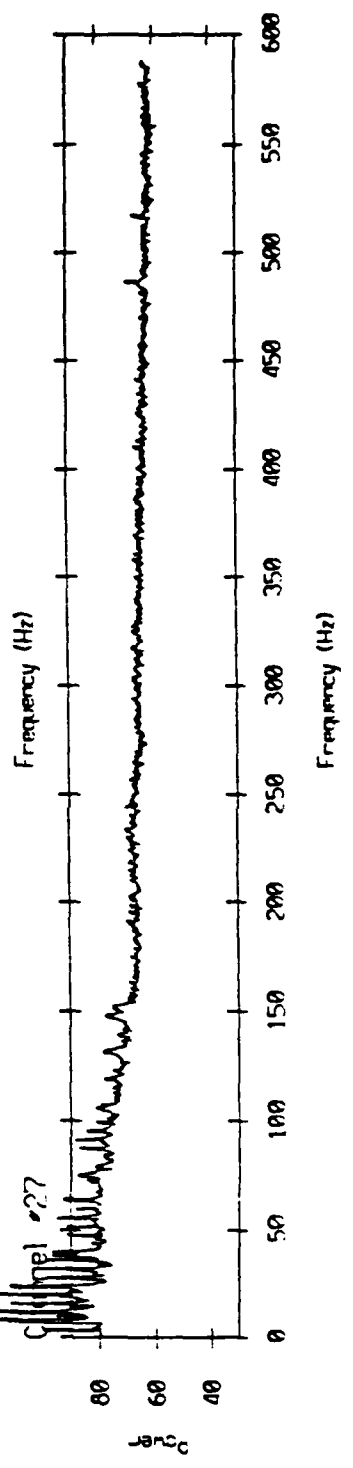
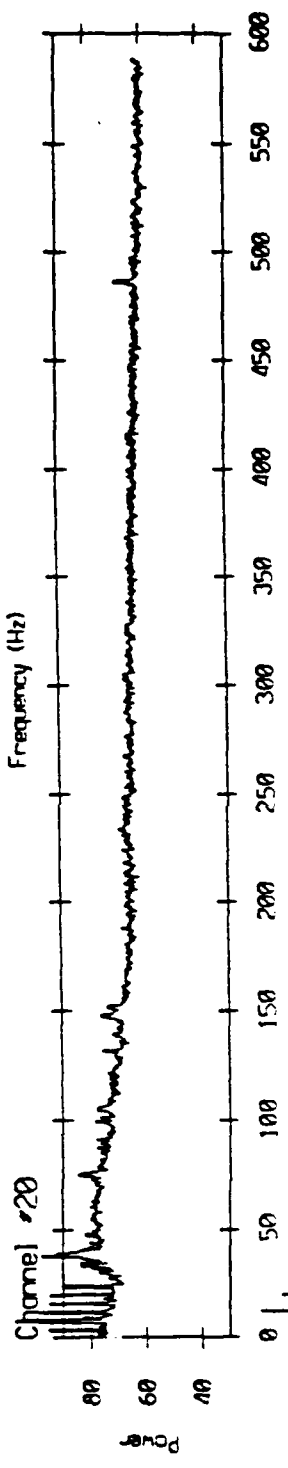
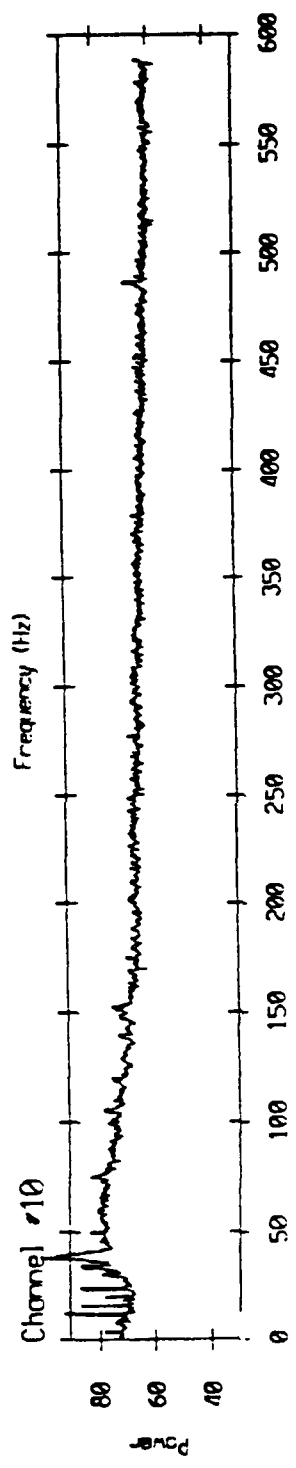
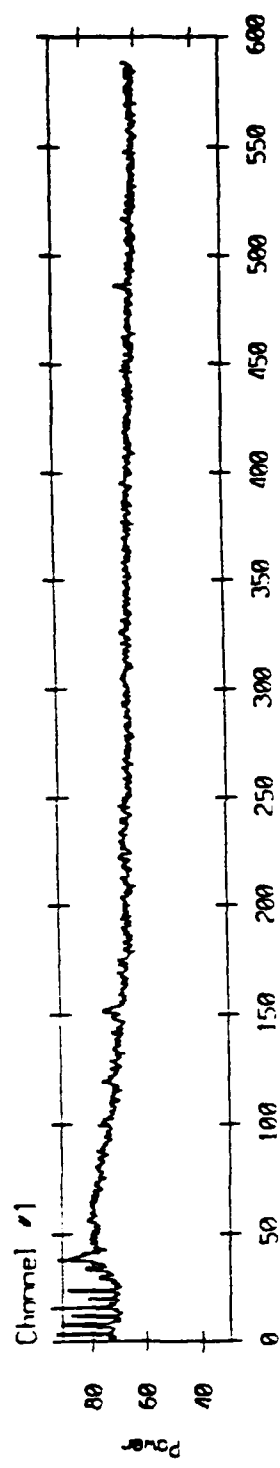


Array Response - 85010 Bin #5902  
f = 200 Hz, KB window (alpha = 1.5)



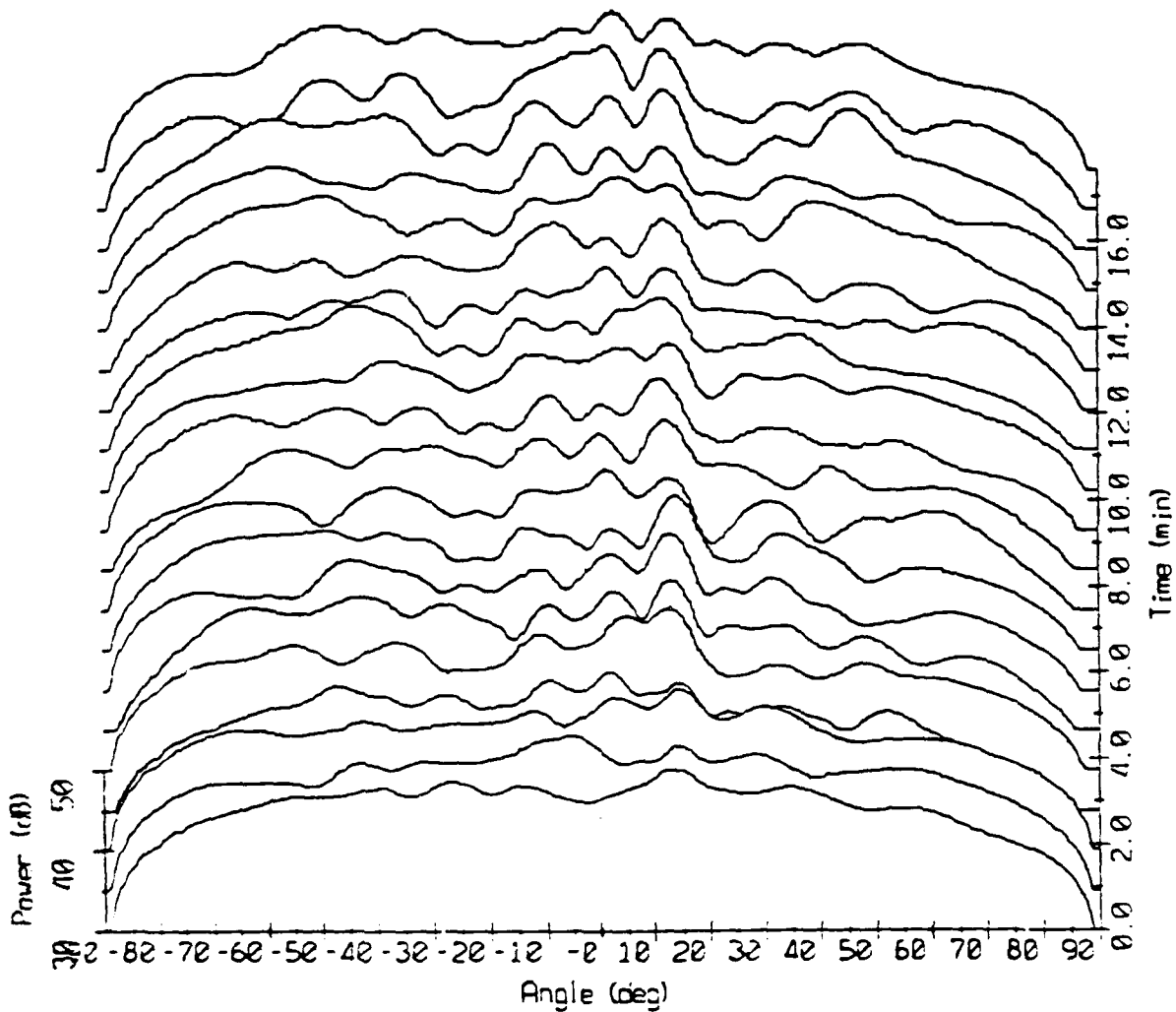


Power Spectrum - 85060.1



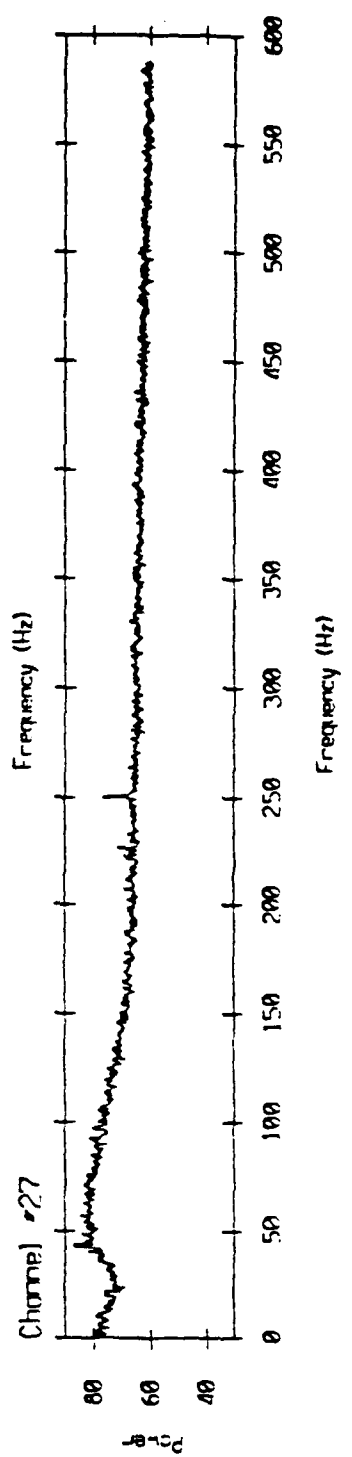
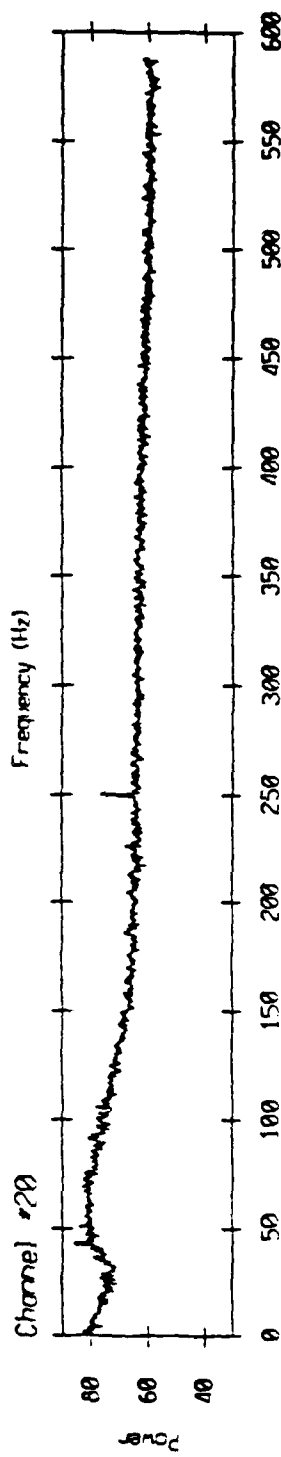
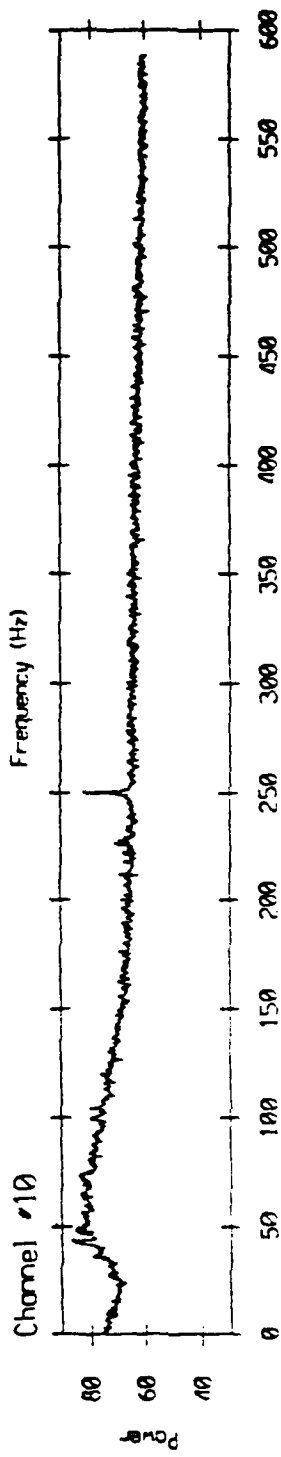
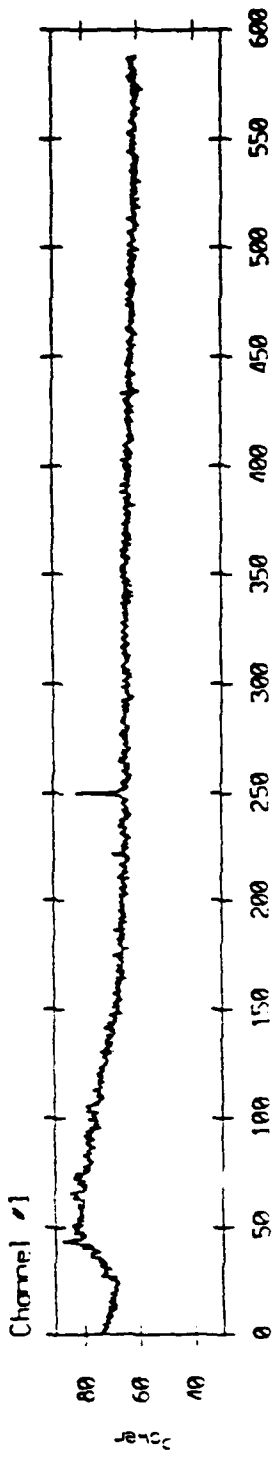


Array Response - 86060 Bin #5490  
f = 200 Hz, KB window (alpha = 1.5)



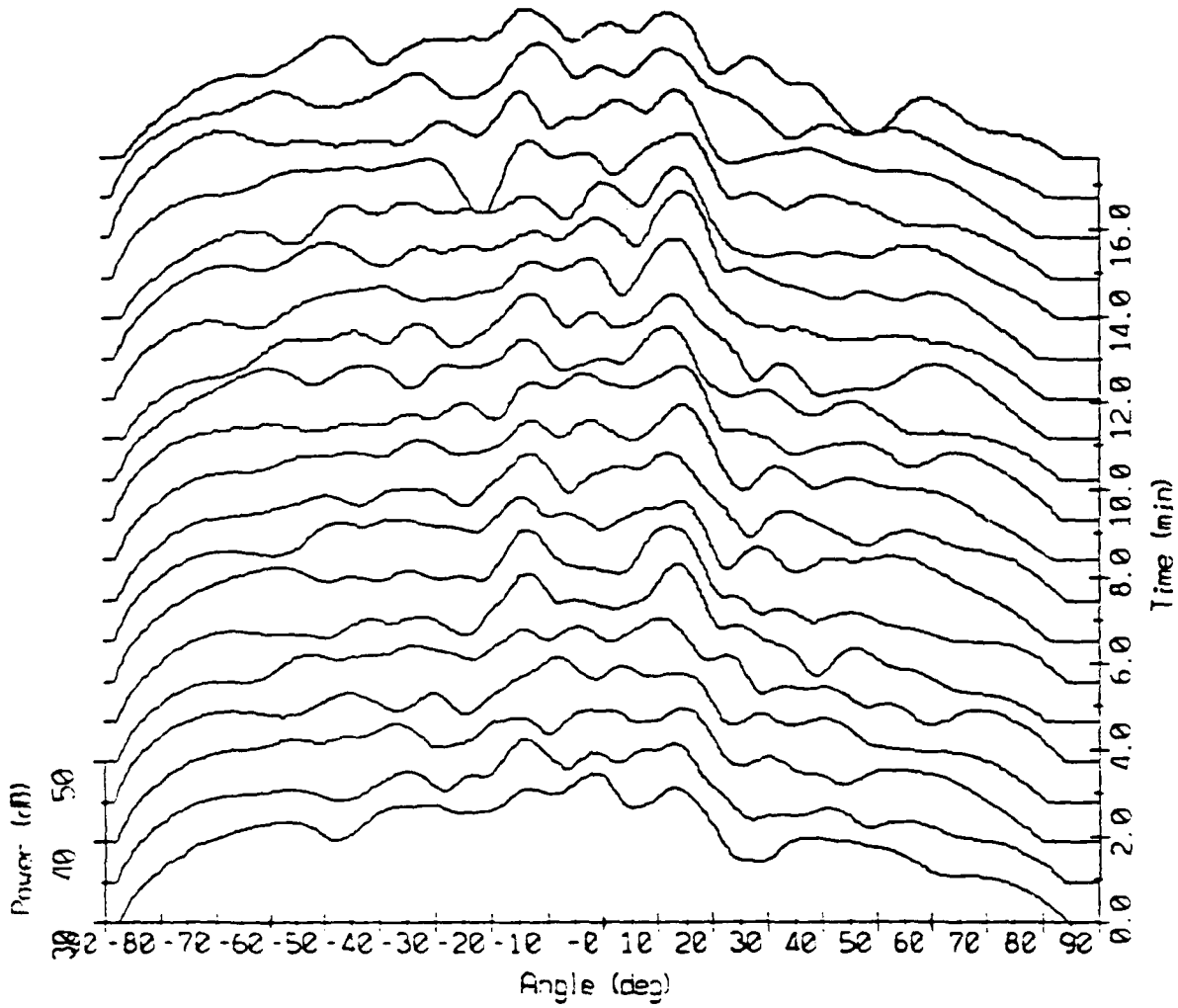


Power Spectrum - 86247.1



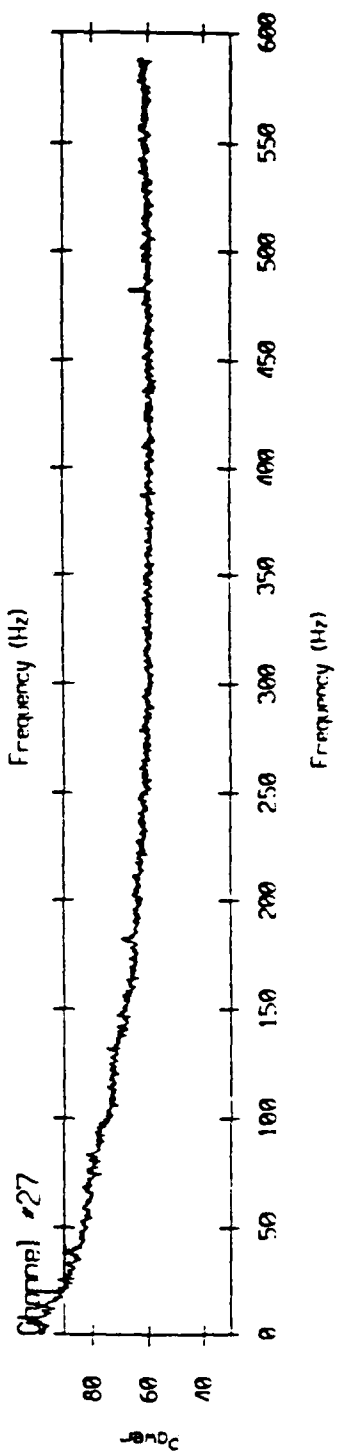
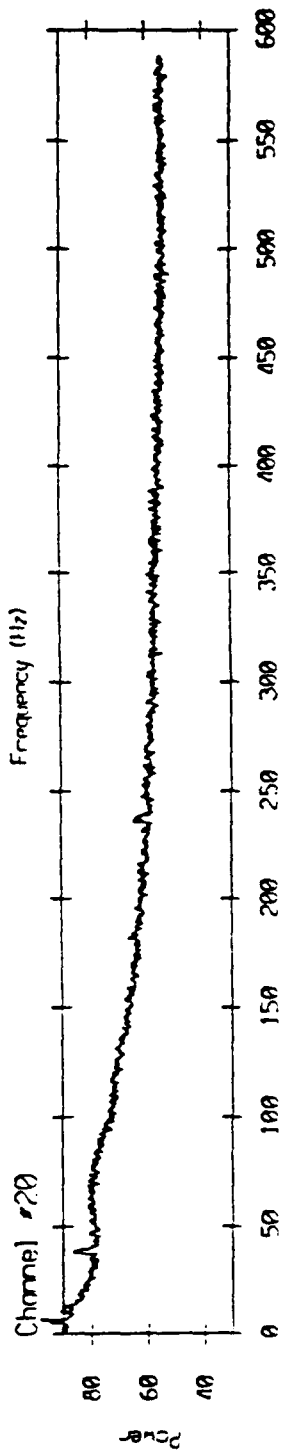
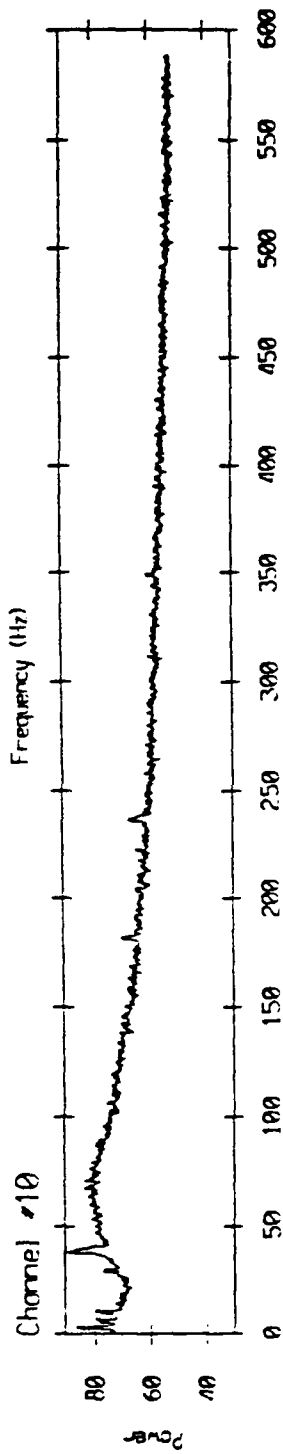
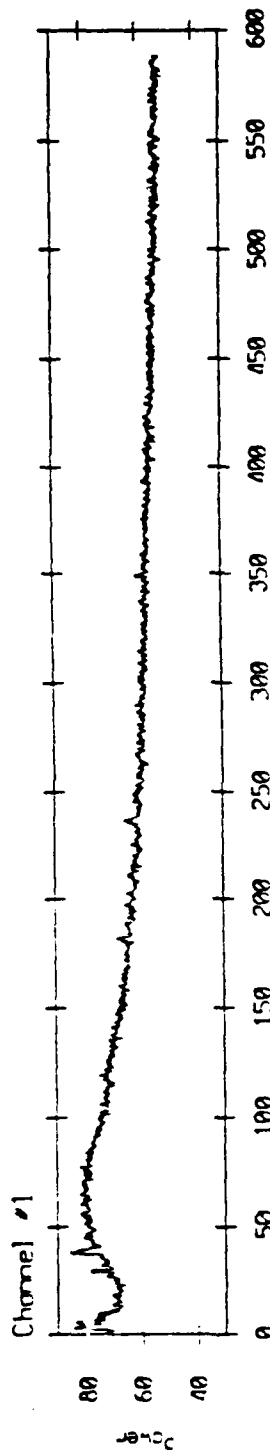


Array Response - 86247 Bin #5490  
f = 200 Hz, KB window (alpha = 1.5)



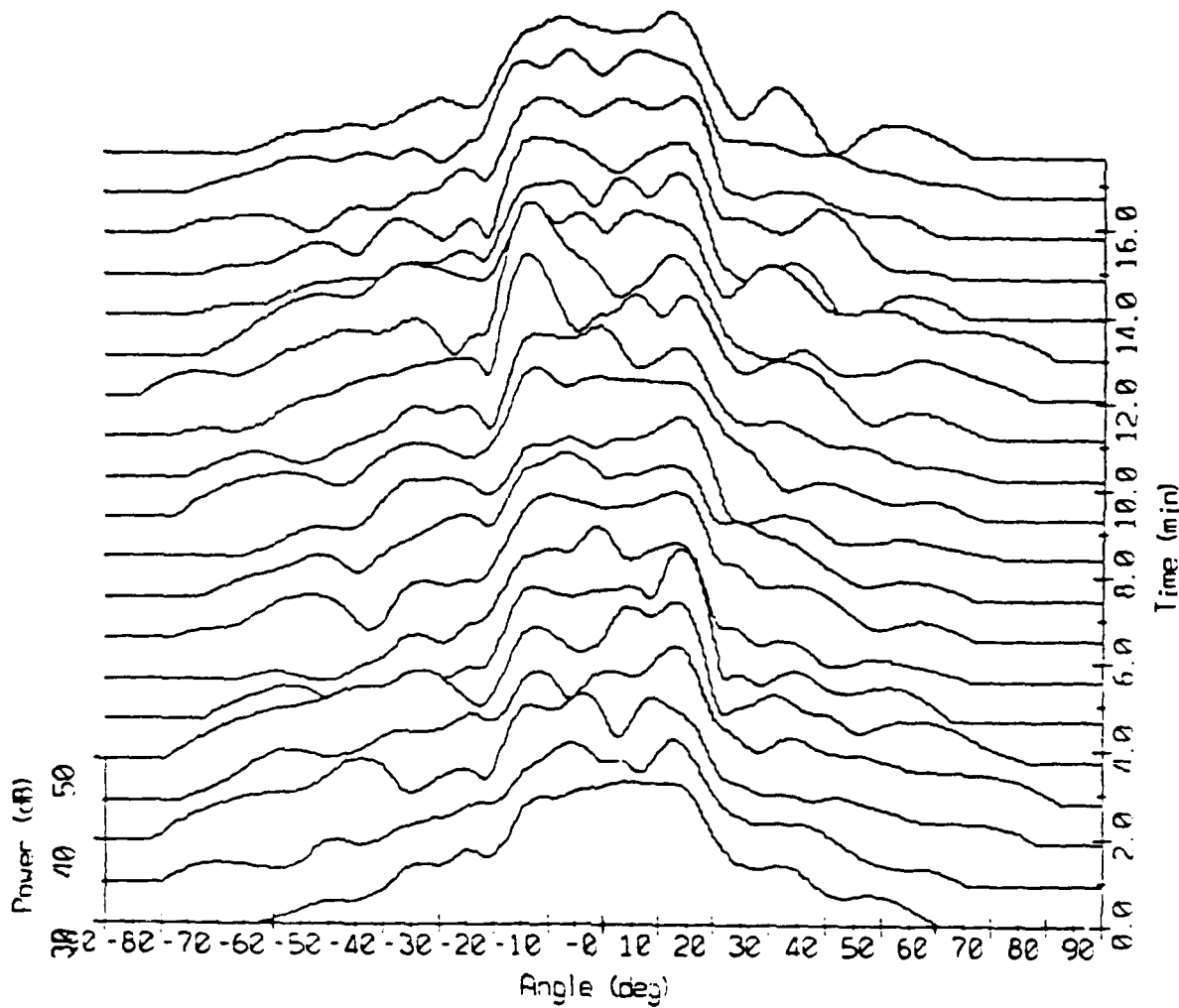


Power Spectrum - 86180.1



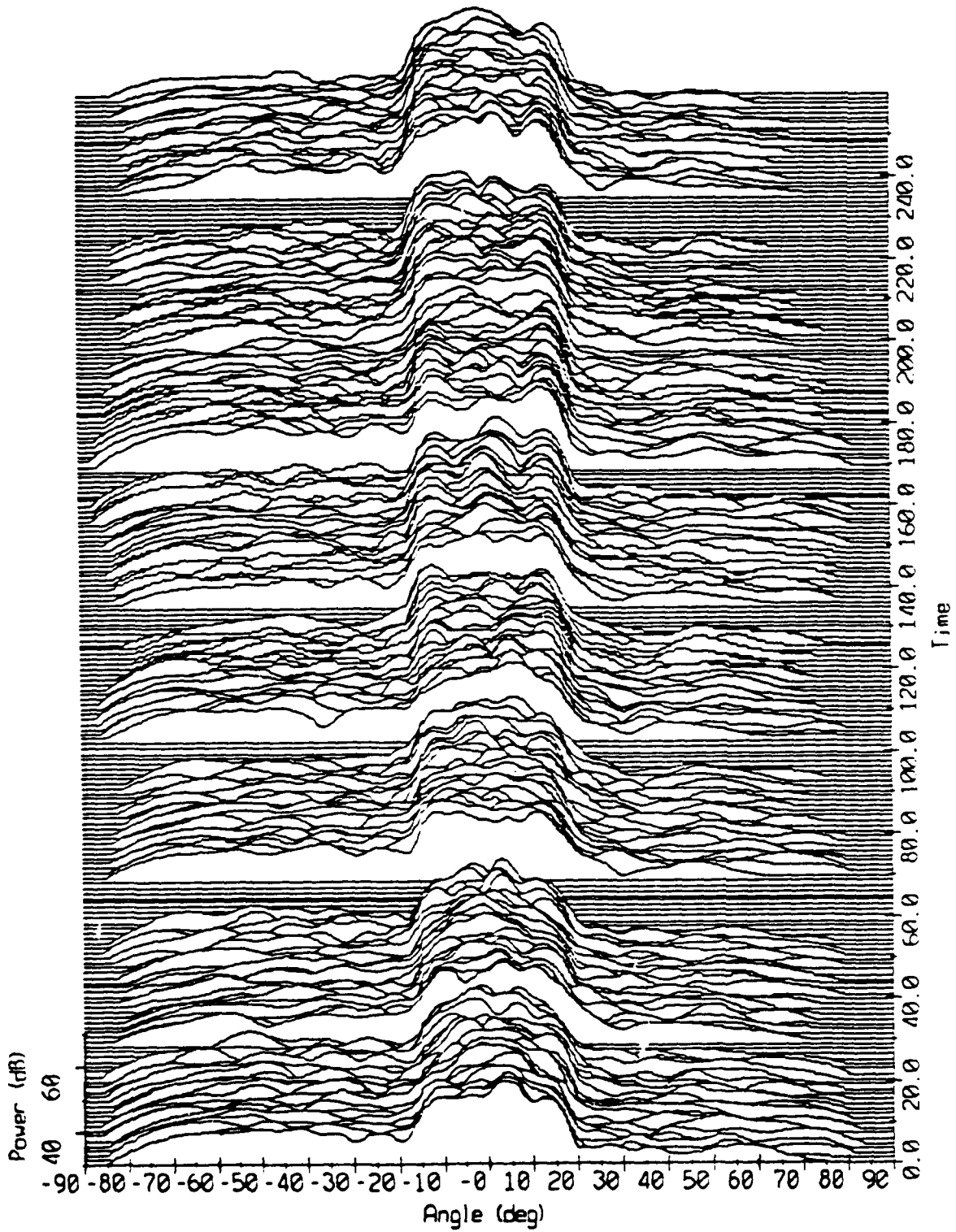


Array Response - 86180 Bin #5490  
 $f = 200$  Hz, KB window ( $\alpha$ ) = 1.5)





Array Response - 85010-85017 Bin #5902  
f = 200 Hz, KB window (alpha = 1.5)





**NOISE MODAL FILTERING TO  
ENHANCE ARRAY GAIN**

**T. YANG (NRL)**



**MODE FILTERING TO ENHANCE ARRAY GAIN**

**BACKGROUND:**

**SIGNAL AND NOISE, REPRESENTED BY A SUMMATION OF NORMAL MODES, HAVE DIFFERENT INTENSITY DISTRIBUTION IN THE MODE SPACE.**

**OBJECTIVE:**

**INVESTIGATE/DEVELOP SIGNAL PROCESSING TECHNIQUES THAT AMPLIFY THOSE MODES WHICH CONTRIBUTE SUBSTANTIALLY TO THE SIGNAL, AND SUPPRESS THOSE MODES WHICH CONTRIBUTE SIGNIFICANTLY TO THE NOISE.**



## OUTLINE

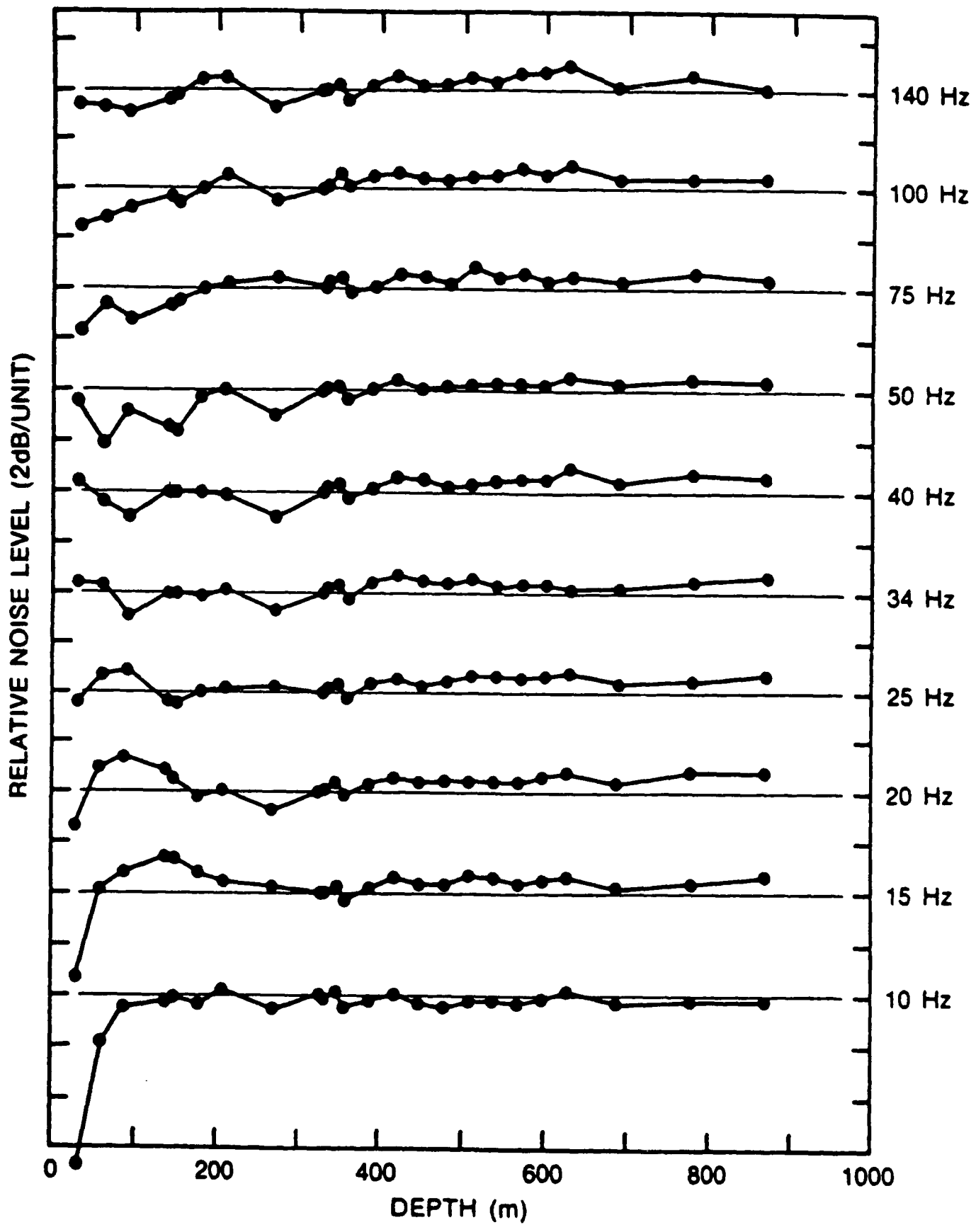
- o LOW FREQUENCY AMBIENT NOISE IN THE ARCTIC
  - SPATIAL CHARACTERISTICS
  - MODAL REPRESENTATION
- o EFFECTIVENESS OF MODE FILTERING IN THE ARCTIC
- o EFFECTIVENESS OF MODE FILTERING IN THE PACIFIC



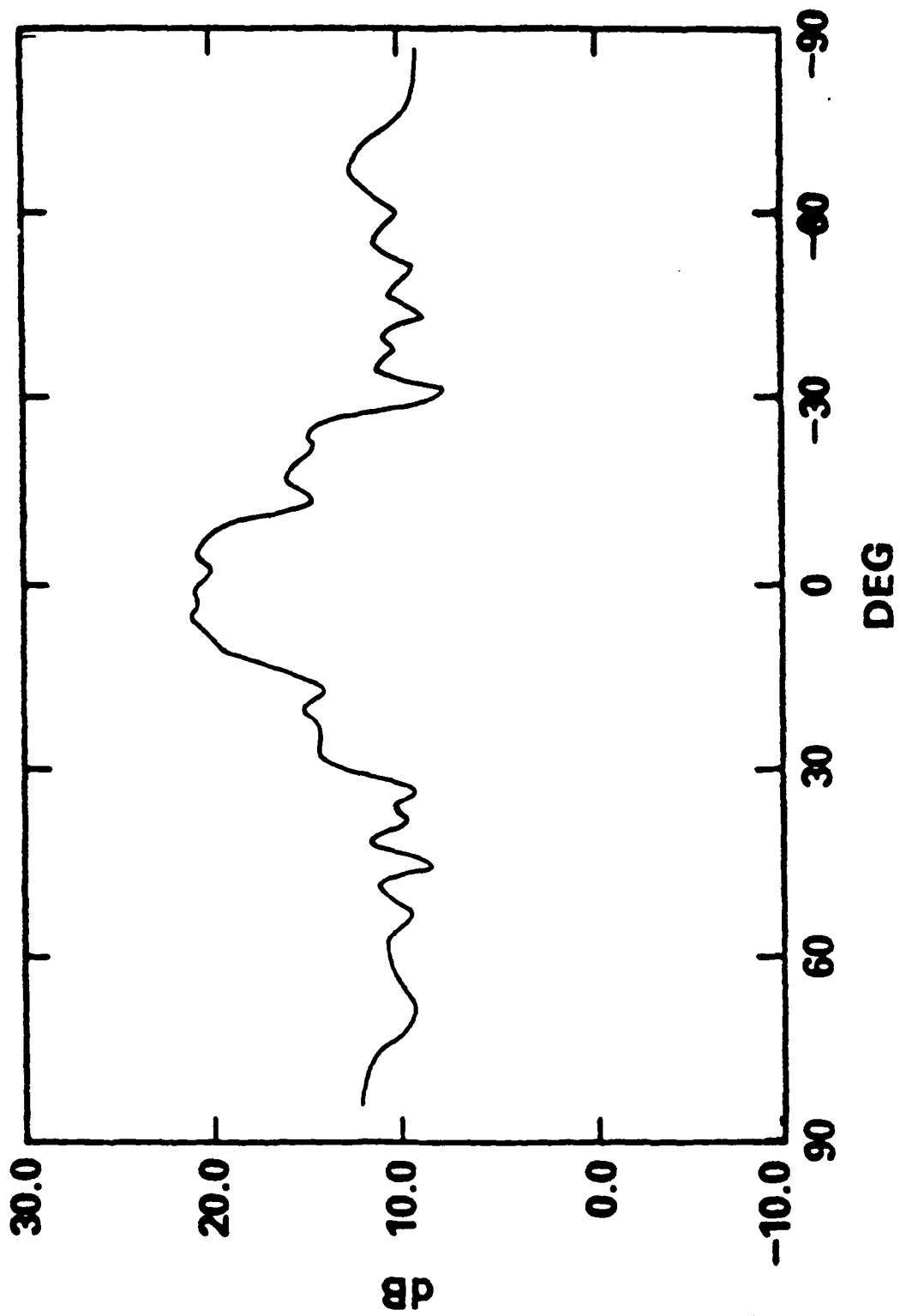
SPATIAL CHARACTERISTICS OF LOW FREQUENCY  
AMBIENT NOISE IN THE ARCTIC

- o NOISE LEVEL VS DEPTH
- o NOISE VERTICAL DIRECTIONALITY
- o SPATIAL COHERENCE





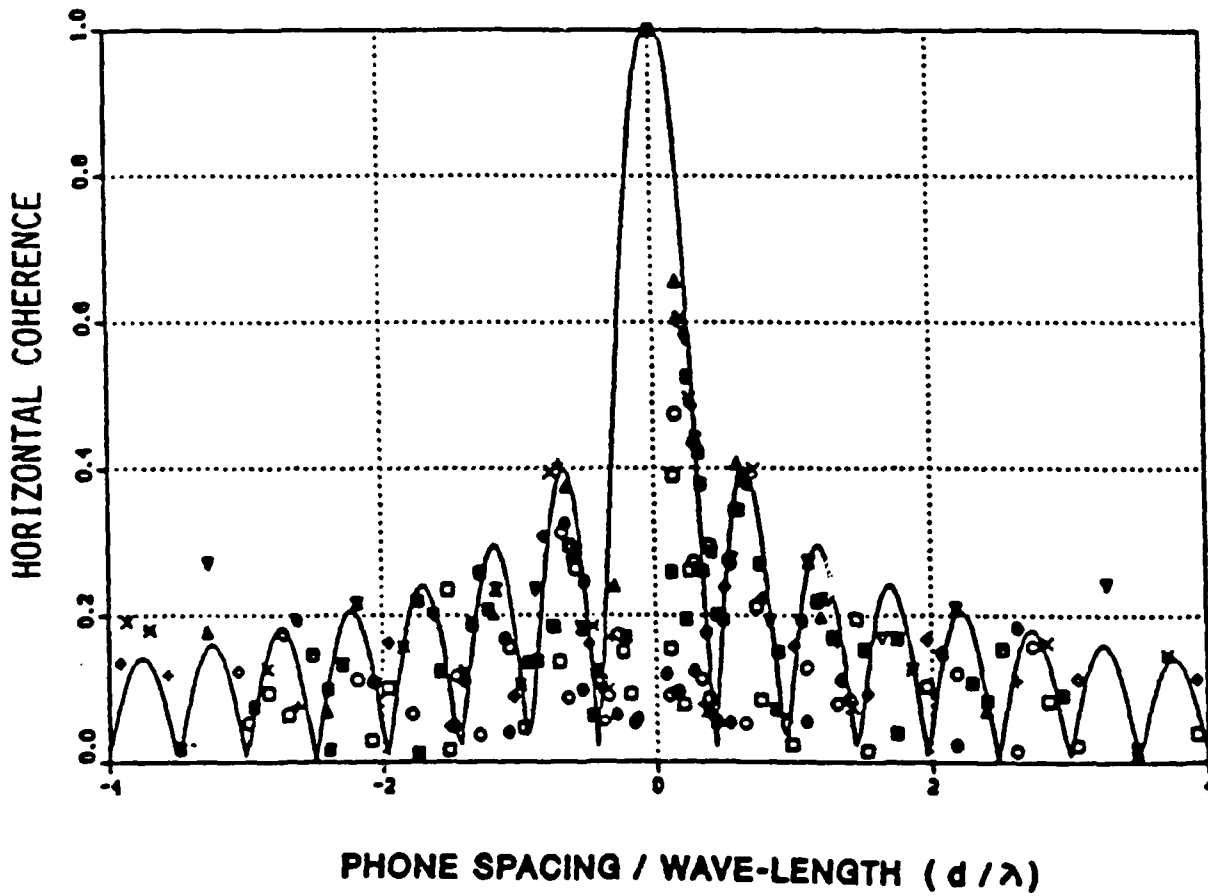
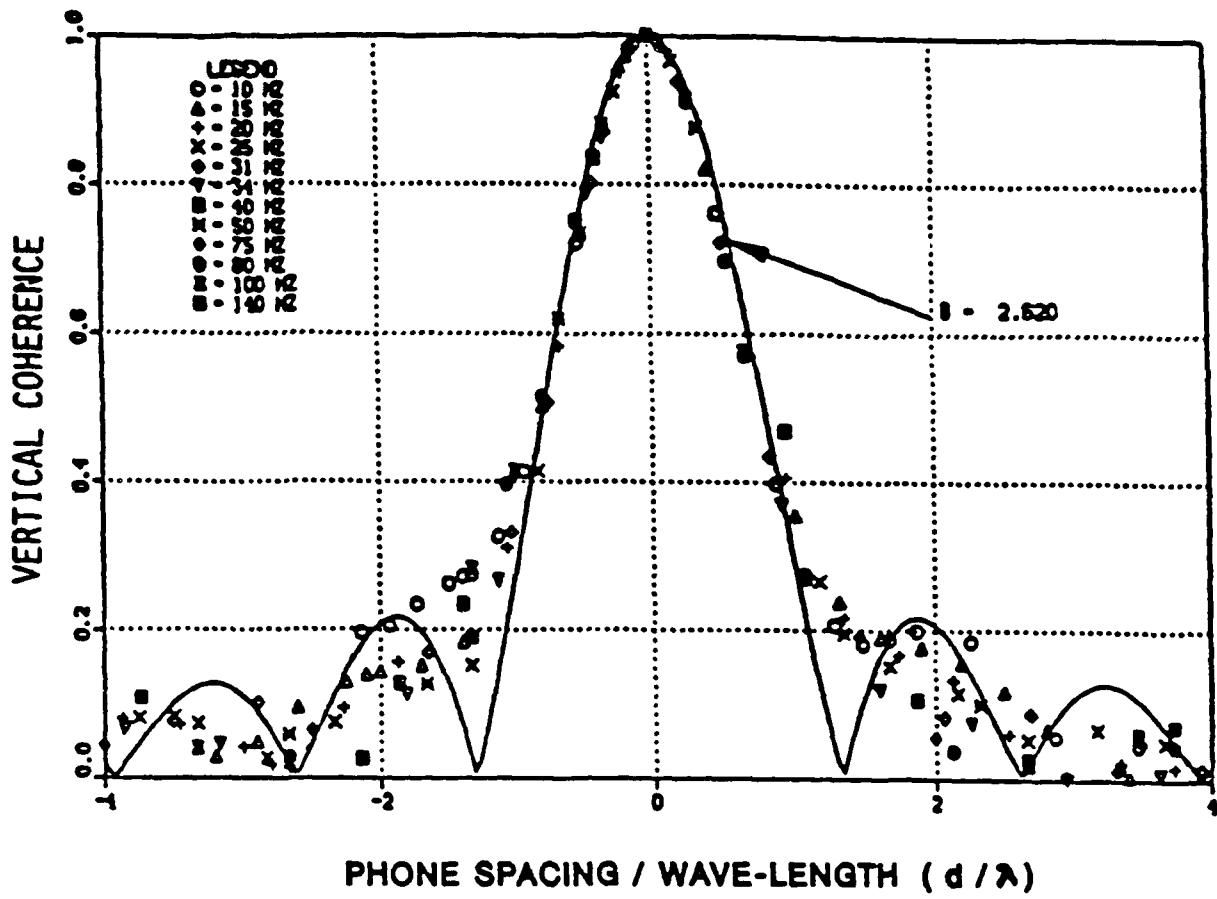






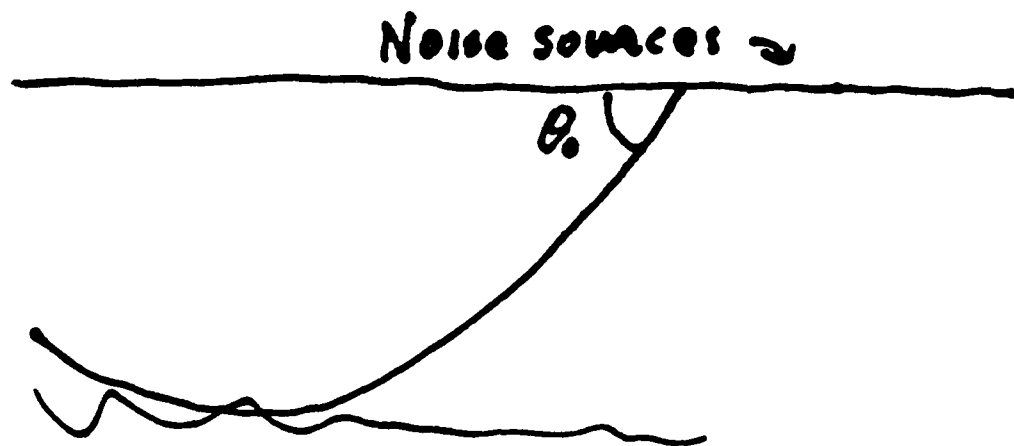








# A Model for Noise Coherence in the Arctic



$$P_V(d) = \frac{\sin(kd\beta)}{kd\beta}$$

Crow-Sherman  
Model

$$\beta = \sin(\theta_0)$$

$$P_H(d) = - \int_0^{\theta_0} \cos\theta J_0(kd\cos\theta) d\theta / \sin\theta_0$$



## MODAL REPRESENTATION OF THE NOISE

OBSERVATION (R. KLEMM):

IF NOISE IS UNCORRELATED IN THE MODE SPACE, THEN THE SPATIAL COHERENCE IS A FUNCTION OF PHONE SEPARATION, AND IS APPROXIMATELY A FUNCTION OF  $D/\lambda$

PROOF:  $p(r) = \sum a_n \exp\{i(k_n r + \phi_n)\}$

$$P_p(n, m) = \langle e^{i\phi_n} e^{-i\phi_m} \rangle$$

$$P(d) = \sum_{n, m} a_n a_m \exp\{i(k_n - k_m)r - k_n d\} P_p(n, m)$$

In general, the spatial correlation depends on the modal phase differences  $(k_n - k_m)r$ . Only for uncorrelated modes, i.e.,

$$P_p(n, m) = 0 \quad \text{for } n \neq m$$

do we get

$$P(d) = \sum_{n=1} a_n^2 \exp(-ik_n d)$$



## INTERPRETATION

LOW (<140 Hz) FREQ. ARCTIC DATA INDICATED THAT THE SPATIAL COHERENCE OF THE AMBIENT NOISE CAN BE REPRESENTED APPROXIMATELY BY A FUNCTION OF  $D/\lambda$ . THIS RESULT SUGGESTS THAT AMBIENT NOISE IS UNCORRELATED IN THE MODE SPACE, (IE., THAT THE NOISE MODAL COVARIANCE MATRIX IS DIAGONAL).

### IMPLICATIONS:

MODAL BEAMFORMING IS POTENTIALLY ROBUST FOR LOW S/N RATIO SIGNAL DETECTION AND LOCALIZATION IN A COLORED NOISE ENVIRONMENT WHERE THE NOISE SOURCES ARE UNCORRELATED







Processor                      Phone Space                      Mode Space

---

Matched-Mode  
(Modal Beamforming)

$$e^+ Q R_s Q e \qquad a_s^+ S a_s$$

$$= |a_s^+ a_s|^2$$


---

Matched-Field

$$e^+ R_s e \qquad a_s^+ H S H a_s$$

$$= |e^+ p|^2 \qquad = |a_s^+ H a_s|^2$$

where  $H = U^+ U = \int \psi_i^+(z) \psi_j(z) dz$

---

Optimum Linear Processor

$$e^+ R_N^{-1} R_s R_N^{-1} e = a_s^+ G^{-1} S G^{-1} a_s$$

$$Q = U H^{-1} H^{-1} U^+$$



## ARRAY OUTPUT S/N

$$S = \begin{pmatrix} s_1 & s_2 & \dots \\ N_1 & N_2 & \dots \end{pmatrix}$$

v CONVENTIONAL

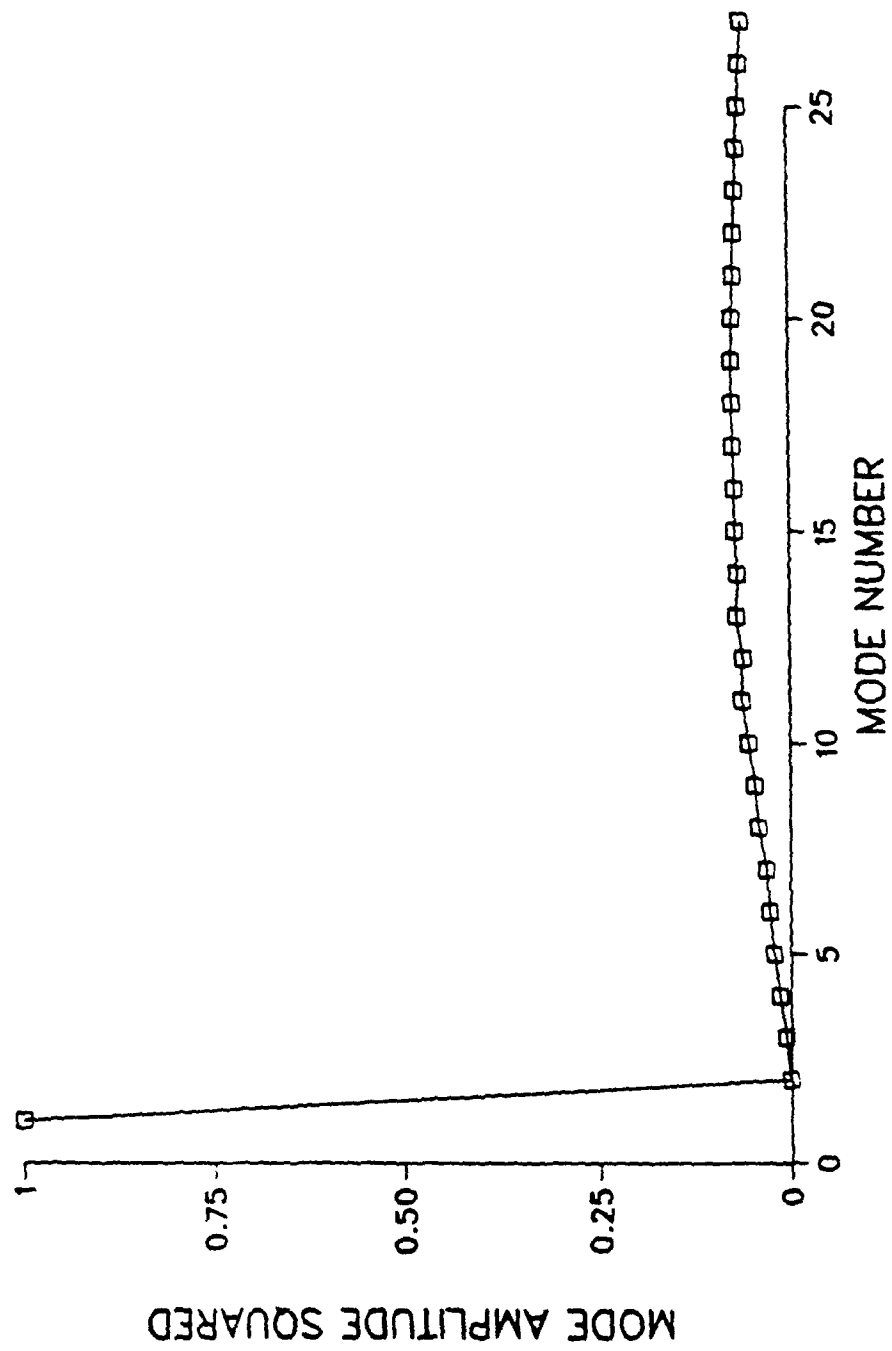
$$\text{OUTPUT S/N} = \frac{\sum s_i^2}{\sum s_i N_i}$$

$\approx 10 \log N$  (White noise)

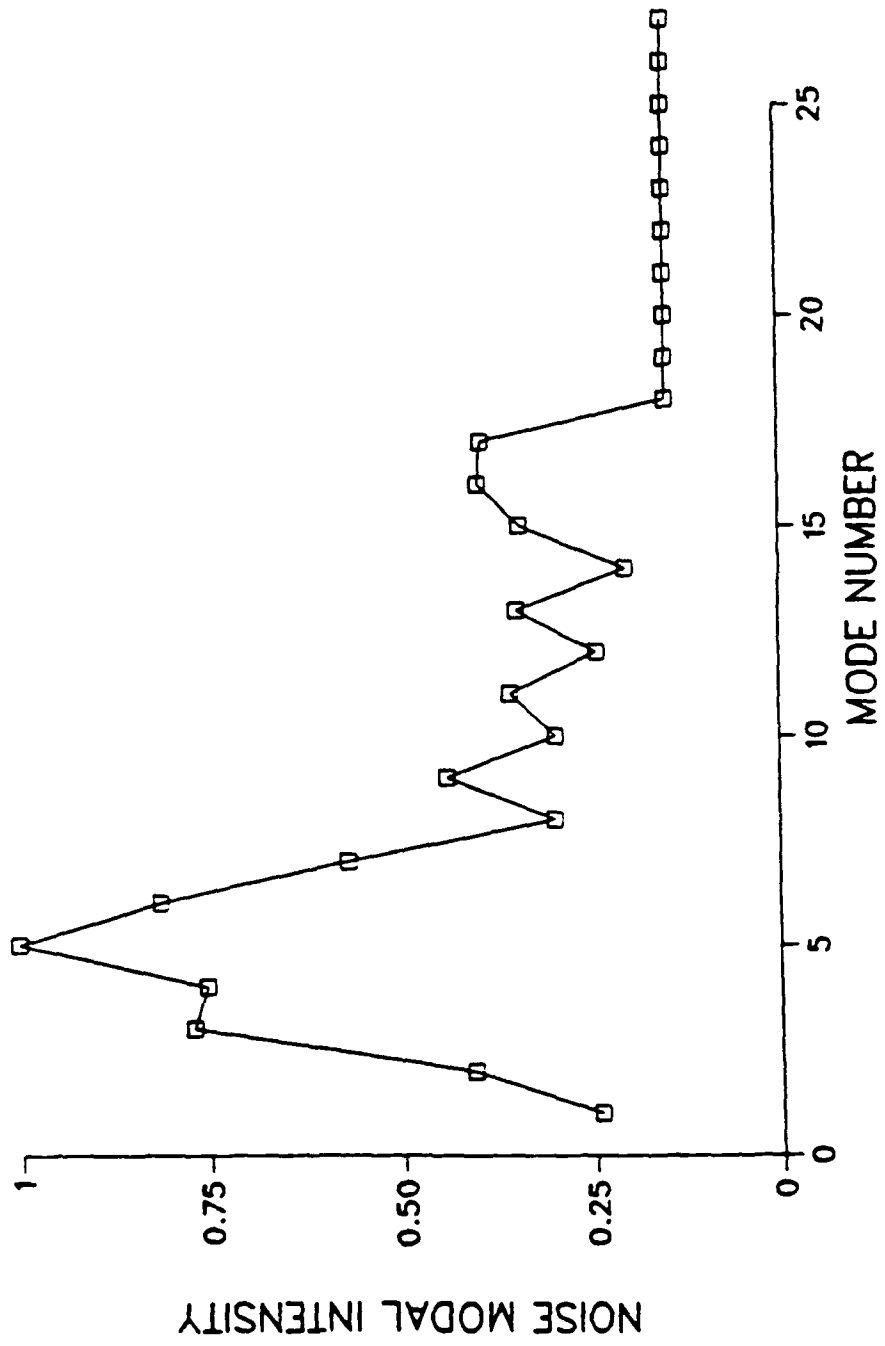
v Optimum

$$\text{OUTPUT S/N} = \sum \frac{s_i}{N_i}$$

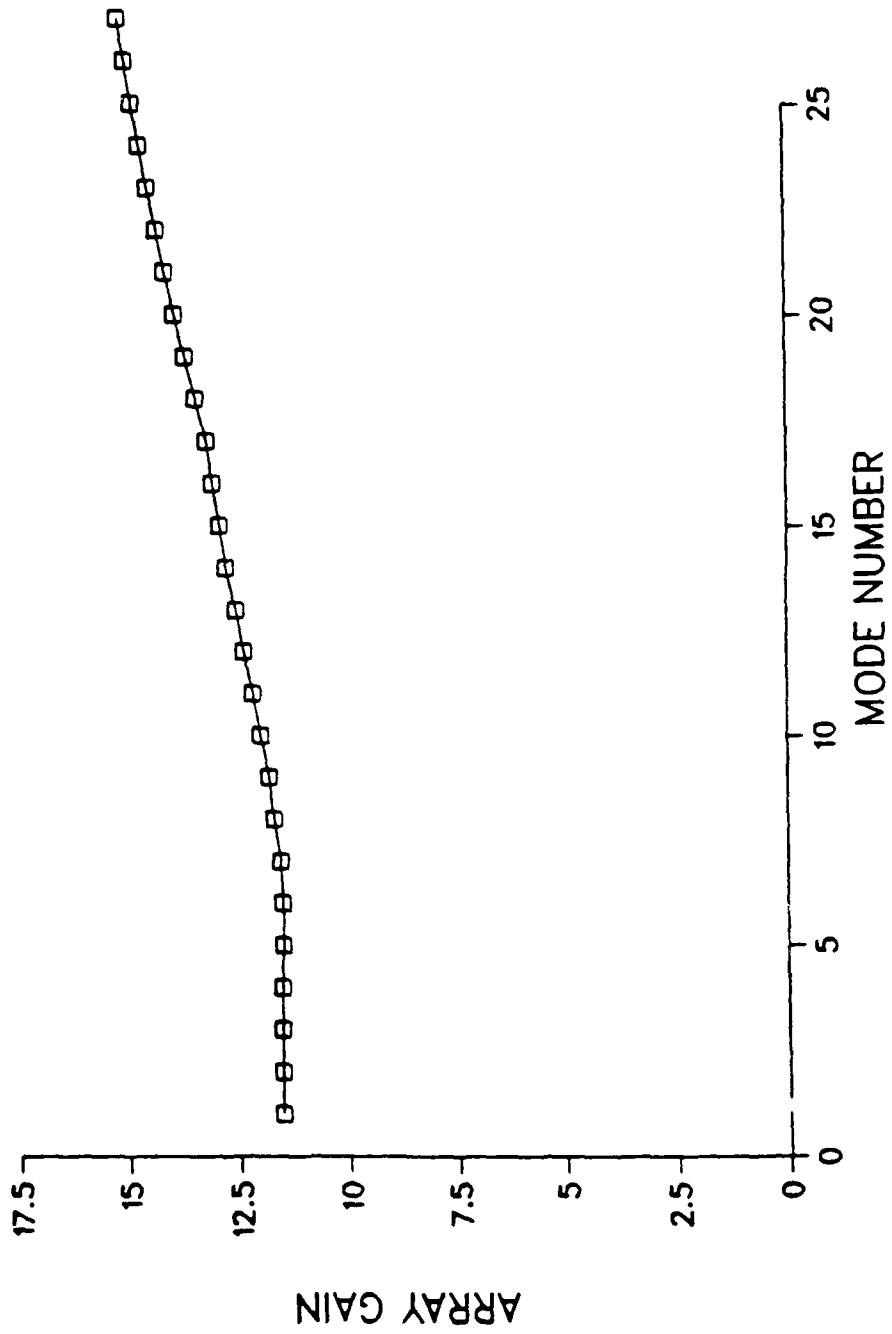




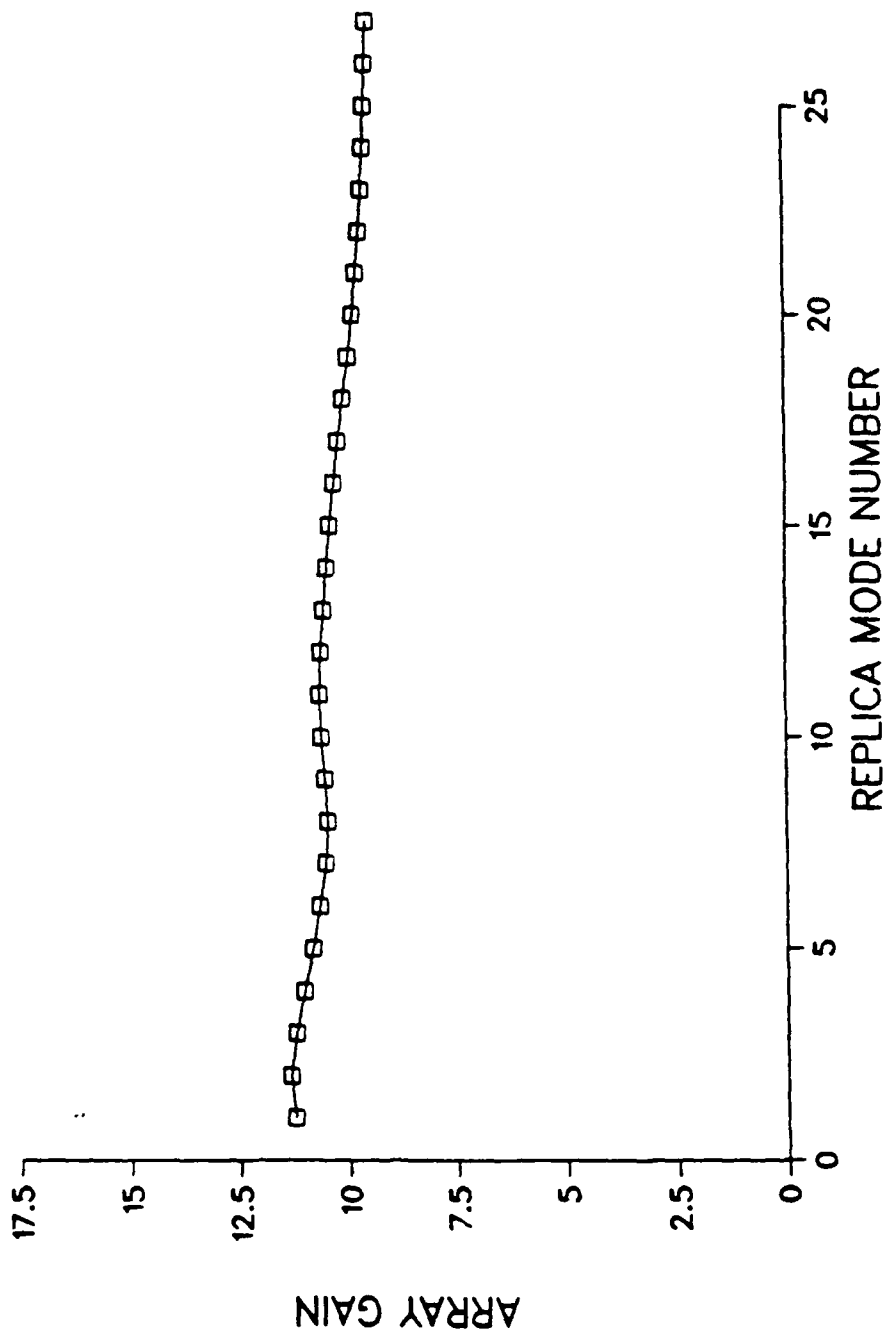




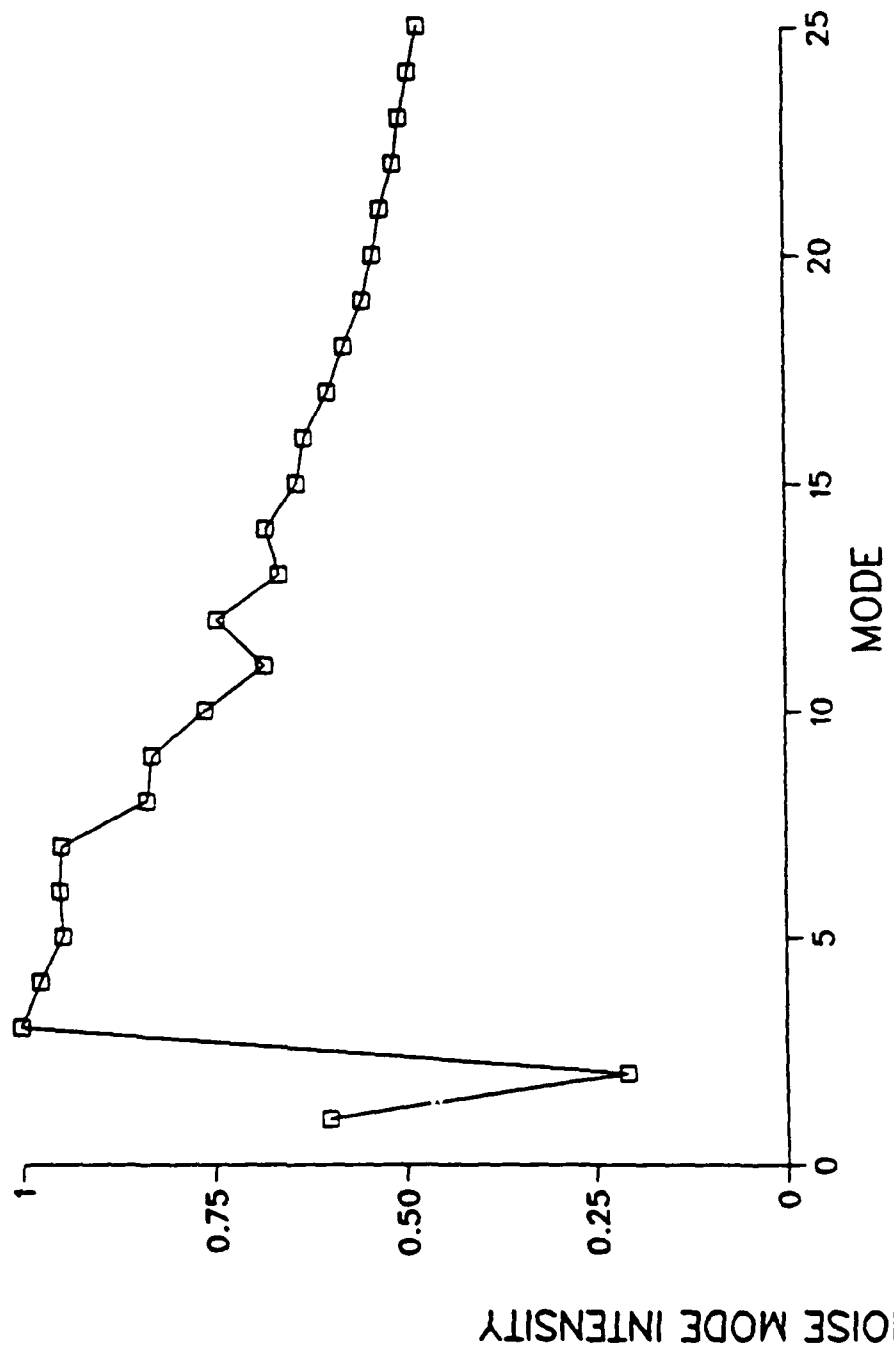




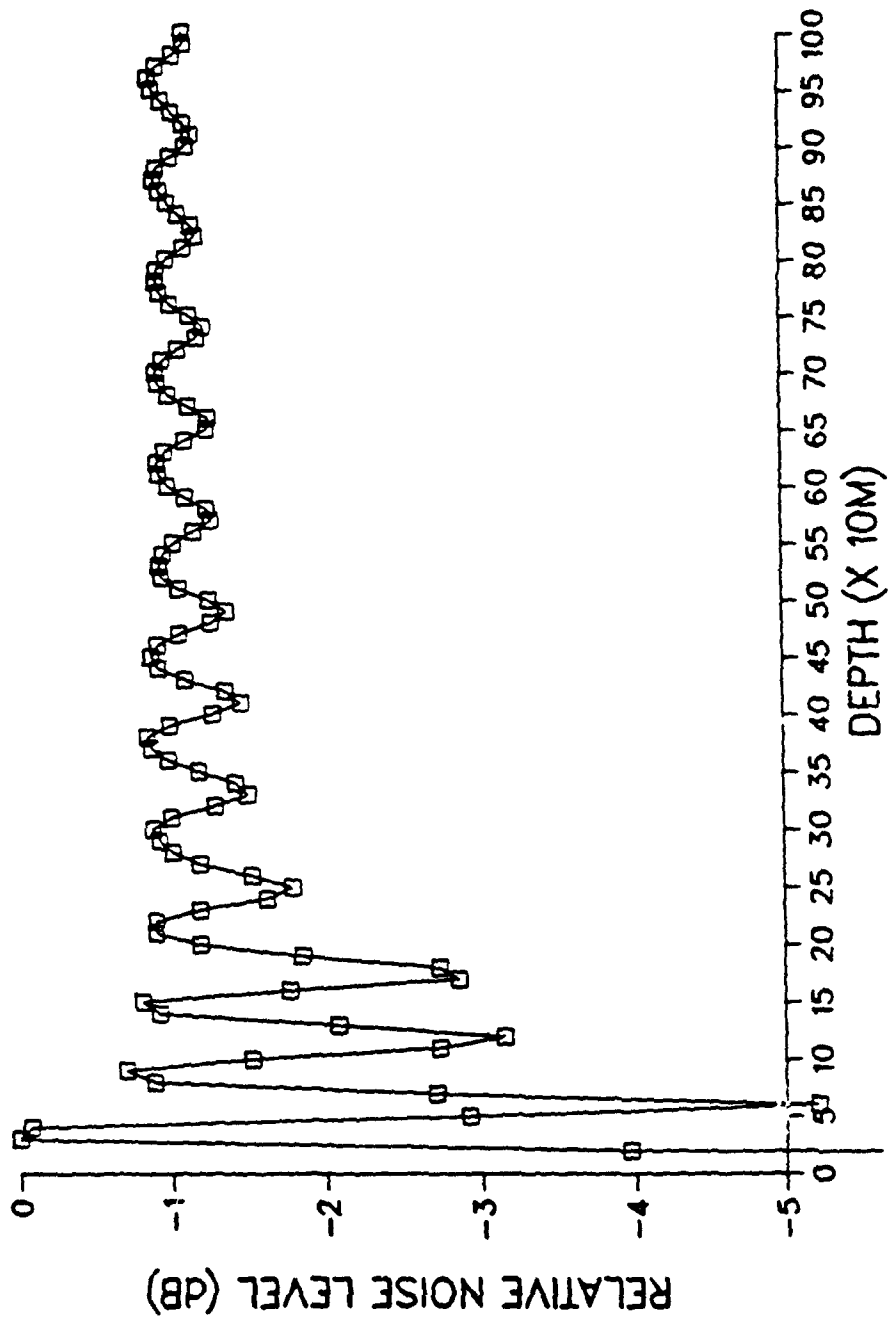






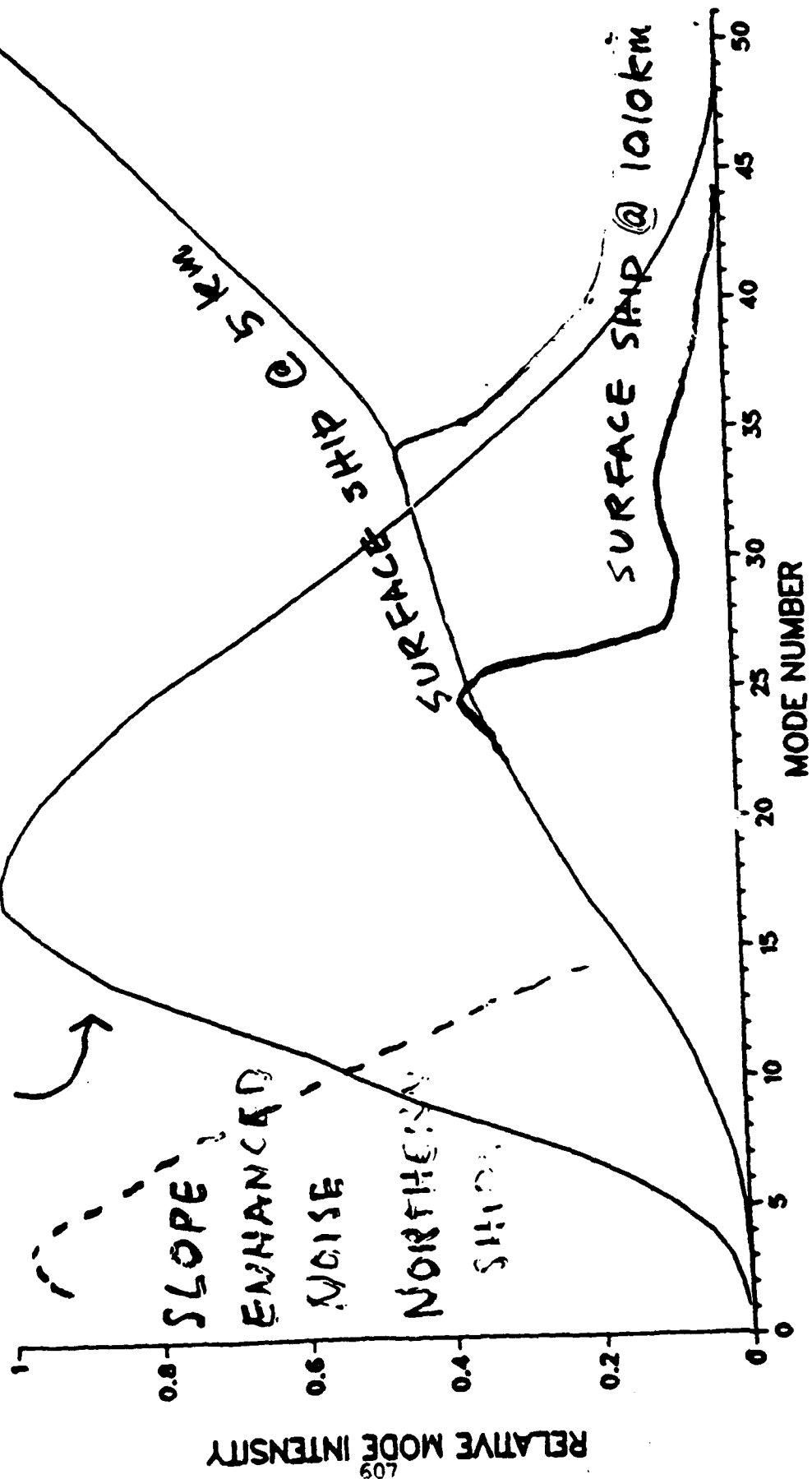






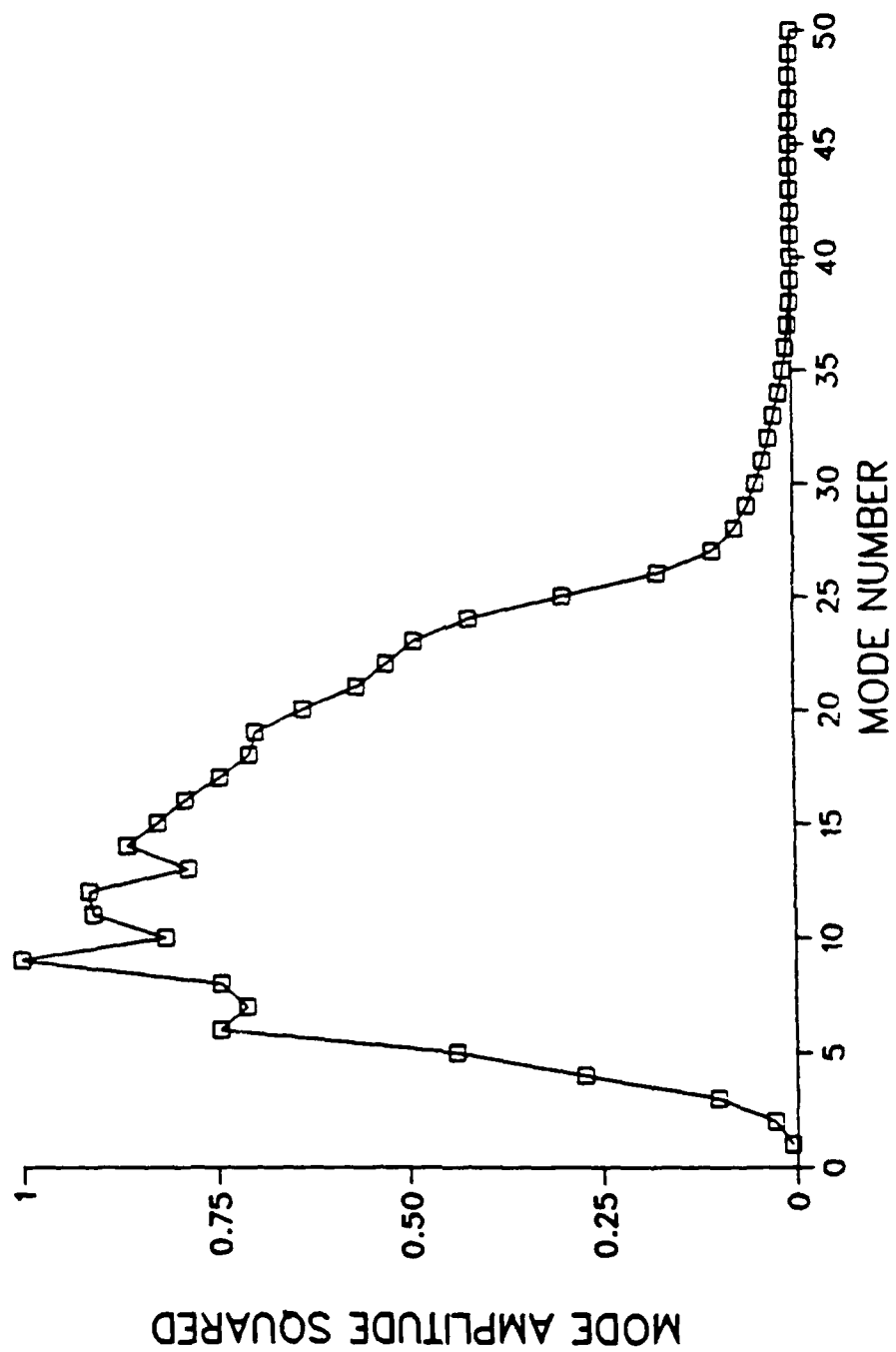


SD: 100M  
R: 1010 km

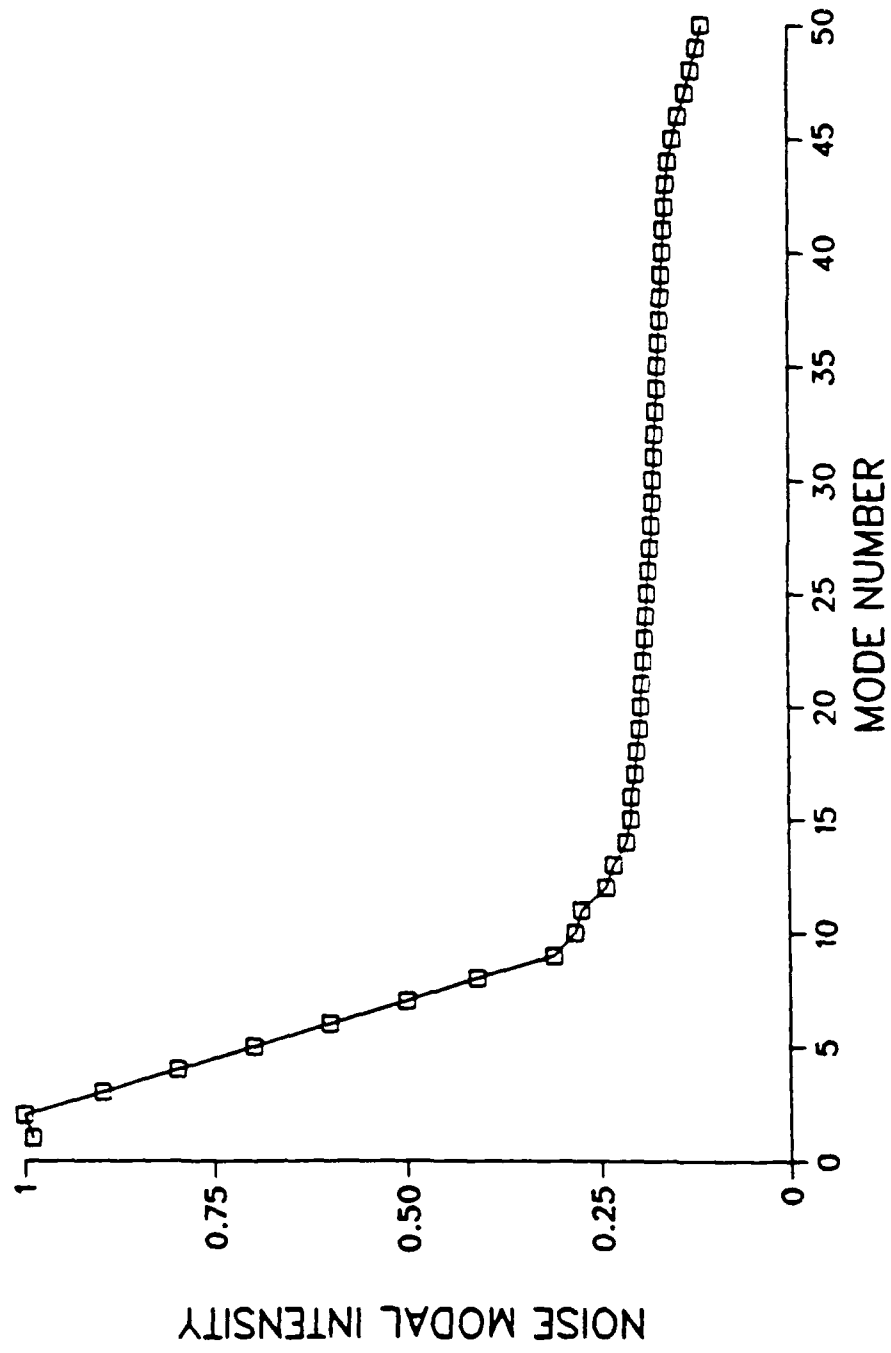


FREQ = 25.00 HZ ECH251010.AM

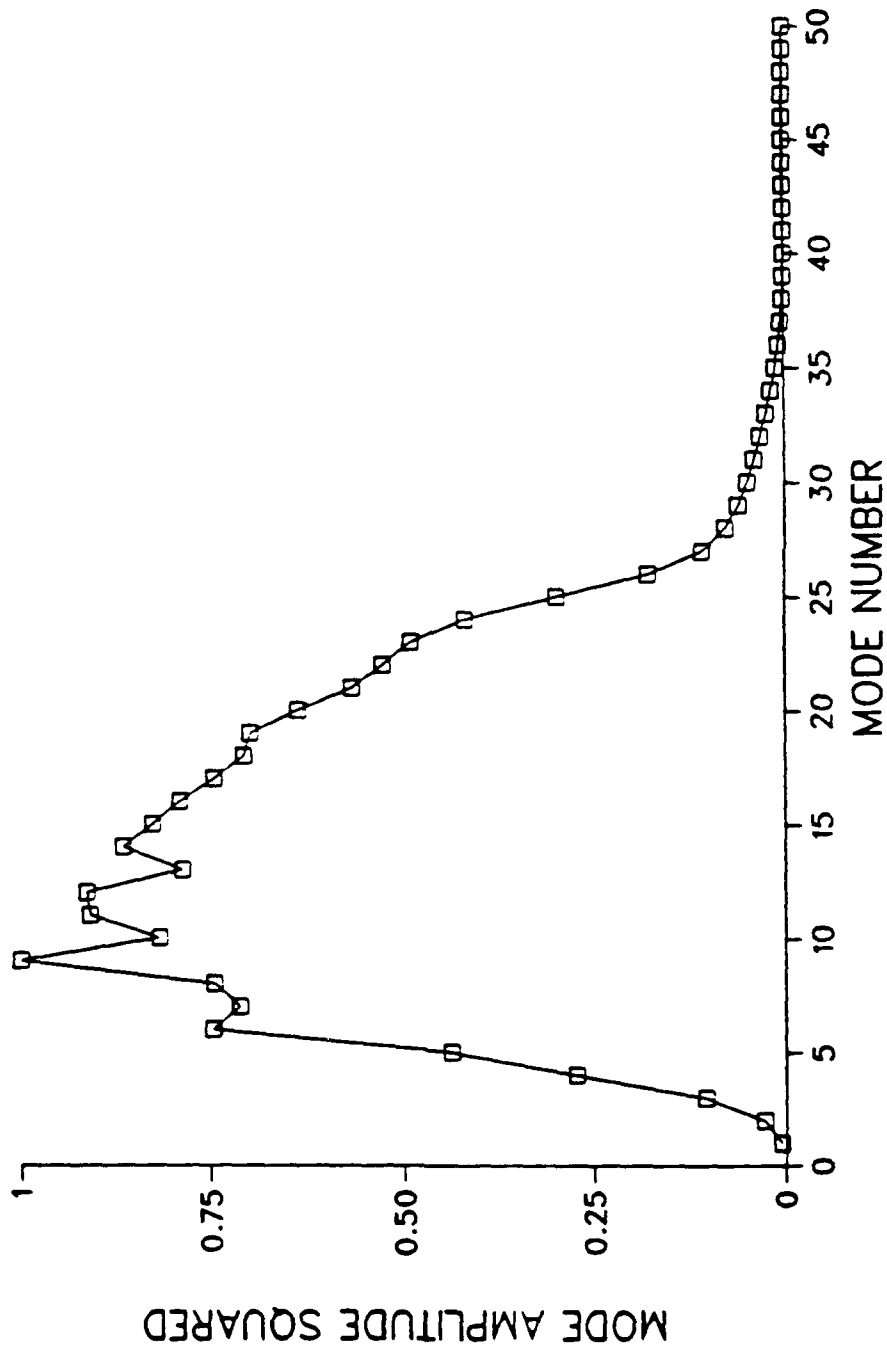




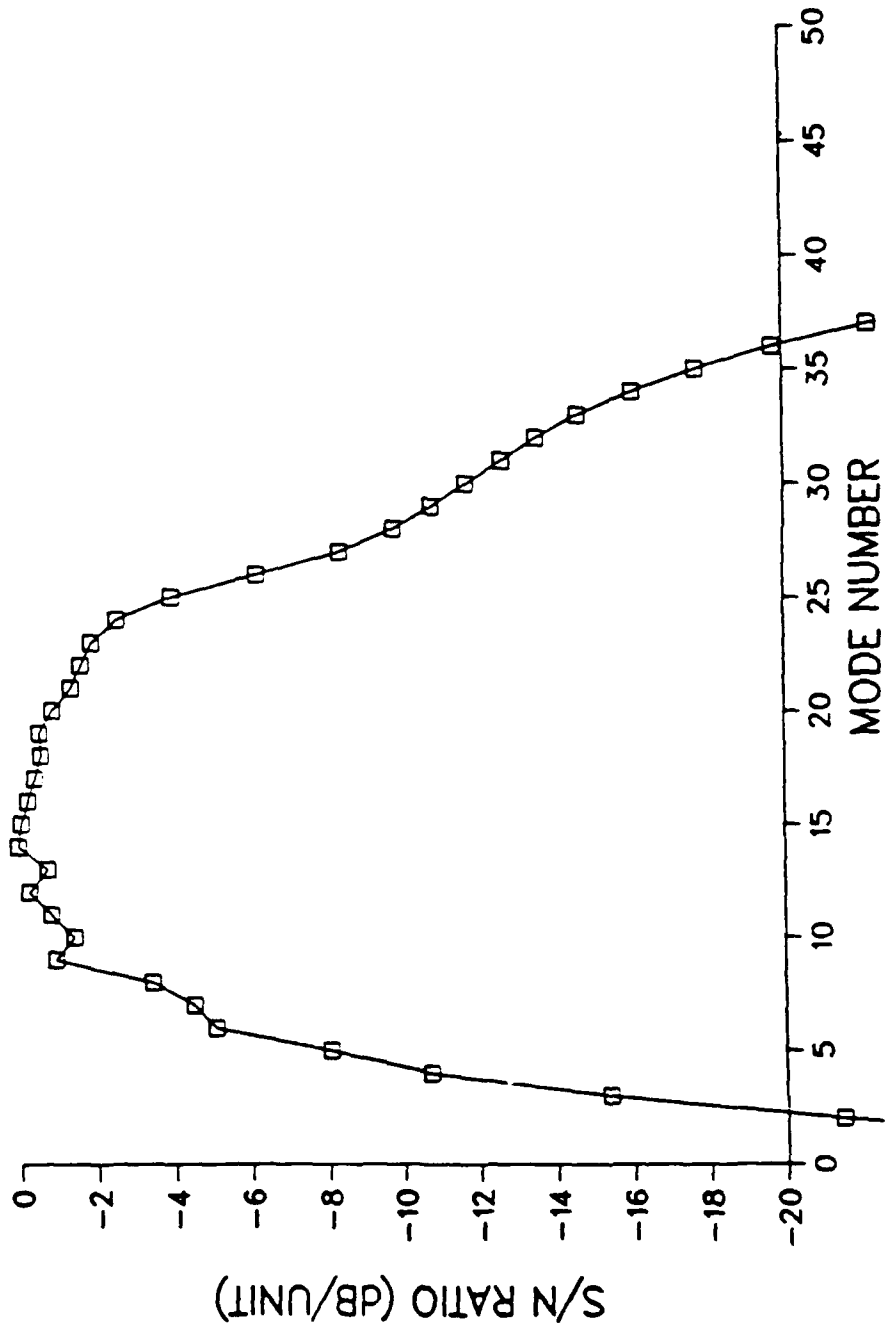




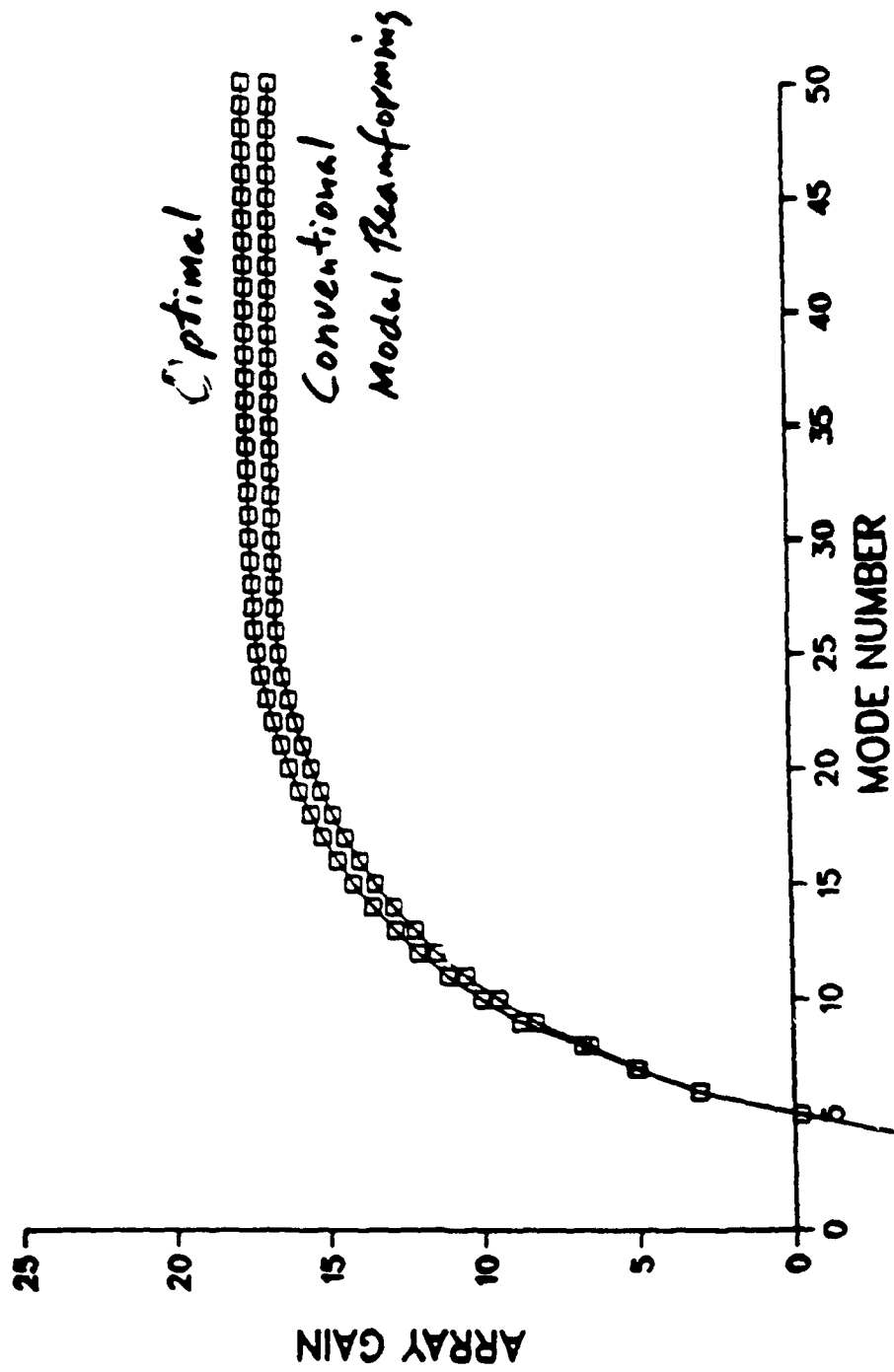














## CONCLUSIONS

- o THE DOMINANT CONTRIBUTION OF ARRAY GAIN COMES FROM MODES WHICH HAVE HIGH SIGNAL CONTENT AND LOW NOISE CONTENT. IT IS ESSENTIAL THAT THESE MODES ARE ACCURATELY FILTERED IN ORDER TO ENHANCE ARRAY GAIN.
- o MODAL BEAMFORMING (MATCHED-MODE) ARRAY GAIN IS OFTEN VERY CLOSE TO THE OPTIMUM ARRAY GAIN FOR A LINEAR PROCESSOR IN A COLORED NOISE ENVIRONMENT.
- o BEAMFORMING IN THE MODE SPACE (MODAL BEAMFORMING IS ONE OF THEM) IS POTENTIALLY ROBUST FOR LOW S/N DETECTION AND LOCALIZATION, IF THE NOISE COVARIANCE MATRIX IS DIAGONAL.



# **OPPORTUNITIES FOR ANALYSIS OF PREVIOUSLY RECORDED DATA**

**J. SHOOTER / S. MITCHELL (ARL:UT)**



**The AEAS  
VLF Data Base**

**Presentation  
to  
Ambient Noise HGI/AEAS Workshop  
20-21 September 1988**

**Environmental Science Group**

**Applied Research Laboratories  
University of Texas at Austin**



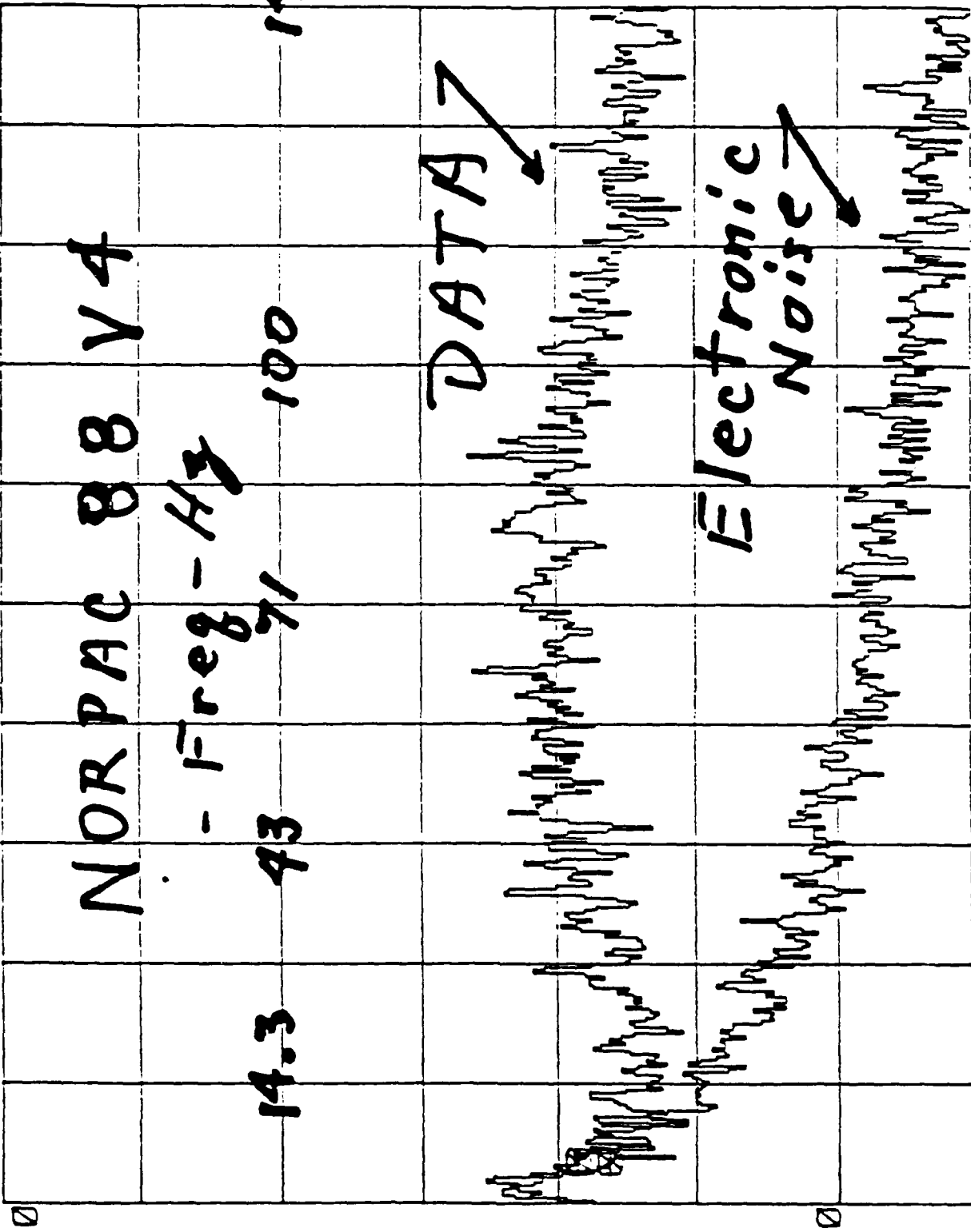
## Background

- Thirteen Years of Data Collection and Analysis, 38 sites -- Archived at ARL:UT
- Most Analysis was Limited to 25 - 600 Hz
  - Low Sponsor interest < 25 Hz
  - Poor VLF SNR at Low Freq on Standard Playback
- Current Focuses
  - Noise Vertical Directionality
  - Spatial Coherence (BB)





LOG B NB G ØDB WTG H B 1.Ø V RMS



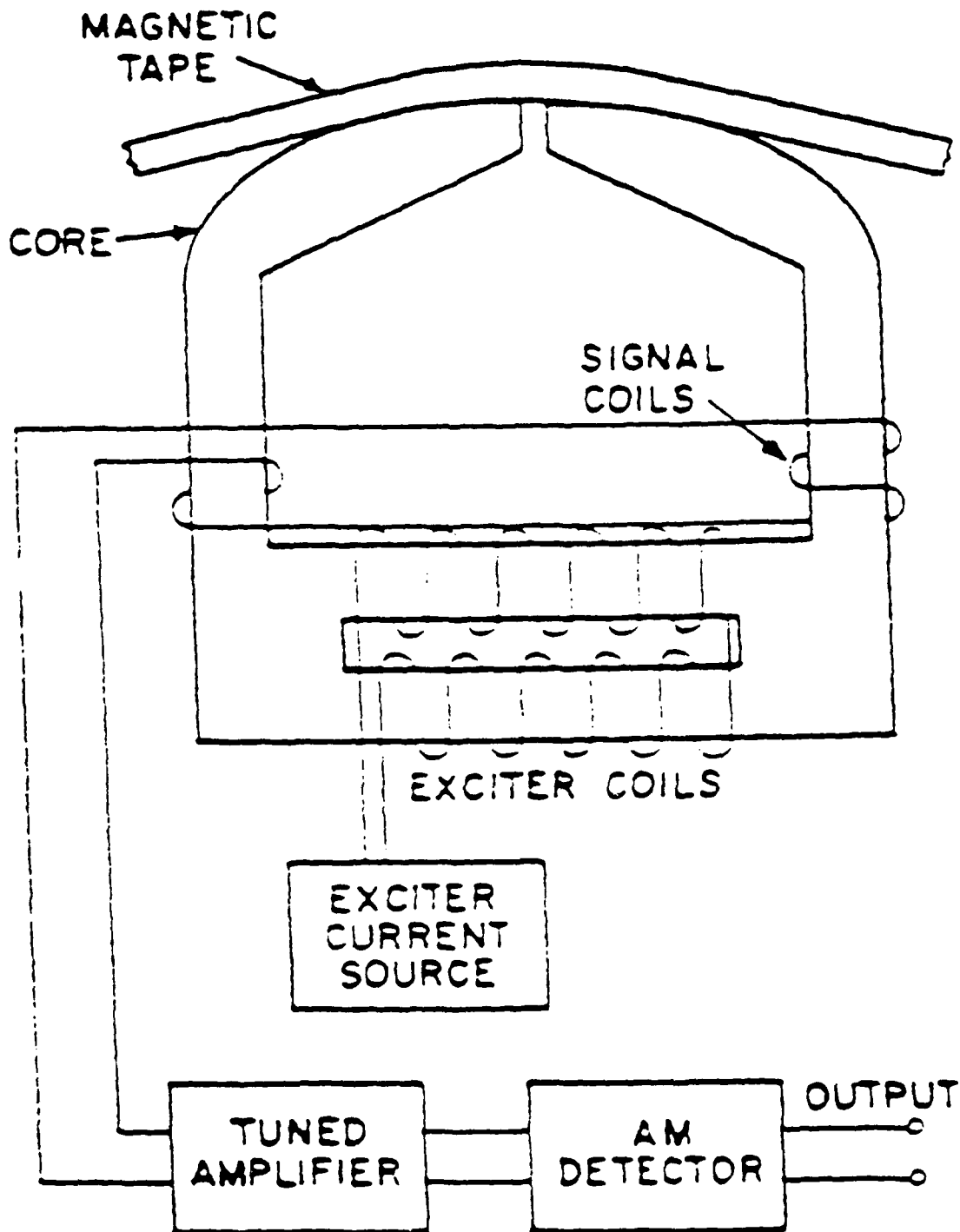
X: 00 700 HZ Y(B) -044.1 DB LIN X HZ 20000 EXPO N 4



## The Analysis of Recordings below 25 Hz

1. Acoustic Data are recorded and calibrated down to 5 Hz
2. Reproduction is possible using Flux responsive heads developed by Teledyne/Geotech





**Flux-responsive head**



## Magnetic Tape Playback

- Conventional Head Output is proportional to Flux Rate ( tape speed )
- Flux Responsive Head Output is proportional to Flux Level



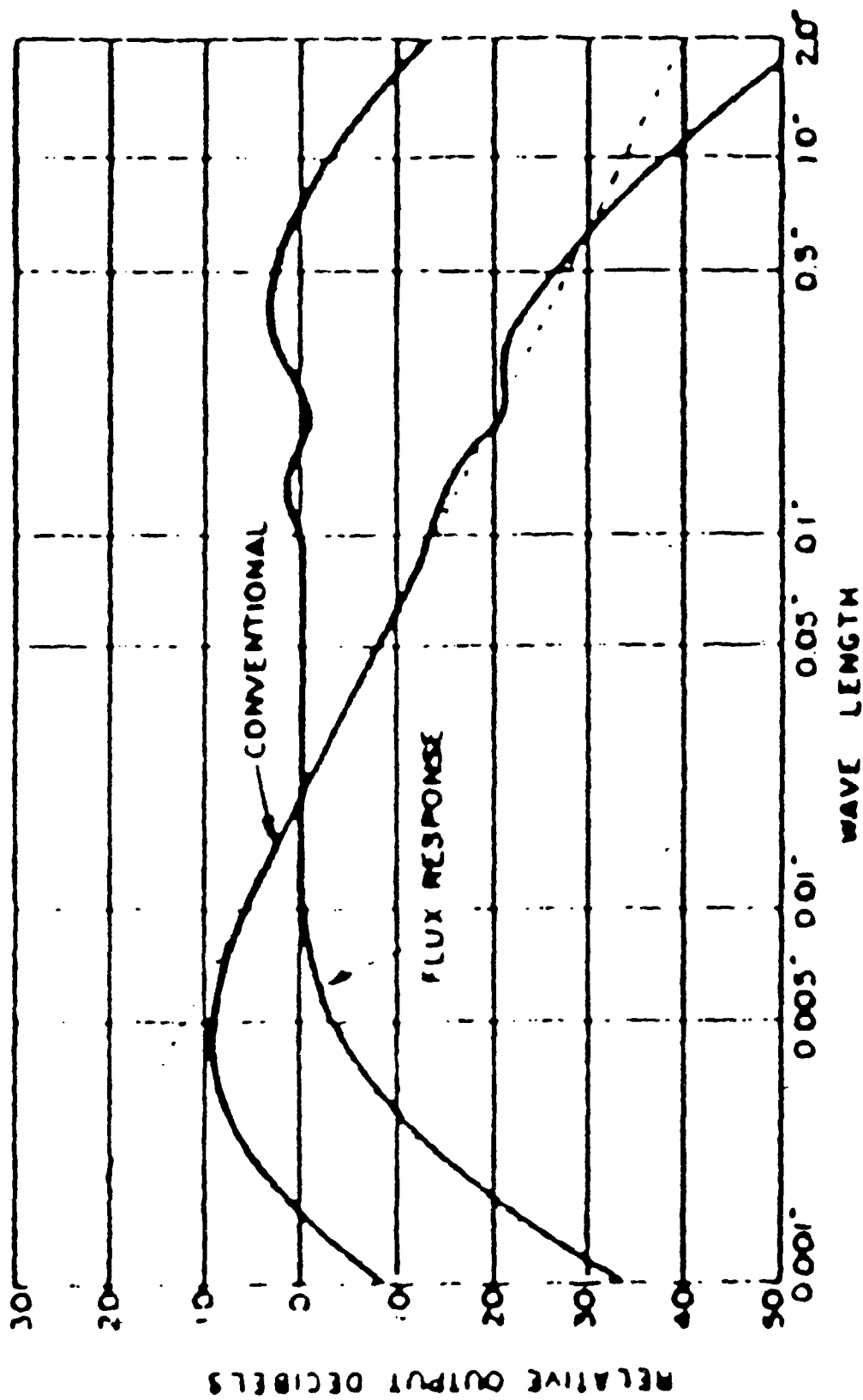


Fig 2 — Playback comparison of the conventional and the flux-response



## **Objectives**

Similar to Objectives at Higher Frequencies

- **Characterization of Spectral Levels**
  1. **Variability over**  
**Ocean Region**  
**Depth**  
**Season**  
**Weather**
  2. **Directionality and Spatial Coherence**  
**at 5 - 50 Hz**
  3. **Compare VLF levels with LF, MF**
- **Characterization of Noise Sources**
  - **Source Level and Radiation Patterns**
  - **Distant Wind, Storms, Microseisms**
- **VLF FL Sensitivity to Geoacoustic**  
**Parameters, Bottom/Sub-bottom**



## Approach

- Obtain Flux responsive heads and Playback Electronics
- Focus on Three Sites
  - Parece Vela Basin 1977
  - Irminger Basin 1982
  - Cascadia Basin 1983
- Digitize and Process Selected Data VLF band ( 5 - 50 Hz), 300 Hz
- Interpret and Analyze results based on FNOC Hindcast, Local Weather, HITS, Local Shipping, and careful Modelling



## VI. DISTRIBUTION LIST

Newell Booth  
ONT  
800 Quincy Street, Room 503  
Arlington, VA 22217-5000

Marshall Bradley  
PSI  
115 Christian Lane  
Slidell, LA 70458

J. Ernest Breeding, Jr.  
NORDA  
Code 245  
Stennis Space Center, MS 39529

John Campbell  
NORDA  
Code 224  
Stennis Space Center, MS 39529

William Carey  
NUSC  
New London, CT 06320

Edward Chaika  
ONR Detachment  
Building 1100  
Stennis Space Center, MS 39529

Johanan L. Codona  
AT&T Bell Labs  
WH14B-419  
Whippany, NJ 07981

J.P. Feuillet  
SPAWAR  
Space & Naval Warfare Command  
Washington, DC 20375

Craig Fisher  
NORDA  
Code 245  
Stennis Space Center, MS 39529

Dr. Edward Franchi  
NORDA  
Code 200  
Stennis Space Center, MS 39529

Herb Freese  
SAIC  
1710 Goodridge Drive  
McLean, VA 22102

R.D. Gaul  
Blue Sea Corporation  
14300 Cornerstone Village Drive  
Suite 317  
Houston, TX 77014

T.G. Goldsberry  
NORDA  
Code 240  
Stennis Space Center, MS 39529

J.T. Gottwald  
G/J Associates  
P.O. Box 3259  
968 Yachtsman Way  
Annapolis, MD 21403

Richard Heitmeyer  
NRL  
Code 512  
Washington, DC 20375

W.S. Hodgkiss  
Marine Physical Lab  
Scripps Institute of Oceanography  
San Diego, CA 92152

E.K. Holmstrom  
COMOCEANSYSPAC  
Box 1390  
Pearl Harbor, HI 96860-7550

Stephanie Kooney  
NORDA  
Code 245  
Stennis Space Center, MS 39529

K.W. Lackie  
ONR/AEAS  
Code 125  
800 N. Quincy Street  
Arlington, VA 22217

Yung P. Lee  
SAIC  
1710 Goodridge Drive  
McLean, VA 22102

Joe Lombardo  
JHU/APL  
Laurel, MD 20707

Jack McDermid  
NORDA  
Code 211  
Stennis Space Center, MS 39529

S.W. Marshall  
BBN  
1300 North 17th St.  
Arlington, VA 22209

Peter Mikhalevsky  
SAIC  
1710 Goodridge Dr.  
(MS T-3-5)  
McLean, VA 22102

S.K. Mitchell  
ARL:UT  
Applied Research Labs  
P.O. Box 8029  
Austin, TX 78713

Joal J. Newcombe  
NORDA  
Code 245  
Stennis Space Center, MS 39529

John Perkins  
NRL  
Code 5160  
Washington, DC 20375-5000

Commanding Officer  
Naval Ocean R&D Activity  
Attn: Code 125P (1)  
Stennis Space Center, MS 39529

William Renner  
SAIC  
1710 Goodridge Drive  
McLean, VA 22102

J.W. Reese  
NOSC  
Code 715  
San Diego, CA 92152

Jack Shooter  
ARL:UT  
P.O. Box 8029  
Austin, TX 78713

R.A. Wagstaff  
NORDA  
Code 245  
Stennis Space Center, MS 39529

James H. Wilson  
WAR, Inc.  
PRL, Inc.  
6309 Carpinteria Avenue  
Carpinteria, CA 93013

A.F. Wittenborn  
Blue Sea Corporation  
3405 Southill  
Austin, TX 78703

T.C. Yang  
NRL  
4555 Overlook Avenue  
Washington, DC 20375

Commanding Officer  
Naval Ocean R&D Activity  
Attn: Code 125L (16)  
Stennis Space Center, MS 39529

UNCLASSIFIED

SECURITY CLASSIFICATION OF THIS PAGE

AD 205 142

REPORT DOCUMENTATION PAGE

1a REPORT SECURITY CLASSIFICATION <b>Unclassified</b>		1b. RESTRICTIVE MARKINGS <b>None</b>	
2a SECURITY CLASSIFICATION AUTHORITY		3 DISTRIBUTION/AVAILABILITY OF REPORT  <b>Approved for public release; distribution is unlimited.</b>	
2b DECLASSIFICATION/DOWNGRADING SCHEDULE			
4. PERFORMING ORGANIZATION REPORT NUMBER(S)  <b>NORDA Technical Note 414</b>		5. MONITORING ORGANIZATION REPORT NUMBER(S)  <b>NORDA Technical Note 414</b>	
6. NAME OF PERFORMING ORGANIZATION  <b>Naval Ocean Research and Development Activity</b>		7a. NAME OF MONITORING ORGANIZATION  <b>Naval Ocean Research and Development Activity</b>	
6c. ADDRESS (City, State, and ZIP Code)  <b>Ocean Acoustics and Technology Directorate Stennis Space Center, Mississippi 39529-5004</b>		7b. ADDRESS (City, State, and ZIP Code)  <b>Ocean Acoustics and Technology Directorate Stennis Space Center, Mississippi 39529-5004</b>	
8a NAME OF FUNDING/SPONSORING ORGANIZATION <b>AEAS, ONRDET* CNR/ONT**</b>	8b OFFICE SYMBOL (If applicable)	9. PROCUREMENT INSTRUMENT IDENTIFICATION NUMBER	
8c. ADDRESS (City, State, and ZIP Code)  <b>*Stennis Space Center, Mississippi 39529-5004 **Arlington, Virginia 22217-5000</b>		10. SOURCE OF FUNDING NOS	
		PROGRAM ELEMENT NO. *62435N **63785N	PROJECT NO. *3511 **0120
		TASK NO. *JOD **500	WORK UNIT NO. *DN258030 **DN258055
11. TITLE (Include Security Classification) <b>Proceedings of the Very Low Frequency (VLF) Ambient Noise Workshop: 20-21 September 1988</b>			
12. PERSONAL AUTHOR(S) <b>R. A. Wagstaff, M. R. Bradley, * L. A. Jagan*</b>			
13a. TYPE OF REPORT <b>Final</b>	13b. TIME COVERED From _____ To _____	14. DATE OF REPORT (Yr., Mo., Day) <b>December 1988</b>	15. PAGE COUNT <b>643</b>
16. SUPPLEMENTARY NOTATION <b>*Planning Systems Incorporated, Slidell, Louisiana 70458</b>			
17. COSATI CODES		18. SUBJECT TERMS (Continue on reverse if necessary and identify by block number)	
FIELD	GROUP	SUB GR	<b>surtass, VLF, ambient noise, towed array, beam noise, acoustic processing</b>
19. ABSTRACT (Continue on reverse if necessary and identify by block number)  <b>A workshop on Very Low Frequency (VLF) Ambient Noise sponsored by the High Gain Initiative (HGI) Program and the ASW Environmental Acoustics Support (AEAS) Program was held at the Stennis Space Center on 20-21 September 1988. The workshop was hosted by the Naval Ocean Research and Development Activity (NORDA). The unclassified presentations made at the workshop are presented here; classified presentations can be found in a companion document. The purpose of the workshop was to assess existing ambient noise measurements and to determine the feasibility of reprocessing some of these data for application to HGI objectives.</b>			
20. DISTRIBUTION/AVAILABILITY OF ABSTRACT <b>UNCLASSIFIED/UNLIMITED <input type="checkbox"/> SAME AS RPT <input checked="" type="checkbox"/> DTIC USERS <input type="checkbox"/></b>		21. ABSTRACT SECURITY CLASSIFICATION <b>Unclassified</b>	
22a. NAME OF RESPONSIBLE INDIVIDUAL <b>R. A. Wagstaff</b>		22b. TELEPHONE NUMBER (Include Area Code) <b>(601) 688-4751</b>	22c. OFFICE SYMBOL <b>Code 245</b>